PARTICLE PROPERTIES DATA BOOKLET

APRIL 1984

From "Review of Particle Properties"
Reviews of Modern Physics
Vol. 56, No. 2, Part II
April 1984

Particle Data Group

M. Aguilar-Benitez, R.N. Cahn,
R.L. Crawford, R. Frosch, G.P. Gopal,
R.E. Hendrick, J.J. Hernandez, G. Höhler,
M.J. Losty, L. Montanet, F.C. Porter,
A. Rittenberg, M. Roos, L.D. Roper,
T. Shimada, R.E. Shrock, N.A. Törnqvist,
T.G. Trippe, W.P. Trower, Ch. Walck,
C.G. Wohl, G.P. Yost, and
B. Armstrong (Technical Associate)

Next edition: April 1986

Printed at CERN
Available from Berkeley and CERN

NOTE

All the information in this booklet is extracted from the "Review of Particle Properties," Rev. Mod. Phys. **56**, No. 2, Part II (April 1984). The reader should refer to that publication for explanations and discussions of the items appearing here, and for more extensive information. In particular, the Review contains complete "Data Card Listings," showing all the data (with references) used in the computation of the values given in the Tables of Particle Properties; also presented in the Listings are data from searches for particles not appearing in the Tables, such as unestablished heavy leptons and weak gauge bosons, quarks, and other unseen or unconfirmed particles. In addition, there are an introductory text and numerous "mini-reviews" which contain, e.g., explanations of nomenclature, comments on the handling of inconsistent data, discussions of individual particles, summaries of partial-wave-analysis results, etc.

Instructions for ordering a copy of the "Review of Particle Properties" are given on the inside back cover of this booklet.

DISCLAIMER

PARTICLE PROPERTIES DATA BOOKLET

APRIL 1984

TABLE OF CONTENTS **PAGE**

PHYSICAL CONSTANTS*

Quantity	Symbol, equation	Value	Uncert. (ppm)
speed of light	c	$2.997\ 924\ 58(1.2)\times10^{10}$ cm s^{-1} (see note**)	0.004
Planck constant	h	$6.626\ 176(36)\times10^{-27}$ erg s	5.4
Planck constant, reduced	$\hbar = h/2\pi$	$1.054\ 588\ 7(57)\times10^{-27}$ erg s	5.4
		$= 6.582\ 173(17)\times10^{-22}$ MeV s	2.6
electron charge magnitude	e	$4.803\ 242(14)\times10^{-10}$ esu	2.9
		$= 1.602\ 189\ 2(46)\times10^{-19}$ coulomb	2.9
conversion constant	$\hbar c$	197.328 58(51) MeV fm	2.6
conversion constant	$(\hbar c)^2$	0.389 385 7(20) GeV^2 mbarn	5.2
electron mass	m_e	$0.511\ 003\ 4(14)$ MeV/c^2 $= 9.109\ 534(47)\times10^{-28}$ g	2.8, 5.1
proton mass	m_p	$938.279\ 6(27)$ MeV/c^2 $= 1.672\ 648\ 5(86)\times10^{-24}$ g	2.8, 5.1
		$= 1.007\ 276\ 470(11)$ amu $= 1836.151\ 52(70)\ m_e$	0.011, 0.38
deuteron mass	m_d	1875.628 0(53) MeV/c^2	2.8
atomic mass unit (amu)	(mass C^{12} atom)/12 = (1 g)/N_A	$931.501\ 6(26)$ MeV/c^2 $= 1.660\ 565\ 5(86)\times10^{-24}$ g	2.8, 5.1
fine structure constant	$\alpha = e^2/\hbar c$	1/137.036 04(11)	0.82
classical electron radius	$r_e = e^2/m_e c^2$	2.817 938 0(70) fm	2.5
electron Compton wavelength	$\lambda_e = \hbar/m_e c = r_e \alpha^{-1}$	$3.861\ 590\ 5(64)\times10^{-11}$ cm	1.6
Bohr radius ($m_{nucleus} = \infty$)	$a_\infty = \hbar^2/m_e e^2 = r_e \alpha^{-2}$	$0.529\ 177\ 06(44)\times10^{-8}$ cm	0.82
Rydberg energy	$hcR_\infty = m_e e^4/2\hbar^2 = m_e c^2 \alpha^2/2$	13.605 804(36) eV	2.6
Thomson cross section	$\sigma_T = 8\pi r_e^2/3$	0.665 244 8(33) barn	4.9
Bohr magneton	$\mu_B = e\hbar/2m_e c$	$5.788\ 378\ 5(95)\times10^{-15}$ MeV gauss^{-1}	1.6
nuclear magneton	$\mu_N = e\hbar/2m_p c$	$3.152\ 451\ 5(53)\times10^{-18}$ MeV gauss^{-1}	1.7
electron cyclotron frequency/field	$\omega_{cycl}^e/B = e/m_e c$	$1.758\ 804\ 7(49)\times10^{7}$ rad s^{-1} gauss^{-1}	2.8
proton cyclotron frequency/field	$\omega_{cycl}^p/B = e/m_p c$	$9.578\ 756(28)\times10^{3}$ rad s^{-1} gauss^{-1}	2.8

gravitational constant	G_N	$6.672\,0(41)\times10^{-8}$ cm^3 g^{-1} s^{-2}	615
grav. acceleration, sea level, 45° lat.	g	980.62 cm s^{-2}	
Fermi coupling constant	$G_F/(\hbar c)^3$	$1.166\,37(2)\times10^{-5}$ GeV^{-2}	17
Avogadro number	N_A	$6.022\,045(31)\times10^{23}$ mol^{-1}	5.1
Boltzmann constant	k	$1.380\,662(44)\times10^{-16}$ erg K^{-1}	32
		$= 8.617\,35(28)\times10^{-5}$ eV K^{-1}	32
molar volume, ideal gas at STP	$N_A k(273.15\text{ K})/(1\text{ atmosphere})$	22 413.83(70) cm^3 mol^{-1}	31
Stefan-Boltzmann constant	$\sigma = \pi^2 k^4/60\hbar^3 c^2$	$5.670\,32(71)\times10^{-5}$ erg s^{-1} cm^{-2} K^{-4}	125

$\pi = 3.141\,592\,653\,589\,793\,238$ $\quad e = 2.718\,281\,828\,459\,045\,235$ $\quad \gamma = 0.577\,215\,664\,901\,532\,861$

1 in = 2.54 cm	1 newton = 10^5 dyne	1 coulomb = $2.997\,924\,58\times10^9$ esu	1 tropical year = $3.155\,69\times10^7$ s
1 Å = 10^{-8} cm	1 joule = 10^7 erg	1 tesla = 10^4 gauss	1 light year = $9.460\,528\times10^{17}$ cm
1 fm = 10^{-13} cm	1 eV = $1.602\,189\,2\times10^{-12}$ erg	1 atm. = $1.013\,25\times10^6$ dyne/cm^2	1 parsec = 3.261 633 light year
1 barn = 10^{-24} cm^2	1 eV/c^2 = $1.782\,676\times10^{-33}$ g	0°C = 273.15 K	1 astro. unit = $1.495\,979\times10^{13}$ cm

* Revised 1984 by Barry N. Taylor, based mainly on the "1973 Least-Squares Adjustment of the Fundamental Constants," by E.R. Cohen and B.N. Taylor, J. Phys. Chem. Ref. Data 2, 663 (1973). The figures in parentheses give the 1-standard-deviation uncertainties in the last digits of the main numbers; the uncertainties in parts per million (ppm) are given in the last column. The uncertainties of the output values of a least-squares adjustment are in general correlated, and the laws of error propagation must be used in calculating additional quantities.

The set of constants resulting from the 1973 adjustment of Cohen and Taylor has been recommended for international use by CODATA (Committee on Data for Science and Technology), and is the most up-to-date, generally accepted set currently available. Since the publication of the 1973 adjustment, new experiments have yielded better values for some of the constants: $N_A = 6.022\,097\,8(63)\times10^{23}$ mol^{-1} (1.04 ppm); $\alpha^{-1} = 137.035\,963(15)$ (0.11 ppm); and $m_p/m_e = 1836.152\,470(79)$ (0.043 ppm). However, since a change in the measured value of one constant usually leads to changes in the adjusted values of others, one must be cautious in using together the values from the 1973 adjustment and the results of more recent experiments.

A new adjustment of the fundamental constants is planned for completion in 1984.

** In October 1983, the Conférence Générale des Poids et Mesures adopted a new definition of the meter. The meter is the length of the path traveled by light in vacuum during a time interval of 1/299 792 458 s. Thus the speed of light is *defined* to be 299 792 458 m/s. For a discussion of this change, see B.W. Petley, Nature 303, 373 (1983).

TABLES OF PARTICLE PROPERTIES

April 1984

M. Aguilar-Benitez, R.N. Cahn, R.L. Crawford, R. Frosch, G.P. Gopal, R.E. Hendrick,
J.J. Hernandez, G. Höhler, M.J. Losty, L. Montanet, F.C. Porter, A. Rittenberg,
M. Roos, L.D. Roper, T. Shimada, R.E. Shrock, N.A. Törnqvist, T.G. Trippe,
W.P. Trower, Ch. Walck, C.G. Wohl, G.P. Yost, and B. Armstrong (Technical Associate)

(Closing date for data: Jan. 1, 1984)

Reprinted from Reviews of Modern Physics, Vol. 56, No. 2, Part II (April 1984)

Stable Particle Table

For additional parameters, see Addendum to this table.

Quantities in italics are new or have changed by more than one (old) standard deviation since April 1982.

Particle	$I^G(J^P)C$ [a]	Mass [b] (MeV)	Mean life [b] (sec) $c\tau$ (cm)	Partial decay mode		
				Mode	Fraction [b]	p or p_{max} [c] (MeV/c)
GAUGE BOSONS						
γ	$0,1(1^-)-$	$(<3\times10^{-33})$	—	stable		

W	*80800 ±2700*	$\Gamma<7$ GeV	$e\nu$	(*seen*)		40400
Z	*92900 ±1600*	$\Gamma<8.5$ GeV	e^+e^-	(*seen*)		46450
			$\mu^+\mu^-$	(*seen*)		46450

→ weak gauge boson searches

LEPTONS

ν_e	$J=\frac{1}{2}$	$(<0.000046)^d$	stable ($>3\times10^8 m_{\nu_e}$ (MeV))	stable		
e	$J=\frac{1}{2}$	0.5110034 ±0.0000014	stable ($>2\times10^{22}$y)	stable		
ν_μ	$J=\frac{1}{2}$	0(<0.50)	stable ($>1.1\times10^5 m_{\nu_\mu}$ (MeV))	stable		
			μ^- ⟶ (or μ^+ →chg. conj.)			
μ	$J=\frac{1}{2}$	105.65932 ±0.00029	2.19709×10^{-6} ±0.00005 $c\tau=6.5867\times10^4$	$e^-\bar{\nu}\nu$	(100	)% 53
				†[$e^-\bar{\nu}\nu\gamma$	(1.4 ± 0.4	)% 53
				$e^-\nu_e\bar{\nu}_\mu$	(<5	)%] 53
				$e^-\bar{\nu}\nu e^+e^-$	(2.2 ± 1.5	)$\times10^{-5}$ 53
				$e^-\gamma$	(<1.7	)$\times10^{-10}$ 53
				$e^-e^+e^-$	(<1.9	)$\times10^{-9}$ 53
				$e^-\gamma\gamma$	(<8.4	)$\times10^{-9}$ 53

Stable Particle Table *(cont'd)*

Particle	$I^G(J^P)C$ [a]	Mass [b] (MeV)	Mean life [b] (sec) $c\tau$ (cm)	Partial decay mode: Mode	Fraction [b]		p or p_{max} [c] (MeV/c)
ν_τ	$J=\frac{1}{2}$	< 164					
			τ^- (or τ^+ → chg. conj.)				
τ	$J=\frac{1}{2}$	1784.2 ±3.2	$(3.4\pm0.5)\times10^{-13}$ $c\tau=0.010$	$\mu^-\bar{\nu}\nu$	(18.5 ± 1.1)%		889
				$e^-\bar{\nu}\nu$	(16.5 ± 0.9)%		892
				hadron$^-$ neutrals	(*48.1* ± *2.0*)%	S=1.1*	
				3(hadron$^\pm$) neutrals	(*17.0* ± *1.3*)%	S=1.2*	
				5(hadron$^\pm$) neutrals	(<1.4)%		
				†[3(hadron$^\pm$)ν	(5 ± 4)%		
				3(hadron$^\pm$)ν(≥1γ)	(12 ± 4)%]		
				†[$\pi^-\nu$	(10.3 ± 1.2)%		887
				$\rho^-\nu$	(22.1 ± 2.4)%		726
				$K^-\nu$	(*1.3* ± *0.5*)%		824
				K^- neutrals	(*small*)%]		
				†[$K^{*-}(892)\nu$	(1.7 ± 0.7)%		669
				$K^{*-}(1430)\nu$	(<0.9)%		323
				$\pi^-\rho^0\nu$	(5.4 ± 1.7)%]		718
				e^- chgd.parts. + μ^- chgd.parts.	(<4)%		

$\mu^-\gamma$	(<5.5	)$\times10^{-4}$	889
$e^-\gamma$	(<6.4	)$\times10^{-4}$	892
$\mu^-\mu^+\mu^-$	(<4.9	)$\times10^{-4}$	876
$e^-\mu^+\mu^-$	(<3.3	)$\times10^{-4}$	886
$\mu^-e^+e^-$	(<4.4	)$\times10^{-4}$	889
$e^-e^+e^-$	(<4.0	)$\times10^{-4}$	892
$\mu^-\pi^0$	(<8.2	)$\times10^{-4}$	884
$e^-\pi^0$	(<2.1	)$\times10^{-3}$	887
μ^-K^0	(<1.0	)$\times10^{-3}$	819
e^-K^0	(<1.3	)$\times10^{-3}$	823
$\mu^-\rho^0$	(<4.4	)$\times10^{-4}$	722
$e^-\rho^0$	(<3.7	)$\times10^{-4}$	726

→ searches for massive neutrinos and lepton mixing
→ ν bounds from astrophysics and cosmology
→ heavy lepton searches

NONSTRANGE MESONS [a]

π^+ ⟶ (or π^- →chg. conj.)

$\pi^\pm$

$I^-(0^-)$ 139.5673 ±0.0007

$m_{\pi^\pm} - m_{\mu^\pm}$ −33.9080 ±0.0008

2.6030×10^{-8} ±0.0023 $c\tau$=780.4

$\mu^+\nu$	100%		30
$e^+\nu$	(*1.232±0.024*)$\times10^{-4}$	S=2.0*	70
†[$\mu^+\nu\gamma$	[e](1.24± 0.25)$\times10^{-4}$		30
$e^+\nu\gamma$	[e](5.6 ± 0.7)$\times10^{-8}$]		70
$e^+\nu\pi^0$	(1.033±0.034)$\times10^{-8}$		5
$e^+\nu e^+e^-$	(<5)$\times10^{-9}$		70
$\mu^+\overline{\nu}_e$	(*<1.5*)$\times10^{-3}$		30
$\mu^+\nu_e$	(*<8*)$\times10^{-3}$		30

Stable Particle Table *(cont'd)*

Particle	$I^G(J^P)C$ [a]	Mass [b] (MeV)	Mean life [b] (sec) $c\tau$ (cm)	Partial decay mode: Mode	Fraction [b]	p or p_{max} [c] (MeV/c)
π^0	$1^-(0^-)+$	134.9630 ±0.0038	0.83×10^{-16} ±0.06 S=1.8*	$\gamma\gamma$	(98.802 ± 0.030)%	67
			$c\tau=2.5\times10^{-6}$	γe^+e^-	(1.198)%	67
				$\gamma\gamma\gamma$	(<3.8)$\times10^{-7}$	67
	$m_{\pi^\pm}-m_{\pi^0}$ =4.6043 ±0.0037			$e^+e^-e^+e^-$	(3.24)$\times10^{-5}$	67
				$\gamma\gamma\gamma\gamma$	(<4)$\times10^{-6}$	67
				e^+e^-	(1.8 ± 0.7)$\times10^{-7}$	67
				$\nu\nu$	(<2.4)$\times10^{-5}$	67
				$\mu^+e^- + \mu^-e^+$	(<7)$\times10^{-8}$	26
η	$0^+(0^-)+$	548.8 ±0.6 S=1.4*	Γ=(0.88 ±0.12)keV	$\gamma\gamma$	(39.0 ± 0.8)%	274
			Neutral decays (70.9 ±0.7)%	$3\pi^0$	(31.8 ± 0.8)% S=1.1*	180
				$\pi^0\gamma\gamma$	(0.10 ± 0.02)%	258
				$\pi^+\pi^-\pi^0$	(23.7 ± 0.5)%	175
				$\pi^+\pi^-\gamma$	(4.91 ± 0.13)%	236
				$e^+e^-\gamma$	(0.50 ± 0.12)%	274
				$\mu^+\mu^-\gamma$	(3.1 ± 0.4)$\times10^{-4}$	253
				e^+e^-	(<3)$\times10^{-4}$	274
				$\mu^+\mu^-$	(6.5 ± 2.1)$\times10^{-6}$	253
			Charged decays (29.1 ±0.7)%	$\pi^+\pi^-e^+e^-$	(0.13 ± 0.13)%	236
				$\pi^+\pi^-\gamma\gamma$	(<0.21)%	236
				$\pi^+\pi^-\pi^0\gamma$	(<6)$\times10^{-4}$	175

				$\pi^+\pi^-$	(<0.15)%	236
				$\pi^0 e^+ e^-$	(<5)$\times 10^{-5}$	258
				$\pi^0 \mu^+ \mu^-$	(<5)$\times 10^{-6}$	211
				$\pi^0 \mu^+ \mu^- \gamma$	(<3)$\times 10^{-6}$	211

STRANGE MESONS [a]

K^+ — (or K^- → chg. conj.)

$K^\pm$	$\frac{1}{2}(0^-)$	493.667 ±0.015	1.2371×10^{-8} ±0.0026 S=1.9* $c\tau$=370.9	$\mu^+\nu$	(63.51± 0.16)%		236
				$\pi^+\pi^0$	(21.17± 0.15)%		205
				$\pi^+\pi^+\pi^-$	(5.59± 0.03)%	S=1.1*	125
				$\pi^+\pi^0\pi^0$	(1.73± 0.05)%	S=1.4*	133
				$\pi^0\mu^+\nu$	(3.18± 0.10)%	S=1.9*	215
				$\pi^0 e^+\nu$	(4.82± 0.05)%	S=1.1*	228
$m_{K^\pm} - m_{K^0} = -4.01$ ±0.13 S=1.1*				† $\mu^+\nu\gamma$	[e] (5.8 ± 3.5)$\times 10^{-3}$		236
				$\pi^+\pi^0\gamma$	[g,e] (2.75± 0.16)$\times 10^{-4}$		205
				$\pi^+\pi^+\pi^-\gamma$	[e] (1.0 ± 0.4)$\times 10^{-4}$		125
				$\pi^0\mu^+\nu\gamma$	[e] (<6)$\times 10^{-5}$		215
				$\pi^0 e^+\nu\gamma$	[e] (3.7 ± 1.4)$\times 10^{-4}$]		228
				$\pi^0\pi^0 e^+\nu$	($1.8\ ^{+\ 2.4}_{-\ 0.6}$)$\times 10^{-5}$		207
				$\pi^+\pi^- e^+\nu$	(3.90± 0.15)$\times 10^{-5}$		203
				$\pi^+\pi^+ e^-\overline{\nu}$	(<1.2)$\times 10^{-8}$		203
				$\pi^+\pi^-\mu^+\nu$	(1.4 ± 0.9)$\times 10^{-5}$		151
				$\pi^+\pi^+\mu^-\overline{\nu}$	(<3.0)$\times 10^{-6}$		151
				$e^+\nu$	(1.54± 0.07)$\times 10^{-5}$		247
				$e^+\nu\gamma$ (SD+) [h]	(1.52± 0.23)$\times 10^{-5}$		247
				$e^+\nu\gamma$ (SD−) [h]	(<1.6)$\times 10^{-4}$		247

(continued next page)

Stable Particle Table *(cont'd)*

Particle	$I^G(J^P)C$ [a]	Mass [b] (MeV)	Mean life [b] (sec) $c\tau$ (cm)	Partial decay mode: Mode	Fraction [b]	p or p_{max} [c] (MeV/c)
$K^\pm$ (continued)				$K^+ \rightarrow$ (or $K^- \rightarrow$ chg. conj.)		
				$\pi^+ e^+ e^-$	$(2.7 \pm 0.5) \times 10^{-7}$	227
				$\pi^- e^+ e^+$	$(<1) \times 10^{-8}$	227
				$\pi^+ \mu^+ \mu^-$	$(<2.4) \times 10^{-6}$	172
				$\pi^+ \gamma\gamma$	[e] $(<8) \times 10^{-6}$	227
				$\pi^+ \gamma\gamma\gamma$	[e] $(<1.0) \times 10^{-4}$	227
				$\pi^+ \nu\bar{\nu}$	$(<1.4) \times 10^{-7}$	227
				$\pi^\mp e^+ \mu^\pm$	$(<7) \times 10^{-9}$	214
				$\pi^+ e^- \mu^+$	$(<5) \times 10^{-9}$	214
				$e^+ \nu\nu\bar{\nu}$	$(<6) \times 10^{-5}$	247
				$\mu^+ \nu\nu\bar{\nu}$	$(<6) \times 10^{-6}$	236
				$\mu^+ \nu e^+ e^-$	$(11 \pm 3) \times 10^{-7}$	236
				$\mu^- \nu e^+ e^+$	$(<2.0) \times 10^{-8}$	236
				$e^+ \nu e^+ e^-$	$(2^{+2}_{-1}) \times 10^{-7}$	247
				$\mu^+ \nu_e$	$(<4) \times 10^{-3}$	236
				$\mu^+ \bar{\nu}_e$	$(<3.3) \times 10^{-3}$	236
				$\pi^0 e^+ \nu_e$	$(<3) \times 10^{-3}$	228
K^0 / $\bar{K}^0$	$\frac{1}{2}(0^-)$	497.67 ±0.13 S=1.1*		50 % K_{Short}, 50% K_{Long}		

K_S^0	$\frac{1}{2}(0^-)$	0.8923×10^{-10} ±0.0022 $c\tau=2.675$	$\pi^+\pi^-$	(68.61 ± 0.24)%		206
			$\pi^0\pi^0$	(31.39)%	S=1.1*	209
			†[$\pi^+\pi^-\gamma$	[e] (1.85 ± 0.10)$\times10^{-3}$]		206
			$\mu^+\mu^-$	(<3.2)$\times10^{-7}$		225
			e^+e^-	(<3.4)$\times10^{-4}$		249
			$\gamma\gamma$	(<4)$\times10^{-4}$		249
			$\pi^+\pi^-\pi^0$	(<8.5)$\times10^{-5}$		133
			$\pi^0\pi^0\pi^0$	(<3.7)$\times10^{-5}$		139
K_L^0	$\frac{1}{2}(0^-)$	5.183×10^{-8} ±0.040 $c\tau=1554$	$\pi^0\pi^0\pi^0$	(21.5 ± 1.0)%	S=1.7*	139
			$\pi^+\pi^-\pi^0$	(12.39 ± 0.20)%	S=1.3*	133
			$\pi^\pm\mu^\mp\nu$	(27.1 ± 0.4)%	S=1.4*	216
			$\pi^\pm e^\mp\nu$	(38.7 ± 0.5)%	S=1.5*	229
			$\pi^+\pi^-$	[i] (0.203 ± 0.005)%	S=1.1*	206
			$\pi^0\pi^0$	[i] (0.094 ± 0.018)%	S=1.5*	209
			†[$\pi e\nu\gamma$	[e] (1.3 ± 0.8)%		229
			$\pi^+\pi^-\gamma$	[e] (4.41 ± 0.32)$\times10^{-5}$]		206
			$\pi^0\gamma\gamma$	(<2.4)$\times10^{-4}$		231
			$\gamma\gamma$	(4.9 ± 0.4)$\times10^{-4}$		249
			$e\mu$	[j] (<6)$\times10^{-6}$		238
			$\mu^+\mu^-$	(9.1 ± 1.9)$\times10^{-9}$		225
			$\mu^+\mu^-\gamma$	(2.8 ± 2.8)$\times10^{-7}$		225
			$\pi^0\mu^+\mu^-$	(<1.2)$\times10^{-6}$		177
			e^+e^-	[j] (<2.0)$\times10^{-7}$		249
			$e^+e^-\gamma$	(1.7 ± 0.9)$\times10^{-5}$		249
			$\pi^0e^+e^-$	(<2.3)$\times10^{-6}$		231
			$\pi^+\pi^-e^+e^-$	(<9)$\times10^{-6}$		206
			$\pi^0\pi^\pm e^\mp\nu$	(6.2 ± 2.0)$\times10^{-5}$		207
			($\pi\mu$ atom) ν	(*1.05 ± 0.11*)$\times10^{-7}$		

$m_{K_L^0} - m_{K_S^0} = 0.5349\times10^{10}\ \hbar\ \text{sec}^{-1}$ ±0.0022

$= 3.521\times10^{-12}$ MeV ±0.014

Stable Particle Table *(cont'd)*

Particle	$I^G(J^P)C$ [a]	Mass [b] (MeV)	Mean life [b] (sec) $c\tau$ (cm)	Partial decay mode: Mode	Fraction [b]		p or p_{max} [c] (MeV/c)
CHARMED NONSTRANGE MESONS [a]							
$D^{\pm}$	$\frac{1}{2}(0^-)$	1869.4 ±0.6	$(9.2^{+1.7}_{-1.2})\times10^{-13}$	D^+ → (or D^- → chg. conj.)			
			$c\tau$=0.028	e^+ anything	(19 $^{+4}_{-3}$)%		
				K^- anything	(16 ± 4)%		
				$\bar{K}^0$ any + K^0 any	(48 ± 15)%		
				K^+ anything	(6.0 ± 3.3)%		
		$m_{D^\pm} - m_{D^0}$= 4.7 ±0.3		η anything	[k] (< 13)%		
				$\mu^+\nu$	(<2)%		932
				† $K^-\pi^+\pi^+$	(4.6 ± 1.1)%	S=1.3*	845
				$K^-\pi^+\pi^+\pi^0$	(2.6 $^{+3.1}_{-1.0}$)%		816
				$K^-\pi^+\pi^+\pi^+\pi^-$	(<4)%		772
				$\bar{K}^0\pi^+$	(1.8 ± 0.5)%		862
				$\bar{K}^0\pi^+\pi^0$	(13 ± 8)%		845
				$\bar{K}^0\pi^+\pi^+\pi^-$	(8.4 ± 3.5)%		814
				$\bar{K}^0K^+$	(0.45± 0.30)%		792
				$K^+K^-\pi^+$	(<0.6)%		744
				$K^+\pi^+\pi^-$	(<0.23)%		845
				$\pi^+\pi^0$	(<0.5)%		925
				$\pi^+\pi^+\pi^-$	(<0.4)%]		908

†[$\bar{K}^{*0}\pi^+$	(<3.7	)%]		714
D^0 (or $\bar{D}^0$ → chg. conj.)				
e^+ anything	(5.3 $^{+2.9}_{-1.3}$	)%		
K^- anything	(44 ± 10	)%	S=1.3*	
$\bar{K}^0$ any + K^0 any	(33 ± 10	)%		
K^+ anything	(8 ± 3	)%		
η anything [k]	(< 13	)%		
†[$K^-\pi^+$	(2.4 ± 0.4	)%		861
$K^-\pi^+\pi^0$	(9.3 ± 2.8	)%		844
$K^-\pi^+\pi^+\pi^-$	(4.6 ± 1.4	)%	S=1.2*	812
$K^-\pi^+\pi^0\pi^0$	(seen	)		815
$\bar{K}^0\pi^0$	(2.2 ± 1.1	)%		860
$\bar{K}^0\pi^+\pi^-$	(4.2 ± 0.8	)%		842
$\pi^+\pi^-$	(7.9 ± 3.8	)$\times10^{-4}$		922
$\pi^+\pi^+\pi^-\pi^-$	(<1.0	)%		880
K^+K^-	(2.7 ± 0.8	)$\times10^{-3}$]		791
†[$K^{*-}\pi^+$	(3.4 ± 1.4	)%		711
$\bar{K}^{*0}\pi^0$	(1.4 $^{+2.3}_{-1.4}$	)%		711
$K^-\rho^+$	(7.2 $^{+3.0}_{-3.1}$	)%		679
$\bar{K}^0\rho^0$	(0.1 $^{+0.6}_{-0.1}$	)%		677
$\bar{K}^{*0}\rho^0$	(0.7 $^{+0.8}_{-0.7}$	)%		423
$K^-\pi^+\rho^0$	(3.9 $^{+1.3}_{-1.6}$	)%		613
$\bar{K}^{*0}\pi^+\pi^-$	(<2.3	)%		685
$K^-A_2^+$	(<0.8	)%]		198

D^0 / $\bar{D}^0$

$J^P = \frac{1}{2}(0^-)$ 1864.7 ±0.6 $(4.4\ ^{+0.8}_{-0.6})\times10^{-13}$ $c\tau$=0.013

$\left|m_{D_1^0} - m_{D_2^0}\right| < 6.5\times10^{-10}$ MeV [ℓ]

$\dfrac{\left|\tau_{D_1^0} - \tau_{D_2^0}\right|}{\text{average}} < 0.55$ [ℓ]

$\dfrac{\Gamma(D^0\to\bar{D}^0\to K^+\pi^-)}{\Gamma(D^0\to K\pi)} < 0.16$

$\dfrac{\Gamma(D^0\to\bar{D}^0\to\mu^-\text{ anything})}{\Gamma(D^0\to\mu^\pm\text{ anything})} < 0.044$

Stable Particle Table *(cont'd)*

Particle	$I^G(J^P)C$ [a]	Mass [b] (MeV)	Mean life [b] (sec) $c\tau$ (cm)	Partial decay mode: Mode	Fraction [b]	p or p_{max} [c] (MeV/c)
CHARMED STRANGE MESON [a]						
				F^+ — (or F^- → chg. conj.)		
$\mathbf{F^\pm}$	$0(0^-)$ [m]	1971 [m] ± 6	$(1.9^{+1.3}_{-0.7})\times10^{-13}$ $c\tau=0.006$	$\phi\pi^+$	(*seen*)	713
				$\eta\pi^+$	(*possibly seen*)	903
				$\eta\pi^+\pi^+\pi^-$	(*possibly seen*)	857
				$\eta'\pi^+\pi^+\pi^-$	(*possibly seen*)	679
				$\phi\rho^+$	(*possibly seen*)	411
BOTTOM MESONS [a]						
				B^+ — (or B^- → chg. conj.)		
$\mathbf{B^\pm}$	$\frac{1}{2}(0^-)$ [n]	5270.8 ± 3.0		$\bar{D}^0\pi^+$	(4.2 ± 4.2)%	2303
				$D^{*-}\pi^+\pi^+$	(4.8 ± 3.0)%	2243
				B^0 (or $\bar{B}^0$ → chg. conj.)		
$\mathbf{B^0}$ $\mathbf{\bar{B}^0}$	$\frac{1}{2}(0^-)$ [n]	5274.2 ± 2.8		$\bar{D}^0\pi^+\pi^-$	(13 ± 9)%	2298
				$D^{*-}\pi^+$	(2.6 ± 1.9)%	2253

$B^{\pm}$, B^0, $\overline{B}^0$ (not separated) [p]			$(14\pm4)\times10^{-13}$ $c\tau$=0.042	$e^{\pm}\nu$ hadrons	(13.0 ± 1.3	)%	
				$\mu^{\pm}\nu$ hadrons	(12.4 ± 3.5	)%	
				D^0 anything	(80 ±28	)%	
				K anything	(seen	)	
				p anything	(>3.6	)%	
				Λ anything	(>2.2	)%	
				e^+e^- anything	(<0.8	)%	
				$\mu^+\mu^-$ anything	(<0.7	)%	
NONSTRANGE BARYONS [a]							
p	$\frac{1}{2}(\frac{1}{2}^+)$	938.2796 ±0.0027	stable (>10^{32}y) [q]	stable			
				$\lvert q_p\rvert - \lvert q_e\rvert < 10^{-21}\lvert q_e\rvert$ [r]			
n	$\frac{1}{2}(\frac{1}{2}^+)$	939.5731 ±0.0027	898±16 $c\tau=2.7\times10^{13}$	$pe^-\overline{\nu}$	100%		1.2
				$p\nu\nu$ (chg.noncons.)	(<9	)$\times10^{-24}$	1.3
	$m_p-m_n=-1.293323$ ±0.000016			$\lvert q_n\rvert < 10^{-21}\lvert q_e\rvert$ [r]			
STRANGENESS −1 BARYONS [a]							
Λ	$0(\frac{1}{2}^+)$	1115.60 ±0.05 S=1.2*	2.632×10^{-10} ±0.020 S=1.6* $c\tau$ =7.89	$p\pi^-$	(64.2	)%	100
				$n\pi^0$	(35.8 ± 0.5	)%	104
				$pe^-\nu$	(8.37± 0.14	)$\times10^{-4}$	163
				$p\mu^-\nu$	(1.57± 0.35	)$\times10^{-4}$	131
	$m_\Lambda-m_{\Sigma^0}=-76.86$ ±0.08			† $[p\pi^-\gamma$	e(8.5 ± 1.4	)$\times10^{-4}]$	100

Stable Particle Table *(cont'd)*

Particle	$I^G(J^P)C$ [a]	Mass [b] (MeV)	Mean life [b] (sec) $c\tau$ (cm)	Partial decay mode: Mode	Fraction [b]	p or p_{max} [c] (MeV/c)
Σ^+	$1(\frac{1}{2}^+)$	1189.36 ±0.06 S=1.8*	0.800×10^{-10} ±0.004 $c\tau$=2.40	$p\pi^0$	(51.64)%	189
				$n\pi^+$	(48.36 ± 0.30)%	185
				$p\gamma$	(1.20 ± 0.13)$\times10^{-3}$ S=1.2*	225
				†[$n\pi^+\gamma$	[e] (4.5 ± 0.5)$\times10^{-4}$]	185
				$\Lambda e^+\nu$	(2.0 ± 0.5)$\times10^{-5}$	71
	$m_{\Sigma^+}-m_{\Sigma^-}$ = −7.97 ±0.07 S=1.3*		$\frac{\Gamma(\Sigma^+\to\ell^+n\nu)}{\Gamma(\Sigma^-\to\ell^-n\nu)}$ < .04	$n\mu^+\nu$	(<3.0)$\times10^{-5}$	202
				$ne^+\nu$	(<5)$\times10^{-6}$	224
				pe^+e^-	(<7)$\times10^{-6}$	225
Σ^0	$1(\frac{1}{2}^+)$ [s]	1192.46 ±0.08	5.8×10^{-20} ±1.3 $c\tau=1.7\times10^{-9}$	$\Lambda\gamma$	100%	74
				Λe^+e^-	[f] (5.45)$\times10^{-3}$	74
				$\Lambda\gamma\gamma$	(<3)%	74
Σ^-	$1(\frac{1}{2}^+)$	1197.34 ±0.05	1.482×10^{-10} ±0.011 S=1.3* $c\tau$=4.44	$n\pi^-$	100%	193
				$ne^-\nu$	(*1.022 ± 0.034*)$\times10^{-3}$	230
				$n\mu^-\nu$	(4.5 ± 0.4)$\times10^{-4}$	210
				$\Lambda e^-\nu$	(5.74 ± 0.27)$\times10^{-5}$	79
	$m_{\Sigma^0}-m_{\Sigma^-}$ = −4.88 ±0.06			†[$n\pi^-\gamma$	[e] (4.6 ± 0.6)$\times10^{-4}$]	193

STRANGENESS −2 BARYONS [a]

Ξ^0	$\frac{1}{2}(\frac{1}{2}^+)$ [s]	1314.9 ±0.6	2.90×10^{-10} ±0.10 $c\tau$=8.69	$\Lambda\pi^0$	100%			135
				$\Lambda\gamma$	(0.5 ± 0.5	)%		184
				$\Sigma^0\gamma$	(<7	)%		117
				$p\pi^-$	(<3.6	)$\times10^{-5}$		299
				$pe^-\nu$	(<1.3	)$\times10^{-3}$		323
	$m_{\Xi^0}-m_{\Xi^-}$	=−6.4 ±0.6		$\Sigma^+e^-\nu$	(<1.1	)$\times10^{-3}$		120
				$\Sigma^-e^+\nu$	(<0.9	)$\times10^{-3}$		112
				$\Sigma^+\mu^-\nu$	(<1.1	)$\times10^{-3}$		65
				$\Sigma^-\mu^+\nu$	(<0.9	)$\times10^{-3}$		49
				$p\mu^-\nu$	(<1.3	)$\times10^{-3}$		309
Ξ^-	$\frac{1}{2}(\frac{1}{2}^+)$ [s]	1321.32 ±0.13	1.641×10^{-10} ±0.016 $c\tau$=4.92	$\Lambda\pi^-$	100%			139
				$\Lambda e^-\nu$	(5.5 ± 0.6	)$\times10^{-4}$	S=2.0*	190
				$\Sigma^0e^-\nu$	(8.7 ± 1.7	)$\times10^{-5}$		123
				$\Lambda\mu^-\nu$	(3.5 ± 3.5	)$\times10^{-4}$		163
				$\Sigma^0\mu^-\nu$	(<8	)$\times10^{-4}$		70
				$n\pi^-$	(<1.9	)$\times10^{-5}$		303
				$ne^-\nu$	(<3.2	)$\times10^{-3}$		327
				$n\mu^-\nu$	(<1.5	)%		313
				$\Sigma^-\gamma$	(<1.2	)$\times10^{-3}$		118
				$p\pi^-\pi^-$	(<4	)$\times10^{-4}$		223
				$p\pi^-e^-\nu$	(<4	)$\times10^{-4}$		304
				$p\pi^-\mu^-\nu$	(<4	)$\times10^{-4}$		250
				$\Xi^0e^-\nu$	(<2.3	)$\times10^{-3}$		6

Stable Particle Table *(cont'd)*

Particle	$I^G(J^P)C$ [a]	Mass [b] (MeV)	Mean life [b] (sec) $c\tau$ (cm)	Partial decay mode: Mode	Fraction [b]	p or p_{max} [c] (MeV/c)
STRANGENESS −3 BARYON [a]						
Ω^-	$0(\frac{3}{2}^+)$ [s]	1672.45 ±0.32	0.819×10^{-10} ±0.027 $c\tau$=2.46	ΛK^-	(68.6 ± 1.3)%	211
				$\Xi^0\pi^-$	(23.4 ± 1.3)%	294
				$\Xi^-\pi^0$	(8.0 ± 0.8)%	290
				$\Xi^0 e^-\nu$	(~1)%	319
				$\Xi^0(1530)\pi^-$	(~2)$\times10^{-3}$	
				$\Lambda\pi^-$	(<1.3)$\times10^{-3}$	449
				$\Xi^-\gamma$	(<3.1)$\times10^{-3}$	314
NONSTRANGE CHARMED BARYON [a]						
Λ_c^+	$0(\frac{1}{2}^+)$ [s]	2282.0 ±3.1 S=1.8*	$(2.3^{+1.0}_{-0.6})\times10^{-13}$ $c\tau$=0.007	$pK^-\pi^+$	(2.2 ± 1.0)%	820
				$p\bar{K}^0$	(1.1 ± 0.7)%	870
				$p\bar{K}^0\pi^+\pi^-$	(<4, seen)%	751
				Λ anything	(33 ±29)%	
				†[$\Lambda\pi^+$	(0.6 ± 0.5)%	861
				$\Lambda\pi^+\pi^+\pi^-$	(< 3.1, seen)%	804
				$\Sigma^0\pi^+$	(seen)]	822

†[pK^{*0}	(0.48 ± 0.30)%	681
$\Delta^{++}K^-$	(0.45 ± 0.27)%	706
$pK^{*-}\pi^+$	(seen)]	575
e^+ anything	(4.5 ± 1.7)%	
†[pe^+ anything	(1.8 ± 0.9)%	
Λe^+ anything	(1.1 ± 0.8)%]	

→ A^+

→ Λ_b^0

→ top hadron searches
→ free quark searches
→ magnetic monopole searches
→ axion searches
→ other stable particle searches

ADDENDUM TO Stable Particle Table

Magnetic Moment

e^- $1.001\,159\,652\,209 \pm .000\,000\,000\,031$ $\frac{e\hbar}{2m_e c}$

μ^- $1.001\,165\,924 \pm .000\,000\,009$ $\frac{e\hbar}{2m_\mu c}$

μ Decay parameters [u]

$\rho = 0.752 \pm 0.003$ $\eta = -0.06 \pm 0.15$ S=1.1*

$\xi P_\mu > 0.9959$ [v] $\delta = 0.755 \pm 0.009$ $h = 1.01 \pm 0.06$

$\alpha' = -0.12 \pm 0.10$ $\beta' = -0.029 \pm 0.037$ $\overline{\eta} = 0.006 \pm 0.080$

$|g_A/g_V| = 0.91^{+0.24}_{-0.06}$ $\phi_{AV} = 180° \pm 9°$

$|g_S/g_V| < 0.29$ $|g_T/g_V| < 0.14$ $|g_P/g_V| < 0.25$

τ Michel parameter

$\rho = 0.72 \pm 0.15$

η

Mode	Left-right asymmetry	Sextant asymmetry	Quadrant asymmetry
$\pi^+\pi^-\pi^0$	$(0.12 \pm .17)\%$	$(0.19 \pm 0.16)\%$	$(-0.17 \pm 0.17)\%$
$\pi^+\pi^-\gamma$	$(0.88 \pm .40)\%$		

$\beta = 0.047 \pm 0.062$ S=1.5*

K

Slope parameters for $K \to 3\pi$ [w]

$K^+ \to \pi^+\pi^+\pi^-$	$g = -0.215 \pm .004$	S=1.4*
$K^- \to \pi^-\pi^-\pi^+$	$g = -0.217 \pm .007$	S=2.5*
$K^\pm \to \pi^0\pi^0\pi^\pm$	$g = 0.607 \pm .030$	S=1.3*
$K_L^0 \to \pi^+\pi^-\pi^0$	$g = 0.670 \pm .014$	S=1.6*

See Data Card Listings for quadratic coefficients.

$\Delta S = -\Delta Q$ in $K_{\ell 3}^0$ decay

Re x = $0.009 \pm .020$ S=1.4*

Im x = $-0.004 \pm .026$ S=1.1*

Form factors for $K_{\ell 3}$ decays [x]

K_{e3}^+: $\lambda_+ = 0.029 \pm 0.004$; $|f_S/f_+| = 0.125 \pm 0.044$; $|f_T/f_+| = 0.22 \pm 0.14$

K_{e3}^0: $\lambda_+ = 0.0300 \pm 0.0016$ S=1.2*; $|f_S/f_+| < 0.04$; $|f_T/f_+| < 0.23$

$K_{\mu 3}^+$: $\lambda_+ = 0.032 \pm 0.008$ S=2.3*; $\lambda_0 = 0.004 \pm 0.007$ S=2.3*; $|f_T/f_+| = 0.02 \pm 0.12$

$K_{\mu 3}^0$: $\lambda_+ = 0.034 \pm 0.005$ S=2.3*; $\lambda_0 = 0.025 \pm 0.006$ S=2.3*; $|f_T/f_+| = 0.12 \pm 0.12$

CP-violation parameters [y,i]

$|\eta_{+-}| = (2.274 \pm .022) \times 10^{-3}$ $|\eta_{00}| = (2.33 \pm .08) \times 10^{-3}$ S=1.1*

$\phi_{+-} = (44.6 \pm 1.2)°$ [f] $\phi_{00} = (54 \pm 5)°$ [f] Re $\epsilon = (1.621 \pm 0.088) \times 10^{-3}$

$|\eta_{+-0}|^2 < 0.12$ $|\eta_{000}|^2 < 0.1$ [f] $\delta = (0.330 \pm .012)\%$

	Magnetic moment ($e\hbar/2m_pc$)	Decay parameters[z]					Coupling Constant Ratios
			Measured		Derived		
			α	ϕ(degree)	γ	Δ(degree)	
p^l	2.7928456 ±.0000011						
n^l	−1.91304184 ±.00000088	$pe^-\nu$					$g_A/g_V=-1.254\pm0.006$ $\phi_{AV}=(180.11\pm0.17)^\circ$
Λ^l	−0.613 ±.004	$p\pi^-$ $n\pi^0$ $pe\nu$	0.642 ± 0.013 0.646 ± 0.044	(−6.5 ± 3.5)°	0.76	(7.7 ± 4.1)°	$g_A/g_V=-0.694\pm0.025$ S=1.3*
Σ^+	2.379 ±.020	$p\pi^0$ $n\pi^+$ $p\gamma$	−0.979 ± 0.016 +0.068 ± 0.013 −0.72 ± 0.29	(36 ± 34)° (167 ± 20)° S=1.1*	0.17 −0.97	(187 ± 6)° $(-73^{+134}_{-10})^\circ$	
Σ^-	*−1.10* *±.05* S=1.5*	$n\pi^-$ $ne^-\nu$ $\Lambda e^-\nu$	−0.068 ± 0.008	(10 ± 15)°	0.98	$(249^{+12}_{-116})^\circ$	$\lvert g_A/g_V\rvert=0.372\pm0.050$ S=1.9* $g_V/g_A=0.01\pm0.10$ S=1.5* $g_{WM}/g_A=2.4\pm1.7$
Ξ^0	−1.250 ±.014	$\Lambda\pi^0$	−0.413 ± 0.022 S=2.0*	(21 ± 12)°	0.85	$(218^{+12}_{-18})^\circ$	
Ξ^-	−1.85 ±.75	$\Lambda\pi^-$ $\Lambda e^-\nu$	−0.434 ± 0.015 S=1.4*	(2 ± 6)° S=1.1*	0.90	(184 ± 12)°	$g_A/g_V=-0.25\pm0.05$
Ω^-		ΛK^-	−0.10 ± 0.38 S=1.2*				

Stable Particle Table *(cont'd)*

→ Indicates an entry in the Stable Particle Data Card Listings not entered in the Stable Particle Table.

* S = Scale factor = $\sqrt{\chi^2/(N-1)}$, where N ≈ number of experiments. S should be ≈1. If S > 1, we have enlarged the error of the mean, $\delta\bar{x}$; i.e., $\delta\bar{x} \to S\delta\bar{x}$. This convention is still inadequate, since if S >> 1 the experiments are probably inconsistent, and therefore the real uncertainty is probably even greater than $S\delta x$. See the Introduction, and ideograms in Stable Particle Data Card Listings.

† Square brackets indicate subreactions of some previous unbracketed decay mode(s). Reactions in one set of brackets may overlap with reactions in another set of brackets. A radiative mode such as $\pi \to \mu\nu\gamma$ is a subreaction of its parent mode $\pi \to \mu\nu$.

a. The strangeness *S*, charm *C*, and bottomness (beauty) *B* of the hadrons which appear in the Table are as follows:

Mesons	*S*	*C*	*B*	Mesons	*S*	*C*	*B*	Baryons	*S*	*C*	*B*
π,η	0	0	0	F^+	+1	+1	0	p,n	0	0	0
K^+,K^0	+1	0	0	F^-	−1	−1	0	Λ,Σ	−1	0	0
$K^-,\overline{K}^0$	−1	0	0	B^+, B^0	0	0	+1	Ξ	−2	0	0
D^+,D^0	0	+1	0	$B^-, \overline{B}^0$	0	0	−1	Ω^-	−3	0	0
$D^-,\overline{D}^0$	0	−1	0					Λ_c^+	0	+1	0

b. Quoted upper limits correspond to a 90% confidence level. Masses, mean lives, and partial rates evaluated assuming equality for particles and antiparticles. See Conservation Laws Section for further details.

c. In decays with more than two bodies, p_{max} is the maximum momentum that any particle can have.

d. 99% confidence level. See footnote in Stable Particle Data Card Listings.

e. See Stable Particle Data Card Listings for energy limits used in this measurement.

f. Theoretical value; see also Stable Particle Data Card Listings.

g. The direct emission branching fraction is $(1.56 \pm .35) \times 10^{-5}$.

h. Structure-dependent part with positive (SD+) and negative (SD−) photon helicity.

i. The $K_S^0 \to \pi\pi$ and $K_L^0 \to \pi\pi$ branching fractions are from our branching fraction and rate fits and do not include results of $K_L^0 - K_S^0$ interference experiments. The $\pi\pi$ rate results are combined with the interference results to obtain the $|\eta_{+-}|$ and $|\eta_{00}|$ values given in the addendum.

j. The stronger limit $<2\times10^{-9}$ of Clark et al., Phys. Rev. Lett. 26, 1667 (1971) is not listed because of possible (but unknown) systematic errors. See Stable Particle Data Card Listings.

k. This is a weighted average of $D^\pm$ (44%) and D^0 (56%) branching fractions.

ℓ. $D_1^0 - D_2^0$ limits inferred from limit on $D^0 \to \overline{D}^0 \to \mu^-$ anything.

m. F mass determined from $\phi\pi$ mode. See note on conflicting F meson results in Stable Particle Data Card Listings. Quantum numbers shown are favored but not yet established.

n. Quantum numbers not measured. Values shown are quark model predictions.

p. Except for the neutral-current decay modes ($\ell^+\ell^-$ anything), only data from Υ(10575) decays are used. Behrends et al. [Phys. Rev. Lett. 50, 881 (1983)] estimate the Υ(10575) $\to B^+B^-$ and Υ(10575) $\to B^0\overline{B}^0$ branching fractions to be 60 ± 2 and $40 \pm 2\%$.

q. Partial mean life for $p \to e^+\pi^0$ mode. For antiprotons the best mean life limit, inferred from observation of cosmic ray $\overline{p}$'s, is $\tau_{\overline{p}} > 10^7$ yrs, the cosmic ray storage time.

r. Limit from neutrality-of-matter experiments. Assumes $|q_n| = |q_p| - |q_e|$.

s. P for Ξ, J^P for Ω^- and Σ^0, and J for Λ_c^+ not yet measured. Values shown are quark model predictions.

t. For limits on electric dipole moment, see Conservation Laws Section. Forbidden by P and T invariance.

u. $|g_A/g_V|$ defined by $g_A^2 = |C_A|^2 + |C_A'|^2$, $g_V^2 = |C_V|^2 + |C_V'|^2$, and $\Sigma[\overline{e}\Gamma_i\mu][\overline{\nu}\Gamma_i(C_i + C_i'\gamma_5)\nu]$; ϕ defined by $\cos\phi = -\mathrm{Re}(C_A^* C_V' + C_A' C_V^*)/g_A g_V$. For more details, see Data Card Listings.

v. Value assumes $\rho = \delta$. P_μ is muon longitudinal polarization from π decay. In standard V-A theory, $P_\mu = 1$ and $\rho = \delta = 3/4$.

w. The definition of the slope parameter of the Dalitz plot is as follows [see also note in Data Card Listings]: $|M|^2 = 1 + g\left(\dfrac{s_3 - s_0}{m_{\pi^+}^2}\right)$

x. For definitions of form factors f_+, f_S, and f_T, and linear t dependences λ_+ and λ_0 of $f_+(t)$ and $f_0(t)$, see note in K^+ section of Data Card Listings.

y. The definition for the CP violation parameters is as follows [see also note in Data Card Listings]:

$$\eta_{+-} = |\eta_{+-}|e^{i\phi_{+-}} = \frac{A(K_L^0 \to \pi^+\pi^-)}{A(K_S^0 \to \pi^+\pi^-)} \qquad \eta_{00} = |\eta_{00}|e^{i\phi_{00}} = \frac{A(K_L^0 \to \pi^0\pi^0)}{A(K_S^0 \to \pi^0\pi^0)}$$

$$\delta = \frac{\Gamma(K_L^0 \to \ell^+) - \Gamma(K_L^0 \to \ell^-)}{\Gamma(K_L^0 \to \ell^+) + \Gamma(K_L^0 \to \ell^-)}, \quad |\eta_{+-0}|^2 = \frac{\Gamma(K_S^0 \to \pi^+\pi^-\pi^0)_{\text{CP viol.}}}{\Gamma(K_L^0 \to \pi^+\pi^-\pi^0)}, \quad |\eta_{000}|^2 = \frac{\Gamma(K_S^0 \to \pi^0\pi^0\pi^0)_{\text{CP viol.}}}{\Gamma(K_L^0 \to \pi^0\pi^0\pi^0)}.$$

z. The definition of these quantities is as follows [for more details and sign convention, see note in Data Card Listings]:

$$\alpha = \frac{2|s||p|\cos\Delta}{|s|^2 + |p|^2} \qquad \beta = \sqrt{1-\alpha^2}\sin\phi \qquad g_A, g_V, g_{WM} \text{ defined by } \langle B_f|\gamma_\lambda(g_V - g_A\gamma_5) + (g_{WM}/m_{B_i})\sigma^{\lambda\nu}q_\nu|B_i\rangle$$

$$\beta = \frac{-2|s||p|\sin\Delta}{|s|^2 + |p|^2} \qquad \gamma = \sqrt{1-\alpha^2}\cos\phi \qquad \phi_{AV} \text{ defined by } g_A/g_V = |g_A/g_V|e^{i\phi_{AV}}$$

Meson Table

April 1984

In addition to the entries in the Meson Table, the Meson Data Card Listings contain all substantial claims for meson resonances. See Contents of Meson Data Card Listings at end of this Table.

Quantities in italics are new or have changed by more than one (old) standard deviation since April 1982.

J^P \ G		0	1	$\frac{1}{2}$
N	+	ϵ/f	ρ	K^*,κ
	−	ω/ϕ	δ	
A	+	η/D	B	K,Q
	−	H	π/A	

$I^G(J^P)C_n$

—— estab.

Mass M (MeV)	Full Width Γ (MeV)	Partial decay mode: Mode	Fraction(%) [Upper limits (%) are 90% CL]	p or p_{max} [b] (MeV/c)
NONSTRANGE MESONS				
$\pi^\pm$ $I^-(0^-)+$ 139.57	0.0	See Stable Particle Table		
π^0 134.96	7.95 eV ±0.55 eV			
η $0^+(0^-)+$ 548.8 ±0.6	0.83 keV ±0.12 keV	Neutral	70.9	See Stable
		Charged	29.1	Particle Table

$\rho(770)$	$1^+(1^-)-$	$769^{\ddagger}$ $\pm 3^{\S}$	$154^{\ddagger}$ $\pm 5^{\S}$	$\pi\pi$	≈ 100	358
				$\pi\gamma$	0.046 ± 0.005	372
				$\mu^+\mu^-$	0.0067 ± 0.0012^d	370
				e^+e^-	0.0046 ± 0.0002^d	384
				$\eta\gamma$	seen‡	189
M and Γ from neutral mode.				For upper limits, see footnote *e*		
$\omega(783)$	$0^-(1^-)-$	782.6 ± 0.2 S=1.1*	9.9 ± 0.3	$\pi^+\pi^-\pi^0$	89.9 ± 0.5	327
				$\pi^0\gamma$	8.7 ± 0.5	380
				$\pi^+\pi^-$	1.4 ± 0.2	366
				$\pi^0\mu^+\mu^-$	0.010 ± 0.002	349
				e^+e^-	0.0067 ± 0.0004 S=1.2*	391
				$\eta\gamma$	seen‡	199
				For upper limits, see footnote *f*		
$\eta'(958)$	$0^+(0^-)+^{\ddagger}$	957.57 ± 0.25	0.29 ± 0.05	$\eta\pi\pi$	65.3 ± 1.6	231
				$\rho^0\gamma$	30.0 ± 1.6	170
				$\omega\gamma$	2.8 ± 0.5	159
				$\gamma\gamma$	1.9 ± 0.2	479
				$\mu^+\mu^-\gamma$	0.009 ± 0.002	467
				For upper limits, see footnote *g*		
S(975) or S*	$0^+(0^+)+$	975^c ± 4 S=1.4*	33^c ± 6	$\pi\pi$	78 ± 3	467
				$K\bar{K}$	22 ± 3	
See note on $\pi\pi$ and $K\bar{K}$ S wave.‡						
$\delta(980)^{\ddagger}$	$1^-(0^+)+$	983^h ± 2	54^h ± 7	$\eta\pi$	seen	320
				$K\bar{K}$	seen	

Meson Table *(cont'd)*

J^P	G \ I	0	1	$\frac{1}{2}$
N	+	ϵ/f	ρ	K^*,κ
	−	ω/ϕ	δ	
A	+	η/D	B	K,Q
	−	H	π/A	

	$I^G(J^P)C_n$ ____ *estab.*	Mass M (MeV)	Full Width Γ (MeV)	Partial decay mode: Mode	Fraction(%) [Upper limits (%) are 90% CL]		p or p_{max} [b] (MeV/c)
$\phi(1020)$	$0^-(1^-)-$	*1019.5* ±*0.1* S=1.2*	4.22 ±0.13	K^+K^-	49.3 ± 1.0	S=1.3*	127
				$K_L K_S$	34.7 ± 1.0	S=1.3*	110
				$\pi^+\pi^-\pi^0$ (incl. $\rho\pi$)	14.8 ± 0.7	S=1.2*	462
				$\eta\gamma$	*1.2 ± 0.2*	S=1.4*	362
				$\pi^0\gamma$	0.14 ± 0.05		501
				e^+e^-	0.031 ± 0.001		510
				$\mu^+\mu^-$	0.025 ± 0.003		499
				$\pi^+\pi^-$	0.02 ± 0.01		490
				For upper limits, see footnote *i*			
H(1190)	$0^-(1^+)-$	1190 ±60	320 ±50	$\rho\pi$	seen		327
Seen in one experiment only.							
B(1235)	$1^+(1^+)-$	1234 ±10[§]	*150* ±*10*[§]	$\omega\pi$	only mode seen		350
				[D/S amplitude ratio = 0.29 ± 0.05]			
				For upper limits, see footnote *j*			
f(1270)	$0^+(2^+)+$	1274 ±5[§]	178 ±20[§]	$\pi\pi$	84.3 ± 1.2		622
				$2\pi^+2\pi^-$	2.9 ± 0.4	S=1.2*	559
				$K\bar{K}$	2.9 ± 0.2		398
				$\gamma\gamma$	0.0015 ± 0.0002		637

				$\pi^+\pi^-2\pi^0$	seen	562
				For upper limits, see footnote *k*		
A(1270) or A_1	$1^-(1^+)\pm$	$1275^{\ddagger}$ ± 30	$315^{\ddagger}$ ± 45	$\rho\pi$	dominant	389
				$\pi(\pi\pi)_{S-wave}$	$< 0.7^{\S}$	599
D(1285)	$0^+(1^+)\pm$	1283 $\pm 5^{\S}$	26 $\pm 5^{\S}$	$K\bar{K}\pi$	11 ± 3	302
				$\eta\pi\pi$	49 ± 6	482
				†[$\delta\pi$	36 ± 7]	236
				4π (prob. $\rho\pi\pi$)‡	40 ± 7	564
$\epsilon(1300)$	$0^+(0^+)\pm$	~1300	200−600	$\pi\pi$	~90	635
				$K\bar{K}$	~10	418
				$\eta\eta$	*possibly seen*	348
See note on $\pi\pi$ and $K\bar{K}$ S wave.‡						
$\pi(1300)$	$1^-(0^-)\pm$	$1300^{\S}$ $\pm 100^{\S}$	200−600	$\rho\pi$	seen	407
				$\pi(\pi\pi)_{S-wave}$	seen	612
Not a well-established resonance.						
$A_2(1320)$	$1^-(2^+)\pm$	1318 $\pm 5^{\S}$	110 $\pm 5^{\S}$	$\rho\pi$	70.1 ± 2.2	419
				$\eta\pi$	14.5 ± 1.2	534
				$\omega\pi\pi$	10.6 ± 2.5	361
				$K\bar{K}$	4.9 ± 0.8	434
				$\eta'\pi$	< 2 (CL=97%)	286
				$\pi\gamma$	0.27 ± 0.06	652
				$\gamma\gamma$	0.0007 ± 0.0002	659
E(1420)‡	$0^+(1^+)\pm$	1418 $\pm 10^{\S}$	52 $\pm 10^{\S}$	$K\bar{K}\pi$ (incl. $K^*\bar{K}+K\bar{K}^*$)	seen	423
				$\eta\pi\pi$	possibly seen	565
				†[$\delta\pi$	possibly seen]	348

Meson Table *(cont'd)*

J^P \ G^C	0	1	$\frac{1}{2}$
N +	ϵ/f	ρ	K^*,κ
N −	ω/ϕ	δ	
A +	η/D	B	K,Q
A −	H	π/A	

$I^G(J^P)C_n$ — *estab.*	Mass M (MeV)	Full Width Γ (MeV)	Partial decay mode: Mode	Fraction(%) [Upper limits (%) are 90% CL]	p or p_{max} [b] (MeV/c)
$\iota(1440)^{\ddagger}$	*1440*[§]	*76*	$K\bar{K}\pi$ (incl. $K^*\bar{K}+K\bar{K}^*$)	*seen*	441
$0^+(0^-)+$	*±10*[§]	*±10*[§]	$\eta\pi\pi$	*seen*	579
			†[$\delta\pi$	*seen*]	366
f'(1525)	1525	70	$K\bar{K}$	dominant	578
$0^+(2^+)+$	±5[§]	±10[§]	$\pi\pi$	possibly seen	750
			$\gamma\gamma$	*0.0011 ± 0.0002*	763
$\rho(1600)$	1590[‡§]	260[‡§]	4π (incl. $\rho\pi^+\pi^-$, $A(1270)\pi$)	*60 ± 7*[§]	733
or ρ'	±20[§]	±100[§]	$\pi\pi$	*23 ± 7*[§]	783
$1^+(1^-)-$			$K^*\bar{K} + \bar{K}^*K$	*9 ± 2*	377
			$\eta\pi\pi$	*7 ± 2*	669
			$\bar{K}K$	*1 ± 0.5*	623
			e^+e^-	*0.003 ± 0.001*	795
$\omega(1670)$	1668	166	3π	seen	806
$0^-(3^-)-$	±5	±15[§]	†[$\rho\pi$	seen]	648
		S=1.1*	5π	seen	740
			†[$\omega\pi\pi$ (prob. $B\pi$)	seen]	616
$A(1680)^{\ddagger}$	1680[§]	250[§]	$f\pi$	53 ± 5	336
or A_3	±30[§]	±50[§]	$\rho\pi$	34 ± 6	656
$1^-(2^-)+$					

				$\pi(\pi\pi)_{S-wave}$	9 ± 5		813
				$K^*\bar{K} + \bar{K}^*K$	*4 ± 1.4*		459
				For upper limits, see footnote ℓ			
$\phi(1680)$ or ϕ'	$0^-(1^-)-$	1685 ±10[§]	*150* ±*30*[§]	$K^*\bar{K} + \bar{K}^*K$	dominant		466
				$\omega\pi\pi$	seen		624
				$K\bar{K}$	seen		683
				e^+e^-	*seen*		842
				$\pi^+\pi^-\pi^0$	*possibly seen*		814
g(1690)	$1^+(3^-)-$	1691 ±5[§]	200 ±20[§]	2π	23.8 ± 1.3		834
				4π (incl. $\pi\pi\rho,\rho\rho,A_2\pi,\omega\pi$)	70.9 ± 1.9		787
				$K\bar{K}\pi$ (incl. $K^*K+K\bar{K}^*$)	*3.8 ± 1.2*		625
				$K\bar{K}$	1.5 ± 0.3	S=1.3*	684
J^P, M, and Γ from the 2π and $K\bar{K}$ modes.							
$\theta(1690)$	$0^+(2^+)+$	*1690* ±*30*	*180* ±*50*	$\eta\eta$	*seen*		643
				$K\bar{K}$	*seen*		683
$\phi(1850)$	$0^-(3^-)-$	*1853* ±*10*	*96* ±*32*	$K\bar{K}$	*seen*		784
				$K^*\bar{K} + \bar{K}^*K$	*seen*		601
h(2030)	$0^+(4^+)+$	2027 ±12	*220* ±*30*	$\pi\pi$	*17 ± 2*		1004
				$K\bar{K}$	$0.7^{+0.4}_{-0.2}$		883
$\eta_c(2980)$	$0^+(0^-)+$	2981 ±6	< 20	$\eta\pi^+\pi^-$	seen		1426
				$2(\pi^+\pi^-)$	seen		1458
				$K^+K^-\pi^+\pi^-$	seen		1343
				$p\bar{p}$	seen		1158

Meson Table *(cont'd)*

J^P	G \ I	0	1	$\frac{1}{2}$
N	+	η/f	ρ	$K^*,\varkappa$
	−	ω/ϕ	δ	
A	+	η/D	B	K,Q
	−	H	π/A	

	$I^G(J^P)C_n$	Mass M	Full Width Γ	Partial decay mode		p or p_{max} [b]
	____ *estab.*	(MeV)	(MeV)	Mode	Fraction(%) [Upper limits (%) are 90% CL]	(MeV/c)
$J/\psi(3100)$	$0^-(1^-)-$	3096.9 ±0.1	0.063 ±0.009	e^+e^-	7.4 ± 1.2	1548
				$\mu^+\mu^-$	7.4 ± 1.2	1545
				hadrons + radiative	85 ± 2	

Decay modes into stable hadrons

†[$2(\pi^+\pi^-)\pi^0$	3.7 ± 0.5	1496
$3(\pi^+\pi^-)\pi^0$	2.9 ± 0.7	1433
$\pi^+\pi^-\pi^0K^+K^-$	1.2 ± 0.3	1368
$4(\pi^+\pi^-)\pi^0$	0.9 ± 0.3	1345
$\pi^+\pi^-K^+K^-$	0.72 ± 0.23	1407
$p\bar{p}\pi^+\pi^-$	0.53 ± 0.06	1107
$2(\pi^+\pi^-)$	0.4 ± 0.1	1517
$3(\pi^+\pi^-)$	0.4 ± 0.2	1466
$n\bar{n}\pi^+\pi^-$	0.38 ± 0.36	1106
$\Xi^-\bar{\Xi}$	0.32 ± 0.08	818
$2(\pi^+\pi^-)K^+K^-$	0.31 ± 0.13	1320
$K^0K^\pm\pi^\mp$	0.26 ± 0.07	1440
$\Sigma^+\bar{\Sigma}^-$	0.24 ± 0.26	988

Decay modes into hadronic resonances

†[$\rho\pi$	1.22 ± 0.12		1449
$\omega 2\pi^+2\pi^-$	0.85 ± 0.34		1392
ρA_2	0.84 ± 0.45		1126
$\omega\pi\pi$	0.68 ± 0.19		1435
$K^{*0}(892)\bar{K}^{*0}(1430)$+c.c.	0.67 ± 0.26		1009
$K^\pm K^{*\mp}(892)$	0.34 ± 0.05		1373
$B^\pm(1235)\pi^\mp$	0.29 ± 0.07		1298
$K^0\bar{K}^{*0}(892)$+c.c.	0.27 ± 0.06		1370
ωf	0.23 ± 0.08	S=1.2*	1143
$\phi\pi^+\pi^-$	0.21 ± 0.09		1365
$\eta' p\bar{p}$	0.18 ± 0.06		596
$\phi K\bar{K}$	0.18 ± 0.08		1176
$\omega p\bar{p}$	0.16 ± 0.03		768

$p\bar{p}\eta$	0.23 ± 0.04	948	$\omega K\bar{K}$	0.16 ± 0.10	1265
$p\bar{p}$	0.22 ± 0.02	1232	$\phi\eta$	0.10 ± 0.06	1320
$p\bar{n}\pi^-$ or $\bar{p}n\pi^+$	0.21 ± 0.02	1174	$\phi f'(1525)$	0.037 ± 0.013	871
$n\bar{n}$	0.18 ± 0.09	1231	$\phi S(975)$	*0.026 ± 0.006*	1184
$p\bar{p}\pi^+\pi^-\pi^0$	0.16 ± 0.06^m	1033	$\pi^\pm A_2^\mp$	< 0.43	1263
$\Sigma^0\bar{\Sigma}^0$	0.13 ± 0.04	988	$K^{*0}(1430)\bar{K}^{*0}(1430)$	< 0.29	606
$\Lambda\bar{\Lambda}$	0.11 ± 0.02	1074	$K^0\bar{K}^{*0}(1430)+$c.c.	< 0.2	1158
$p\bar{p}\pi^0$	0.11 ± 0.01	1176	$K^\pm K^{*\mp}(1430)$	< 0.2	1159
$2(K^+K^-)$	0.07 ± 0.03	1131	$\phi 2\pi^+ 2\pi^-$	< 0.15	1318
K^+K^-	0.022 ± 0.008	1468	$\phi\eta'$	< 0.13	1192
$\pi^+\pi^-$	0.011 ± 0.005	1542	$K^{*0}(892)\bar{K}^{*0}(892)$	< 0.05	1261
$\Lambda\bar{\Sigma}$	< 0.015	1032	ϕf	< 0.037	1037
$K_S^0K_L^0$	$< 0.009]$	1466	$\omega f'(1525)$	$< 0.016]$	1003

Radiative decay modes

†$[\gamma 2(\pi^+\pi^-)$	*0.49 ± 0.17*	1517
$\gamma\rho\rho$	*seen*	1344
$\gamma\iota(1440) \to \gamma K\bar{K}\pi$	0.42 ± 0.12^n	1214
$\gamma\eta'$	0.36 ± 0.05	1400
γf	0.15 ± 0.04	1286
$\gamma\eta$	0.086 ± 0.009	1500
$\gamma\pi^0$	0.007 ± 0.005	1546

Radiative decay modes (cont'd)

$\gamma\eta_c(2980)$	*seen*	114
$\gamma\theta(1690)$	*seen*	1087
$\gamma\eta\pi\pi$	*seen*	1487
$\gamma D(1285)$	< 0.6	1283
2γ	< 0.05	1548
$\gamma f'(1525)$	< 0.03	1173
$\gamma p\bar{p}$	< 0.01	1232
3γ	$< 0.006]$	1548

Meson Table *(cont'd)*

J^P \ G^N	0	1	$\frac{1}{2}$
N +	ϵ/f	ρ	K^*,κ
N −	ω/ϕ	δ	
A +	η/D	B	K,Q
A −	H	π/A	

$I^G(J^P)C_n$ ___ *estab.*	Mass M (MeV)	Full Width Γ (MeV)	Partial decay mode: Mode	Fraction(%) [Upper limits (%) are 90% CL]	p or p_{max} [b] (MeV/c)
$\chi(3415)$ $0^+(0^+)+$	3415.0 ±1.0		$2(\pi^+\pi^-)$ (incl. $\pi\pi\rho$)	4.3 ± 0.9	1679
			$\pi^+\pi^-K^+K^-$ (incl. $\pi K\bar{K}^*$)	3.4 ± 0.9	1580
			$3(\pi^+\pi^-)$	1.7 ± 0.6	1633
			$\pi^+\pi^-$	0.9 ± 0.2	1702
			$\gamma J/\psi(3100)$	0.8 ± 0.3	303
			K^+K^-	0.8 ± 0.2	1635
			$p\bar{p}\pi^+\pi^-$	0.6 ± 0.2	1320
			For upper limits, see footnote *o*		
$\chi(3510)$ $0^+(1^+)+$	3510.0 ±0.6		$\gamma J/\psi(3100)$	28 ± 3	389
			$3(\pi^+\pi^-)$	2.4 ± 0.9	1683
			$2(\pi^+\pi^-)$ (incl. $\pi\pi\rho$)	1.8 ± 0.5	1727
			$\pi^+\pi^-K^+K^-$ (incl. $\pi K\bar{K}^*$)	1.0 ± 0.4	1632
			$\pi^+\pi^-p\bar{p}$	0.15 ± 0.10	1381
			For upper limits, see footnote *p*		
$\chi(3555)$ $0^+(2^+)+$	3555.8 ±0.6		$\gamma J/\psi(3100)$	15.5 ± 1.8	429
			$2(\pi^+\pi^-)$ (incl. $\pi\pi\rho$)	2.3 ± 0.5	1750
			$\pi^+\pi^-K^+K^-$ (incl. $\pi K\bar{K}^*$)	2.0 ± 0.5	1656
			$3(\pi^+\pi^-)$	1.2 ± 0.8	1706
			$\pi^+\pi^-p\bar{p}$	0.35 ± 0.14	1410

				$\pi^+\pi^-$	0.20 ± 0.11	1772
				K^+K^-	0.16 ± 0.12	1708
				For upper limits, see footnote *q*		
$\psi(3685)$	$0^-(1^-)-$	3686.0 ±0.1	0.215 ±0.040	e^+e^-	0.9 ± 0.1	1843
				$\mu^+\mu^-$	0.8 ± 0.2	1840
				hadrons + radiative	98.1 ± 0.3	
	$m_{\psi(3685)} - m_{\psi(3100)} = 589.06 \pm 0.13$					
	Radiative decay modes			Decay modes into hadrons		
†[	$\gamma\chi(3415)$	8.2 ± 1.4	261	†[$J/\psi\pi^+\pi^-$	33 ± 2	477
	$\gamma\chi(3510)$	8.0 ± 1.3	172		$J/\psi\pi^0\pi^0$	17 ± 2	481
	$\gamma\chi(3555)$	7.4 ± 1.3	128		$J/\psi\eta$	2.8 ± 0.6[§]	196
	$\gamma\eta_c(2980)$	0.43 ± 0.26	638		$2(\pi^+\pi^-)\pi^0$	0.35 ± 0.15	1799
	$\gamma\eta'(3590)$	0.2 to 1.3	91		$\pi^+\pi^-K^+K^-$	0.16 ± 0.04	1726
	$\gamma\pi^0$	< 0.5 (CL=95%)	1841		$J/\psi\pi^0$	0.10 ± 0.03	528
	$\gamma\eta$	< 0.02	1802		$p\bar{p}\pi^+\pi^-$	0.08 ± 0.02	1491
	$\gamma\eta'$	< 0.02	1719		$K^{*0}(892)K^-\pi^+ + cc.$	0.067 ± 0.025	1674
	$\gamma\iota(1440) \to \gamma K\bar{K}\pi$	$< 0.012^n$]	1562		$2(\pi^+\pi^-)$	0.05 ± 0.01	1817
					$\rho^0\pi^+\pi^-$	0.042 ± 0.015	1751
					$p\bar{p}$	0.019 ± 0.005	1586
					$3(\pi^+\pi^-)$	0.015 ± 0.010	1774
					K^+K^-	0.010 ± 0.007	1776
					$\pi^+\pi^-$	0.008 ± 0.005	1838
					$\rho\pi$	< 0.1	1760
					$\Lambda\bar{\Lambda}$	< 0.04]	1467

Meson Table *(cont'd)*

J^P \ G	0	1	$\frac{1}{2}$
N +	ϵ/f	ρ	K^*_χ
N −	ω/ϕ	δ	
A +	η/D	B	K,Q
A −	H	π/A	

$I^G(J^P)C_n$ ___ *estab.*	Mass M (MeV)	Full Width Γ (MeV)	Mode	Partial decay mode: Fraction(%) [Upper limits (%) are 90% CL]	p or p_{max} [b] (MeV/c)
$\psi(3770)$ (1⁻)−	3770 ±3	25 ±3	e^+e^-	0.0011 ±0.0002	1885
			$D\bar{D}$	dominant	242
	$m_{\psi(3770)} - m_{\psi(3685)} = 83.9 \pm 2.4$ S=1.8*				
$\psi(4030)$ (1⁻)−	4030[§] ±5[§]	52 ±10	e^+e^-	0.0014 ±0.0004	2015
			hadrons	dominant	
			$D\bar{D}$	*seen*	752
			$D\bar{D}^* + D^*\bar{D}$	*seen*	559
			$D^*\bar{D}^*$	*seen*	177
$\psi(4160)$ (1⁻)−	4159 ±20	78 ±20	e^+e^-	0.0010 ±0.0004	2079
			hadrons	dominant	
$\psi(4415)$ (1⁻)−	4415 ±6	43 ±20[§]	e^+e^-	0.0010 ±0.0003 S=1.4*	2207
			hadrons	dominant	
$\Upsilon(9460)$ (1⁻)−	9460.0 ±0.3	0.0443 ±0.0066	$\mu^+\mu^-$	2.9 ±0.5	4729
or $\Upsilon(1S)$	S=1.6*		e^+e^-	2.5 ±0.5	4730
			$\tau^+\tau^-$	*3.4 ±0.8*	4381
$\chi_b(9875)$ ( )+	*9872.9*		$\gamma\Upsilon(9460)$	*seen*	404
or $\chi_b(1\,^3P_0)^r$	*±5.8*				

$\chi_b(9895)$ or $\chi_b(1\,^3P_1)'$	( )+	*9894.5 ±3.5*		$\gamma\Upsilon(9460)$	*43 ± 11*	425
$\chi_b(9915)$ or $\chi_b(1\,^3P_2)'$	( )+	*9914.6 ±2.4*		$\gamma\Upsilon(9460)$	*20.0 ± 4.4*	444
$\Upsilon(10025)$ or $\Upsilon(2S)$	$(1^-)=$	10023.4 ±0.3	0.0296 ±0.0047	$\mu^+\mu^-$	*1.9 ± 1.8*	5011
				e^+e^-	1.6 ± 0.3	5012
				$\Upsilon(9460)\pi\pi$	*19.5 ± 1.7*	476
	$m_{\Upsilon(10025)} - m_{\Upsilon(9460)} = 563.3 \pm 0.4$			$\gamma\chi_b(9875)$	*3.5 ± 1.4*	149
				$\gamma\chi_b(9895)$	*5.9 ± 1.4*	128
				$\gamma\chi_b(9915)$	*6.1 ± 1.4*	108
$\chi_b(10255)$ or $\chi_b(2\,^3P_1)'$	( )+	*10253.7 ±3.4*		$\gamma\Upsilon(9460)$	*seen*	763
				$\gamma\Upsilon(10025)$	*seen*	228
$\chi_b(10270)$ or $\chi_b(2\,^3P_2)'$	( )+	*10271.0 ±2.4*		$\gamma\Upsilon(9460)$	*seen*	779
				$\gamma\Upsilon(10025)$	*seen*	245
$\Upsilon(10355)$ or $\Upsilon(3S)$	$(1^-)=$	10355.5 ±0.5	*0.0177 ±0.0051*	e^+e^-	*2.0 ± 0.7*	5178
				$\mu^+\mu^-$	*3.3 ± 2.0*	5177
				$\Upsilon(9460)\pi^+\pi^-$	*5.1 ± 1.1*	814
	$m_{\Upsilon(10355)} - m_{\Upsilon(9460)} = 895.5 \pm .6$			$\Upsilon(10025)\pi^+\pi^-$	*3 ± 3*	177
				$\gamma\chi_b(10235)$	*7.6 ± 3.5*	122
				$\gamma\chi_b(10255)$	*15.6 ± 4.2*	101
				$\gamma\chi_b(10270)$	*12.7 ± 4.1*	84
$\Upsilon(10575)$ or $\Upsilon(4S)$	$(1^-)=$	10573 ±4	14 ±5	e^+e^-	0.0017 ± 0.0007	5286
	$m_{\Upsilon(10575)} - m_{\Upsilon(9460)} = 1113 \pm 4$					

Meson Table *(cont'd)*

J^P	G \ I	0	1	$\frac{1}{2}$
N	+	ϵ/f	ρ	K^*,κ
	−	ω/ϕ	δ	
A	+	η/D	B	K,Q
	−	H	π/A	

$I^G(J^P)C_n$ ——— *estab.*

Mass M (MeV)	Full Width Γ (MeV)	Partial decay mode: Mode	Fraction(%) [Upper limits (%) are 90% CL]	p or p_{max} [b] (MeV/c)

STRANGE MESONS

K^+	$1/2(0^-)$	493.67		See Stable Particle Table		
K^0		497.67				
$K^*(892)$	$1/2(1^-)$	892.1	51.3	$K\pi$	≈ 100	288
		±0.4	±1.0	$K\gamma$	0.10 ± 0.01	309
		S=1.4*	S=1.1*	$K\pi\pi$	< 0.05	216
M and Γ from charged mode; $m^0 - m^\pm = 6.7 \pm 1.2$ MeV.						
$Q(1280)$	$1/2(1^+)$	$1270^{\S}$	$90^{\S}$	$K\rho$	42 ± 6	45
or Q_1		$\pm 10^{\S}$	$\pm 20^{\S}$	$\kappa(1350)\pi$	28 ± 4	
				$K^*(892)\pi$	16 ± 5	298
				$K\omega$	11 ± 2	
				$K\epsilon$	3 ± 2	
$\kappa(1350)$	$1/2(0^+)$	~1350	~250	$K\pi$	seen	574
See note on $K\pi$ S wave.[‡]						
$Q(1400)$	$1/2(1^+)$	1406	184	$K^*(892)\pi$	94 ± 6	403
or Q_2		±10	±9	$K\rho$	3 ± 3	299
				$K\epsilon$	2 ± 2	
				$K\omega$	1 ± 1	285

K*(1430)	1/2(2$^+$)	1425[§] ±5[§]	100[§] ±10[§]	Kπ	44.8 ± 2.3	S=2.7*	618
				K*(892)π	24.5 ± 2.0	S=1.1*	417
				K*(892)ππ	13.0 ± 2.6	S=1.1*	366
				Kρ	8.8 ± 1.0	S=1.2*	324
				Kω	4.2 ± 1.5		310
				Kη	5 ± 5[§]		485
				Kγ	*0.24 ± 0.05*		627
L(1770)[‡]	1/2(2$^-$)	~1770[§]	~200[§]	K*(1430)π	dominant		286
				K*(892)π	seen		651
				Kf	seen		
				Kφ	*seen*		816
See note on L(1770).[‡]							
K*(1780)[‡] or K*	1/2(3$^-$)	1780 ±10[§]	160 ±20[§]	Kππ	large		796
				†Kρ	large		620
				†K*(892)π	large		657
				Kπ	17 ± 5[§]		815
See note on K*(1780).[‡]							
K*(2060)	1/2(4$^+$)	*2060*[§] *±30*[§]	*210*[§] *±40*[§]	Kπ	*7 ± 1*		966
				K*(892)ππ	*seen*		809
				ρKπ	*seen*		751
				ωKπ	*seen*		744
Not a well-established resonance.				K*(892)πππ	*seen*		775

Meson Table *(cont'd)*

J^P	G \ I	0	1	$\frac{1}{2}$
N	+	ϵ/f	ρ	K^*,κ
	−	ω/ϕ	δ	
A	+	η/D	B	K,Q
	−	H	π/A	

$I^G(J^P)C_n$ ____ *estab.*

Mode	Fraction(%) [Upper limits (%) are 90% CL]	p or p_{max} [b] (MeV/c)
CHARMED, NONSTRANGE MESONS		
D^+ $1/2(0^-)$ 1869.4	See Stable Particle Table	
D^0 1864.7		
$D^{*+}(2010)$ $1/2(1^-)$ 2010.1 ±0.7 — < 2.0	$D^0\pi^+$	64 ± 11 39
	$D^+\pi^0$	28 ± 9 38
	$D^+\gamma$	8 ± 7 136
$m_{D^{*+}} - m_{D^0} = 145.4 \pm 0.2$ MeV		
$D^{*0}(2010)$ $1/2(1^-)$ 2007.2 ±2.1 — < 5	$D^0\pi^0$	55 ± 15 44
	$D^0\gamma$	45 ± 15 137
CHARMED, STRANGE MESON		
F^+ $0(0^-)$ 1971	See Stable Particle Table	
BOTTOM, NONSTRANGE MESON		
B^+ $1/2(0^-)$ 5271	See Stable Particle Table	
B^0 5274		

→ Indicates an entry in the Meson Data Card Listings not entered in the Meson Table. We do not regard these as established resonances. All the entries in the Listings can be found in the Table of Contents of the Meson Data Card Listings immediately following these footnotes.

‡ See Meson Data Card Listings.

* Quoted error includes scale factor $S = \sqrt{\chi^2/(N-1)}$. See footnote to Stable Particle Table.

† Square brackets indicate a subreaction of the previous (unbracketed) decay mode(s).

§ This is only an educated guess; the error given is larger than the error on the average of the published values. (See the Meson Data Card Listings for the latter.)

a. ΓM is approximately the half-width of the resonance when plotted against M^2.

b. For decay modes into ≥ 3 particles, p_{max} is the maximum momentum that any of the particles in the final state can have. The momenta have been calculated by using the averaged central mass values, without taking into account the widths of the resonances.

c. From pole position ($M - i\Gamma/2$).

d. The e^+e^- branching fraction is from $e^+e^- \to \pi^+\pi^-$ experiments only. The $\omega\rho$ interference is then due to $\omega\rho$ mixing only, and is expected to be small. See note in the Meson Data Card Listings. The $\mu^+\mu^-$ branching fraction is compiled from 3 experiments, each possibly with substantial $\omega\rho$ interference. The error reflects this uncertainty; see notes in the Meson Data Card Listings. If $e\mu$ universality holds, $\Gamma(\rho^0 \to \mu^+\mu^-) = \Gamma(\rho^0 \to e^+e^-) \times 0.99785$.

e. Empirical limits on fractions for other decay modes of $\rho(770)$ are $\pi^\pm\eta < 0.8\%$ (CL=84%), $\pi^+\pi^+\pi^-\pi^- < 0.15\%$, $\pi^\pm\pi^+\pi^-\pi^0 < 0.2\%$ (CL=84%).

f. Empirical limits on fractions for other decay modes of $\omega(783)$ are $\pi^+\pi^-\gamma < 5\%$, $\pi^0\pi^0\gamma < 1\%$, η + neutral(s) < 1.5%, $\mu^+\mu^- < 0.02\%$.

g. Empirical limits on fractions for other decay modes of $\eta'(958)$ are $\pi^+\pi^- < 2\%$ (CL=84%), $\pi^+\pi^-\pi^0 < 5\%$ (CL=84%), $\pi^+\pi^+\pi^-\pi^- < 1\%$ (CL=95%), $\pi^+\pi^+\pi^-\pi^-\pi^0 < 1\%$ (CL=84%), $6\pi < 1\%$, $\pi^+\pi^-e^+e^- < 0.6\%$, $\pi^0e^+e^- < 1.3\%$ (CL=84%), $\eta e^+e^- < 1.1\%$, $\pi^0\rho^0 < 4\%$, $\eta\mu^+\mu^- < 1.5 \times 10^{-5}$, $\pi^0\mu^+\mu^- < 6 \times 10^{-5}$.

h. The mass and width are from the $\eta\pi$ mode only. If the $K\bar{K}$ channel is strongly coupled, the width may be larger.

i. Empirical limits on fractions for other decay modes of $\phi(1020)$ are $\pi^+\pi^-\gamma < 0.7\%$, $\omega\gamma < 5\%$ (CL=84%), $\rho\gamma < 2\%$ (CL=84%), $2\pi^+2\pi^-\pi^0 < 1\%$ (CL=95%), $2\pi^+2\pi^- < 0.1\%$.

j. Empirical limits on fractions for other decay modes of B(1235) are $\pi\pi < 15\%$, $K\bar{K} < 2\%$ (CL=84%), $4\pi < 50\%$ (CL=84%), $\phi\pi < 1.5\%$ (CL=84%), $\eta\pi < 25\%$, $(\bar{K}K)^\pm\pi^0 < 8\%$, $K_SK_S\pi^\pm < 2\%$, $K_SK_L\pi^\pm < 6\%$.

k. Empirical limits (CL=95%) on fractions for other decay modes of f(1270) are $\eta\pi\pi < 1\%$, $K^0K^-\pi^+ + \text{c.c.} < 0.4\%$, $\eta\eta < 2\%$.

ℓ. Empirical limits on fractions for other decay modes of A(1680) are $\eta\pi < 10\%$, $5\pi < 10\%$.

m. Includes $p\bar{p}\pi^+\pi^-\gamma$ and excludes $p\bar{p}\eta$, $p\bar{p}\omega$, $p\bar{p}\eta'$.

n. See E(1420) mini-review.

o. Empirical limits on fractions for other decay modes of $\chi(3415)$ are $2\gamma < 0.17\%$, $p\bar{p} < 0.11\%$.

p. Empirical limits on fractions for other decay modes of $\chi(3510)$ are ($\pi^+\pi^-$ and K^+K^-) < 0.2%, $\gamma\gamma < 0.16\%$, $p\bar{p} < 0.13\%$.

q. Empirical limits on fractions for other decay modes of $\chi(3555)$ are $2\gamma < 0.06\%$, $p\bar{p} < 0.10\%$, $J/\psi\pi^+\pi^-\pi^0 < 1.5\%$.

r. Spectroscopic labeling for these states is theoretical, pending experimental information.

Meson Table *(cont'd)*

Contents of Meson Data Card Listings

Non-strange (S = 0; C,B = 0)									Strange (|S| = 1; C,B = 0)	
entry		$I^G(J^P)C_n$	entry		$I^G(J^P)C_n$	entry		$I^G(J^P)C_n$	entry	I (J^P)
π		$1^-(0^-)+$	ω	(1670)	$0^-(3^-)-$	→ e^+e^-	(1100—2200)	(1^-)	K	$1/2(0^-)$
η		$0^+(0^-)+$	A'	(1680)	$1^-(2^-)+$	→ $\bar{N}N$	(1200—3600)		K* (892)	$1/2(1^-)$
ρ	(770)	$1^+(1^-)-$	ϕ	(1680)	$0^-(1^-)-$	→ X	(1900—3600)		Q (1280)	$1/2(1^+)$
ω	(783)	$0^-(1^-)-$	g	(1690)	$1^+(3^-)-$	η_c	(2980)	0^+ +	κ (1350)	$1/2(0^+)$
η'	(958)	$0^+(0^-)+$	θ	(1690)	$0^+(\ ^+)+$	J/ψ	(3100)	$0^-(1^-)-$	Q (1400)	$1/2(1^+)$
S	(975)	$0^+(0^+)+$	→ η	(1700)	$^+$	χ	(3415)	$0^+(0^+)+$	→ K (1400)	$1/2(0^-)$
δ	(980)	$1^-(0^+)+$	→ S	(1730)	$0^+(0^+)+$	χ	(3510)	$0^+(1^+)+$	K* (1430)	$1/2(2^+)$
ϕ	(1020)	$0^-(1^-)-$	→ π	(1770)	$1^-(0^-)+$	χ	(3555)	$0^+(2^+)+$	→ L (1580)	$1/2(2^-)$
H	(1190)	$0^-(1^+)-$	→ f	(1810)	$0^+(2^+)+$	→ η_c	(3590)	+	→ K* (1650)	$1/2(1^-)$

	B	(1235) $1^+(1^+)-$
→	g_S	(1240) $0^+(0^+)+$
→	ρ	(1250) $1^+(1^-)-$
	f	(1270) $0^+(2^+)+$
	A	(1270) $1^-(1^+)+$
→	η	(1275) $0^+(0^-)+$
	D	(1285) $0^+(1^+)+$
	ϵ	(1300) $0^+(0^+)+$
	π	(1300) $1^-(0^-)+$
	A_2	(1320) $1^-(2^+)+$
	E	(1420) $0^+(1^+)+$
	ι	(1440) $0^+(0^-)+$
	f′	(1525) $0^+(2^+)+$
→	D	(1530) $0^+(1^+)+$
	ρ	(1600) $1^+(1^-)-$

	ϕ	(1850) 0
→	S	(1935)
	h	(2030) $0^+(4^+)+$
→	δ	(2040) $1^-(4^+)+$
→	A	(2050) $1^-(3^+)+$
→	A	(2100) $1^-(2^-)+$
→	ρ	(2150) $1^+(1^-)-$
→	ϵ	(2150) $0^+(2^+)+$
→	ξ	(2220) 0 ($^+$)
→	g_T	(2240) $0^+(2^+)+$
→	ρ	(2250) $1^+(3^-)-$
→	ϵ	(2300) $0^+(4^+)+$
→	ρ	(2350) $1^+(5^-)-$
→	δ	(2450) $1^-(6^+)$
→	r	(2510) $0^+(6^+)$

	ψ	(3685) $0^-(1^-)-$
	ψ	(3770) $(1^-)-$
	ψ	(4030) $(1^-)-$
	ψ	(4160) $(1^-)-$
	ψ	(4415) $(1^-)-$
	Υ	(9460) $(1^-)-$
	χ_b	(9875) ( )+
	χ_b	(9895) ( )+
	χ_b	(9915) ( )+
	Υ	(10025) $(1^-)-$
→	χ_b	(10235) ( )+
	χ_b	(10255) ( )+
	χ_b	(10270) ( )+
	Υ	(10355) $(1^-)-$
	Υ	(10575) $(1^-)-$

	L	(1770) $1/2(2^-)$
	K*	(1780) $1/2(3^-)$
→	K	(1830) $1/2(0^-)$
	K*	(2060) $1/2(4^+)$
→	K	(2250) $1/2(2^-)$
→	K	(2320) $1/2(3^+)$
→	K	(2500) $1/2(4^-)$
Charmed ($\|C\| = 1$)		
	D	$1/2(0^-)$
	D*	(2010) $1/2(1^-)$
	F	0 (0^-)
→	F*	(2140)
Bottom (Beauty) ($\|B\| = 1$)		
B		
→ Exotics		

Baryon Table

April 1984

The following short list gives the name, the nominal mass, the quantum numbers (where known), and the status of each of the Baryon States in the Data Card Listings. States with 3- or 4-star status are included in the Baryon Table below; the others are omitted because the evidence for the existence of the effect and/or for its interpretation as a resonance is open to question.

N(939) P11	****	Δ(1232) P33	****	Z0(1780) P01	*	Σ(1193) P11	****	Ξ(1318) P11	****		
N(1440) P11	****	Δ(1550) P31	*	Z0(1865) D03	*	Σ(1385) P13	****	Ξ(1530) P13	****		
N(1520) D13	****	Δ(1600) P33	**	Z1(1900) P13	*	Σ(1480)	*	Ξ(1630)	*		
N(1535) S11	****	Δ(1620) S31	****	Z1(2150)	*	Σ(1560)	**	Ξ(1680)	**		
N(1540) P13	*	Δ(1700) D33	****	Z1(2500)	*	Σ(1580) D13	**	Ξ(1820) 13	***		
N(1650) S11	****	Δ(1900) S31	***			Σ(1620) S11	**	Ξ(1940)	**		
N(1675) D15	****	Δ(1905) F35	****	Λ(1116) P01	****	Σ(1660) P11	***	Ξ(2030) 1	***		
N(1680) F15	****	Δ(1910) P31	****	Λ(1405) S01	****	Σ(1670) D13	****	Ξ(2120)	*		
N(1700) D13	***	Δ(1920) P33	***	Λ(1520) D03	****	Σ(1690)	**	Ξ(2250)	**		
N(1710) P11	***	Δ(1930) D35	***	Λ(1600) P01	***	Σ(1750) S11	***	Ξ(2370) 1	**		
N(1720) P13	****	Δ(1940) D33	*	Λ(1670) S01	****	Σ(1770) P11	*	Ξ(2500)	*		
N(1990) F17	**	Δ(1950) F37	****	Λ(1690) D03	****	Σ(1775) D15	****				
N(2000) F15	**	Δ(2150) S31	*	Λ(1800) S01	***	Σ(1840) P13	*	Ω(1672) P03	****		
N(2080) D13	**	Δ(2200) G37	*	Λ(1800) P01	***	Σ(1880) P11	**	Λ_c(2282)	****		
N(2090) S11	*	Δ(2300) H39	**	Λ(1820) F05	****	Σ(1915) F15	****				

N(2100) P11	*	Δ(2350) D35	*	Λ(1830) D05	****	Σ(1940) D13	***	Σ_c(2450)	**
N(2190) G17	****	Δ(2390) F37	*	Λ(1890) P03	****	Σ(2000) S11	*		
N(2200) D15	**	Δ(2400) G39	**	Λ(2000)	*	Σ(2030) F17	****	Λ(2460)	*
N(2220) H19	****	Δ(2420) H311	****	Λ(2020) F07	*	Σ(2070) F15	*	Λ_b(5500)	*
N(2250) G19	****	Δ(2750) I313	**	Λ(2100) G07	****	Σ(2080) P13	**		
N(2600) I111	***	Δ(2950) K315	**	Λ(2110) F05	***	Σ(2100) G17	*	Dibaryons	
N(2700) K113	**	Δ(~3000)		Λ(2325) D03	*	Σ(2250)	***	NN(2170) 1D2	**
N(~3000)				Λ(2350)	***	Σ(2455)	**	NN(2250) 3F3	**
				Λ(2585)	**	Σ(2620)	**	NN(?)	*
						Σ(3000)	*	ΛN(2130) 3S1	**
						Σ(3170)	*	ΞN(?)	*

****	Good, clear, and unmistakable.
***	Good, but in need of clarification or not absolutely certain.
**	Not established; needs confirmation.
*	Evidence weak; could disappear.

Baryon Table *(cont'd)*

Particle [a]	$I(J^P)L_{2I\cdot 2J}$ [b]	P_{beam} [c] (GeV/c) $\sigma = 4\pi\lambda^2$ (mb)	Mass [d] M (MeV)	Full [e] width Γ (MeV)	Partial decay modes Mode [f]	Fraction [g] (%)	p [h] (MeV/c)
S=0 I=1/2 NUCLEON RESONANCES (N)							
p	$1/2(1/2^+)$		938.3		See Stable Particle Table		
n			939.6				
N(1440)	$1/2(1/2^+)P'_{11}$	p = 0.61	1400 to	120 to	$N\pi$	50-70	397
		σ = 31.0	1480	350	$N\eta$	8-18	†
				(200)	$N\pi\pi$	~30	342
					$\Delta\pi$	12-28 *	143
					$N\rho$	~ 7	†
					$N\epsilon$	~ 5	†
N(1520)	$1/2(3/2^-)D'_{13}$	p = 0.74	1510 to	100 to	$N\pi$	50-60	456
		σ = 23.5	1530	140	$N\eta$	~0.1	149
				(125)	$N\pi\pi$	35-50	410
					$\Delta\pi$	15-25 *	228
					$N\rho$	15-25	†
					$N\epsilon$	< 5	†
N(1535)	$1/2(1/2^-)S'_{11}$	p = 0.76	1520 to	100 to	$N\pi$	35-50	467
		σ = 22.5	1560	250	$N\eta$	~35	182
				(150)	$N\pi\pi$	~ 5	422

					[$\Delta\pi$	~ 1] *	242
					[$N\rho$	~ 3]	†
					[$N\epsilon$	~ 2]	†
N(1650)	$1/2(1/2^-)S''_{11}$	p = 0.96	1620 to	100 to	$N\pi$	55-65	547
		σ = 16.4	1680	200	$N\eta$	~1.5	346
				(150)	ΛK	~ 8	161
					ΣK	3-10	†
					$N\pi\pi$	~30	511
					[$\Delta\pi$	4-15] *	344
					[$N\rho$	~20]	†
					[$N\epsilon$	< 5]	†
N(1675)	$1/2(5/2^-)D'_{15}$	p = 1.01	1660 to	120 to	$N\pi$	30-40	563
		σ = 15.4	1690	180	$N\eta$	~ 1	374
				(155)	ΛK	~0.1	209
					$N\pi\pi$	55-70	529
					[$\Delta\pi$	50-65] *	364
					[$N\rho$	~ 5]	†
N(1680)	$1/2(5/2^+)F'_{15}$	p = 1.01	1670 to	110 to	$N\pi$	55-65	567
		σ = 15.2	1690	140	$N\eta$	< 1	379
				(125)	ΛK	not seen	218
					$N\pi\pi$	~40	532
					[$\Delta\pi$	~12] *	369
					[$N\rho$	~10]	†
					[$N\epsilon$	~20]	†

Baryon Table *(cont'd)*

Particle [a]	$I(J^P)L_{2I\cdot 2J}$ [b]	P_{beam} [c] (GeV/c) $\sigma = 4\pi\lambda^2$ (mb)	Mass [d] M (MeV)	Full [e] width Γ (MeV)	Partial decay modes Mode [f]	Fraction [g] (%)		p [h] (MeV/c)
N(1700)	$1/2(3/2^-)D''_{13}$	p = 1.05 σ = 14.5	1670 to 1730	70 to 120 (100)	Nπ Nη ΛK Nππ Δπ Nρ Nε	8-12 ~ 4 ~0.2 ~85 15-40 ~ 5 <40	* †	580 400 250 547 385 † †
N(1710)	$1/2(1/2^+)P''_{11}$	p = 1.07 σ = 14.2	1680 to 1740	90 to 130 (110)	Nπ Nη ΛK ΣK Nππ Δπ Nρ Nε	10-20 ~25 ~15 2-10 >50 10-25 25-65 15-40	* †	587 410 264 138 554 393 48 †
N(1720)	$1/2(3/2^+)P''_{13}$	p = 1.09 σ = 13.9	1690 to 1800	125 to 250 (200)	Nπ Nη ΛK ΣK	10-20 ~3.5 ~ 5 2-5		594 420 278 162

					$N\pi\pi$	~70	561
					$\Delta\pi$	~20 *	401
					$N\rho$	45-70	104
					$N\epsilon$	~20	†
N(2190)	$1/2(7/2^-)G_{17}$	p = 2.07	2120 to	200 to	$N\pi$	~14	888
		σ = 6.21	2230	500	$N\eta$	~ 3	790
				(350)	ΛK	~0.3	712
N(2220)	$1/2(9/2^+)H_{19}$	p = 2.14	2150 to	300 to	$N\pi$	~18	905
		σ = 5.97	2300	500	$N\eta$	~0.5	811
				(400)	ΛK	~0.2	732
N(2250)	$1/2(9/2^-)G'_{19}$	p = 2.21	2130 to	200 to	$N\pi$	~10	923
		σ = 5.74	2270	500	$N\eta$	~ 2	831
				(300)	ΛK	~0.3	754
N(2600)	$1/2(11/2^-)I_{111}$	p = 3.12	2580 to	>300	$N\pi$	~ 5	1126
		σ = 3.86	2700	(400)			

Baryon Table *(cont'd)*

Particle [a]	$I(J^P)L_{2I\cdot 2J}$ [b]	P_{beam} [c] (GeV/c) $\sigma = 4\pi\lambda^2$ (mb)	Mass [d] M (MeV)	Full [e] width Γ (MeV)	Partial decay modes Mode [f]	Fraction [g] (%)	p [h] (MeV/c)
		S=0 I=3/2 DELTA RESONANCES (Δ)					
Δ(1232)	$3/2(3/2^+)P'_{33}$	p = 0.30 σ = 94.8	1230 to 1234	110 to 120 (115)	Nπ Nγ	99.4 0.6	227 259
Δ(1620)	$3/2(1/2^-)S'_{31}$	p = 0.91 σ = 17.7	1600 to 1650	120 to 160 (140)	Nπ Nππ [Δπ Nρ] *	25-35 ~70 35-50 <40	526 488 318 †
Δ(1700)	$3/2(3/2^-)D'_{33}$	p = 1.05 σ = 14.5	1630 to 1740	190 to 300 (250)	Nπ Nππ [Δπ Nρ] *	10-20 ~85 <50 ~40	580 547 385 †
Δ(1900)	$3/2(1/2^-)S''_{31}$	p = 1.44 σ = 9.71	1850 to 2000	130 to 300 (150)	Nπ ΣK	6-12 ~10	710 410
Δ(1905)	$3/2(5/2^+)F_{35}$	p = 1.45 σ = 9.62	1890 to 1920	250 to 400 (300)	Nπ ΣK Nππ	8-15 < 3 ~80	713 415 687

					[$\Delta\pi$	10-30] *	542
					[$N\rho$	~60]	421
$\Delta(1910)$	$3/2(1/2^+)P''_{31}$	p = 1.46	1850 to	200 to	$N\pi$	20-25	716
		σ = 9.54	1950	330	ΣK	2-20	421
				(220)	$N\pi\pi$	>40	691
					[$\Delta\pi$	small] *	545
					[$N\rho$	<40]	426
$\Delta(1920)$	$3/2(3/2^+)P'''_{33}$	p = 1.48	1860 to	190 to	$N\pi$	14-20	722
		σ = 9.38	2160	300	ΣK	~ 5	431
				(250)			
$\Delta(1930)$	$3/2(5/2^-)D'_{35}$	p = 1.50	1890 to	150 to	$N\pi$	4-14	729
		σ = 9.21	1960	350	ΣK	<10	441
				(250)			
$\Delta(1950)$	$3/2(7/2^+)F'_{37}$	p = 1.54	1910 to	200 to	$N\pi$	35-45	741
		σ = 8.91	1960	340	ΣK	< 1	460
				(240)	$N\pi\pi$	~60	716
					[$\Delta\pi$	~40] *	574
					[$N\rho$	~20]	469
$\Delta(2420)$	$3/2(11/2^+)H_{311}$	p = 2.64	2380 to	300 to	$N\pi$	5-15	1023
		σ = 4.68	2450	500			
				(300)			

Baryon Table *(cont'd)*

Particle [a]	$I(J^P)L^b_{I,2J}$	P^c_{beam} (GeV/c) $\sigma = 4\pi\lambda^2$ (mb)	Mass [d] M (MeV)	Full [e] width Γ (MeV)	Partial decay modes Mode	Fraction [g] (%)	p [h] (MeV/c)
		S=−1 I=0 LAMBDA RESONANCES (Λ)					
Λ	$0(1/2^+)$		1115.6		See Stable Particle Table		
Λ(1405)	$0(1/2^-)S'_{01}$	Below K^-p threshold	1405 ±5[i]	40±10[i]	Σπ	100	152
Λ(1520)	$0(3/2^-)D'_{03}$	p = 0.395 σ = 82.3	1519.5 ±1.0[i]	15.6±1.0[i]	$N\bar{K}$ Σπ Λππ Σππ Λγ	45±1 42±1 10±1 0.9±0.1 0.8±0.2	244 267 252 152 351
Λ(1600)	$0(1/2^+)P'_{01}$	p = 0.58 σ = 41.6	1560 to 1700	50 to 250 (150)	$N\bar{K}$ Σπ	15-30 10-60	343 336
Λ(1670)	$0(1/2^-)S''_{01}$	p = 0.74 σ = 28.5	1660 to 1680	25 to 50 (35)	$N\bar{K}$ Σπ Λη	15-25 20-60 15-35	414 393 64

$\Delta(1690)$	$0(3/2^-)D''_{03}$	$p = 0.78$ $\sigma = 26.1$	1685 to 1695	50 to 70 (60)	$N\bar{K}$ $\Sigma\pi$ $\Lambda\pi\pi$ $\Sigma\pi\pi$	20-30 20-40 ~25 ~20	433 409 415 350
$\Delta(1800)$	$0(1/2^-)S'''_{01}$	$p = 1.01$ $\sigma = 17.5$	1720 to 1850	200 to 400 (300)	$N\bar{K}$ $\Sigma\pi$ $\Sigma(1385)\pi$ $N\bar{K}^*(892)$	25-40 seen seen seen	528 493 345 †
$\Delta(1800)$	$0(1/2^+)P''_{01}$	$p = 1.01$ $\sigma = 17.5$	1750 to 1850	50 to 250 (150)	$N\bar{K}$ $\Sigma\pi$ $\Sigma(1385)\pi$ $N\bar{K}^*(892)$	20-50 10-40 seen 30-60	528 493 345 †
$\Delta(1820)$	$0(5/2^+)F'_{05}$	$p = 1.06$ $\sigma = 16.5$	1815 to 1825	70 to 90 (80)	$N\bar{K}$ $\Sigma\pi$ $\Sigma(1385)\pi$	55-65 8-14 5-10	545 508 362
$\Delta(1830)$	$0(5/2^-)D_{05}$	$p = 1.08$ $\sigma = 16.0$	1810 to 1830	60 to 110 (95)	$N\bar{K}$ $\Sigma\pi$ $\Sigma(1385)\pi$	3-10 35-75 >15	553 515 371
$\Delta(1890)$	$0(3/2^+)P'_{03}$	$p = 1.21$ $\sigma = 13.6$	1850 to 1910	60 to 200 (100)	$N\bar{K}$ $\Sigma\pi$ $\Sigma(1385)\pi$ $N\bar{K}^*(892)$	20-35 3-10 seen seen	599 559 420 233

Baryon Table *(cont'd)*

Particle [a]	$I(J^P)L^b_{I,2J}$	P^c_{beam} (GeV/c) $\sigma = 4\pi\lambda^2$ (mb)	Mass [d] M (MeV)	Full [e] width Γ (MeV)	Partial decay modes Mode	Fraction [g] (%)	p [h] (MeV/c)
Λ(2100)	$0(7/2^-)G_{07}$	p = 1.68 σ = 8.68	2090 to 2110	100 to 250 (200)	$N\bar{K}$	25-35	751
					$\Sigma\pi$	~ 5	704
					$\Lambda\eta$	< 3	617
					ΞK	< 3	483
					$\Lambda\omega$	< 8	443
					$N\bar{K}^*(892)$	10-20	514
Λ(2110)	$0(5/2^+)F''_{05}$	p = 1.70 σ = 8.53	2090 to 2140	150 to 250 (200)	$N\bar{K}$	5-25	757
					$\Sigma\pi$	10-40	711
					$\Lambda\omega$	seen	455
					$\Sigma(1385)\pi$	seen	589
					$N\bar{K}^*(892)$	10-60	524
Λ(2350)	$0(9/2^+)$	p = 2.29 σ = 5.85	2340 to 2370	100 to 250 (150)	$N\bar{K}$	~12	915
					$\Sigma\pi$	~10	867
S=−1 I=1 SIGMA RESONANCES (Σ)							
Σ	$1(1/2^+)$		(+)1189.4 (0)1192.5 (−)1197.3		See Stable Particle Table		

$\Sigma(1385)$	$1(3/2^+)P'_{13}$	Below	(+)1382.3±0.4	35±1	$\Lambda\pi$	88±2	208
		K^-p	S=1.6[j]	S=1.0[j]	$\Sigma\pi$	12±2	127
		threshold	(0)1382.0±2.5	~35			
			S=1.6[j]				
			(−)1387.4±0.6	40±2			
			S=2.2[j]	S=1.9[j]			
$\Sigma(1660)$	$1(1/2^+)P'_{11}$	p = 0.72	1630 to	40 to	$N\bar{K}$	10-30	405
		σ = 29.9	1690	200	$\Lambda\pi$	seen	439
				(100)	$\Sigma\pi$	seen	385
$\Sigma(1670)$	$1(3/2^-)D''_{13}$	p = 0.74	1665 to	40 to	$N\bar{K}$	7-13	414
		σ = 28.5	1685	80	$\Lambda\pi$	5-15	447
				(60)	$\Sigma\pi$	30-60	393
$\Sigma(1750)$	$1(1/2^-)S''_{11}$	p = 0.91	1730 to	60 to	$N\bar{K}$	10-40	486
		σ = 20.7	1800	160	$\Lambda\pi$	seen	507
				(90)	$\Sigma\pi$	< 8	455
					$\Sigma\eta$	15-55	81
$\Sigma(1775)$	$1(5/2^-)D_{15}$	p = 0.96	1770 to	105 to	$N\bar{K}$	37-43	508
		σ = 19.0	1780	135	$\Lambda\pi$	14-20	525
				(120)	$\Sigma\pi$	2-5	474
					$\Sigma(1385)\pi$	8-12	324
					$\Lambda(1520)\pi$	17-23	198
$\Sigma(1915)$	$1(5/2^+)F'_{15}$	p = 1.26	1900 to	80 to	$N\bar{K}$	5-15	618
		σ = 12.8	1935	160	$\Lambda\pi$	seen	622
				(120)	$\Sigma\pi$	seen	577
					$\Sigma(1385)\pi$	< 5	440

Baryon Table *(cont'd)*

Particle [a]	$I(J^P)L^b_{I,2J}$	P_{beam} [c] (GeV/c) $\sigma = 4\pi\lambda^2$ (mb)	Mass [d] M (MeV)	Full [e] width Γ (MeV)	Partial decay modes Mode	Fraction [g] (%)	p [h] (MeV/c)
Σ(1940)	$1(3/2^-)D^{'''}_{13}$	p = 1.32 σ = 12.1	1900 to 1950	150 to 300 (220)	$N\bar{K}$	<20	637
					Λπ	seen	639
					Σπ	seen	594
					Σ(1385)π	seen	460
					Λ(1520)π	seen	354
					Δ(1232)$\bar{K}$	seen	410
					$N\bar{K}^*$(892)	seen	320
Σ(2030)	$1(7/2^+)F_{17}$	p = 1.52 σ = 9.93	2025 to 2040	150 to 200 (180)	$N\bar{K}$	17-23	702
					Λπ	17-23	700
					Σπ	5-10	657
					Ξ K	< 2	412
					Σ(1385)π	5-15	529
					Λ(1520)π	10-20	430
					Δ(1232)$\bar{K}$	10-20	498
					$N\bar{K}^*$(892)	< 5	438
Σ(2250)	1(?)	p = 2.04 σ = 6.76	2210 to 2280	60 to 150 (100)	$N\bar{K}$	<10	851
					Λπ	seen	842
					Σπ	seen	803

Particle [a]	$I(J^P)L_{2I\cdot 2J}$ [b]	Mass [d] M (MeV)	Full [e] width Γ (MeV)	Partial decay modes: Mode	Fraction (%)	p [h] (MeV/c)
S=−2 I=1/2 CASCADE RESONANCES (Ξ)						
Ξ	$1/2(1/2^+)$	(0)1314.9 (−)1321.3		See Stable Particle Table		
$\Xi(1530)$	$1/2(3/2^+)P_{13}$	(0)1531.8±0.3 S = 1.3[j] (−)1535.0±0.6	9.1±0.5 10.1±1.9	$\Xi\pi$	100	148
$\Xi(1820)$	$1/2(3/2^-)$	1823 ±6[i]	20^{+15}_{-10}[i]	$\Lambda\bar{K}$ $\Sigma\bar{K}$ $\Xi\pi$ $\Xi(1530)\pi$	~45 ~10 small ~45	396 306 413 231
$\Xi(2030)$	$1/2(?^?)$	2024 ±6[i]	16^{+15}_{-5}[i]	$\Lambda\bar{K}$ $\Sigma\bar{K}$ $\Xi\pi$ $\Xi(1530)\pi$	~20 ~80 small small	587 524 573 418
OTHER BARYONS						
Ω^-	$0(3/2^+)$	1672.4		See Stable Particle Table		
Λ_c^+	$0(1/2^+)$	2282		See Stable Particle Table		

Baryon Table *(cont'd)*

→ Each arrow in the left-hand margin indicates there is an entry in the Data Card Listings for a baryon that is not well enough established (status less than 3 stars) to be included here. There is a short list of *all* the baryons in the Listings, whatever their status, at the front of this Table.

f. This mode is energetically forbidden when the nominal mass of the decaying resonance (and of any resonance in the final state) is used, but is in fact allowed due to the nonzero widths of the resonance(s).

*. The modes in brackets are subreactions of the $N\pi\pi$ mode.

a. The nominal mass here (in MeV) is used for identification. See column 4 for the actual mass.

b. When there is more than one baryon with the same quantum numbers, one prime is attached to the spectroscopic symbol for the first of them (e.g., S'_{11}), two primes to the second, etc.

c. The quantities here are calculated using the nominal mass of column 1.

d. Usually a conservatively large range of masses rather than a statistical average of the various determinations of the mass is given. In these cases, the mass determinations are nearly entirely from various phase-shift analyses of more or less the same data. It is thus not appropriate to treat the determinations as independent measurements or to average them together. The masses, widths, and branching fractions in this Table are Breit-Wigner parameters. The Data Card Listings also include pole parameters where they are available.

e. Usually a conservatively large range of widths rather than a statistical average of the various determinations of the width is given (see note *d* for the reason). The nominal value in parentheses is then simply a best guess.

f. For information on the $N\gamma$ decay modes, see the Note on N and Δ Resonances in the Listings.

g. Most of the inelastic branching fractions come from partial-wave analyses, and these determine $\sqrt{xx'}$, where x and x′ are the elastic and inelastic branching fractions, not x′ directly. Thus any uncertainty (and it is often considerable) in x carries over into x′. When x′ so determined is really poorly known, we here simply note that the mode is seen. The values of $\sqrt{xx'}$ are given in the Data Card Listings.

h. For a 2-body decay mode, this is the momentum of the decay products in the rest frame of the decaying particle. For a mode with more than two decay products, this is the maximum momentum any of the products can have in this frame. The nominal mass of column 1 is used, as is the nominal mass of any resonance in the final state.

i. The error given here is only an educated guess. It is larger than the error on the weighted average of the published values (the error on this average is given in the Listings).

j. The error given here has been scaled up by the "$\bar{S}$ factor" (see the * footnote to the Stable Particle Table for how S is defined) because the various measurements disagree more seriously than one would expect from statistics.

CLEBSCH-GORDAN COEFFICIENTS, SPHERICAL HARMONICS, AND D FUNCTIONS

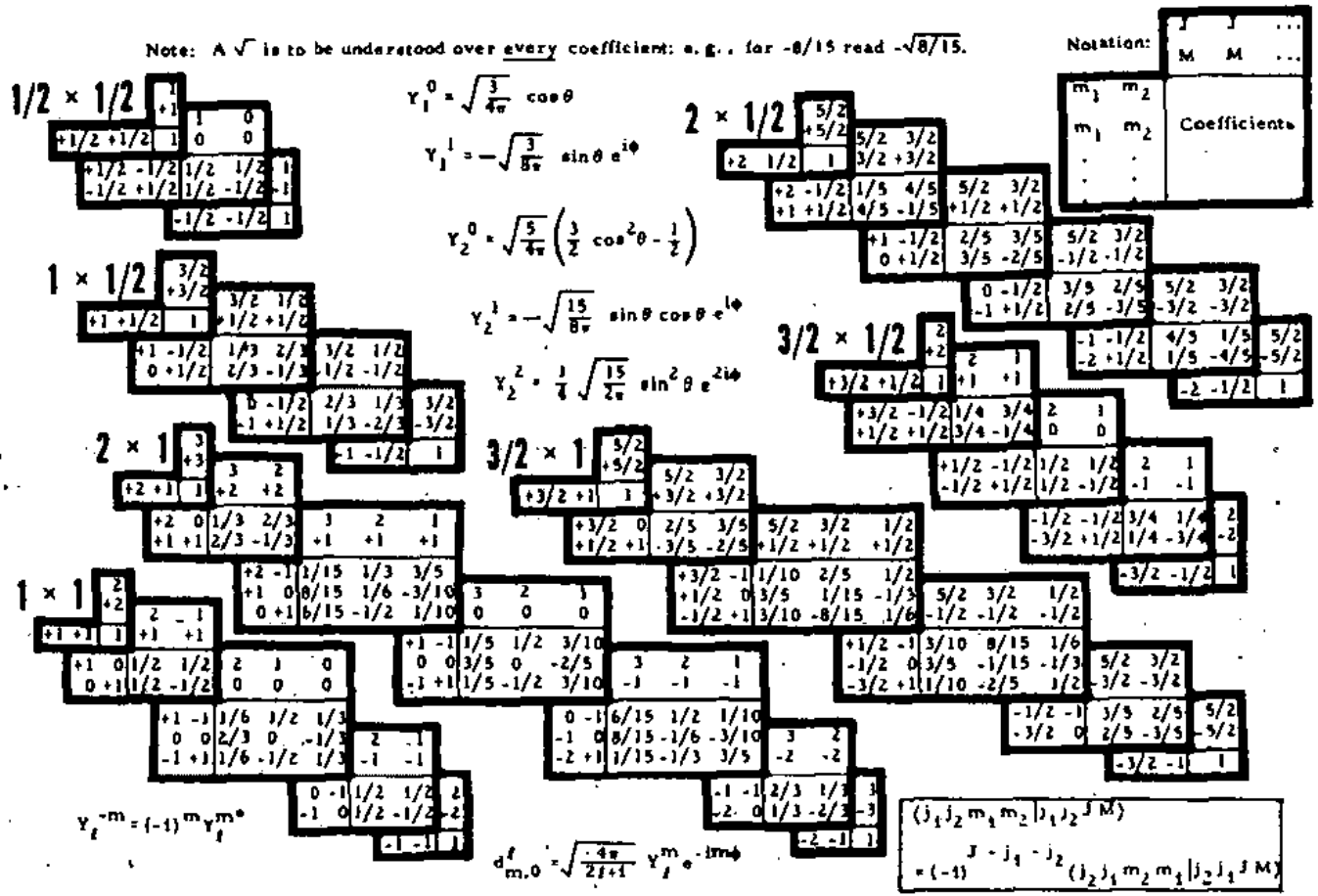

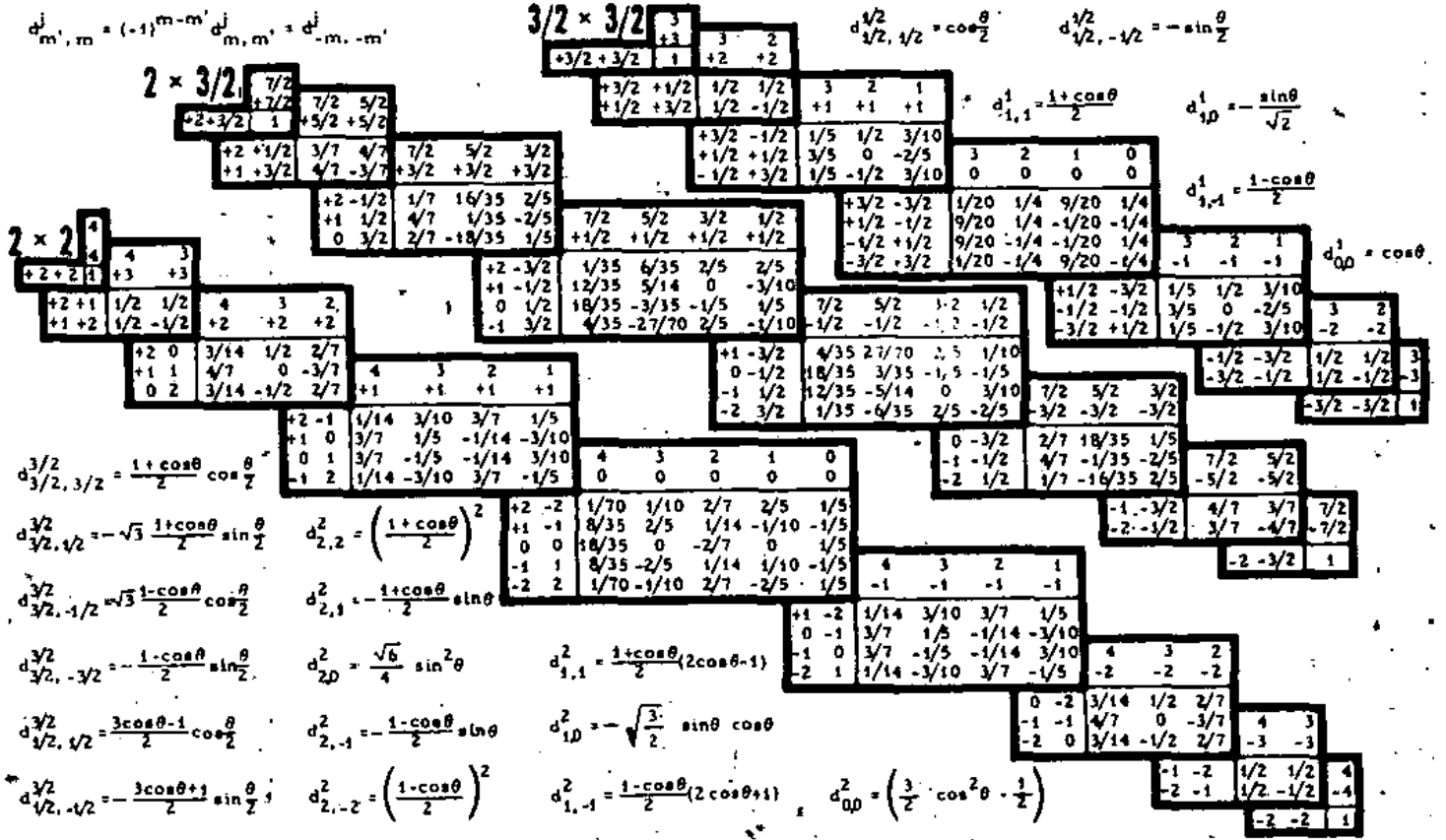

Sign convention is that of Wigner (*Group Theory*, Academic Press, New York, 1959), also used by Condon and Shortley (*The Theory of Atomic Spectra*, Cambridge Univ. Press, New York, 1953), Rose (*Elementary Theory of Angular Momentum*, Wiley, New York, 1957), and Cohen (*Tables of the Clebsch-Gordan Coefficients*, North American Rockwell Science Center, Thousand Oaks, Calif., 1974). The signs and numbers in the current tables have been calculated by computer programs written independently by Cohen and at LBL. (Table extended April 1974.)

SU(3) ISOSCALAR FACTORS

The most commonly used isoscalar factors, corresponding to the singlet, octet, and decuplet content of $8 \otimes 8$ and $10 \otimes 8$, are displayed at the right. The notation uses particle names to identify the coefficients, so that the pattern of relative couplings can be seen at a glance. We illustrate the use of the coefficients by example; see J.J de Swart, Rev. Mod Phys. 35, 916 (1963) for detailed explanation and phase conventions.

A $\sqrt{}$ is understood over every integer in the matrices; the exponent ½ is a reminder of this. For example, in de Swart's notation the $\Xi \to \Omega K$ element of our $10 \to 10 \otimes 8$ matrix reads

$$\left(\begin{array}{cc|c} 10 & 8 & 10 \\ 0 \; -2 & ½ \; 1 & ½ \; -1 \end{array}\right) = \frac{-\sqrt{6}}{\sqrt{24}} .$$

Intramultiplet relative decay strengths can be read directly from our matrices. Thus, the partial widths for $\Delta \to (N\pi)_{I=3/2}$ and $\Omega^* \to (\Xi\bar{K})_{I=0}$ are in the ratio

$$\frac{\Gamma(\Omega^* \to (\Xi\bar{K})_{I=0})}{\Gamma(\Delta \to (N\pi)_{I=3/2})} = \frac{12}{6} \times (\text{phase space factors}) .$$

Supplying isospin Clebsch-Gordan coefficients, one obtains, e.g.,

$$\frac{\Gamma(\Omega^{*-} \to \Xi^0 K^-)}{\Gamma(\Delta^+ \to p\pi^0)} = \frac{1/2}{2/3} \times \frac{12}{6} \times \text{p.s.f.} = \frac{3}{2} \times \text{p.s.f.}$$

Partial widths for $8 \to 8 \otimes 8$ involve a linear superposition of 8_1 (symmetric) and 8_2 (antisymmetric) couplings. For example,

$$\Gamma(\Xi^* \to \Xi\pi) \sim \left(-\sqrt{\frac{9}{20}} g_1 + \sqrt{\frac{3}{12}} g_2 \right)^2 .$$

The relation between g_1, g_2 (with de Swart's normalization) and the standard D,F couplings appearing in the interaction Lagrangian,

$$\mathcal{L} = -\sqrt{2} D \, \mathrm{Tr}([\bar{B},B]_+ M) + \sqrt{2} F \, \mathrm{Tr}([\bar{B},B]_- M) ,$$

is

$$D = \frac{\sqrt{30}}{40} g_1 , \quad F = \frac{\sqrt{6}}{24} g_2 .$$

Thus,

$$\Gamma(\Xi^* \to \Xi\pi) \sim (1 - 2\alpha)^2$$

where $\alpha \equiv D/(D+F)$.

$1 \to 8 \otimes 8$

$$(\Lambda)_1 \to \left(N\bar{K} \quad \Sigma\pi \quad \Lambda\eta \quad \Xi K \right)_{8 \otimes 8} = \frac{1}{\sqrt{8}} \left(2 \quad 3 \quad -1 \quad -2 \right)^{\frac{1}{2}}$$

$8_1 \to 8 \otimes 8$

$$\begin{pmatrix} N \\ \Sigma \\ \Lambda \\ \Xi \end{pmatrix}_{8_1} \to \begin{pmatrix} N\pi & N\eta & \Sigma K & \Lambda K \\ N\bar{K} & \Sigma\pi & \Lambda\pi & \Sigma\eta & \Xi K \\ & N\bar{K} & \Sigma\pi & \Lambda\eta & \Xi K \\ & \Sigma\bar{K} & \Lambda\bar{K} & \Xi\pi & \Xi\eta \end{pmatrix}_{8 \otimes 8} = \frac{1}{\sqrt{20}} \begin{pmatrix} 9 & -1 & -9 & -1 \\ -6 & 0 & 4 & 4 & -6 \\ 2 & -12 & -4 & -2 \\ 9 & -1 & -9 & -1 \end{pmatrix}^{\frac{1}{2}}$$

$8_2 \to 8 \otimes 8$

$$\begin{pmatrix} N \\ \Sigma \\ \Lambda \\ \Xi \end{pmatrix}_{8_2} \to \begin{pmatrix} N\pi & N\eta & \Sigma K & \Lambda K \\ N\bar{K} & \Sigma\pi & \Lambda\pi & \Sigma\eta & \Xi K \\ & N\bar{K} & \Sigma\pi & \Lambda\eta & \Xi K \\ & \Sigma\bar{K} & \Lambda\bar{K} & \Xi\pi & \Xi\eta \end{pmatrix}_{8 \otimes 8} = \frac{1}{\sqrt{12}} \begin{pmatrix} 3 & 3 & 3 & -3 \\ 2 & 8 & 0 & 0 & -2 \\ 6 & 0 & 0 & 6 \\ 3 & 3 & 3 & -3 \end{pmatrix}^{\frac{1}{2}}$$

$10 \to 8 \otimes 8$

$$\begin{pmatrix} \Delta \\ \Sigma \\ \Xi \\ \Omega \end{pmatrix}_{10} \to \begin{pmatrix} & N\pi & & \Sigma K & \\ N\bar{K} & \Sigma\pi & \Lambda\pi & \Sigma\eta & \Xi K \\ & \Sigma\bar{K} & \Lambda\bar{K} & \Xi\pi & \Xi\eta \\ & & \Xi\bar{K} & & \end{pmatrix}_{8 \otimes 8} = \frac{1}{\sqrt{12}} \begin{pmatrix} & -6 & & 6 & \\ -2 & 2 & -3 & 3 & 2 \\ & 3 & -3 & 3 & \\ & & 12 & & \end{pmatrix}^{\frac{1}{2}}$$

$8 \to 10 \otimes 8$

$$\begin{pmatrix} N \\ \Sigma \\ \Lambda \\ \Xi \end{pmatrix}_{8} \to \begin{pmatrix} & \Delta\pi & \Sigma K & \\ \Delta\bar{K} & \Sigma\pi & \Sigma\eta & \Xi K \\ & \Sigma\pi & \Xi K & \\ \Sigma\bar{K} & \Xi\pi & \Xi\eta & \Omega K \end{pmatrix}_{10 \otimes 8} = \frac{1}{\sqrt{15}} \begin{pmatrix} & -12 & 3 & \\ 8 & -2 & -3 & 2 \\ & -9 & 6 & \\ 3 & -3 & -3 & 6 \end{pmatrix}^{\frac{1}{2}}$$

$10 \to 10 \otimes 8$

$$\begin{pmatrix} \Delta \\ \Sigma \\ \Xi \\ \Omega \end{pmatrix}_{10} \to \begin{pmatrix} \Delta\pi & \Delta\eta & \Sigma K & \\ \Delta\bar{K} & \Sigma\pi & \Sigma\eta & \Xi K \\ \Sigma\bar{K} & \Xi\pi & \Xi\eta & \Omega K \\ & \Xi\bar{K} & \Omega\eta & \end{pmatrix}_{10 \otimes 8} = \frac{1}{\sqrt{24}} \begin{pmatrix} & 15 & 3 & 6 & \\ 8 & 8 & 0 & -8 \\ 12 & 3 & -3 & -6 \\ & & 12 & -12 & \end{pmatrix}^{\frac{1}{2}}$$

SU(N) MULTIPLETS AND YOUNG DIAGRAMS

This note tells how SU(n) particle multiplets are identified or labeled, how to find the number of particles in a multiplet from its label, how to draw the Young diagram for a multiplet, and how to use Young diagrams to determine the overall multiplet structure of a composite system, such as a 3-quark or a meson-baryon system.

(1) **Multiplet labels** — An SU(n) multiplet is uniquely identified by a string of (n−1) nonnegative integers: $(\alpha,\beta,\gamma,\cdots)$. Any such set of integers specifies a multiplet. For an SU(2) multiplet such as an isospin multiplet, the single integer α is the number of *steps* from one end of the multiplet to the other (i.e., it is one fewer than the number of particles in the multiplet). In SU(3), the two integers α and β are the numbers of steps across the top and bottom levels of the multiplet diagram. Thus the labels for the SU(3) octet and decuplet

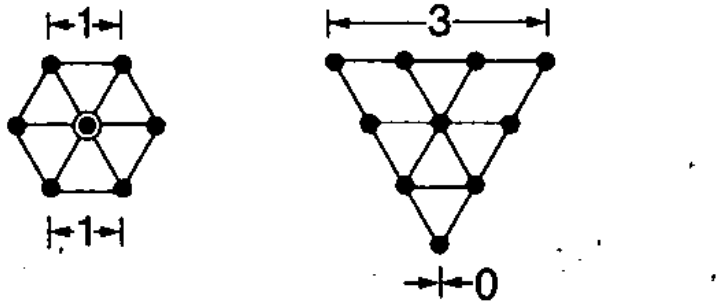

are (1,1) and (3,0). For larger n, the interpretation of the integers in terms of the geometry of the multiplets, which exist in an (n−1)-dimensional space, is not so readily apparent.

The label for the SU(n) singlet is (0,0,...,0). In a flavor SU(n), the n quarks together form a (1,0,...,0) multiplet, and the n antiquarks belong to a (0,...,0,1) multiplet. These two multiplets are *conjugate* to one another, which means their labels are related by $(\alpha,\beta,\ldots) \longleftrightarrow (\ldots,\beta,\alpha)$.

(2) **Number of particles** — The number of particles in a multiplet, $N = N(\alpha,\beta,\ldots)$, is given as follows (note the pattern of the equations). In SU(2), $N = N(\alpha)$ is

$$N = \frac{(\alpha+1)}{1} .$$

In SU(3), $N = N(\alpha,\beta)$ is

$$N = \frac{(\alpha+1)}{1}\cdot\frac{(\beta+1)}{1}\cdot\frac{(\alpha+\beta+2)}{2}$$

In SU(4), $N = N(\alpha,\beta,\gamma)$ is

$$N = \frac{(\alpha+1)}{1}\cdot\frac{(\beta+1)}{1}\cdot\frac{(\gamma+1)}{1}\cdot\frac{(\alpha+\beta+2)}{2}\cdot\frac{(\beta+\gamma+2)}{2}\cdot\frac{(\alpha+\beta+\gamma+3)}{3}$$

Note that there is no factor with $(\alpha+\gamma+2)$: only a *consecutive* sequence of the label integers appears in any factor. One more example should make the pattern clear for any SU(n). In SU(5), $N = N(\alpha,\beta,\gamma,\delta)$ is

$$N = \frac{(\alpha+1)}{1}\cdot\frac{(\beta+1)}{1}\cdot\frac{(\gamma+1)}{1}\cdot\frac{(\delta+1)}{1}\cdot\frac{(\alpha+\beta+2)}{2}\cdot\frac{(\beta+\gamma+2)}{2}\times$$

$$\frac{(\gamma+\delta+2)}{2}\cdot\frac{(\alpha+\beta+\gamma+3)}{3}\cdot\frac{(\beta+\gamma+\delta+3)}{3}\cdot\frac{(\alpha+\beta+\gamma+\delta+4)}{4}$$

Multiplets that are conjugate to one another obviously have the same number of particles, but so can other multiplets. For example, the SU(4) multiplets (3,0,0) and (1,1,0) each have 20 particles.

(3) **Young diagrams** — A Young diagram consists of an array of boxes (or some other symbol) arranged in one or more *left-justified* rows, with each row being *at least as long* as the row beneath. The correspondence between a diagram and a multiplet label is: The top row juts out α boxes to the right past the end of the second row, the second row juts out β boxes to the right past the end of the third row, etc. A diagram in SU(n) has at most n rows. There can be any number of "completed" columns of n boxes buttressing the left of a diagram; these don't affect the label. Thus in SU(3) the diagrams

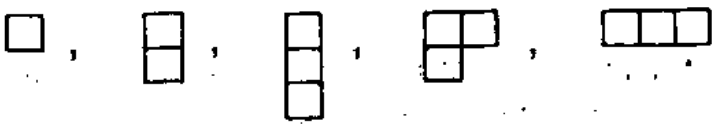

represent the multiplets (1,0), (0,1), (0,0), (1,1), and (3,0). In any SU(n), the quark multiplet is represented by a single box, the anti-quark multiplet by a column of (n−1) boxes, and a singlet by a completed column of n boxes.

(4) **Coupling multiplets together** — The following recipe tells how to find the multiplets that occur in coupling two multiplets together. To couple together more than two multiplets, first couple two, then couple the third with each of the multiplets obtained from the first two, etc.

First a definition: A sequence of the letters *a,b,c,...* is *admissible* if at any point in the sequence at least as many *a*'s have been reached as *b*'s, at least as many *b*'s have been reached as *c*'s, etc. Thus *abcd* and *aabcb* are admissible sequences and *abb* and *acb* are not. Now the recipe:

(a) Draw the Young diagrams for the two multiplets, but in one of the diagrams replace the boxes in the first row with *a*'s, the boxes in the second row with *b*'s, etc. The unlettered diagram forms the *upper left-hand corner* of all the enlarged diagrams constructed below.

(b) Add the *a*'s from the lettered diagram to the unlettered diagram to form all possible legitimate Young diagrams that have no more than one *a* per column. (All the *a*'s appear in each new diagram.)

(c) Use the *b*'s to further enlarge the diagrams already obtained, subject to the same rules. Throw away any diagram in which the sequence of letters formed by reading *right to left* in the first row, then the second row, etc., is not admissible.

(d) Proceed as in (c) with the *c*'s, etc.

Thus, for example, the calculation to find the multiplets that can occur in a system made up of two SU(3) octets (one might be the π-meson octet, the other the N-baryon octet) is as follows:

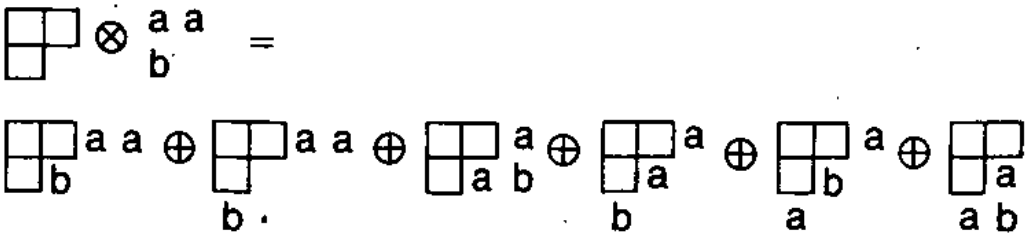

where only the diagrams with admissible sequences and with fewer than four rows (since n = 3) have been kept. In terms of multiplet labels, the above may be written

$$(1,1) \otimes (1,1) = (2,2) \oplus (3,0) \oplus (0,3) \oplus (1,1) \oplus (1,1) \oplus (0,0)\,,$$

or in terms of numbers of particles,

$$8 \otimes 8 = 27 \oplus 10 \oplus \overline{10} \oplus 8 \oplus 8 \oplus 1\,.$$

The product of the numbers of the left is equal to the sum on the right. (See the section on the Nonrelativistic Quark Model for results for 3-quark systems.)

TESTS OF CONSERVATION LAWS*

INTRODUCTION

In response to the current interest in tests of conservation laws, we have made a list of experimental limits on all weak and electromagnetic decays, mass differences, and moments, whose observation would violate conservation laws. The list is in two parts, "Number Conservation Laws," i.e., lepton, baryon, hadronic flavor, and charge conservation, and "Discrete Space Time Symmetries," i.e. C, P, T, CP, and CPT. The references for these data can be found in the Stable Particle Section of the Data Card Listings in this Review. A discussion of these tests follows.

CONSERVATION OF LEPTON NUMBERS

Present experimental evidence and the standard electroweak theory are consistent with the absolute conservation of three separate lepton numbers: electron number L_e, muon number L_μ, and τ-number L_τ. Searches for violations are of the following types:

a) $\Delta L = 2$ for one type of lepton. The best limit comes from the search for neutrinoless double beta decay $(Z,A) \rightarrow (Z+2,A) + e^- + e^-$. The best laboratory limit is $t_{1/2} > 2\times10^{22}$ yr for ^{76}Ge [E. Bellotti et al., Phys. Lett. **121B**, 72 (1983)].

b) Conversion of one lepton type to another. For purely leptonic processes, the best limit is on $\mu \rightarrow e\gamma$. For semileptonic processes, the best limit comes from the coherent conversion process in a muonic atom $\mu^- + (Z,A) \rightarrow e^- + (Z,A)$. Of special interest is the case in which the hadronic flavor also changes, as in $K_L \rightarrow \mu^\pm e^\mp$. Limits on the conversion of τ into e or μ are found in τ decay and are much less stringent that those for $\mu \rightarrow$ e conversion.

c) Conversion of one type of lepton into another type of antilepton. The case most studied is $\mu^- + (Z,A) \rightarrow e^+ + (Z-2,A)$.

d) Relation to neutrino mass. If neutrinos have masses then it is expected even in the standard electroweak theory that separate lep-

ton numbers are not conserved. With small neutrino masses this would be observed first in neutrino oscillations which have been the subject of extensive experimental searches. If the $\Delta L = 2$ type of violation occurs, it is expected that neutrinos will have a nonzero mass of the Majorana type.

CONSERVATION OF HADRONIC FLAVORS

The conversion of quarks of a given charge, (d,s,b) or (u,c,t), into one another is forbidden in strong and electromagnetic interactions by the conservation of hadron flavors: S (strangeness), C (charm), B (bottomness), and T (topness). The weak interactions violate these conservation laws as a result of the Cabibbo or Kobayashi-Maskawa mixing (see Appendix III in the complete Review of Particle Properties). The way in which these conservation laws are violated is tested as follows:

a) $\Delta S = \Delta Q$ rule. In the semileptonic decay of strange particles, the strangeness change equals the change in charge of the hadrons. Tests come from limits on decay rates such as $\Sigma^+ \to ne^+\nu$ and from a detailed analysis of $K_L \to \pi e\nu$, which yields the parameter x. A corresponding rule for charm decays is $\Delta C = \Delta Q$.

b) Change of flavor by 2 units. In the standard model this occurs only in second-order weak interactions. The one example for which this has been measured is the $\Delta S = 2$ $K^0 - \bar{K}^0$ mixing, which is directly measured by $m(K_S) - m(K_L)$. A limit on the $\Delta C = 2$ $D^0 - \bar{D}^0$ mixing provides a limit on $|m(D_1^0) - m(D_2^0)|$.

c) Flavor-changing neutral-currents. In the standard model the neutral-current interactions do not change flavor. The low rate of $K_L \to \mu^+\mu^-$ puts limits on such interactions; the nonzero value for this rate is attributed to a combination of the weak and electromagnetic interactions. The best test should come from a limit on $K^+ \to \pi^+\nu\bar{\nu}$, which occurs in the standard model only as a second-order weak process with a branching fraction of 10^{-10} to 10^{-11}. Limits for charm-changing or bottom-changing neutral currents are much less stringent.

CPT INVARIANCE

General principles of relativistic field theory require invariance under the combined transformation CPT. The simplest tests of CPT invariance are the equality of the masses and lifetimes of a particle and its antiparticle. The best test comes from a limit on the mass difference between K^0 and $\bar{K}^0$. Any such mass difference contributes to the CP-violating parameter ϵ. In fact ϵ can be explained by a CPT-conserving but CP-violating mixing of K^0 and $\bar{K}^0$, which yields a prediction that $\phi_{+-} \approx 44°$, while a $K^0 - \bar{K}^0$ mass difference would yield $\phi_{+-} \approx 44° + 90°$. It is thus possible to deduce that $|m(K^0) - m(\bar{K}^0)| < 10^{-4} |m(K_S) - m(K_L)| < 3\times10^{-10}$ eV. Also, an upper limit on $|m(D^0) - m(\bar{D}^0)|$ can be derived from the bound $|m(D_1^0) - m(D_2^0)| < 0.65\times10^{-9}$ MeV (inferred from bound on $D^0 \to \bar{D}^0 \to \mu^-$ anything), given an input value of, or bound on, the CP-violation parameter ϵ for $D^0 - \bar{D}^0$ mixing.

CP AND T INVARIANCE

Given CPT invariance, CP violation and T violation are equivalent. So far the only evidence for CP or T violation comes from the measurements of η_{+-}, η_{00}, and the semileptonic decay charge asymmetry for K_L. Other searches for CP or T violation should be divided into (a) those that involve weak interactions or parity violation, and (b) those that involve processes allowed by the strong or electromagnetic interactions. In class (a) the most sensitive is probably the search for an electric dipole moment of the neutron, which requires both P and T violation to be nonzero. Class (b) searches involve looking for C or T violation in strong or electromagnetic processes. Examples are the search for C violation in η decay, believed to be an electromagnetic process, and the search for T violation in a number of nuclear and electromagnetic reactions.

---

* Prepared April 1984 by R.E. Shrock, T.G. Trippe, and L. Wolfenstein.

Quantity[a]	Value[b]	Conservation Law Tested
$\mu^+ \to e^+\bar{\nu}_e\nu_\mu$ / all	$< 5 \times 10^{-2}$	Lepton family number[c,d]
$\to e^+\gamma$ / all	$< 1.7 \times 10^{-10}$	Lepton family number[d]
$\to e^+e^+e^-$ / all	$< 1.9 \times 10^{-9}$	" " "
$\to e^+\gamma\gamma$ / all	$< 8.4 \times 10^{-9}$	" " "
$\mu^- S_{32} \to e^- S_{32}$ / all	$< 7 \times 10^{-11}$	" " "
coupling for $(\mu^+e^- \to \mu^-e^+)_{bound}$	$< 42\ G_F$	" " "
$\tau^+ \to \mu^+\gamma$ / all	$< 5.5 \times 10^{-4}$	" " "
$\to e^+\gamma$ / all	$< 6.4 \times 10^{-4}$	" " "
$\to \mu^+\mu^+\mu^-$ / all	$< 4.9 \times 10^{-4}$	" " "
$\to e^+\mu^+\mu^-$ / all	$< 3.3 \times 10^{-4}$	" " "
$\to \mu^+e^+e^-$ / all	$< 4.4 \times 10^{-4}$	" " "
$\to e^+e^+e^-$ / all	$< 4.0 \times 10^{-4}$	" " "
$\to \mu^+\pi^0$ / all	$< 8.2 \times 10^{-4}$	" " "
$\to e^+\pi^0$ / all	$< 2.1 \times 10^{-3}$	" " "
$\to \mu^+K^0$ / all	$< 1.0 \times 10^{-3}$	" " "
$\to e^+K^0$ / all	$< 1.3 \times 10^{-3}$	" " "
$\to \mu^+\rho^0$ / all	$< 4.4 \times 10^{-4}$	" " "
$\to e^+\rho^0$ / all	$< 3.7 \times 10^{-4}$	" " "
$\pi^+ \to \mu^+\nu_e$ / all	$< 8.0 \times 10^{-3}$[e]	" " "
$K^+ \to \pi^+e^+\mu^-$ / all	$< 7 \times 10^{-9}$	" " "
$\to \pi^+e^-\mu^+$ / all	$< 5 \times 10^{-9}$	" " "
$\to \mu^+\nu_e$ / all	$< 4 \times 10^{-3}$[e]	" " "
$\to \mu^-\nu e^+e^+$ / all	$< 2 \times 10^{-8}$	" " "
$K_L^0 \to e\mu$ / charged	$< 8 \times 10^{-6}$	" " "

ν oscillations and lepton mixing effects in particle decays	See Data Card Listings	" " "
$\mu^- S_{32} \to e^+ Si^*_{32}$ / all	$< 9 \times 10^{-10}$	Total lepton number[f]
$\mu^- I_{127} \to e^+ Sb^{stable}_{127}$ / all	$< 3 \times 10^{-10}$	" " "
$\pi^+ \to \mu^+ \overline{\nu}_e$ / all	$< 1.5 \times 10^{-3}$[e]	" " "
$K^+ \to \pi^- e^+ e^+$ / all	$< 1 \times 10^{-8}$	" " "
$\to \pi^- e^+ \mu^+$ / all	$< 7 \times 10^{-9}$	" " "
$\to \mu^+ \overline{\nu}_e$ / all	$< 3.3 \times 10^{-3}$[e]	" " "
$\to e^+ \pi^0 \overline{\nu}_e$ / all	$< 3 \times 10^{-3}$[e]	" " "
neutrinoless double beta decay	See Data Card Listings	" " "
τ_p / BR($p \to e^+ \pi^0$)	$< 1 \times 10^{32}$ years	Baryon number
mean time for $n \to \overline{n}$ trans.	> 1.0 year	" "
e mean life	$> 2 \times 10^{22}$ years	Charge
$n \to p\overline{\nu\nu}$ / $pe^-\overline{\nu}$	$< 9 \times 10^{-24}$	"
Re x from $K^0 \to \pi e \nu$	0.009 ± 0.020	$\Delta S = \Delta Q$[g]
Im x from $K^0 \to \pi e \nu$	-0.004 ± 0.026	"
$K^+ \to \pi^+ \pi^+ e^- \nu$ / all	$< 1.2 \times 10^{-8}$	"
$\to \pi^+ \pi^+ \mu^- \nu$ / all	$< 3 \times 10^{-6}$	"
$\Sigma^+ \to n e^+ \nu$ / all	$< 5 \times 10^{-6}$	"
$\to n \mu^+ \nu$ / all	$< 3 \times 10^{-5}$	"
$(\Sigma^+ \to n \ell^+ \nu) / (\Sigma^- \to n \ell^- \overline{\nu})$	< 0.04	"
$\Xi^0 \to \Sigma^- e^+ \nu$ / all	$< 9 \times 10^{-4}$	"
$\to \Sigma^- \mu^+ \nu$ / all	$< 9 \times 10^{-4}$	"
$\to p e^- \nu$ / all	$< 1.3 \times 10^{-3}$	$\Delta S = 2$ forbidden[g]
$\to p \mu^- \nu$ / all	$< 1.3 \times 10^{-3}$	" "
$\Xi^- \to n e^- \nu$ / all	$< 3.2 \times 10^{-3}$	" "
$\to n \mu^- \nu$ / all	$< 1.5 \times 10^{-2}$	" "
$\to p \pi^- e^- \nu$ / all	$< 4 \times 10^{-4}$	" "
$\to p \pi^- \mu^- \nu$ / all	$< 4 \times 10^{-4}$	" "

Number Conservation Laws (cont'd)

Quantity[a]	Value[b]	Conservation Law Tested
$\bar{\Xi}^0 \to p\pi^-$ / all	$< 3.6 \times 10^{-5}$	$\Delta S=2$ forbidden[g]
$\bar{\Xi}^- \to n\pi^-$ / all	$< 1.9 \times 10^{-5}$	" "
$\to p\pi^-\pi^-$ / all	$< 4 \times 10^{-4}$	" "
$\Omega^- \to \Lambda\pi^-$ / all	$< 3.1 \times 10^{-3}$	" "
$m_{K_L} - m_{K_S}$	$(3.521 \pm 0.014) \times 10^{-12}$ MeV	" "
$(D^0 \to \bar{D}^0 \to K^+\pi^-)/(D^0 \to K\pi)$	< 0.16	$\Delta C=2$ forbidden[g]
$(D^0 \to \bar{D}^0 \to \mu^-$ anything$)/(D^0 \to \mu^+$ anything$)$	< 0.044	" "
$\lvert m_{D_1^0} - m_{D_2^0}\rvert$ (from previous limit)	$< 6.5 \times 10^{-10}$ MeV	" "
$K_L^0 \to \mu^+\mu^-$ / all	$(9.1 \pm 1.9) \times 10^{-9}$	no flav. chng. neut. curr.[g]
$\to e^+e^-$ / all	$< 2.0 \times 10^{-7}$	" " " " "
$\to \mu^+\mu^-\gamma$ / all	$(2.8 \pm 2.8) \times 10^{-7}$	" " " " "
$\to e^+e^-\gamma$ / all	$(1.7 \pm 0.9) \times 10^{-5}$	" " " " "
$\to \pi^0\mu^+\mu^-$ / all	$< 1.2 \times 10^{-6}$	" " " " "
$\to \pi^0e^+e^-$ / all	$< 2.3 \times 10^{-6}$	" " " " "
$\to \pi^+\pi^-e^+e^-$ / all	$< 9 \times 10^{-6}$	" " " " "
$K_S^0 \to \mu^+\mu^-$ / all	$< 3.2 \times 10^{-7}$	" " " " "
$\to e^+e^-$ / all	$< 3.4 \times 10^{-4}$	" " " " "
$K^+ \to \pi^+e^+e^-$ / all	$(2.7 \pm 0.5) \times 10^{-7}$	" " " " "
$\to \pi^+\mu^+\mu^-$ / all	$< 2.4 \times 10^{-6}$	" " " " "
$\to \pi^+\nu\bar{\nu}$ / all	$< 1.4 \times 10^{-7}$	" " " " "
$B \to e^+e^-$ anything / all	$< 8 \times 10^{-3}$	" " " " "
$\to \mu^+\mu^-$ anything / all	$< 7 \times 10^{-3}$	" " " " "

Quantity[a]	Value[b]	Symmetry Tested or Violated
$\pi^0 \to \gamma\gamma\gamma$ / all	$< 3.8 \times 10^{-7}$	C
$(e^+e^-)_{J=1} \to \gamma\gamma\gamma$ / all	$(5 \pm 3) \times 10^{-4}$[h]	C
$\eta \to e^+e^-\pi^0$ / all	$< 5 \times 10^{-5}$	C (single photon process)
$\eta \to \mu^+\mu^-\pi^0$ / all	$< 5 \times 10^{-6}$	C (single photon process)
$\eta \to \pi^+\pi^-\pi^0$ parameters:		
left-right asymmetry	$(1.2 \pm 1.7) \times 10^{-3}$	C
sextant asymmetry	$(1.9 \pm 1.6) \times 10^{-3}$	C
quadrant asymmetry	$(-1.7 \pm 1.7) \times 10^{-3}$	C
$\eta \to \pi^+\pi^-\gamma$ parameters:		
left-right asymmetry	$(8.8 \pm 4.0) \times 10^{-3}$	C
beta (D-wave)	0.047 ± 0.062	C
$\eta \to \pi^+\pi^-$ / all	$< 1.5 \times 10^{-3}$	P and CP
e electric dipole moment	$< 3 \times 10^{-24}$ e cm	T and P
μ electric dipole moment	$(3.7 \pm 3.4) \times 10^{-19}$ e cm	T and P
p electric dipole moment	$< 4 \times 10^{-21}$ e cm	T and P
n electric dipole moment	$(2.3 \pm 2.3) \times 10^{-25}$ e cm	T and P
Λ electric dipole moment	$< 1.5 \times 10^{-16}$ e cm	T and P
α' / a from $\mu \to e\bar{\nu}\nu$	-0.12 ± 0.10	T
β' / a from $\mu \to e\bar{\nu}\nu$	-0.029 ± 0.037	T
Im ξ in $K^{\pm}_{\mu 3}$ decay (from transverse μ pol.)	-0.017 ± 0.025	T
Im ξ in $K^{0}_{\mu 3}$ decay (from transverse μ pol.)	-0.020 ± 0.022	T

Discrete Space Time Symmetries (cont'd)

Quantity[a]	Value[b]	Symmetry Tested or Violated
$\phi(g_A) - \phi(g_V)$ for n	$(180.11 \pm 0.17)^\circ$	T (0 ° or 180°)
n 3-vector corr. coeff.	-0.0007 ± 0.0014	T
$K^\pm \to \pi^\pm\pi^+\pi^-$ rate difference / average	$(0.07 \pm 0.12)\%$	CP
$K^\pm \to \pi^\pm 2\pi^0$ rate difference / average	$(-0.03 \pm 0.55)\%$	CP
$K^\pm \to \pi^\pm\pi^0\gamma$ rate difference / average	$(0.9 \pm 3.3)\%$	CP
$K \to 3\pi^\pm$ slope $(g^+ - g^-)$ / sum	$(-0.7 \pm 0.5)\%$	CP
$\lvert\eta_{+-0}\rvert^2 = \Gamma(K_S^0 \to \pi^+\pi^-\pi^0) / \Gamma(K_L^0 \to \pi^+\pi^-\pi^0)$	< 0.12	CP
$\lvert\eta_{000}\rvert^2 = \Gamma(K_S^0 \to 3\pi^0) / \Gamma(K_L^0 \to 3\pi^0)$	< 0.1	CP
Charge asymm. j in $K_L^0 \to \pi^+\pi^-\pi^0$	0.0011 ± 0.0008	CP
$K_L^0 \to (\mu^+\pi^-\nu - \mu^-\pi^+\nu)$ / sum	$(0.319 \pm 0.038)\%$	CP (violated)
$K_L^0 \to (e^+\pi^-\nu - e^-\pi^+\nu)$ / sum	$(0.333 \pm 0.014)\%$	CP (violated)
$\lvert\eta_{00}\rvert = \lvert A(K_L^0 \to \pi^0\pi^0)/A(K_S^0 \to \pi^0\pi^0)\rvert$	$(2.33 \pm 0.08) \times 10^{-3}$	CP (violated)
$\lvert\eta_{+-}\rvert = \lvert A(K_L^0 \to \pi^+\pi^-)/A(K_S^0 \to \pi^+\pi^-)\rvert$	$(2.274 \pm 0.022) \times 10^{-3}$	CP (violated)
ϕ_{+-}: phase of η_{+-}	$(44.6 \pm 1.2)^\circ$	CP (violated)
ϕ_{00}: phase of η_{00}	$(54 \pm 5)^\circ$	CP (violated)
Re ϵ	$(1.621 \pm 0.088) \times 10^{-3}$	CP (violated)
$(g_{e^+} - g_{e^-})$ / average	$(2.2 \pm 6.4) \times 10^{-11}$	CPT
$(g_{\mu^+} - g_{\mu^-})$ / average	$(-2.6 \pm 1.6) \times 10^{-8}$	CPT
$(\mu_p^\mu - \mu_{\bar{p}}^\mu)$ / average	$(-1 \pm 7) \times 10^{-3}$	CPT

$\pi^+ - \pi^-$ mass difference / average	$(2 \pm 5) \times 10^{-4}$	CPT
$K^+ - K^-$ mass difference / average	$(-0.6 \pm 1.8) \times 10^{-4}$	CPT
$\lvert K^0 - \bar{K}^0 \rvert$ mass difference / average	$< 6 \times 10^{-19}$	CPT
$p - \bar{p}$ mass difference / average	$(7 \pm 4) \times 10^{-5}$	CPT
$\Lambda - \bar{\Lambda}$ mass difference / average	$(7 \pm 7) \times 10^{-6}$	CPT
$\Xi^- - \bar{\Xi}^+$ mass difference / average	$(1.1 \pm 2.7) \times 10^{-4}$	CPT
$\Omega^- - \bar{\Omega}^+$ mass difference / average	$(-4 \pm 6) \times 10^{-4}$	CPT
$\mu^+ - \mu^-$ mean life difference / average	$(3 \pm 8) \times 10^{-5}$	CPT
$\pi^+ - \pi^-$ mean life difference / average	$(5 \pm 7) \times 10^{-4}$	CPT
$K^+ - K^-$ mean life difference / average	$(1.1 \pm 0.9) \times 10^{-3}$	CPT
$\Lambda - \bar{\Lambda}$ mean life difference / average	$(4.4 \pm 8.5) \times 10^{-2}$	CPT
$\Xi^- - \bar{\Xi}^+$ mean life difference / average	(0.02 ± 0.18)	CPT
$K^\pm \to \mu^\pm \nu$ rate difference / average	$(-0.54 \pm 0.41)\%$	CPT
$K^\pm \to \pi^\pm \pi^0$ rate difference / average	$(0.8 \pm 1.2)\%$	CPT[i]

a. Branching fractions are described by a shorthand notation, e.g., "$\mu^+ \to e^+\gamma$/all" means $\Gamma(\mu^+ \to e^+\gamma)/\Gamma(\mu^+ \to \text{all})$.
b. Limits are given at 90% confidence level while errors are given as ± 1 standard deviation.
c. Test of additive vs. multiplicative lepton family number conservation.
d. Lepton family number conservation means separate conservation of e-number, μ-number, and τ-number.
e. These limits are derived from the analysis of neutrino oscillation experiments.
f. Violation of total lepton number conservation also implies violation of lepton family number conservation.
g. Can be violated in second-order weak interactions.
h. Orthopositronium data are from Liu and Roberts, Phys. Rev. Lett. **16**, 67 (1966).
i. Neglecting photon channels. See, e.g., A. Pais and S.B. Treiman, Phys. Rev. **D12**, 2744 (1975).

KINEMATICS, DECAYS, AND SCATTERING

A. LORENTZ TRANSFORMATIONS

The energy E and three-momentum $\vec{p}$ of a particle form a four-vector $p = (E, \vec{p})$. Viewed from a second frame with velocity $\vec{v} = \beta c\hat{z}$ relative to the original frame, the components of p are $(E', \vec{p}')$, where

$$E' = \gamma E - \beta\gamma p_z ,$$

$$p_z' = \gamma p_z - \beta\gamma E ,$$

$$p_x' = p_x ; \; p_y' = p_y ,$$

and where $\gamma = (1 - \beta^2)^{-1/2}$. It follows that the scalar product of two momenta, $p_1 \cdot p_2 = E_1 E_2 - \vec{p}_1 \cdot \vec{p}_2$, is invariant, that is, frame independent.

If $\vec{p}$ makes an angle θ with the z-axis, then $\vec{p}'$ makes an angle θ' with the z-axis,

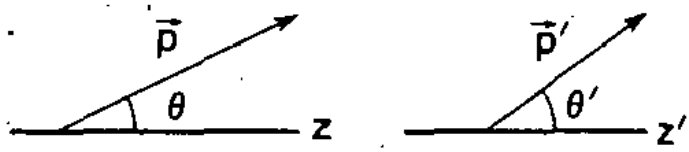

where

$$\tan\theta' = \frac{|\vec{p}| \sin\theta}{\gamma |\vec{p}| \cos\theta - \beta\gamma E}$$

In particular, if the unprimed frame is the center of mass and the primed frame is the lab, and if the velocity of the center of mass in the lab frame is $\beta^* \hat{z}$, we use $\beta = -\beta^*$ above to find (denoting $p_{cm} = |\vec{p}_{cm}|$)

$$\tan\theta_{lab} = \frac{p_{cm} \sin\theta_{cm}}{\gamma^* p_{cm} \cos\theta_{cm} + \beta^* \gamma^* E_{cm}}$$

If $\beta^* > p_{cm}/E_{cm}$, the particle is necessarily moving forward in the lab and

$$(\tan\theta_{lab})_{max} = \frac{p_{cm}}{\gamma^* E_{cm}} \frac{1}{\sqrt{\beta^{*2} - p_{cm}^2/E_{cm}^2}}$$

We denote $p_\perp = p_\perp{}' = |\vec{p}| \sin\theta_{cm}$. Then given a fixed p_{cm} and E_{cm}, as, for example, in a two-to-two scattering process, as θ_{cm} varies from 0 to 2π the lab momentum describes an ellipse:

$$\frac{(p_z' - \beta^* \gamma^* E_{cm})^2}{\gamma^{*2} p_{cm}^2} + \frac{p_\perp'^2}{p_{cm}^2} = 1 .$$

B. DECAYS

B.1.a Two-body kinematics:

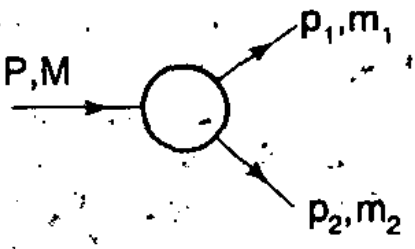

In the rest frame of the decaying particle,

$$E_1 = \frac{M^2 + m_1^2 - m_2^2}{2M} ,$$

$$|\vec{p}_1| = \left[\frac{[M^2 - (m_1 + m_2)^2][M^2 - (m_1 - m_2)^2]}{4M^2} \right]^{1/2} .$$

B.1.b Two-body partial decay rate: If $\mathscr{M}$ is the Lorentz invariant matrix element (see Section D below), the partial decay rate in the rest frame of the decaying particle is

$$d\Gamma = \frac{1}{32\pi^2} |\mathscr{M}|^2 \frac{|\vec{p}_1| \, d\Omega}{M^2} ,$$

where $d\Omega$ is the differential solid angle in the rest frame of the decaying particle.

B.2.a Three-body kinematics:

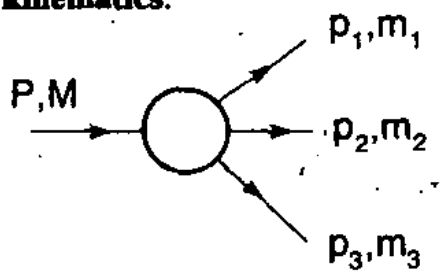

We denote

$$p_{12} = p_1 + p_2 \,, \; m_{12}^2 = p_{12}^2 \,, \text{ etc.}$$

Then

$$m_{12}^2 + m_{23}^2 + m_{13}^2 = M^2 + m_1^2 + m_2^2 + m_3^2 \,.$$

The invariant mass of the pair 1-2 is related to the energy of particle 3 in the rest frame of M,

$$m_{12}^2 = (P - p_3)^2 = M^2 + m_3^2 - 2ME_3 \,.$$

B.2.b Dalitz plot: If the orientation of the decaying particle is ignored, there are two kinematic variables, which may be chosen to be m_{12}^2 and m_{13}^2. For fixed m_{12}^2, the range of m_{13}^2 is determined by letting $\vec{p}_1$ be parallel or antiparallel to $\vec{p}_3$. In the rest frame of $(p_1 + p_2)$, the energy of particle 3 is $E_3^* = (M^2 - m_{12}^2 - m_3^2)/(2m_{12})$, and that of particle 1 is $E_1^* = (m_{12}^2 + m_1^2 - m_2^2)/(2m_{12})$. Thus for a given m_{12}^2,

$$(m_{13}^2)_{\max} = (E_1^* + E_3^*)^2 - \left(\sqrt{E_1^{*2} - m_1^2} - \sqrt{E_3^{*2} - m_3^2} \right)^2$$

$$(m_{13}^2)_{\min} = (E_1^* + E_3^*)^2 - \left(\sqrt{E_1^{*2} - m_1^2} + \sqrt{E_3^{*2} - m_3^2} \right)^2 .$$

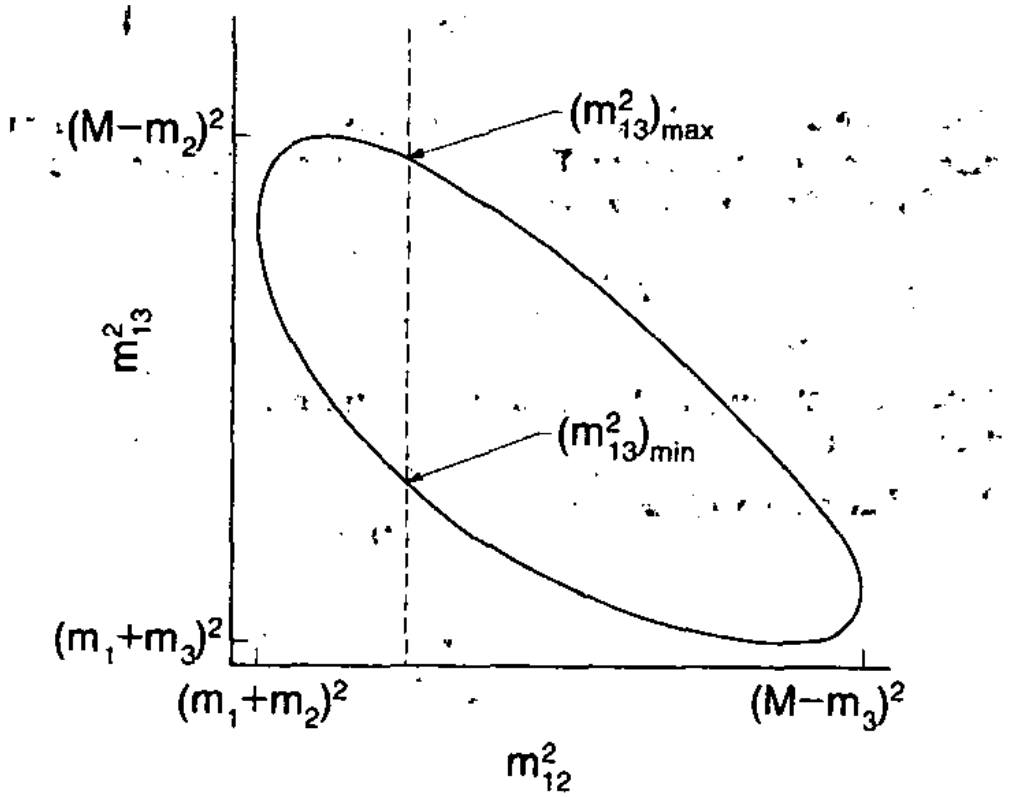

The scatter plot in m_{12}^2 and m_{13}^2 is called a Dalitz plot. Phase space density is uniform across the plot. See below.

B.2.c Three-body phase space: Fixing the energies E_1 and E_2 of two of the final state particles in the M rest frame determines the relative orientation of the three outgoing particles. Their momenta may then be regarded as a rigid body whose orientation with respect to the initial particle is specified by the Euler angles α, β, and γ. The partial decay rate in the M rest frame is

$$d\Gamma = \frac{(2\pi)^{-5}}{16M} |\mathcal{M}|^2 \, dE_1 \, dE_2 \, d\alpha \, d\cos\beta \, d\gamma \, .$$

If the angles are integrated out, we have the Dalitz plot form,

$$d\Gamma = \frac{(2\pi)^{-3}}{8M} |\mathcal{M}|^2 \, dE_1 \, dE_2 = \frac{(2\pi)^{-3}}{32M^3} |\mathcal{M}|^2 \, dm_{12}^2 dm_{23}^2 \, .$$

An alternative expression is

$$d\Gamma = \frac{(2\pi)^{-5}}{16M^2} |\mathcal{M}|^2 \, |\vec{p}_1^{\,*}| \, |\vec{p}_3| \, dm_{12} \, d\Omega_1^* \, d\Omega_3 \, ,$$

where

$$|\vec{p}_1^{\,*}| = \left[\frac{[m_{12}^2 - (m_1 + m_2)^2][m_{12}^2 - (m_1 - m_2)^2]}{4m_{12}^2} \right]^{1/2}$$

is the momentum of particle 1 in the rest frame of m_{12},

$$|\vec{p}_3| = \left[\frac{[M^2 - (m_{12} + m_3)^2][M^2 - (m_{12} - m_3)^2]}{4M^2} \right]^{1/2}$$

is the momentum of particle 3 in the M rest frame, $d\Omega_1^*$ is the solid angle element for particle 1 in the 1-2 rest frame, and $d\Omega_3$ is the solid angle element for particle 3 in the M rest frame.

B.3 n-body phase space:

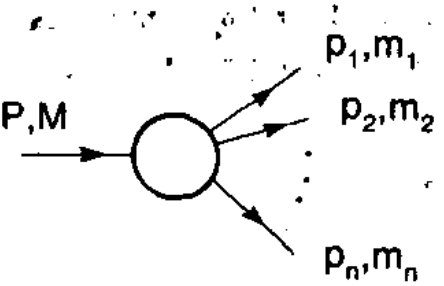

The partial decay rate in the M rest frame is

$$d\Gamma = \frac{(2\pi)^4}{2M} |\mathcal{M}|^2 \, d\Phi_n(P; p_1, \cdots, p_n) ,$$

where

$$d\Phi_n(P; p_1, \cdots, p_n) = \delta^4(P - \sum_{i=1}^{n} p_i) \prod_{i=1}^{n} \frac{d^3 p_i}{(2\pi)^3 2E_i} .$$

In particular,

$$d\Phi_2(P; p_1, p_2) = (2\pi)^{-6} \frac{|\vec{p}_1^{\,*}|}{4M} d\Omega_1^* ,$$

where $|\vec{p}_1^{\,*}|$ is the momentum of particle 1 in the M rest frame and $d\Omega_1^*$ is the solid angle element in the same frame.

Phase space for n particles can be related to that for $n-1$ by treating particles 1 and 2 as a single system of momentum $p_{12} = p_1 + p_2$ and mass squared $m_{12}^2 = p_{12}^2$. Thus

$$d\Phi_n(P; p_1, p_2, \cdots, p_n) = d\Phi_{n-1}(P; p_{12}, p_3, \cdots, p_n)$$

$$\times d\Phi_2(p_{12}; p_1, p_2) (2\pi)^3 dm_{12}^2 .$$

C. SCATTERING

Throughout Section C, we set $\hbar = 1$, $c = 1$. Use $\hbar c = 197.3$ MeV fermi, and $(\hbar c)^2 = 0.3894$ GeV^2 mb for conversions.

C.1 Partial waves: The amplitude in the center of mass for elastic scattering of spinless particles may be written in a partial wave expansion

$$f(k,\theta) = \frac{1}{k} \sum_{\ell} (2\ell+1) \, a_\ell \, P_\ell(\cos\theta) ,$$

where k is the c.m. momentum, θ is the c.m. scattering angle, $a_\ell = (\eta_\ell e^{2i\delta_\ell} - 1)/2i$, $0 \leq \eta_\ell \leq 1$, and δ_ℓ is the phase shift of the ℓ^{th} partial wave. For purely elastic scattering, $\eta_\ell = 1$. The differential cross section is

$$\frac{d\sigma}{d\Omega} = |f(k,\theta)|^2 .$$

The optical theorem is

$$\sigma_{tot} = \frac{4\pi}{k} \text{ Im } f(k,0) ,$$

and the cross section in the ℓ^{th} partial wave is

$$\sigma_\ell = \frac{4\pi}{k^2} (2\ell + 1) \, |a_\ell|^2 \leq \frac{4\pi (2\ell + 1)}{k^2} .$$

The partial-wave amplitude a_ℓ can be displayed in an Argand plot.

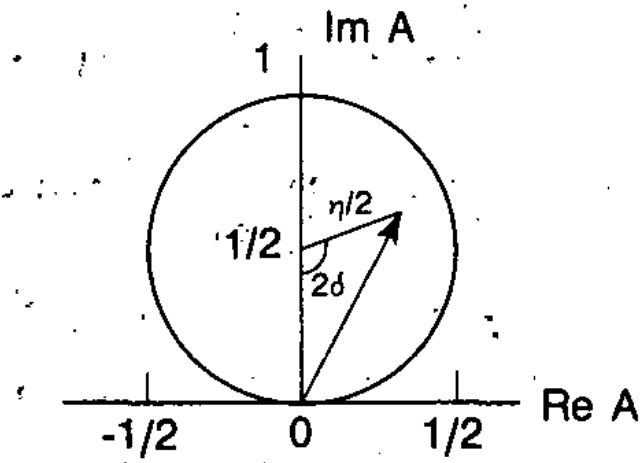

The usual Lorentz invariant matrix element $\mathcal{M}$ (see Section D below) for the elastic process is related to $f(k,\theta)$ by

$$\mathcal{M} = -8\pi\sqrt{s}\, f(k,\theta) ,$$

so

$$\sigma_{tot} = -\frac{1}{2k\sqrt{s}} \text{Im}\mathcal{M}(t=0) ,$$

where s and t are the center-of-mass energy squared and momentum transfer squared, respectively (see Section C.3.a).

C.2 Resonances: The Breit-Wigner form for a_ℓ with a resonance at c.m. energy E_R, elastic width Γ_{el}, and total width Γ_{tot} is

$$a_\ell = \frac{\frac{1}{2}\Gamma_{el}}{E_R - E - \frac{i}{2}\Gamma_{tot}} ,$$

where E is the c.m. energy. This gives a circle in the Argand plot with center $ix_{el}/2$ and radius $x_{el}/2$, where $x_{el} = \Gamma_{el}/\Gamma_{tot}$. The quantity x_{el} is called the elasticity. The amplitude has a pole at $E = E_R - i\Gamma_{tot}/2$.

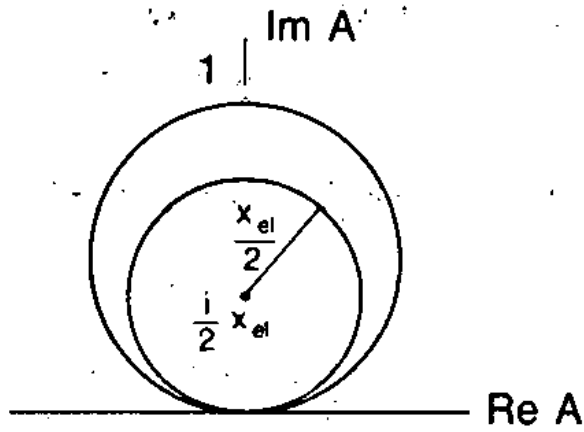

The Breit-Wigner cross section for a spin-J resonance produced in the collision of particles of spin S_1 and S_2 is

$$\sigma_{BW}(E) = \frac{(2J+1)}{(2S_1+1)(2S_2+1)} \frac{\pi}{k^2} \frac{B_{in}B_{out}\Gamma_{tot}^2}{(E-E_R)^2 + \Gamma_{tot}^2/4},$$

where k is the c.m. momentum, E is the c.m. energy, and B_{in} and B_{out} are the branching fractions of the resonance into the entrance and exit channels. The $2S + 1$ factors are the multiplicities of the incident spin states, so they are replaced by 2 for photons, etc.

C.3.a Two-body scattering kinematics:

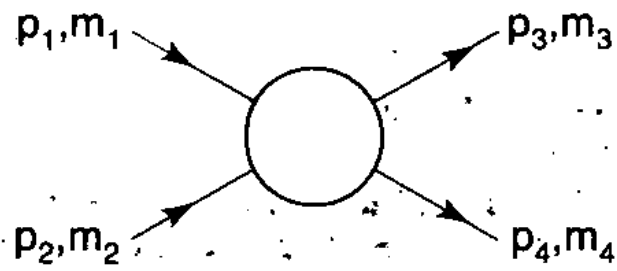

In the center of mass,

$$E_{1cm} = \frac{s + m_1^2 - m_2^2}{2\sqrt{s}},$$

$$p_{1cm} = \left[\frac{[s-(m_1+m_2)^2][s-(m_1-m_2)^2]}{4s} \right]^{1/2}$$

$$= \frac{p_{1lab} m_2}{\sqrt{s}} ,$$

where $\sqrt{s}$ is the total c.m. energy. The Lorentz invariant Mandelstam variables are

$$s = (p_1+p_2)^2 = (p_3+p_4)^2$$

$$= m_1^2 + 2E_1E_2 - 2\vec{p}_1\cdot\vec{p}_2 + m_2^2 ,$$

$$t = (p_1-p_3)^2 = (p_2-p_4)^2$$

$$= m_1^2 - 2E_1E_3 + 2\vec{p}_1\cdot\vec{p}_3 + m_3^2 ,$$

$$u = (p_1-p_4)^2 = (p_2-p_3)^2$$

$$= m_1^2 - 2E_1E_4 + 2\vec{p}_1\cdot\vec{p}_4 + m_4^2 ,$$

and they satisfy

$$s+t+u = m_1^2 + m_2^2 + m_3^2 + m_4^2 .$$

If θ_{cm} is the c.m. scattering angle between particles 1 and 3, then (denoting $p_{1cm} = |\vec{p}_{1cm}|$, $p_{3cm} = |\vec{p}_{3cm}|$)

$$t = (E_{1cm} - E_{3cm})^2 - (p_{1cm} - p_{3cm})^2 - 4p_{1cm}p_{3cm}\sin^2(\theta_{cm}/2) .$$

For $\theta_{cm} = 0$, $-t$ is a minimum.

C.3.b Two-body differential cross sections: In the center of mass or lab,

$$\frac{d\sigma}{dt} = \frac{1}{64\pi s} \frac{1}{p_{1cm}^2} |\mathcal{M}|^2 .$$

In the center of mass,

$$\frac{d\sigma}{d\Omega_{cm}} = \frac{p_{1cm}p_{3cm}}{\pi} \frac{d\sigma}{dt}$$

C.4 n-body differential cross sections:

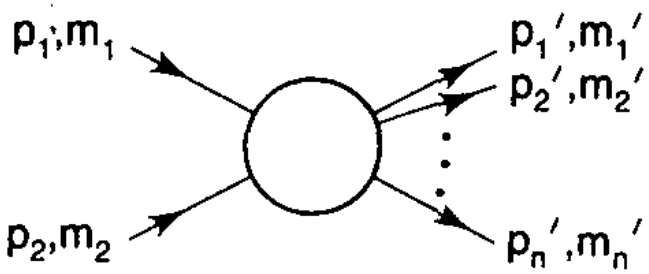

In the c.m. or lab

$$d\sigma = \frac{(2\pi)^4 |\mathcal{M}|^2}{4\sqrt{(p_1 \cdot p_2)^2 - m_1^2 m_2^2}} \, d\Phi_n(p_1 + p_2; p_1', p_2', \cdots, p_n') ,$$

where n-body phase space, $d\Phi_n$, is described in Section B.3 above.

Note that $\sqrt{(p_1 \cdot p_2)^2 - m_1^2 m_2^2} = p_{1lab} m_2 = p_{1cm} \sqrt{s}$.

C.5.a Leptoproduction kinematics:

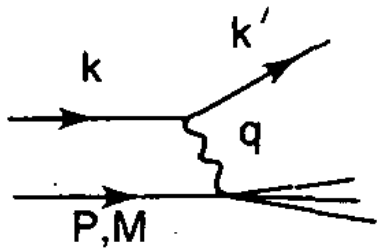

$q = k - k'$ is the four-momentum transferred to the target.

Invariant quantities:

$\nu = \frac{q \cdot P}{M} = E - E'$ is the lepton's energy loss in the lab (in earlier literature sometimes $\nu = q \cdot P$). Here, E and E′ are the initial and final lepton energies in the lab.

$Q^2 = -q^2 = 2(EE' - \vec{k} \cdot \vec{k}') - m_\ell^2 - m_{\ell'}^2$ where $m_\ell (m_{\ell'})$ is the initial (final) lepton mass. If $EE' \sin^2(\theta/2) \gg m_\ell^2$, $m_{\ell'}^2$, then

$\simeq 4EE' \sin^2(\theta/2)$, where θ is the lepton's scattering angle in the lab.

$x = \frac{Q^2}{2M\nu}$ In the parton model, x is the fraction of the target nucleon's momentum carried by the struck quark. See section on Quark Parton Model.

$y = \frac{q\cdot P}{k\cdot P} = \frac{\nu}{E}$ is the fraction of the lepton's energy lost in the lab.

$W^2 = (P+q)^2 = M^2 + 2M\nu - Q^2$ is the mass squared of the system recoiling against the lepton.

C.5.b Leptoproduction cross sections:

$$\frac{d^2\sigma}{dx\,dy} = 2M\nu E\frac{d^2\sigma}{d\nu\,dQ^2} = \frac{2\pi M\nu}{E'}\frac{d^2\sigma}{d\Omega_{lab}\,dE'} = 2xME\frac{d^2\sigma}{dx\,dQ^2}.$$

C.5.b.i Electroproduction structure functions:

$$\frac{d^2\sigma}{dx\,dy} = \frac{8\pi\alpha^2 ME}{Q^4}\left[\frac{1+(1-y)^2}{2}2xF_1^{em} + (1-y)(F_2^{em} - 2xF_1^{em}) - \frac{M}{2E}xyF_2^{em}\right].$$

$F_1^{em}(x, Q^2)$ and $F_2^{em}(x, Q^2)$ are the (unpolarized) structure functions, which are, in the naive parton model, independent of Q^2.

C.5.b.ii Neutrino production structure functions:

$$\frac{d^2\sigma^{\nu}}{dx\,dy} = \frac{G_F^2 ME}{\pi}\left[(1-y-\frac{M}{2E}xy)\,F_2^{\nu} + \frac{y^2}{2}2xF_1^{\nu} + (y-\frac{y^2}{2})xF_3^{\nu}\right],$$

$$\frac{d^2\sigma^{\bar{\nu}}}{dx\,dy} = \frac{G_F^2 ME}{\pi}\left[(1-y-\frac{M}{2E}xy)\,F_2^{\bar{\nu}} + \frac{y^2}{2}2xF_1^{\bar{\nu}} - (y-\frac{y^2}{2})xF_3^{\bar{\nu}}\right].$$

The structure functions $F_i^{\gamma,\bar{\nu}}$ are related to quark distributions in the parton model (see section on Quark Parton Model). There are separate F_i's for neutral- and charged-current processes.

C.6.a e^+e^- annihilation: For pointlike spin-1/2 fermions in the c.m., the differential cross section for $e^+e^- \to f\bar{f}$ via single photon annihilation is

$$\frac{d\sigma}{d\Omega} = \frac{\alpha^2}{4s}\beta\left[1 + \cos^2\theta + (1-\beta^2)\sin^2\theta\right]e_Q^2 ,$$

where β is the velocity of the final state fermion in the center of mass, and where e_Q is the charge of the fermion in units of the proton charge. For $\beta \to 1$,

$$\sigma = \frac{4\pi\alpha^2}{3s}e_Q^2 = \frac{86.8\, e_Q^2\ \text{nb}}{s(\text{GeV}^2)} .$$

C.6.b e^+e^- two-photon process: In the equivalent photon approximation, the cross section for $e^+e^- \to e^+e^-X$ is related to the cross section for $\gamma\gamma \to X$ by

$$d\sigma_{e^+e^- \to e^+e^-X}(s) = \eta^2 \int d\omega\, f(\omega)\, d\sigma_{\gamma\gamma \to X}(\omega s) ,$$

where

$$\eta \approx \frac{\alpha}{2\pi}\ell n\left[\frac{s}{4m_e^2}\right]$$

and

$$f(\omega) = \frac{1}{\omega}\left[(2+\omega)^2 \ell n\frac{1}{\omega} - 2(1-\omega)(3+\omega)\right] .$$

For the production of a resonance of mass m_R and spin J,

$$\sigma(e^+e^- \to e^+e^-R) = \eta^2 \frac{(2J+1)8\pi^2\,\Gamma(R \to \gamma\gamma)}{m_R s} f\left(\frac{m_R^2}{s}\right) .$$

C.7 Inclusive hadronic reactions: A particle's momentum can be parametrized by selecting a particular direction for the z-axis and writing

$$(E = m_\perp \cosh y,\ p_z = m_\perp \sinh y,\ p_x,\ p_y) ,$$

where

$$m_\perp^2 = m^2 + p_x^2 + p_y^2 ,$$

$$y = \frac{1}{2}\ell n\left(\frac{E+p_z}{E-p_z}\right) = \ell n\left(\frac{E+p_z}{m_\perp}\right) = \tanh^{-1}\left(\frac{p_z}{E}\right).$$

The variable y is called the rapidity. A boost in the z-direction then modifies y by $y \to y + \Delta$, where $\gamma = \cosh\Delta$, $\beta = \tanh\Delta$. Thus the shape of the distribution dN/dy is invariant under such a boost, and

$$E\frac{d^3\sigma}{d^3p} = \frac{d^3\sigma}{dy\,d^2p_\perp}.$$

Feynman's x variable is defined to be

$$x = \left(\frac{p_z}{p_{z\,max}}\right)_{cm} \approx \frac{2p_{z\,cm}}{\sqrt{s}} \approx \frac{2m_\perp \sinh y_{cm}}{\sqrt{s}}.$$

For y_{cm} not small ($e^{-2y_{cm}} \ll 1$)

$$x \approx \frac{m_\perp}{\sqrt{s}}\, e^{y_{cm}}$$

and

$$(y_{cm})_{max} = \ell n\frac{\sqrt{s}}{m}.$$

D. LORENTZ INVARIANT AMPLITUDES

The quantity $-i\mathcal{M}$ is determined in perturbation theory by the Feynman rules. Our convention above is consistent with the Appendices of Bjorken and Drell except that fermion spinors are normalized so that $\bar{u}u = 2m$, etc. In particular, the S-matrix for two-body scattering is

$$\langle p_1' p_2' | S | p_1 p_2\rangle = I - i(2\pi)^4\delta^4(p_1 + p_2 - p_1' - p_2')$$

$$\times \frac{\mathcal{M}(p_1,p_2;p_1',p_2')}{(2E_1)^{1/2}(2E_2)^{1/2}(2E_1')^{1/2}(2E_2')^{1/2}},$$

where the states are normalized so

$$\langle p' | p\rangle = (2\pi)^3\delta^3(\vec{p} - \vec{p}').$$

C.M. ENERGY, MOMENTUM VS. BEAM MOMENTUM

$$E_{cm}dE_{cm} = m_p dT_{beam} = m_p v_{beam} dP_{beam} = m_p dP_{beam}$$

PBEAM (GEV/C)	C. M. ENERGY (GEV)				MOMENTUM IN C. M. (GEV/C)			
	$\gamma p, \nu p$ $\approx ep$	πp	Kp	pp	$\gamma p, \nu p$ $\approx ep$	πp	Kp	pp
0.00	.938	1.078	1.432	1.877	.000	.000	.000	.000
0.02	.958	1.079	1.432	1.877	.020	.017	.013	.010
0.04	.977	1.083	1.433	1.877	.038	.035	.026	.020
0.06	.996	1.089	1.434	1.878	.056	.052	.039	.030
0.08	1.015	1.096	1.436	1.878	.074	.068	.052	.040
0.10	1.033	1.105	1.439	1.879	.091	.085	.065	.050
0.12	1.051	1.116	1.441	1.880	.107	.101	.078	.060
0.14	1.069	1.127	1.445	1.882	.123	.117	.091	.070
0.16	1.087	1.139	1.448	1.883	.138	.132	.104	.080
0.18	1.104	1.152	1.453	1.885	.153	.147	.116	.090
0.20	1.121	1.165	1.457	1.887	.167	.161	.129	.099
0.22	1.137	1.178	1.462	1.889	.182	.175	.141	.109
0.24	1.154	1.192	1.468	1.892	.195	.189	.153	.119
0.26	1.170	1.206	1.473	1.894	.209	.202	.166	.129
0.28	1.186	1.219	1.480	1.897	.222	.215	.178	.138
0.30	1.201	1.233	1.486	1.900	.234	.228	.189	.148
0.32	1.217	1.247	1.493	1.903	.247	.241	.201	.158
0.34	1.232	1.261	1.500	1.906	.259	.253	.213	.167
0.36	1.247	1.275	1.507	1.910	.271	.265	.224	.177
0.38	1.262	1.288	1.514	1.913	.282	.277	.235	.186
0.40	1.277	1.302	1.522	1.917	.294	.288	.247	.196
0.42	1.292	1.315	1.530	1.921	.305	.300	.258	.205
0.44	1.306	1.329	1.538	1.925	.316	.311	.268	.214
0.46	1.320	1.342	1.546	1.929	.327	.322	.279	.224
0.48	1.335	1.356	1.554	1.934	.337	.332	.290	.233
0.50	1.349	1.369	1.563	1.938	.348	.343	.300	.242
0.52	1.362	1.382	1.571	1.943	.358	.353	.310	.251
0.54	1.376	1.395	1.580	1.947	.368	.363	.321	.260
0.56	1.390	1.408	1.589	1.952	.378	.373	.331	.269
0.58	1.403	1.421	1.598	1.957	.388	.383	.341	.278
0.60	1.416	1.434	1.607	1.962	.397	.393	.350	.287
0.62	1.430	1.447	1.616	1.968	.407	.402	.360	.296
0.64	1.443	1.459	1.625	1.973	.416	.412	.370	.304
0.66	1.456	1.472	1.634	1.978	.425	.421	.379	.313
0.68	1.468	1.484	1.643	1.984	.434	.430	.388	.322
0.70	1.481	1.496	1.653	1.989	.443	.439	.397	.330
0.72	1.494	1.509	1.662	1.995	.452	.448	.406	.339
0.74	1.506	1.521	1.671	2.001	.461	.457	.415	.347
0.76	1.519	1.533	1.681	2.007	.470	.465	.424	.355
0.78	1.531	1.545	1.690	2.013	.478	.474	.433	.364
0.80	1.543	1.557	1.699	2.019	.486	.482	.442	.372
0.82	1.555	1.569	1.709	2.025	.495	.490	.450	.380
0.84	1.567	1.580	1.718	2.031	.503	.499	.459	.388
0.86	1.579	1.592	1.728	2.037	.511	.507	.467	.396
0.88	1.591	1.604	1.737	2.043	.519	.515	.475	.404
0.90	1.603	1.615	1.747	2.050	.527	.523	.484	.412
0.92	1.615	1.627	1.756	2.056	.535	.531	.492	.420
0.94	1.626	1.638	1.765	2.062	.542	.538	.500	.428
0.96	1.638	1.649	1.775	2.069	.550	.546	.508	.435
0.98	1.649	1.661	1.784	2.075	.558	.554	.515	.443

PBEAM (GEV/C)	C. M. ENERGY (GEV)				MOMENTUM IN C. M. (GEV/C)			
	$\gamma p, \nu p$ $\rightarrow ep$	πp	Kp	pp	$\gamma p, \nu p$ $\rightarrow ep$	πp	Kp	pp
1.00	1.660	1.672	1.794	2.082	.565	.561	.523	.451
1.05	1.688	1.699	1.817	2.098	.584	.580	.542	.470
1.10	1.716	1.726	1.840	2.115	.601	.598	.561	.488
1.15	1.743	1.753	1.863	2.132	.619	.615	.579	.506
1.20	1.770	1.780	1.887	2.149	.636	.633	.597	.524
1.25	1.796	1.806	1.909	2.167	.653	.650	.614	.541
1.30	1.822	1.831	1.932	2.184	.669	.666	.631	.559
1.35	1.848	1.857	1.955	2.201	.686	.682	.648	.575
1.40	1.873	1.882	1.977	2.219	.701	.698	.664	.592
1.45	1.898	1.906	2.000	2.236	.717	.714	.680	.608
1.50	1.922	1.931	2.022	2.254	.732	.729	.696	.624
1.55	1.947	1.955	2.044	2.272	.747	.744	.712	.640
1.60	1.970	1.978	2.065	2.289	.762	.759	.727	.656
1.65	1.994	2.002	2.087	2.307	.776	.773	.742	.671
1.70	2.018	2.025	2.109	2.325	.791	.788	.756	.686
1.75	2.041	2.048	2.130	2.342	.805	.802	.771	.701
1.80	2.064	2.071	2.151	2.360	.818	.816	.785	.716
1.85	2.086	2.093	2.172	2.378	.832	.829	.799	.730
1.90	2.109	2.115	2.193	2.395	.845	.843	.813	.744
1.95	2.131	2.137	2.213	2.413	.859	.856	.827	.758
2.0	2.153	2.159	2.234	2.430	.872	.869	.840	.772
2.1	2.196	2.202	2.274	2.465	.897	.895	.866	.799
2.2	2.238	2.244	2.314	2.500	.922	.920	.892	.826
2.3	2.280	2.286	2.353	2.534	.947	.944	.917	.852
2.4	2.320	2.326	2.392	2.568	.970	.968	.941	.877
2.5	2.360	2.366	2.430	2.602	.994	.991	.965	.901
2.6	2.400	2.405	2.468	2.636	1.02	1.01	.989	.926
2.7	2.439	2.444	2.505	2.669	1.04	1.04	1.01	.949
2.8	2.477	2.482	2.542	2.702	1.06	1.06	1.03	.972
2.9	2.514	2.520	2.578	2.735	1.08	1.08	1.06	.995
3.0	2.551	2.556	2.613	2.768	1.10	1.10	1.08	1.02
3.1	2.588	2.593	2.649	2.800	1.12	1.12	1.10	1.04
3.2	2.624	2.629	2.683	2.832	1.14	1.14	1.12	1.06
3.3	2.660	2.664	2.718	2.863	1.16	1.16	1.14	1.08
3.4	2.695	2.699	2.752	2.895	1.18	1.18	1.16	1.10
3.5	2.729	2.734	2.785	2.926	1.20	1.20	1.18	1.12
3.6	2.763	2.768	2.818	2.957	1.22	1.22	1.20	1.14
3.7	2.797	2.801	2.851	2.987	1.24	1.24	1.22	1.16
3.8	2.830	2.835	2.884	3.018	1.26	1.26	1.24	1.18
3.9	2.863	2.868	2.916	3.048	1.28	1.28	1.26	1.20
4.0	2.896	2.900	2.947	3.077	1.30	1.29	1.27	1.22
4.1	2.928	2.932	2.979	3.107	1.31	1.31	1.29	1.24
4.2	2.960	2.964	3.010	3.136	1.33	1.33	1.31	1.26
4.3	2.992	2.996	3.041	3.165	1.35	1.35	1.33	1.27
4.4	3.023	3.027	3.071	3.194	1.37	1.36	1.34	1.29
4.5	3.054	3.058	3.101	3.223	1.38	1.38	1.36	1.31
4.6	3.084	3.088	3.131	3.251	1.40	1.40	1.38	1.33
4.7	3.115	3.118	3.161	3.279	1.42	1.41	1.40	1.34
4.8	3.144	3.148	3.190	3.307	1.43	1.43	1.41	1.36
4.9	3.174	3.178	3.220	3.335	1.45	1.45	1.43	1.38

PBEAM (GEV/C)	C. M. ENERGY (GEV)				MOMENTUM IN C. M. (GEV/C)			
	$\gamma p, \nu p$ $\approx ep$	πp	Kp	pp	$\gamma p, \nu p$ $\approx ep$	πp	Kp	pp
5.0	3.204	3.207	3.248	3.363	1.46	1.46	1.44	1.40
5.5	3.347	3.350	3.389	3.497	1.54	1.54	1.52	1.48
6.0	3.484	3.487	3.524	3.627	1.62	1.61	1.60	1.55
6.5	3.616	3.619	3.655	3.753	1.69	1.69	1.67	1.63
7.0	3.744	3.747	3.781	3.875	1.75	1.75	1.74	1.70
7.5	3.867	3.870	3.902	3.993	1.82	1.82	1.80	1.76
8.0	3.987	3.989	4.021	4.108	1.88	1.88	1.87	1.83
8.5	4.103	4.105	4.135	4.220	1.94	1.94	1.93	1.89
9.0	4.215	4.218	4.247	4.329	2.00	2.00	1.99	1.95
9.5	4.325	4.328	4.356	4.436	2.06	2.06	2.05	2.01
10	4.432	4.435	4.462	4.540	2.12	2.12	2.10	2.07
11	4.639	4.642	4.668	4.741	2.22	2.22	2.21	2.18
12	4.837	4.839	4.864	4.934	2.33	2.33	2.31	2.28
13	5.027	5.030	5.053	5.120	2.43	2.43	2.41	2.38
14	5.211	5.213	5.236	5.300	2.52	2.52	2.51	2.48
15	5.388	5.390	5.412	5.474	2.61	2.61	2.60	2.57
16	5.559	5.561	5.582	5.642	2.70	2.70	2.69	2.66
17	5.726	5.727	5.748	5.806	2.79	2.79	2.78	2.75
18	5.887	5.889	5.909	5.965	2.87	2.87	2.86	2.83
19	6.044	6.046	6.066	6.120	2.95	2.95	2.94	2.91
20	6.198	6.199	6.218	6.272	3.03	3.03	3.02	2.99
25	6.913	6.915	6.932	6.979	3.39	3.39	3.38	3.36
30	7.562	7.563	7.578	7.621	3.72	3.72	3.71	3.69
35	8.158	8.160	8.174	8.214	4.03	4.02	4.02	4.00
40	8.715	8.716	8.729	8.766	4.31	4.31	4.30	4.28
45	9.237	9.238	9.251	9.286	4.57	4.57	4.56	4.55
50	9.732	9.733	9.745	9.778	4.82	4.82	4.81	4.80
60	10.65	10.65	10.66	10.69	5.28	5.28	5.28	5.26
70	11.50	11.50	11.51	11.54	5.71	5.71	5.71	5.69
80	12.29	12.29	12.30	12.32	6.11	6.11	6.10	6.09
90	13.03	13.03	13.04	13.06	6.48	6.48	6.48	6.46
100	13.73	13.73	13.74	13.76	6.83	6.83	6.83	6.82
200	19.40	19.40	19.40	19.42	9.68	9.67	9.67	9.66
300	23.75	23.75	23.75	23.76	11.9	11.9	11.9	11.8
400	27.41	27.41	27.42	27.43	13.7	13.7	13.7	13.7
500	30.65	30.65	30.65	30.66	15.3	15.3	15.3	15.3
600	33.57	33.57	33.57	33.58	16.8	16.8	16.8	16.8
700	36.26	36.26	36.26	36.27	18.1	18.1	18.1	18.1
800	38.76	38.76	38.76	38.77	19.4	19.4	19.4	19.4
900	41.11	41.11	41.11	41.12	20.5	20.5	20.5	20.5
1000	43.33	43.33	43.33	43.34	21.7	21.7	21.7	21.6
2000	61.27	61.27	61.27	61.28	30.6	30.6	30.6	30.6
5000	96.87	96.87	96.87	96.87	48.4	48.4	48.4	48.4
10000	137.0	137.0	137.0	137.0	68.5	68.5	68.5	68.5
20000	193.7	193.7	193.7	193.7	96.9	96.9	96.9	96.9
50000	306.3	306.3	306.3	306.3	153	153	153	153
100000	433.2	433.2	433.2	433.2	217	217	217	217
200000	612.6	612.6	612.6	612.6	306	306	306	306
500000	968.6	968.6	968.6	968.6	484	484	484	484
1000000	1370	1370	1370	1370	685	685	685	685

STANDARD MODEL OF ELECTROWEAK INTERACTIONS

The couplings of the photon, $W^{\pm}$, and Z to fundamental fermions are

$$\bar{\psi}\gamma^{\mu}\left[eQA_{\mu} + \frac{e}{\sqrt{2}\sin\theta_W}\left(T^{+}W_{\mu}^{+} + T^{-}W_{\mu}^{-}\right) + \frac{e}{\sin\theta_W\cos\theta_W}\left(T_3 - \sin^2\theta_W Q\right)Z_{\mu}\right]\psi ,$$

where

$$\psi = \begin{pmatrix} u \\ d' \end{pmatrix}, \begin{pmatrix} c \\ s' \end{pmatrix}, \begin{pmatrix} t \\ b' \end{pmatrix}, \begin{pmatrix} \nu_e \\ e^- \end{pmatrix}, \begin{pmatrix} \nu_\mu \\ \mu^- \end{pmatrix}, \begin{pmatrix} \nu_\tau \\ \tau^- \end{pmatrix};$$

for mixing effects defining d′, s′, and b′ see the section on Cabibbo and Kobayashi-Maskawa Mixing;

T^{+} = $\frac{1}{2}(1-\gamma_5)\times$ weak isospin raising operator ($T^{\pm}$ act on left-handed fermions);

T_3 = $\frac{1}{2}(1-\gamma_5)\times$ third component of weak isospin, (i.e., 1/2 for ν_e, ν_μ, ν_τ, u, c, t; $-1/2$ for e^-, μ^-, τ^-, d, s, b);

Q = electric charge operator, in units of proton charge;

θ_W = weak mixing angle;

A = electromagnetic vector potential.

Thus, for example, the Weν coupling is

$$\left(\frac{e}{\sqrt{2}\sin\theta_W}\right)\left[W_{\mu}^{-}\bar{e}\,\gamma^{\mu}\,\frac{1}{2}(1-\gamma_5)\nu + W_{\mu}^{+}\bar{\nu}\,\gamma^{\mu}\,\frac{1}{2}(1-\gamma_5)e\right]$$

and the Zu$\bar{u}$ coupling is

$$\left(\frac{e}{\sin\theta_W\cos\theta_W}\right)Z_{\mu}\bar{u}\gamma^{\mu}\left[\frac{1}{4}(1-\gamma_5) - \frac{2}{3}\sin^2\theta_W\right]u .$$

The physical neutral fields A and Z are mixtures of W_3, the partner of $W^{\pm}$, and another field B:

$$A = W_3\sin\theta_W + B\cos\theta_W , \quad Z = W_3\cos\theta_W - B\sin\theta_W .$$

The SU(2) × U(1) gauge couplings g and g′ appear as

$$gW_{\mu}\cdot T + g'B_{\mu}\frac{Y}{2} ,$$

where electric charge Q, T_3, and Y/2 are connected by $Q = T_3 + Y/2$. The couplings and mixing angle are related by $\tan\theta_W = g'/g$, $\sin\theta_W = e/g$.

In lowest order

$$M_W^2 = \frac{\pi\alpha}{\sqrt{2}\sin^2\theta_W G_F} \simeq \left(\frac{37.3\ \text{GeV}}{\sin\theta_W}\right)^2,$$

$$M_Z^2 = M_W^2/\cos^2\theta_W .$$

See Appendix I of this Review (found only in complete version, not in booklet) for more details.

Branching fractions of the $W^\pm$ and Z are predicted to be roughly

$$\begin{aligned} &BR(W^+ \to e^+\nu_e) = 0.08, \quad && BR(W^+ \to u\bar{d}) = 0.24, \\ &BR(Z \to \nu_e\bar{\nu}_e) = 0.06, && BR(Z \to e^+e^-) = 0.03, \\ &BR(Z \to u\bar{u}) = 0.10, && BR(Z \to d\bar{d}) = 0.13, \text{ etc.} \end{aligned}$$

and similarly for the other generations, assuming there is no suppression for phase space even for the t quark. The total widths are expected to be (with $\sin^2\theta_W \simeq 0.21$): $\Gamma(W) \simeq 2.8$ GeV and $\Gamma(Z) \simeq 2.8$ GeV.

CABIBBO & KOBAYASHI-MASKAWA MIXING

The quark mass eigenstates are not the weak eigenstates. The unitary matrix connecting them is known as the Kobayashi-Maskawa matrix. It generalizes to three generations the Cabibbo mixing which includes only the first two generations. The K-M matrix can be parametrized by three angles θ_1, θ_2, and θ_3 and a phase $e^{i\delta}$, as described in Appendix III (found in the full Review of Particle Properties, not in the data booklet). Independent of such a parametrization we can write

$$\begin{pmatrix} d' \\ s' \\ b' \end{pmatrix} = \begin{pmatrix} V_{ud} & V_{us} & V_{ub} \\ V_{cd} & V_{cs} & V_{cb} \\ V_{td} & V_{ts} & V_{tb} \end{pmatrix} \begin{pmatrix} d \\ s \\ b \end{pmatrix}.$$

The primed quarks are the weak eigenstates, while the unprimed ones are the mass eigenstates. The analysis in Appendix III leads to an estimate of the K-M matrix:

$$\begin{pmatrix} 0.9705 \text{ to } 0.9770 & 0.21 \text{ to } 0.24 & 0. \text{ to } 0.014 \\ 0.21 \text{ to } 0.24 & 0.971 \text{ to } 0.973 & 0.036 \text{ to } 0.070 \\ 0. \text{ to } 0.024 & 0.036 \text{ to } 0.069 & 0.997 \text{ to } 0.999 \end{pmatrix}.$$

QUARK PARTON MODEL FOR DEEP INELASTIC SCATTERING

In the naive parton model, the number of quarks, $q(x)dx$, of type q carrying a fraction between x and $x+dx$ of the proton's momentum (in a frame in which it is large) is independent of the Q^2 of the scattering. (In more complete QCD models there is a logarithmic dependence on Q^2.) Thus deep inelastic leptoproduction probes u(x), d(x), $\bar{u}(x)$, etc. In particular, the structure functions for scattering from a proton (see section on Kinematics, Decays, and Scattering) are determined by these:

$$F_2^{\nu CC} = 2x\left[d(x) + s(x) + \bar{u}(x) + \bar{c}(x)\right]$$

$$xF_3^{\nu CC} = 2x\left[d(x) + s(x) - \bar{u}(x) - \bar{c}(x)\right]$$

$$F_2^{\bar{\nu}CC} = 2x\left[u(x) + c(x) + \bar{d}(x) + \bar{s}(x)\right]$$

$$xF_3^{\bar{\nu}CC} = 2x\left[u(x) + c(x) - \bar{d}(x) - \bar{s}(x)\right]$$

$$F_2^{em} = x\left[\frac{4}{9}\left(u(x) + \bar{u}(x)\right) + \frac{1}{9}\left(d(x) + \bar{d}(x)\right) + \cdots\right]$$

$$F_2^{\nu NC} = 2\rho^2 x\left\{\left[\frac{1}{4} - \frac{2}{3}\sin^2\theta_W + \frac{8}{9}\sin^4\theta_W\right]\left[u(x) + \bar{u}(x)\right] + \left[\frac{1}{4} - \frac{1}{3}\sin^2\theta_W + \frac{2}{9}\sin^4\theta_W\right]\left[d(x) + \bar{d}(x)\right]\right\}$$

$$xF_3^{\nu NC} = 2\rho^2 x\left\{\left[\frac{1}{4} - \frac{2}{3}\sin^2\theta_W\right]\left[u(x) - \bar{u}(x)\right] + \left[\frac{1}{4} - \frac{1}{3}\sin^2\theta_W\right]\left[d(x) - \bar{d}(x)\right]\right\}$$

$F_2 = 2xF_1$ (in all cases. This is the Callan-Gross relation, and ignores parton transverse momentum.)

$$F_i^{\bar{\nu}NC} = F_i^{\nu NC}.$$

Here $\rho = M_W^2/(M_Z^2\cos^2\theta_W)$. See section on the Standard Model of Electroweak Interactions and Appendix I of this Review (found only in complete version, not in booklet).

NONRELATIVISTIC QUARK MODEL

A. QUANTUM NUMBERS

Each quark has spin 1/2. The additive quantum numbers (other than baryon number = 1/3) of the known (and presumed) quarks are shown in the table.

	Quark type (flavor)					
Quantum number	d	u	s	c	b	t
$\mathscr{Q}$ — electric charge	$-\frac{1}{3}$	$+\frac{2}{3}$	$-\frac{1}{3}$	$+\frac{2}{3}$	$-\frac{1}{3}$	$+\frac{2}{3}$
$\mathscr{I}_z$ — z-component of isospin	$-\frac{1}{2}$	$+\frac{1}{2}$	0	0	0	0
$\mathscr{S}$ — strangeness	0	0	−1	0	0	0
$\mathscr{C}$ — charm	0	0	0	+1	0	0
$\mathscr{B}$ — bottomness	0	0	0	0	−1	0
$\mathscr{T}$ — topness	0	0	0	0	0	+1

With these conventions the strangeness $\mathscr{S}$ of the K^+ is +1 and the bottomness $\mathscr{B}$ of the B^+ is +1.

The G-parity operator is defined to be $G = Ce^{-i\pi I_y}$, where C is the charge conjugation operator. The mesons with $\mathscr{S} = \mathscr{C} = \mathscr{B} = \mathscr{T} = 0$ are eigenstates of G. If a meson is also an eigenstate of the charge conjugation operator with charge conjugation C, then $G = C(-1)^I$, where I is its isospin; all the other particles in the same isomultiplet have the same value of G: $G(\pi^{\pm}) = G(\pi^0) = -1$, $G(\rho^{\pm}) = G(\rho^0) = +1$, etc.

B. MESONS

Nearly all known mesons can be understood as bound states of a quark q and an antiquark $\bar{q}'$ (the flavors of q and q′ may be different). If the orbital angular momentum of the $q\bar{q}'$ state is L, then the parity $P = (-1)^{L+1}$. A state $q\bar{q}$ of a quark and its own antiquark is also an eigenstate of charge conjugation with $C = (-1)^{L+S}$, where the spin S = 0 or 1. The L = 0 states are the pseudoscalars, $J^P = 0^-$, and the vectors, $J^P = 1^-$. See table below.

Standard quark model assignments for some of the known mesons. Some assignments, especially for 0^{++}, are controversial. Note that only the states in the $u\bar{u}$, $d\bar{d}$, $s\bar{s}$, $c\bar{c}$, and $b\bar{b}$ columns and the neutral states in the I = 1 column are eigenstates of charge conjugation C.

$^{2S+1}L_J$	J^{PC}	$u\bar{u}$, $d\bar{d}$, $s\bar{s}$ I = 0	$u\bar{d}$, $u\bar{u}$, $d\bar{d}$ I = 1	$\bar{s}u$, $\bar{s}d$ I = 1/2	$c\bar{u}$, $c\bar{d}$ I = 1/2	$c\bar{s}$ I = 0	$c\bar{c}$ I = 0	$\bar{b}u$, $\bar{b}d$ I = 1/2	$b\bar{b}$ I = 0
$^1S_0$	0^{-+}	η, η'	π	K	D	F	η_c	B	
$^3S_1$	1^{--}	ϕ, ω	ρ	K*(892)	D*(2010)		J/ψ		T
$^1P_1$	1^{+-}	H	B(1235)	Q_B					
$^3P_0$	0^{++}	S(975), ϵ	δ	κ			χ(3415)		χ_b(9875)
$^3P_1$	1^{++}	D(1285), E	A(1270)	Q_A			χ(3510)		χ_b(9895)
$^3P_2$	2^{++}	f', f	A_2	K*(1430)			χ(3555)		χ_b(9915)
$^1D_2$	2^{-+}		A(1680)						
$^3D_1$	1^{--}						ψ(3770)		
$^3D_2$	2^{--}			L(1770)					
$^3D_3$	3^{--}	ω(1670)	g	K*(1780)					

States in the "normal" spin-parity series, $P = (-1)^J$, must, according to the above, have $S = 1$ and hence $CP = +1$. Thus mesons with normal spin-parity and $CP = -1$ are forbidden in the $q\bar{q}'$ quark model. The $J^{PC} = 0^{--}$ state is forbidden as well. Mesons with such J^{PC} could exist, but would lie outside the $q\bar{q}'$ model.

States with the same J^P and additive quantum numbers can mix (if they are eigenstates of charge conjugation, they must also have the same value of C). Thus the physical $J^P = 1^+$, strangeness $\mathcal{S} = 1$ states, Q(1280) and Q(1400), are mixtures of Q_A and Q_B. The $\psi(3770)$ is a mixture of $^3S_1$ and $^3D_1$. The η and η' are mixtures of the SU(3) octet and singlet states.

For the pseudoscalar mesons, the Gell-Mann-Okubo formula is

$$m_\eta^2 = \frac{1}{3}(4m_K^2 - m_\pi^2),$$

assuming no octet-singlet mixing. However, the octet η_8 and singlet η_1 mix because of SU(3) breaking. The physical states η and η' are given by

$$\eta = \eta_8 \cos\theta_P - \eta_1 \sin\theta_P$$

$$\eta' = \eta_8 \sin\theta_P + \eta_1 \cos\theta_P .$$

These combinations diagonalize the mass-squared matrix

$$M^2 = \begin{pmatrix} M_{11}^2 & M_{18}^2 \\ M_{18}^2 & M_{88}^2 \end{pmatrix},$$

where $M_{88}^2 = \frac{1}{3}(4m_K^2 - m_\pi^2)$. It follows that

$$\tan^2\theta_P = \frac{M_{88}^2 - m_\eta^2}{m_{\eta'}^2 - M_{88}^2} .$$

The sign of θ_P is meaningful in the quark model. If

$$\eta_1 = (u\bar{u} + d\bar{d} + s\bar{s})/\sqrt{3}$$

$$\eta_8 = (u\bar{u} + d\bar{d} - 2s\bar{s})/\sqrt{6},$$

then the matrix element M_{18}^2, which is due mostly to the strange quark mass, is negative. From the relation

$$\tan\theta_P = \frac{M_{88}^2 - m_\eta^2}{M_{18}^2},$$

we find $\theta_P < 0$.

For the vector mesons we replace $\pi \to \rho$, $K \to K^*$, $\eta \to \phi$, and $\eta' \to \omega$, so

$$\phi = \omega_8 \cos\theta_V - \omega_1 \sin\theta_V$$

$$\omega = \omega_8 \sin\theta_V + \omega_1 \cos\theta_V .$$

For "ideal *mixing*," $\phi = s\bar{s}$, $\tan\theta_V = 1/\sqrt{2}$, so $\theta_V \approx 35.3°$. Experimentally, θ_V is near 35°, the sign being determined by a formula analogous to that for $\tan\theta_P$. Following this procedure we find the mixing angles below. There are uncertainties of a few degrees arising from electromagnetic mass splittings and uncertainties in resonance masses.

Singlet-octet mixing for the pseudoscalar, vector, and tensor mesons. The sign conventions are as above. The value of θ_{quad} is obtained from the equations above, and θ_{lin} is obtained by replacing $m^2 \to m$ throughout. Of the two isosinglets, the mostly octet one is listed first.

J^{PC}	Nonet Members	θ_{quad}	θ_{lin}
0^{-+}	π, K, η, η'	$-10°$	$-23°$
1^{--}	ρ, K*(892), ϕ, ω	39°	36°
2^{++}	A_2, K*(1430), f′, f	28°	26°
3^{--}	g(1690), K*(1780), ϕ(1850), ω(1670)	29°	28°

C. BARYONS

All the established baryons are apparently 3-quark (qqq) states, and each such state is an SU(3) color singlet, a completely antisymmetric state of the three possible colors. Since the quarks are fermions, the state function for any baryon must be antisymmetric under interchange of any two of its quarks. Thus the state is *symmetric* under interchange of the quantum labels other than color.

$$|qqq\rangle_A = |\text{color}\rangle_A \times |\text{space, spin, flavor}\rangle_S ,$$

where the subscripts S and A indicate symmetry or antisymmetry under interchange of any two of the quarks. Note the contrast with the state function for the three nucleons in ^{3}H or ^{3}He:

$$|NNN\rangle_A = |\text{space, spin, isospin}\rangle_A .$$

This difference has major implications for internal structure, magnetic moments, etc. (For a nice discussion, see Ref. 1.)

Few of the baryons containing c or heavier quarks have yet been discovered, so we restrict further attention to baryons made up of just d, u, and s quarks. The three flavors imply a flavor SU(3), which requires that baryons made of these quarks belong to the multiplets on the right side of

$$3 \otimes 3 \otimes 3 = 10_S \oplus 8_M \oplus 8_M \oplus 1_A$$

(see the section on SU(n) Multiplets and Young Diagrams). Here the subscripts indicate symmetric, mixed-symmetric, or antisymmetric states under interchange of any two quarks. The figure shows particle assignments in these multiplets. States Λ_8 and Λ_1

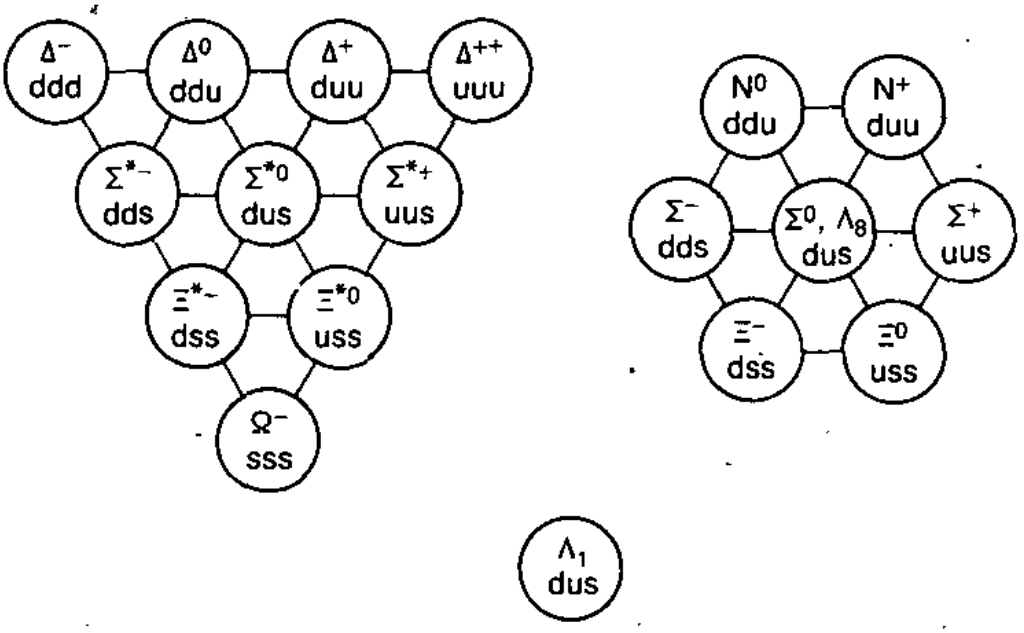

that have the same spin and parity can mix; an example is the mainly octet D_{03} $\Lambda(1690)$ and mainly singlet D_{03} $\Lambda(1520)$. The formalism is the same as for $\eta-\eta'$ or $\phi-\omega$ mixing (see above), except that for baryons the mass M instead of M^2 is used. The section SU(3) Isoscalar Factors shows how relative decay rates in, say, $\mathbf{10} \to \mathbf{8} \otimes \mathbf{8}$ decays may be calculated. A summary of results of fits to the observed baryon masses and decay rates for the best-known SU(3) multiplets is given in Appendix II of our 1982 edition.[2]

Flavor and spin may be combined in a flavor-spin SU(6) in which the six basic states are $d\uparrow$, $d\downarrow$, $\cdots$, $s\downarrow$ ($\uparrow$, $\downarrow$ = spin up, down). Then the baryons belong to the multiplets on the right side of

$$\mathbf{6} \otimes \mathbf{6} \otimes \mathbf{6} = \mathbf{56}_S \oplus \mathbf{70}_M \oplus \mathbf{70}_M \oplus \mathbf{20}_A .$$

These SU(6) multiplets decompose into flavor SU(3) multiplets as follows:

$$\mathbf{56} = {}^4\mathbf{10} \oplus {}^2\mathbf{8}$$

$$\mathbf{70} = {}^2\mathbf{10} \oplus {}^4\mathbf{8} \oplus {}^2\mathbf{8} \oplus {}^2\mathbf{1}$$

$$\mathbf{20} = {}^2\mathbf{8} \oplus {}^4\mathbf{1} ,$$

where the superscript $(2S+1)$ gives the net spin S of the quarks for each particle in the SU(3) multiplet. The $J^P = 1/2^+$ octet containing the nucleon and the $J^P = 3/2^+$ decuplet containing the $\Delta(1232)$ together make up the "ground-state" 56-plet in which the orbital angular momenta between the quarks are zero (so that the spatial part of the state function is trivially symmetric). The **70** and **20** require some excitation of the spatial part of the state function in order to make the overall state function symmetric.

The quark model for baryons is extensively reviewed in Ref. 3.

---

1. F.E. Close, in *Quarks and Nuclear Forces* (Springer-Verlag, 1982), p. 56.
2. Particle Data Group, Phys. Lett. **111B** (1982).
3. A.J.G. Hey and R.L. Kelly, Phys. Reports **96**, 71 (1983).

PROBABILITY AND STATISTICS

A. PROBABILITY DISTRIBUTIONS AND CONFIDENCE LEVELS

We give here properties of the three probability distributions most commonly used in high energy physics: normal (or Gaussian), chi-squared (χ^2), and Poisson. We *warn* the reader that there is no universal convention for the term "confidence level"; thus, explicit definitions that correspond to common usage are given for each distribution. It is explained below how confidence levels for all three distributions may be extracted from the following figure.

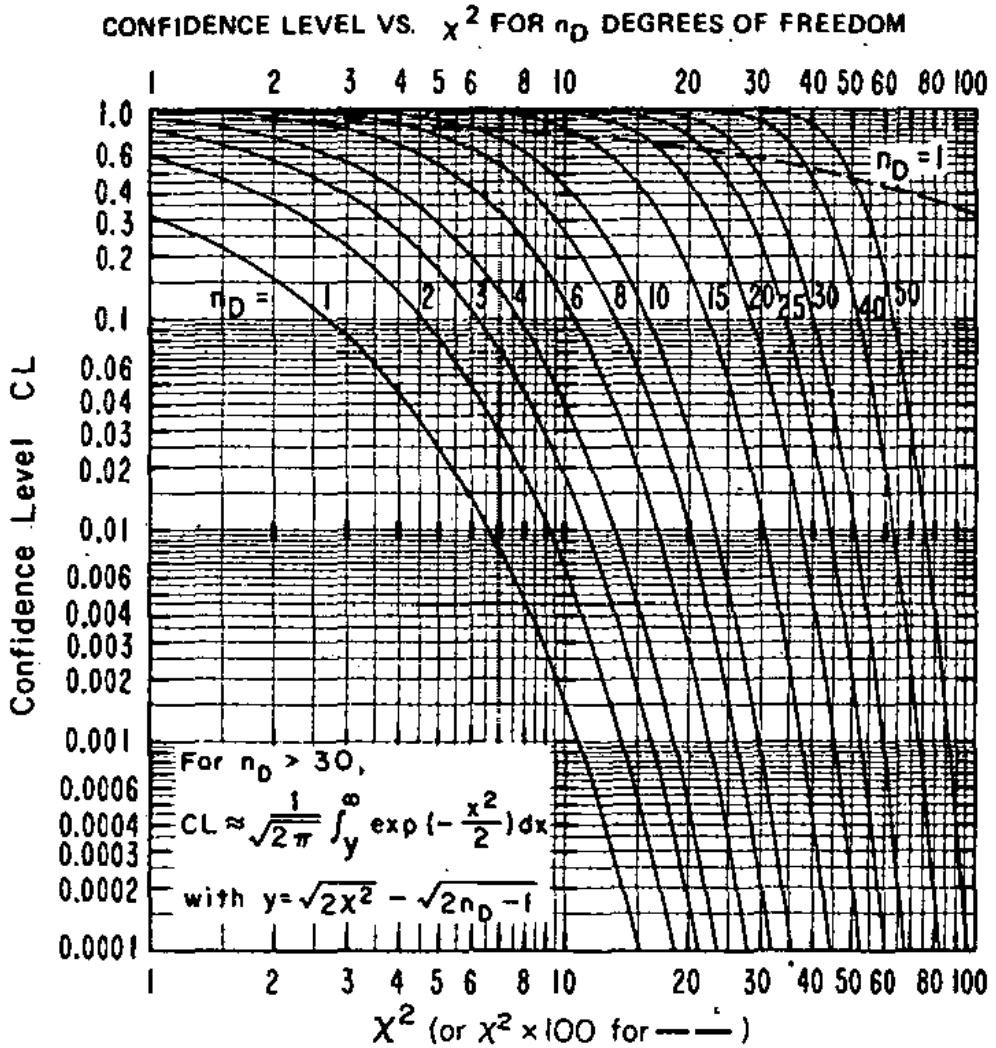

A.1 Normal distribution

The normal distribution with mean $\bar{x}$ and standard deviation σ (variance σ^2) is:

$$P(x)dx = \frac{1}{\sigma\sqrt{2\pi}}\, e^{-(x-\bar{x})^2/2\sigma^2} dx\,. \qquad (1)$$

The *confidence level* associated with an observed deviation δ from the mean is the probability that $|x-\bar{x}| > \delta$, i.e.,

$$CL = 2\int_{\bar{x}+\delta}^{\infty} dx\, P(x)\,, \qquad (2)$$

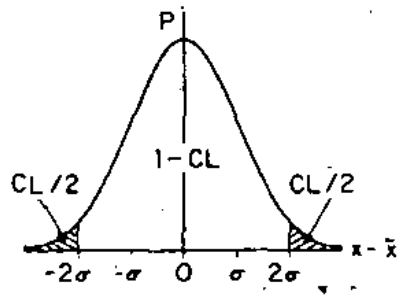

since the distribution is symmetric about $\bar{x}$. The small figure in Eq. (2) is drawn with $\delta = 2\sigma$. CL is given by the ordinate of the $n_D = 1$ curve in the large figure at $\chi^2 = (\delta/\sigma)^2$. The confidence level for $\delta = 1\sigma$ is 31.7%; 2σ, 4.6%; 3σ, 0.3%. The *odds* against exceeding δ, (1−CL)/CL, for $\delta = 1\sigma$ are 2.15:1; 2σ, 21:1; 3σ, 370:1; 4σ, 16,000:1; 5σ, 1,700,000:1. Relations between σ and other measures of the *width*: probable error (CL = 0.5) = 0.67σ; mean absolute deviation = 0.80σ; RMS deviation = σ; half width at half maximum = 1.18σ.

A.2 χ^2 distribution

The χ^2 distribution for n_D degrees of freedom is:

$$P_{n_D}(\chi^2)d\chi^2 = \frac{1}{2^h\Gamma(h)}\,(\chi^2)^{h-1}\, e^{-\chi^2/2} d\chi^2 \quad (\chi^2 \geq 0), \qquad (3)$$

where h (for "half") = $n_D/2$. The mean and variance are n_D and $2n_D$ respectively. In evaluating Eq. (3) one may use *Stirling's approximation*: $\Gamma(h) \cong 2.507\, e^{-h}\, h^{(h-1/2)}(1 + 0.0833/h)$, which is accurate to ± 0.1% for all $h \geq 1/2$. The *confidence level* associated with a given value of n_D and an observed value of χ_0^2 is the probability of the χ^2 exceeding the observed value, i.e.,

$$CL = \int_{\chi_0^2}^{\infty} d\chi^2\, P_{n_D}(\chi^2) \qquad (4)$$

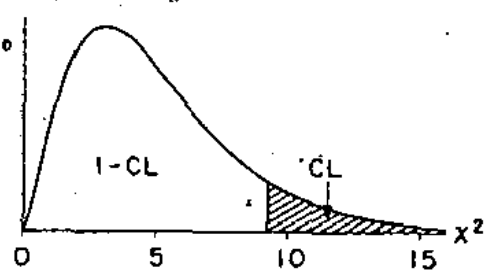

The small figure in Eq. (4) is drawn with $n_D = 5$ and CL = 10%. CL is plotted as a function of χ^2 for several values of n_D in the large figure. For *large* n_D, χ^2 becomes normally distributed about

n_D. Thus,

$$y_1 = (\chi^2 - n_D)/\sqrt{2n_D}$$

becomes normally distributed with unit standard deviation and mean zero. A *better* approximation is that χ, not χ^2, becomes n mally distributed; specifically

$$y_2 = \sqrt{2\chi^2} - \sqrt{2n_D - 1}$$

approaches normality with unit standard deviation and mean ze For small CL's in particular, y_2 is much more accurate than y_1. Thus, for $n_D = 50$ and $\chi^2 = 80$, the true CL = 0.45%, but y_1 is 3. corresponding to a CL of 0.13%, while y_2 is 2.7 corresponding to CL of 0.35%.

A.3 Poisson distribution

The Poisson distribution with mean $\bar{n}$ is:

$$P_{\bar{n}}(n) = \frac{e^{-\bar{n}}\bar{n}^n}{n!} \quad (n = 0, 1, 2, \cdots).$$

The variance is equal to the mean. *Confidence levels* for Poisson distributions are usually defined in terms of quantities called "*upper limits*" as follows: The confidence level associated with a given upper limit N and an observed value n_0 of n is the probab ity that $n > n_0$ if $\bar{n} = N$, i.e.,

$$CL = \sum_{n=n_0+1}^{\infty} P_N(n) = 1 - \sum_{n=0}^{n_0} P_N(n)$$

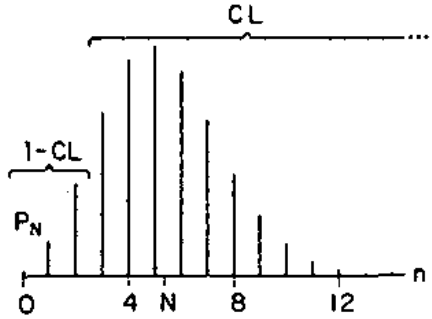

The small figure in Eq. (8) is drawn with $n_0 = 2$ and CL = 90%. useful relation between Poisson and χ^2 confidence levels allows to look up this quantity on the large figure. Specifically, the qua tity 1−CL is given by the ordinate of the $n_D = 2(n_0+1)$ curve a $\chi^2 = 2N$. Thus, 90% confidence level upper limits for $n_0 = 0$, and 2 are given by half the χ^2 value corresponding to an ordinat of 0.1 on the $n_D = 2$, 4, and 6 curves, respectively; the values are = 2.3, 3.9, and 5.3.

Tables of confidence levels for all three of these distributions, the relation between Poisson and χ^2 confidence levels, and numerous other useful tables and relations may be found in Ref.

B. STATISTICS

Suppose one is presented with N independent data, $y_n \pm \sigma_n$, and it is desired to make some *inference* about the "true" value of the quantity represented by these data. For this purpose we interpret each datum y_n as a single sample point drawn randomly (and independently of the other data) from a distribution having true mean $\overline{y}_n$ (which we wish to estimate) and variance σ_n^2. We do not require that they be normally distributed. (Identification of the true σ_n with the σ_n datum is often an *approximation* which may become seriously inaccurate when σ_n is an appreciable fraction of y_n.) Some methods of estimation commonly used in high energy physics are given below; see Ref. 2 for numerous applications. Section B.1 deals with the case in which all $\overline{y}_n$ are the same, e.g., several different measurements of the same quantity; Sec. B.2 deals with the case in which $\overline{y}_n = \overline{y}(x_n)$, where x_n represents some set of independent variables, e.g., cross-section measurements at various values of energy and angle, $x_n = \{E_n, \theta_n\}$.

B.1 Single mean and variance estimates

(1) If the y_n represent a set of values all supposedly drawn from a single distribution with mean $\overline{y}$ and variance σ^2 (i.e., the σ_n are all the same, but their common value is unknown), then

$$\hat{y} = \frac{1}{N} \sum_{n=1}^{N} y_n \quad \text{and} \tag{9}$$

$$\hat{\sigma}^2 = \frac{1}{N-1} \sum_{n=1}^{N} (y_n - \hat{y})^2 = \frac{N}{N-1} \left[\langle (y^2) \rangle - (\hat{y})^2 \right] \tag{10}$$

are unbiased estimates of $\overline{y}$ and σ^2; the angular brackets denote an average over the data. The variance of $\hat{y}$ is σ^2/N. If the parent distribution is normal and N is large, the variance of $\hat{\sigma}^2$ is $2\sigma^4/N$.

(2) If the y_n are independent estimates of the same $\overline{y}$, and the σ_n are known, then the weighted average

$$\hat{y} = \frac{1}{w} \sum_n w_n y_n, \tag{11}$$

where $w_n = 1/\sigma_n^2$ and $w = \Sigma w_n$, is an appropriate unbiased estimate of $\overline{y}$. This choice of weighting factors in Eq. (11) minimizes the variance of the estimate; the variance is $1/w$.

B.2 Linear least-squares fit

We wish to determine the best fit of independent unbiased data $y_n \pm \sigma_n$, measured at points x_n, to the form $y(x) = \Sigma a_i f_i(x)$, where

the f_i are known, linearly independent functions (e.g., Legendre polynomials) one-to-one over the allowed range of x. The estimates for the linear coefficients a_i which minimize the sum of the squared deviations are

$$\hat{a}_i = \sum_{j,n} V_{ij} f_j(x_n) y_n / \sigma_n^2 . \tag{12}$$

Here V is the covariance matrix of the fitted parameters

$$V_{ij} = \overline{(\hat{a}_i - \bar{a}_i)(\hat{a}_j - \bar{a}_j)}, \tag{13}$$

where the overbar denotes the unknown true value; V is estimated by

$$(V^{-1})_{ij} = \sum_n f_i(x_n) f_j(x_n) / \sigma_n^2 . \tag{14}$$

The estimated variance of an interpolated or extrapolated value of y at point x, $\hat{y} = \Sigma \hat{a}_i f_i(x)$, is:

$$(\hat{y} - \bar{y})^2 |_{est} = \sum_{ij} V_{ij} f_i(x) f_j(x) . \tag{15}$$

For the case of a *straight line fit*, $y(x) = a + bx$, one obtains the following estimates of a and b,

$$\hat{a} = (S_y S_{xx} - S_x S_{xy})/D, \tag{16}$$

$$\hat{b} = (S_1 S_{xy} - S_x S_y)/D,$$

where

$$S_1, S_x, S_y, S_{xx}, S_{xy} = \sum (1, x_n, y_n, x_n^2, x_n y_n)/\sigma_n^2 , \tag{17}$$

respectively, and

$$D = S_1 S_{xx} - S_x^2 .$$

The covariance matrix of the fitted parameters is:

$$\begin{pmatrix} V_{aa} & V_{ab} \\ V_{ab} & V_{bb} \end{pmatrix} = \frac{1}{D} \begin{pmatrix} S_{xx} & -S_x \\ -S_x & S_1 \end{pmatrix} . \tag{18}$$

The estimated variance of an interpolated or extrapolated value of y at point x is:

$$(\hat{y}-\overline{y})^2\big|_{est} = \frac{1}{S_1} + \frac{S_1}{D}\left(x - \frac{S_x}{S_1}\right)^2 . \tag{19}$$

A least-squares fit gives estimates for the a_i [Eq.(12)] with the smallest variance, under the conditions that the expansion of y in terms of $a_i f_i$ is the correct model and that the y_n are independent, unbiased measurements whose variances σ_n^2 are known.

C. ERROR PROPAGATION

Suppose one wishes to calculate the value and error of a function of some other quantities with errors, e.g., in a Monte Carlo program. Let $\{y\}$ be a set of random variables with means $\{\overline{y}\}$ and covariance matrix V. Then the mean and variance of a function of these variables are approximately (to second order in $\{y-\overline{y}\}$):

$$\overline{f} \simeq f(\{\overline{y}\}) + \frac{1}{2}\sum_{mn} V_{mn}\left(\frac{\partial^2 f}{\partial y_m \partial y_n}\right)_{\{y\}=\{\overline{y}\}} , \tag{20}$$

$$\overline{(f-\overline{f})^2} \simeq \sum_{mn} V_{mn}\left(\frac{\partial f}{\partial y_m}\right)_{\{y\}=\{\overline{y}\}}\left(\frac{\partial f}{\partial y_n}\right)_{\{y\}=\{\overline{y}\}} \tag{21}$$

E.g., the mean and variance of a function of a *single variable* with mean $\overline{y}$ and variance σ^2 are

$$\overline{f} \simeq f(\overline{y}) + \frac{1}{2}\sigma^2 f''(\overline{y}) , \tag{22}$$

$$\overline{(f-\overline{f})^2} \simeq \sigma^2 f'(\overline{y})^2 . \tag{23}$$

Note that these equations will usually be applied by substituting measured quantities, $\{\bar{y}\}$ say, for the true means, $\{\overline{y}\}$. If, as is often the case, $\bar{y}_n - \overline{y}_n$ is of order $\sqrt{V_{nn}}$, then the second-order terms in Eqs. (20) and (22) may be small compared with the first-order errors introduced by the substitution.

---

1. M. Abramowitz and I. Stegun, eds., *Handbook of Mathematical Functions* (Dover, New York, 1972).
2. W.T. Eadie, D. Drijard, F.E. James, M. Roos, and B. Sadoulet, *Statistical Methods in Experimental Physics* (North Holland, Amsterdam and London, 1971); S.L. Meyer, *Data Analysis for Scientists and Engineers* (John Wiley and Sons, Inc., New York, 1975); A.G. Frodesen, O. Skjeggestad, and H. Tøfte, *Probability and Statistics in Particle Physics* (Universitetsforlaget, Oslo, Norway, 1979).

PARTICLE DETECTORS, ABSORBERS, AND RANGES*

A. DETECTOR PARAMETERS

In this section we give various parameters for common detectors. The quoted numbers are usually based on some typical apparatus, and obviously should be regarded as rough approximations, valid only for preliminary design when applied to other cases. A more detailed introduction to detectors can be found in "A Consumer's Guide to Particle Detectors," by D.J. Miller, Rutherford Lab Report RL-76-072, July 1976.

A.1 Scintillators: The photon yield in the frequency range of practical photomultiplier tubes is $\simeq 1\gamma$ per 100 eV of charged particle ionization energy loss in plastic scintillator[1] and $\simeq 1\gamma/25$ eV in NaI.[1,2]

A.2 Cerenkov:[3] The half-angle θ_c of the Cerenkov cone aperture in terms of the velocity β and the index of refraction n is:

$$\theta_c = \arccos\left(\frac{1}{\beta n}\right) \simeq \left[2\left(1-\frac{1}{\beta n}\right)\right]^{1/2}.$$

The threshold velocity is: $\beta_t = 1/n$; $\gamma_t = 1/\sqrt{1-\beta_t^2}$. Therefore, $\beta_t\gamma_t = 1/\sqrt{2\delta+\delta^2}$, where $\delta = n-1$. Values of δ for various commonly used gases are given as a function of pressure and wavelength in Ref. 4; for values at atmospheric pressure, see the Table of Atomic and Nuclear Properties, following.

The number of photons N per cm of path length is given by:

$$N = \frac{\alpha}{c}\int\left(1-\frac{1}{\beta^2 n^2}\right)2\pi d\nu = \frac{\alpha}{c}\beta_t^2\int\left(\frac{1}{\beta_t^2\gamma_t^2}-\frac{1}{\beta^2\gamma^2}\right)2\pi d\nu$$

$$\simeq 500\sin^2\theta_c/\text{cm (visible spectrum)}.$$

A.3 Photon collection: In addition to the photon yield, one should take into account the light collection efficiency ($\lesssim$10% for typical 1-cm-thick scintillator), the attenuation length ($\simeq$1 to 4 m for typical scintillators[5]), and the quantum efficiency of the photomultiplier cathode ($\lesssim$25%).

A.4 Typical detector characteristics:

Detector Type	Accuracy (rms)	Resolution Time	Dead Time
Bubble chamber	$\simeq \pm 10$ to $\simeq \pm 150\mu$	$\simeq$ 1 ms	$\simeq 1/20$ s[a]
Streamer chamber	$\pm 300\mu$	$\simeq$ 2 μs	$\simeq$100 ms
Proportional chamber	$\geqslant \pm 300\mu$[b,c]	$\simeq$ 50 ns	$\simeq$200 ns
Drift chamber	± 50 to 300μ	$\simeq$ 2 ns[d]	$\simeq$100 ns
Scintillator	—	$\simeq$150 ps	$\simeq$ 10 ns
Emulsion	$\pm 1\mu$	—	—
Silicon strip	$\pm 5\mu$	*e*	*e*

[a] Multiple pulsing time.
[b] 300μ is for 1 mm pitch.
[c] Delay line cathode readout can give $\pm 150\mu$ parallel to anode wire.
[d] For two chambers.
[e] Limited at present by noise and readout time of attached electronics.

A.5 Shower detectors: We give below typical energy resolutions (FWHM) for an incident electron in the 1 GeV range; E is in GeV. For a fixed number of radiation lengths, FWHM in the last three detectors would be expected to be proportional to $\sqrt{t}$ for t (= plate thickness) $\geqslant$ 0.2 radiation lengths.[6] For all detectors, operational resolution may be up to 50% worse due to dead areas, non-normally incident tracks, and other effects.

NaI (20 rad. lengths):[7] $\dfrac{2\%}{E^{1/4}}$

Lead glass (14 rad. lengths):[8] $\dfrac{10-12\%}{\sqrt{E}}$

Lead-liquid argon (15.75 rad. lengths):[6] $\dfrac{16\%}{\sqrt{E}}$
(42 cells: 1.1 mm lead, 2 mm liquid argon, 2.3 mm lead-G10, 2 mm liquid argon)

Lead-scintillator sandwich (12.5 rad. lengths):[9] $\dfrac{17\%}{\sqrt{E}}$
(66 cells: 1 mm lead, 5 mm scintillator)

Proportional wire shower chamber (17 rad. lengths):[10] $\dfrac{40\%}{\sqrt{E}}$
(36 cells: 0.474 rad. length type-metal + Al, 9.5 mm 80% Ar - 20% CH_4 gas)

A.6 dE/dx resolution in Argon: Particle identification (relativistic, Q = 1 incident particles) by dE/dx is dependent on the width of the distribution:

Multiple-sample Ar gas counters (no lead):[11]

$$\text{FWHM}\,\frac{\left(\left.\frac{dE}{dx}\right|_{\text{most probable}}\right)}{\left.\frac{dE}{dx}\right|_{\text{most probable}}} = 0.96N^{-0.46}(tp)^{-0.32};$$

N = no. samples, t = thickness per sample (cm), p = pressure (atm.); most commonly used chamber gases (except Xe) give approximately the same resolution.

A.7. Proportional chamber wire instability: The limit on the voltage V for a wire tension T, due to mechanical effects when the electrostatic repulsion of adjacent wires exceeds the restoring force of wire tension, is given by (MSKA)[12]

$$V < \frac{S}{\ell C}\sqrt{4\pi\epsilon_0 T},$$

where s, ℓ, and C are the wire spacing, length, and capacitance per unit length. An approximation to C for chamber half-gap t and wire diameter d (good for $s \lesssim t$) gives[13]

$$V \lesssim 59T^{1/2}\left[\frac{t}{\ell} + \frac{s}{\pi\ell}\,\ell n\left(\frac{s}{\pi d}\right)\right],$$

where V is in kV, and T is in grams-weight equivalent.

A.8 Proportional and drift chamber potentials: The potential distributions and fields in a proportional or drift chamber can usually be calculated with good accuracy from the exact formula for the potential around an array of parallel line charges q (coul/m) along z and located at y = 0, x = 0, ± s, ± 2s,...,

$$V(x,y) = -\frac{q}{4\pi\epsilon_0}\,\ell n\left\{4\left[\sin^2\left(\frac{\pi x}{s}\right) + \sinh^2\left(\frac{\pi y}{s}\right)\right]\right\}.$$

Errors from the presence of cathodes, mechanical defects, TPC-type edge effects, etc., are usually small and are beyond the scope of this review.

A.9 Silicon strip detectors: These are silicon diodes operated with a reverse bias voltage V (typically 30-300 volts) sufficient to deplete the sensitive volume of most mobile charge carriers (electrons and holes). The active (depletion layer) thickness t is given in a simple model by (MKSA)

$$t = \sqrt{\frac{2\epsilon V}{ne}} = \sqrt{2\rho\mu\epsilon V},$$

where

n = number of impurity centers/m^3
e = electron charge
ϵ = dielectric constant $\simeq$ 105 pF/m $\simeq$ 11.9 ϵ_0
ρ = resistivity $\simeq$ 10-200 Ω-m
μ = majority charge carrier mobility
$\simeq$ 0.13-0.15 m^2/volt-sec (electrons)
$\simeq$ 0.045-0.06 m^2/volt-sec (holes).

A minimum-ionizing particle has a Landau energy-loss distribution with average energy loss 39 keV/100 μm and full width at half-maximum of $0.071t/\beta^2$ keV, where t is the detector thickness in microns and $\beta = v_{inc}/c$. The width is usually increased further by electronic noise ($\sigma \sim$1-10 keV) and for thin layers by a Gaussian contribution due to atomic effects [$\sigma \sim (0.3\text{-}0.4)\sqrt{t}$ keV]. The average energy required to produce an electron-hole pair is 3.62 eV, from which one can estimate total charge of either sign released. Silicon detectors can tolerate integrated charged-particle fluxes of up to $\sim 10^{14}$-$10^{18}/m^2$ and still operate as efficient detectors.

B. COSMIC RAY FLUXES

The fluxes of particles of different types depend on the latitude, their energy, and the conditions of measurement. Some typical sea-level values[14] for charged particles are given below:

I_v flux per unit solid angle about vertical direction crossing unit horizontal area
J_1 perpendicular component of total flux crossing unit horizontal area from above
J_2 total flux crossing unit horizontal area

	Total Intensity	Hard Component	Soft Component	
I_v	1.1×10^2	0.8×10^2	0.3×10^2	$m^{-2}\,sec^{-1}\,sterad^{-1}$
J_1	1.8×10^2	1.3×10^2	0.5×10^2	$m^{-2}\,sec^{-1}$
J_2	2.4×10^2	1.7×10^2	0.7×10^2	$m^{-2}\,sec^{-1}$

Very approximately, about 75% of all particles at sea level are penetrating, and are muons. The sea-level vertical flux ratio for protons to muons (both charges together) is about 3½% at 1 GeV/c, decreasing to about ½% at 10 GeV/c.

The muon flux at sea level has a mean energy of 2 GeV and a differential spectrum falling as E^{-2}, steepening smoothly to $E^{-3.6}$ above a few TeV. The angular distribution is $\cos^2\theta$, changing to $\sec\theta$ at energies above a TeV, where θ is the zenith angle at production. The $+-$ charge ratio is 1.25-1.30. The mean energy of muons originating in the atmosphere is roughly 300 GeV at slant depths $\gtrsim$ a few hundred meters. Beyond slant depths of $\sim$10 km water-equivalent, the muons are due primarily to in-the-earth neutrino interactions (roughly 1/8 interaction $\text{ton}^{-1}\ \text{year}^{-1}$ for $E_\nu >$ 300 MeV, $\sim$ constant throughout the earth).[15] Muons from this source arrive with a mean energy of 20 GeV, and have a flux of $2\times10^{-9}\ \text{m}^{-2}\ \text{sec}^{-1}\ \text{sterad}^{-1}$ in the vertical direction and about twice that in the horizontal,[16] down at least as far as the deepest mines.

C. PASSAGE OF PARTICLES THROUGH MATTER

C.1 Energy loss rates for heavy charged projectiles: A heavy projectile (much more massive than an electron) of charge $Z_{inc}e$, incident at speed βc ($\beta \gg 1/137$) through a slowing medium, dissipates energy principally via interactions with the electrons of the medium. The mean rate of such energy loss per unit path length x, called the stopping power, is given by the Bethe-Bloch equation:[17]

$$\left(\frac{dE}{dx}\right)_{inc} = \frac{D\, Z_{med}\, \rho_{med}}{A_{med}} \left(\frac{Z_{inc}}{\beta}\right)^2$$

$$\times \left[\ell n\left(\frac{2m_e\gamma^2\beta^2c^2}{I}\right) - \beta^2 - \frac{\delta}{2} - \frac{C}{Z_{med}}\right]\left\{1 + \nu\right\},$$

where $D = 4\pi N_A r_e^2 m_e c^2 = 0.3070$ MeV cm^2/g (see Physical Constants Table). Mean range and energy loss figures appear at the end of this section.

Here, Z_{med} and A_{med} are the charge and mass numbers of the medium and ρ_{med} is the mass density of the medium; I, δ, C, and ν are phenomenological functions. Frequently, the values of δ, C, and ν are negligibly small; the parameter I characterizes the binding of the electrons of the medium. As a rule of thumb, we may estimate I for an idealized medium as $I \approx 16\ (Z_{med})^{0.9}$ eV when

$Z_{med} > 1$. For realistic media the value of I will vary at the 10% level from this estimate. Variations of this order occur due to atomic effects such as completion of a shell, also due to chemical binding, and even due to the phase of the substance. Hydrogen, perhaps the most sensitive, has I of about 15 eV in the atomic mode, rising to about 19.2 eV as H_2 gas and to 21.8 eV as H_2 liquid.[18] For many substances, the transition from gas to solid is accompanied by a 20-30% increase in I.[18] We may *approximately* treat media which are chemical mixtures or compounds by computing

$$\frac{dE}{dx} \approx \sum_{n=1}^{N} \left(\frac{dE}{dx} \right)_n ,$$

with $(dE/dx)_n$ appropriate to the n^{th} chemical constituent (using $\rho_{med}^{(n)}$ as the partial density in the formula for dE/dx).[19] For many chemical compounds, small corrections to this additivity rule may be found in Ref. 18.

The function δ represents the density effect upon the energy loss rate; it is non-negligible only for highly relativistic projectiles in denser media.[20] For ultra-relativistic projectiles, δ approaches $2\ell n\gamma$ + constant, where the value of the constant depends upon the density of the medium as well as its chemical composition.

The function C represents shell corrections to the energy loss rate.[17] These effects are non-negligible only for projectiles with speeds not much faster than the speeds of the fastest electrons bound in the medium.

The function ν represents corrections due to higher order electrodynamics.[21] These effects become important when $|Z_{inc}/\beta|$ is comparable to 137. For relativistic unit-charge projectiles, $|\nu|$ is of the order of 1%; positively charged projectiles lose energy more rapidly than do their charge conjugates.[21,22]

For nonrelativistic projectiles, our formulae above are inapplicable. At the very slowest speeds, total energy loss rates are believed to be proportional to β, rising through a peak at projectile speeds comparable to atomic speeds (β on the order of αc), after having passed through a smaller peak (due to elastic Coulomb collisions with the *nuclei* of the slowing medium[23]) at intermediate speeds. For example, for protons in Si, $dE/dx = 61.23\ \beta$ GeV/(gm cm^{-2}) for $\beta < 0.005$; the peak occurs at $\beta = 0.0126$ where dE/dx = 522 MeV/(gm cm^{-2}). In some cases, energy loss rates depend significantly upon the relation of the projectile trajectory to the crystalline structure of the slowing medium.[24]

For relativistic projectiles, $(dE/dx)_{inc}$ falls rapidly with increas-

ing β until reaching a minimum around $\beta = 0.96$ (almost independent of medium), followed by a slow rise. Because of the density effect, the quantity in square brackets approaches $\ell n\gamma$ + constant for large γ.

The quantity $(dE/dx)_{inc}\delta x$ is the *mean* total energy loss via interactions with electrons of the medium in a layer of thickness δx. For any finite δx, Poisson fluctuations can cause the actual energy loss to deviate from the mean. For thin layers, the distribution is broad and skewed, being peaked below $(dE/dx)\delta x$, and having a long tail toward large energy losses.[25] Only for a very thick layer $[(dE/dx)\delta x >> 2m_e\beta^2\gamma^2c^2]$ will the distribution of energy losses become nearly Gaussian. The large fluctuations of the total energy loss rate from the mean are due to a small number of collisions involving large energy transfers. The fluctuations are greatly reduced for the so-called restricted energy loss rate, described in Section C.4.

C.2 Ionization yields: Physicists frequently relate total energy loss to the number of ion pairs produced near the projectile's track. This relation becomes complicated for relativistic projectiles due to the wandering of energetic knock-on electrons whose ranges exceed the dimensions of the fiducial volume. For a qualitative appraisal of the nonlocality of energy deposition by such modestly energetic knock-on electrons in various media, see Ref. 26. Furthermore, the mean local energy dissipation per local ion pair produced, W, while essentially constant for relativistic projectiles, increases at slow projectile speeds.[27] The numerical value of W for gases can be surprisingly sensitive to trace amounts of various contaminants.[27] Of course, in addition to the preceding effects, practical ionization yields may be greatly influenced by subsequent recombinations and other factors.[28]

C.3 Energetic knock-on electrons: For a relativistic point-charge projectile, the production of high energy (kinetic energy $T >> I$) electrons is given by:[29]

$$\frac{d^2N}{dTdx} = \frac{1}{2}D\left(\frac{Z_{med}}{A_{med}}\right)\left(\frac{Z_{inc}}{\beta}\right)^2\rho_{med}\frac{1}{T^2}F,$$

for $I << T << T_{max}$, where

$$T_{max} = \frac{2m_e\beta^2\gamma^2c^2}{1 + 2\gamma\frac{m_e}{M_{inc}} + \left(\frac{m_e}{M_{inc}}\right)^2},$$

M_{inc} is the mass of the incident projectile, and all other quantities except F are as in Sec. C.1. F ($\simeq 1$ for $T \ll T_{max}$) is a factor dependent upon the spin of the projectile.
For spin-0 projectiles,

$$F = 1 - \beta^2\frac{T}{T_{max}};$$

for spin-1/2 projectiles,

$$F = 1 - \beta^2\frac{T}{T_{max}} + \frac{1}{2}\left(\frac{T}{T_{inc} + M_{inc}c^2}\right)^2,$$

where T_{inc} is the kinetic energy of the projectile;
for electrons incident,

$$F = \beta^2T^2\left[\frac{T_{inc}}{T(T_{inc} - T)} - \frac{1}{T_{inc}}\right]^2;$$

and for positrons incident,

$$F = \beta^2\left[1 - \frac{T}{T_{inc}} + \left(\frac{T}{T_{inc}}\right)^2\right]^2.$$

For incident electrons, the indistinguishability of projectile and target means that the range of T is only up to $T_{inc}/2$. For additional formulas see Ref. 30. Our formula is inaccurate for T close to I; for $2I \lesssim T \lesssim 10I$, the $1/T^2$ dependence above becomes $\simeq T^{-\eta}$ with $3 \lesssim \eta \lesssim 5$.[31]

C.4 Rates of restricted energy loss for relativistic charged projectiles: The variability of energy loss for heavy projectiles is due primarily to the variability in the production of energetic knock-on electrons. Bremsstrahlung and pair-production processes make this variability even greater for electrons than for heavy particles as projectiles (see, e.g., the figure "Fractional Energy Loss for Electrons and Positrons in Lead," following). If an instrument, such as a bubble chamber, is capable of isolating these high-energy-loss interactions, then it is appropriate to consider the rate of energy

loss excluding them, i.e., a restricted energy loss rate. The mean energy loss rate via all collisions which have energy transfer T such that $T \leq E_{max} \ll T_{max}$ is:[17]

$$\left(\frac{dE}{dx} \right)_{\leq E_{max}} = \frac{1}{2} D \frac{Z_{med} \rho_{med}}{A_{med}} \left(\frac{Z_{inc}}{\beta} \right)^2 \times \left[\ell n \left(\frac{E_{max} T_{max}}{I^2} \right) - \beta^2 - \delta - \frac{2C}{Z_{med}} \right].$$

Notice the overall factor of 1/2. See Sec. C.1 above for definitions of the quantities in this equation.

The density effect causes the restricted energy loss rate to approach a constant, the Fermi plateau value, for the fastest projectiles.

C.5 Multiple scattering through small angles: As a charged particle traverses a medium it is deflected by many small-angle elastic scatterings. The bulk of this deflection is due to elastic Coulomb scattering from the nuclei within the medium, hence the usual identification as multiple Coulomb scattering (note, however, that strong interactions do contribute to the total multiple scattering for hadronic projectiles). For both Coulomb and strong interactions, the Central Limit Theorem provides little useful guidance in establishing the precise nature of the distribution of the total deflections resulting from multiple scattering. The true distribution is roughly Gaussian only for small deflection angles, while it shows much greater probability for large-angle scatterings ($\gtrsim$ a few θ_0, see below, depending on absorber) than the Gaussian would suggest. These tails on the distribution (a few per cent of peak height in the region where the Gaussian part becomes negligible) are more pronounced for hadrons than for muons as projectiles. The large-angle behavior of these distributions is best estimated by computing the exact distribution for the vectorial sum of the largest deflections based upon the true elastic scattering cross section of the projectile against the medium,[32] or, when applicable, by interpolation from tabular data.[33] An easier alternative which may suffice for noncritical applications would be to use a Gaussian approximation with the following width:[34]

$$\theta_0 = \frac{14.1 \text{ MeV/c}}{p\beta} Z_{inc} \sqrt{L/L_R} \left[1 + \frac{1}{9} \log_{10} \left(L/L_R \right) \right] \text{(radians)},$$

where p, β, and Z_{inc} are the momentum (in MeV/c), velocity, and charge number of the incident particle, and L/L_R is the thickness, in radiation lengths, of the scattering medium. L_R for certain materials is given in the Table of Atomic and Nuclear Properties of Materials, following. See also Sec. C.7 below. The angle, θ_0, is a fit to Moliere[32] theory, accurate to about 5% for $10^{-3} < L/L_R < 10$ except for very light elements or low velocity where the error is about 10 to 20%. In this Gaussian approximation, θ_0 has the meaning

$$\theta_0 = \theta_{\text{plane}}^{\text{rms}} = \frac{1}{\sqrt{2}}\,\theta_{\text{space}}^{\text{rms}}.$$

The nonprojected (space) and projected (plane) angular distributions are given approximately[32] by the Gaussian forms:

$$\frac{1}{2\pi\theta_0^2}\exp\left(-\frac{\theta_{\text{space}}^2}{2\theta_0^2}\right)d\Omega,$$

$$\frac{1}{\sqrt{2\pi}\,\theta_0}\exp\left(-\frac{\theta_{\text{plane}}^2}{2\theta_0^2}\right)d\theta_{\text{plane}},$$

where θ is the deflection angle.

Other quantities are sometimes used to describe the amount of multiple Coulomb scattering: the auxiliary quantities ψ_{plane}, y_{plane}, and s_{plane} (see the figure) obey:

$$\psi_{\text{plane}}^{\text{rms}} = \frac{1}{\sqrt{3}}\,\theta_{\text{plane}}^{\text{rms}} = \frac{1}{\sqrt{3}}\theta_0,$$

$$y_{\text{plane}}^{\text{rms}} = \frac{1}{\sqrt{3}}\,L\,\theta_{\text{plane}}^{\text{rms}} = \frac{1}{\sqrt{3}}L\theta_0,$$

and

$$s_{\text{plane}}^{\text{rms}} = \frac{1}{4\sqrt{3}}\,L\,\theta_{\text{plane}}^{\text{rms}} = \frac{1}{4\sqrt{3}}L\theta_0.$$

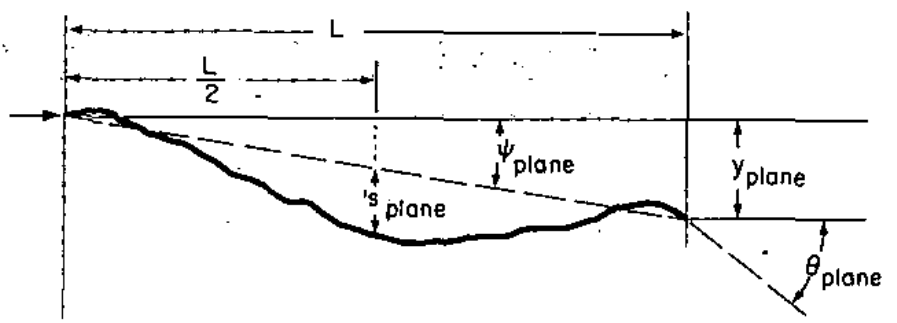

All the quantitative estimates in this section apply only in the limit of small θ_{plane}^{rms} and in the absence of large-angle scatters.

C.6 Longitudinal distribution of electromagnetic showers: A photon of energy $E \geq 0.1$ GeV converting in a semi-infinite medium produces an electromagnetic cascade whose intensity initially increases with depth and then falls off. The average number of $e^{\pm}$ with kinetic energy above 1.5 MeV, crossing a plane at a depth of L radiation lengths from the beginning of the medium, in a material of atomic number Z, calculated using the Monte Carlo program EGS,[35] can be fit by the empirical formula[36]

$$N = N_0 L^a e^{-bL},$$

where $N_0 = 5.51\ E(GeV)\ \sqrt{Z}\ b^{a+1}/\Gamma(a+1)$ and $b = 0.634 - 0.0021\ Z$. For $Z \geq 26$, $a = 2.0 - Z/340 + (0.664 - Z/340)\ell n\ E$. For $Z = 13$, $a = 1.77 - 0.52\ell n\ E$. The maximum intensity, N_{max}, occurs at the depth $L = a/b$. The maximum error of the fit occurs in the vicinity of this depth and is less than $0.15\ N_{max}$. The integral of the tail, $\int_{1.5a/b}^{\infty} N\ dL$ is fit to better than 2.5%. The total longitudinally projected $e^{\pm}$ path length, $\int_0^{\infty} N\ dL = 5.51\ E\ \sqrt{Z}$, is less than the total $e^{\pm}$ path length due primarily to multiple Coulomb scattering.

C.7 Radiation length: For the passage of electromagnetically interacting particles through a medium it is convenient to measure thickness in terms of radiation length.[37] For most electromagnetic processes (Bremsstrahlung, Coulomb scattering, showering, pair production, etc.), over large energy intervals, some or all of the dependence upon the medium is contained in the radiation length.

The radiation length may be defined as the distance L_R over which a high energy electron ($\gtrsim$ 1 GeV for most materials) loses all but a fraction 1/e of its energy to Bremsstrahlung, on average. For a homogeneous monoatomic medium, $Z \geq 5$,

$$\frac{1}{L_R} = \frac{4\alpha r_e^2 N_A Z^2}{A}\left\{\ell n\left(\frac{184.15}{Z^{1/3}}\right) + \frac{1}{Z}\ell n\left(\frac{1194}{Z^{2/3}}\right) - 1.202\alpha^2 Z^2 + 1.0369\alpha^4 Z^4 - \frac{1.008\alpha^6 Z^6}{1+\alpha^2 Z^2}\right\} \equiv \frac{Z^2\left\{\ \right\}}{716.405A},$$

where α, r_e, and N_A are found in the Physical Constants Table, and Z and A are the atomic number and weight of the medium. For $Z < 5$, a more complex numerical calculation is required. Radiation lengths for many substances are tabulated in the Table of Atomic and Nuclear Properties of Materials, following. For media which are chemical mixtures or compounds,

$$\frac{1}{L_R} \approx \sum_i \frac{f_i}{L_R^i} ,$$

where f_i is the fraction by mass of atoms of type i, radiation length L_R^i. Chemical binding can lower L_R from this, typically by a few per cent.

For electrons of energy below about one GeV, the average fractional energy loss per unit length decreases as the energy decreases (see Fractional Energy Loss for Electrons and Positrons in Lead figure, following). With distances measured in units of L_R, dependence of the Bremsstrahlung fractional energy loss upon Z of the medium in the low energy region ($\gtrsim$ 10 MeV) is of order a few percent or less.

For photons of infinite energy, the total pair-production cross section is

$$\sigma = \frac{7}{9}(A/L_R N_A) .$$

This is accurate to within a few per cent down to ~1 GeV for most materials. For energies below about 1 GeV, the cross section varies in a manner which may be determined from the Photon Mass Attenuation figures, following. See also Contributions to Photon Cross Section in Carbon and Lead figure, following.

C.8 Electron practical range: The electron "practical range" — a common measure of straight-line penetration distance — is shorter than the total path length because of multiple Coulomb scattering, which becomes increasingly important as the electron slows down. E.g., for a fast electron the rms projected angle due to multiple Coulomb scattering reaches 1 radian by the time the electron has slowed to 0.4 MeV in hydrogen, 1.5 MeV in carbon, 9 MeV in copper, and 24 MeV in lead. Electrons which have energy less than 0.2 MeV in Ar, 1.5 MeV in Cu, 3.5 MeV in Sn, and 5 MeV in Pb are likely to deposit 10% of their energy *behind* their starting plane. The practical range, R_p, is defined as that absorber thickness obtained by extrapolating to zero the linearly decreasing part of the curve of penetration probability vs. absorber thickness. Data for Al

in the T range up to about 10 MeV are available, and fit (to $\sim \pm 10\%$) $R_p = AT[1\text{-}B/(1+CT)]$ mg cm^{-2}, a form suggested in Ref. 38, with A=0.55 mg cm^{-2} keV^{-1}, B = 0.9841, and C = 0.0030 keV^{-1}. At this penetration depth, 90 - 95% of the incident electrons have stopped. Data for other elements are sketchy, but suggest that higher-Z ($\lesssim$50) elements have $1 \lesssim R_p/R_p(\text{Al}) \lesssim 1.4$ below $\sim$10 keV, and $0.6 \lesssim R_p/R_p(\text{Al}) \lesssim 1$ above $\sim$ 100 keV. The "critical energy" (above which the energy loss due to bremsstrahlung exceeds that due to ionization, and showering becomes important) is 400 MeV for hydrogen, 100 MeV for carbon, 25 MeV for copper, and 10 MeV for lead. The mean positron range may differ from the mean electron range by several percent. See Refs. 39 and 40. Electron energy deposition and penetration probability vs. range are discussed in Refs. 26, 41, and 42.

---

* Revised April 1984 by Sherwood Parker, Ray Hagstrom, and Geoff Hall.

1. *Methods of Experimental Physics*, L.C.L. Yuan and C.-S. Wu, editors, Academic Press, 1961, Vol. 5A, p.127.
2. R.K. Swank, Ann. Rev. Nucl. Sci. 4, 137 (1954), and G.T. Wright, Proc. Phys. Soc. B68, 929 (1955).
3. *Methods of Experimental Physics*, L.C.L. Yuan and C.-S. Wu, editors, Academic Press, 1961, Vol. 5A, p.163.
4. E.R. Hayes, R.A. Schluter, and A. Tamosaitis, "Index and Dispersion of Some Cerenkov Counter Gases," ANL-6916 (1964).
5. Nuclear Enterprises Catalogue.
6. D. Hitlin et al., Nucl. Instr. and Meth. 137, 225 (1976). See also W.J. Willis and V. Radeka, Nucl. Instr. and Meth. 120, 221 (1974), for a more detailed discussion.
7. E.B. Hughes et al., IEEE Transactions on Nuclear Science NS-19, No. 3, 126 (1972).
8. M. Holder et al., Phys. Letters 40B, 141 (1972), and J.S. Beale et al., "A Lead-Glass Cerenkov Detector for Electrons and Photons," CERN Writeup, Intl. Conf. on Instrumentation in H.E.P., Frascati (1973).
9. W. Hofmann et al., DESY 81/045 (July 1981). See also S.L. Stone et al., Nucl. Instr. and Meth. 151, 387 (1978).
10. R.L. Anderson et al., "Tests of Proportional Wire Shower Counter and Hadron Calorimeter Modules," SLAC-PUB-2039 (1977).
11. W.W.M. Allison and J.H. Cobb, "Relativistic Charged Particle Identification by Energy-Loss," Ann. Rev. Nucl. Part. Sci. 30, 253 (1980).
12. T. Trippe, CERN NP Internal Report 69-18 (1969).
13. S. Parker and R. Jones, LBL-797 (1972), and P. Morse and H. Feshbach, *Methods of Theoretical Physics*, McGraw-Hill, New York, 1953, p.1236.
14. B. Rossi, Rev. Mod. Phys. 20, 537 (1948). See also C. Grupen, "News from Cosmic Rays at High Energies," Siegen University preprint SI-84-01; flux ratio for protons at sea-level from G. Brook and A.W. Wolfendale, Proc. of the Phys. Soc. of London, Vol. 83 (1964), p. 843.
15. J.G. Learned, F. Reines, and A. Soni, Phys. Rev. Lett. 43, 907 (1979).
16. M.F. Crouch et al., Phys. Rev. D18, 2239 (1978).
17. U. Fano, Ann. Rev. Nucl. Sci. 13, 1 (1963).
18. M.J. Berger and S.M. Seltzer, "Mean Excitation Energies for Use in Bethe's

Stopping-Power Formula", p. 57-74, Proceedings of Hawaii Conference on Charge States and Dynamic Screening of Swift Ions (1982).
19. H.A. Bethe and J. Ashkin, *Experimental Nuclear Physics*, Vol. 1, E. Segrè, editor, John Wiley, New York, 1959.
20. A. Crispin and G.N. Fowler, Rev. Mod. Phys. **42**, 290 (1970); R.M. Sternheimer, S.M. Seltzer, and M.J. Berger, "The Density Effect for the Ionization Loss of Charged Particles in Various Substances," BNL preprint 31435, to be published in Atomic Data & Nucl. Data Tables.
21. For Z^3 calculations with Z = 1, see J.D. Jackson and R.L. McCarthy, Phys. Rev. **B6**, 4131 (1972).
22. For an approximate treatment of high-Z projectiles, see P.B. Eby and S.H. Morgan, Phys. Rev. **A5**, 2536 (1972).
23. See, for instance, G. Sidenius, Det Kong. Danske Viden. Selskab Mat.-Fysk. Med. **39**, No. 4 (1974).
24. See, for instance, S. Datz, "Atomic Collisions in Solids" in "Structure and Collisions of Ions and Atoms," Springer Verlag, Berlin, 1978, p. 309.
25. See, for instance, K.A. Ispirian, A.T. Margarian, and A.M. Zverev, Nucl. Instr. and Meth. **117**, 125 (1974).
26. L.V. Spencer "Energy Dissipation by Fast Electrons," Nat'l Bureau of Standards Monograph No. 1 (1959).
27. "Average Energy Required to Produce an Ion Pair," ICRU Report No. 31 (1979).
28. N. Hadley et al., "List of Poisoning Times for Materials," Lawrence Berkeley Lab Report TPC-LBL-79-8 (1981).
29. B. Rossi, *High Energy Particles*, Prentice-Hall, Inc., Englewood Cliffs, NJ, 1952.
30. For unit-charge projectiles, see E.A. Uehling, Ann. Rev. Nucl. Sci. **4**, 315 (1954). For highly charged projectiles, see J.A. Doggett and L.V. Spencer, Phys. Rev. **103**, 1597 (1956). A Lorentz transformation is needed to convert these center-of-mass data to knock-on energy spectra.
31. N.F. Mott and H.S.W. Massey, *The Theory of Atomic Collisions*, Oxford Press, London, 1965.
32. For a thorough discussion of simple formulae for single scatters and methods of compounding these into multiple-scattering formulae, see W.T. Scott, Rev. Mod. Phys. **35**, 231 (1963). For detailed summaries of formulae for computing single scatters, see J.W. Motz, H. Olsen, and H.W. Koch, Rev. Mod. Phys. **36**, 881 (1964).
33. E.V. Hungerford and B.W. Mayes, Atomic Data and Nuclear Data Tables **15**, 477 (1975).
34. V.L. Highland, Nucl. Inst. and Meth. **129**, 497 (1975) and important modification Nucl, Inst. and Meth. **161**, 171 (1979).
35. R. Ford and W. Nelson, SLAC-210 (1978).
36. A similar form has been used by E. Longo and I. Sestili, Nucl. Inst. and Meth. **128**, 283 (1975), and J. Sass and M. Spiro, CERN $\overline{p}p$ Tech. Note 78-32 (1978).
37. Y.S. Tsai, Rev. Mod. Phys. **46**, 815 (1974).
38. K.-H. Weber, Nucl. Instr. and Meth. **25**, 261 (1964).
39. M.J. Berger and S.M. Seltzer, NASA SP-3012 (1964) and SP-3036 (1966).
40. P. Trower, UCRL-2426, Vol. III, Rev. (1966).
41. S.M. Seltzer, "Transmission of Electrons through Foils," NBSIR **74**, 457 (1974).
42. M.J. Berger and S.M. Seltzer, "Stopping Powers and Ranges of Electrons and Positrons" (2^{nd} Ed.), U.S. National Bureau of Standards Report NBSIR 82-2550-A (1982).

Atomic and Nuclear Properties of Materials*

Material	Z	A	Nuclear[a] total cross section σ_T [barn]	Nuclear[b] inelastic cross section σ_I [barn]	Nuclear[c] collision length λ_T [g/cm^2]	Nuclear[c] interaction length λ_I [g/cm^2]	dE/dx min[d] $\overline{\Delta E}$ [MeV/(g/cm^2)]	dE/dx min[d] E_{mp}, 1 cm [MeV] () is for gas [keV]	Radiation length[e] L_{rad} [g/cm^2]	Radiation length[e] [cm] () is for gas	Density[f] [g/cm^3] () is for gas [g/ℓ]	Refractive index n[f] () is $(n-1)\times10^6$ for gas
H_2	1	1.01	0.0387	0.033	43.3	50.8	4.12	(0.19)	61.28	865	0.0708(0.090)	1.112(140)
D_2	1	2.01	0.073	0.061	45.7	53.7	2.07	(0.17)	122.6	757	0.162(0.177)	1.128
He	2	4.00	0.133	0.102	49.9	65.1	1.94	(0.16)	94.32	755	0.125(0.178)	1.024(35)
Li	3	6.94	0.211	0.157	54.6	73.4	1.58	0.70	82.76	155	0.534	—
Be	4	9.01	0.268	0.199	55.8	75.2	1.61	2.61	65.19	35.3	1.848	—
C	6	12.01	0.331	0.231	60.2	86.3	1.78	3.57	42.70	18.8	2.265[g]	—
N_2	7	14.01	0.379	0.265	61.4	87.8	1.82	(0.93)	37.99	44.5	0.808(1.25)	1.205(300)
O_2	8	16.00	0.420	0.292	63.2	91.0	1.82	(1.31)	34.24	28.7	1.14(1.43)	1.22(266)
Ne	10	20.18	0.507	0.347	66.1	96.6	1.73	(0.75)	28.94	24.0	1.207(0.90)	1.092(67)
Al	13	26.98	0.634	0.421	70.6	106.4	1.62	3.81	24.01	8.9	2.70	—
Si	14	28.09	0.660	0.440	70.6	106.0	1.66	3.36	21.82	9.36	2.33	—
Ar	18	39.95	0.868	0.566	76.4	117.2	1.51	(1.30)	19.55	14.0	1.40(1.78)	1.233(283)
Fe	26	55.85	1.120	0.703	82.8	131.9	1.48	10.7	13.84	1.76	7.87	—
Cu	29	63.54	1.232	0.782	85.6	134.9	1.44	11.85	12.86	1.43	8.96	—
Sn	50	118.69	1.967	1.21	100.2	163	1.26	8.3	8.82	1.21	7.31	—
Xe	54	131.30	2.120	1.29	102.8	169	1.24	(3.57)	8.48	2.77	3.057(5.89)	(705)
W	74	183.85	2.767	1.65	110.3	185	1.16	21.1	6.76	0.35	19.3	—
Pb	82	207.19	2.960	1.77	116.2	194	1.13	11.7	6.37	0.56	11.35	—
U	92	238.03	3.378	1.98	117.0	199	1.09	19.3	6.00	≈0.32	≈18.95	—

Air, 20°C, 1 atm. (STP in paren.)	62.0	90.0	1.82	(1.12)	36.66	(30420)	0.001205(1.29)	1.000273(293)
H_2O	60.1	84.9	2.03	1.72	36.08	36.1	1.00	1.33
Shielding concrete [h]	67.4	99.9	1.70	3.68	26.7	10.7	2.5	—
SiO_2 (quartz)	67.0	99.2	1.72	3.28	27.05	12.3	2.2	1.458
H_2 (bubble chamber 26°K)	43.3	50.8	4.12	0.20	61.28	≈1000	≈0.063 [i]	1.100
D_2 (bubble chamber 31°K)	45.7	53.7	2.07	0.22	122.6	≈900	≈0.140 [i]	1.110
H-Ne mixture (50 mole percent) [j]	65.0	94.5	1.84	0.59	29.70	73.0	0.407	1.092
Ilford emulsion G5	82.0	134	1.44	4.79	11.0	2.89	3.815	—
NaI	94.8	152	1.32	4.13	9.49	2.59	3.67	1.775
BaF_2	92.1	146	1.35	3.78	9.91	2.05	4.83	1.56
BGO ($Bi_4Ge_3O_{12}$)	97.4	156	1.27	8.07	7.98	1.12	7.1	2.15
Polystyrene, scintillator (CH) [k]	58.4	82.0	1.95	1.72	43.8	42.4	1.032	1.581
Lucite, Plexiglas ($C_5H_8O_2$)	59.2	83.6	1.95	1.98	40.55	≈34.4	1.16-1.20	≈1.49
Polyethylene (CH_2)	56.9	78.8	2.09	1.68	44.8	≈47.9	0.92-0.95	—
Mylar ($C_5H_4O_2$)	60.2	85.7	1.86	2.24	39.95	28.7	1.39	—
Borosilicate glass (Pyrex) [e]	66.2	97.6	1.72	3.32	28.3	12.7	2.23	1.474
CO_2	62.4	90.5	1.82	(1.92)	36.2	(18310)	(1.977)	(410)
Methane CH_4	54.7	74.0	2.41	(0.91)	46.5	(64850)	0.423(0.717)	(444)
Isobutane C_4H_{10}	56.3	77.4	2.22	(3.43)	45.2	(16930)	(2.67)	(1270)
Freon 12 (CCl_2F_2) gas, 26°C, 1 atm. [m]	70.6	106	1.62	4.49	23.7	4810	4.93	1.001080
Silica Aerogel [n]	65.5	95.7	1.83	0.28	29.85	≈150	0.1-0.3	$1.0+0.25\rho$
G10 plate [o]	62.6	90.2	1.87	2.7	33.0	19.4	1.7	—

* Table revised April 1984 by Joachim Engler. For details, see Report KfK 3386B, Kernforschungzentrum, D 7500 Karlsruhe, P.O. Box 3640, FRG.

a. σ_{total} at 80-240 GeV for neutrons ($\approx \sigma$ for protons) from Murthy et al., Nucl. Phys. **B92**, 269 (1975).

b. $\sigma_{inelastic} = \sigma_{total} - \sigma_{elastic} - \sigma_{quasielastic}$; for neutrons at 60-375 GeV from Roberts et al., Nucl. Phys., **B159**, 56 (1979). For protons and other particles, see Carroll et al., Phys. Lett. **80B**, 319 (1979); note that $\sigma_I(p) \approx \sigma_I(n)$.

c. Mean free path between collisions (λ_T) or inelastic interactions (λ_I), calculated from $\lambda = A/(N \times \sigma)$.

d. For minimum-ionizing protons and pions. $\overline{\Delta E}$ is energy loss per g/cm^2 from Barkas and Berger, *Tables of Energy Losses and Ranges of Heavy Charged Particles*, NASA-SP-3013 (1964). For electrons and positrons see: M.J. Berger and S.M. Seltzer, *Stopping Powers and Ranges of Electrons and Positrons* (2nd Ed.), U.S. National Bureau of Standards report NBSIR 82-2550-A (1982). E_{mp} is the most probable deposited energy in one cm, in MeV for solids and liquids, in keV for gases. E_{mp} varies with depth in a nonproportional manner. (See Sec. C.1 preceding.) Parentheses refer to gaseous form at STP (0°C, 1 atm.).

e. From Y.S. Tsai, Rev. Mod. Phys. **46**, 815 (1974). Corrections for molecular binding applied for H_2, and D_2. Parentheses refer to gaseous form at STP (0°C, 1 atm.).

f. Values for solids, or the liquid phase at boiling point, except as noted. Values in parentheses for gaseous phase at STP (0°C, 1 atm.). Refractive index given for sodium D line.

g. For pure graphite; industrial graphite density may vary 2.1 - 2.3 g/cm^3.

h. Standard shielding blocks, typical composition O_2 52%, Si 32.5%, Ca 6%, Na 1.5%, Fe 2%, Al 4%, plus reinforcing iron bars. The attenuation length, $\ell = 115 \pm 5$ g/cm^2, is also valid for earth (typical $\rho = 2.15$), from CERN-LRL-RHEL Shielding exp., UCRL-17841 (1968).

i. Density may vary about ±3%, depending on operating conditions.

j. Values for typical working conditions with H_2 target: 50 mole percent, 29°K, 7 atm.

k. Typical scintillator; e.g., PILOT B and NE 102A have an atomic ratio H/C = 1.10.

ℓ. Main components: 80% SiO_2 + 12% B_2O_3 + 5% Na_2O.

m. Used in Cerenkov counters. Values at 26°C and 1 atm. Indices of refraction from E.R. Hayes, R.A. Schluter, and A. Tamosaitis, ANL-6916 (1964).

n. n(SiO_2) + 2n(H_2O) used in Cerenkov counters, ρ = density in g/cm^3. From M. Cantin et al., Nucl. Instr. Meth. **118**, 177 (1974).

o. G10-plate, typical 60% SiO_2 and 40% Epoxy.

Mean Range and Energy Loss in Lead, Copper, Aluminum, and Carbon

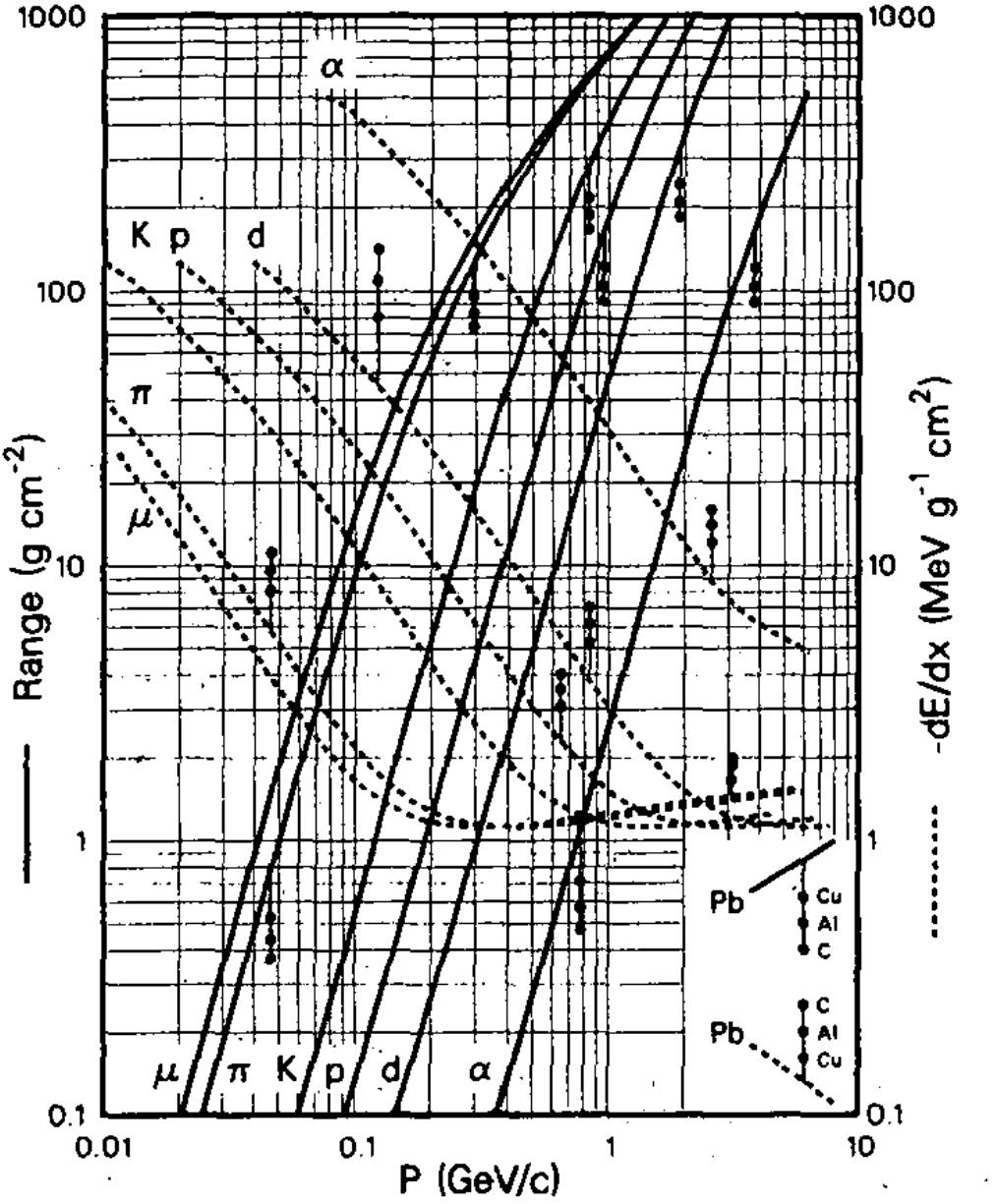

Mean range and energy loss due to ionization for the indicated particles in Pb, with scaling to Cu, Al, and C indicated, using Bethe-Bloch equation (Section C.1 above) with corrections. Calculated by M.J. Berger, using ionization potentials and density effect corrections as discussed in M.J. Berger and S.M. Seltzer, "Stopping Powers and Ranges of Electrons and Positrons," (2nd ed.), U.S. National Bureau of Standards Report NBSIR 82-2550-A (1982). The average ionization potentials (I) assumed were: Pb (823 eV), Cu (322 eV), Al (166 eV), and C (78.0 eV). Figure indicates total path length; observed range may be smaller (by ~ 1 % - 2% in heavy elements) due to multiple scattering, primarily from small energy-loss collisions with nuclei. The functional forms have not been experimentally verified to better than roughly ± 1%. For higher energies refer to discussion by Cobb ["A Study of Some Electromagnetic Interactions of High Velocity Particles with Matter," University of Oxford Report HEP/T/55 (1973)] and by Turner ["Penetration of Charged Particles in Matter: A Symposium," National Academy of Sciences, Washington D.C. (1970), p. 48]. Scaling to other beam particles is, to a good approximation, described by the expression on the next page.

Mean Range and Energy Loss in Liquid Hydrogen

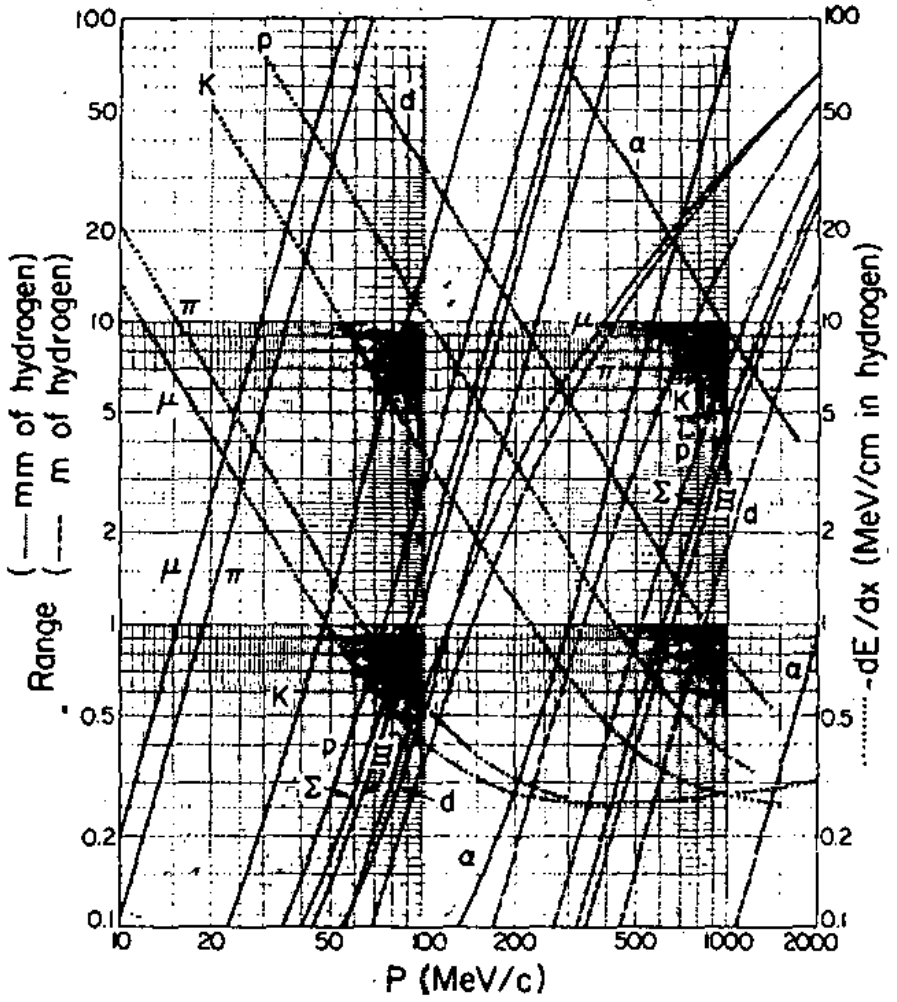

Range and energy loss in liquid hydrogen bubble chamber, based on Bethe-Bloch equation (Section C.1 above), using an average ionization potential for H_2 of I = 20.0 eV, which is an approximate average of the experimental result of Garbincius and Hyman [Phys. Rev. A2, 1834 (1970)] and the theoretical result of Ford and Browne [Phys. Rev. A7, 418 (1973)]. Bubble chamber conditions are chosen to be those of Garbincius and Hyman: parahydrogen of density = 0.0625 g/cm^3 (note: range $\propto$ 1/density), with vapor-pressure 60.8 lb/in^2 (absolute) and temperature 26.2°K. The functional dependence of the Bethe-Bloch equation is not experimentally verified to better than about ± 1% over large momentum ranges. It should be noted that the number of bubbles per cm of a track in a bubble chamber is nearly proportional to $1/\beta^2$, not dE/dx. For the linear portions of the range curves, $R \propto p^{3.6}$. ***Scaling law for particles of other mass or charge (except electrons):*** for a given medium, the range R_b of any beam particle with mass M_b, charge z_b, and momentum p_b is given in terms of the range R_a of any other particle with mass M_a, charge z_a, and momentum $p_a = p_b M_a/M_b$ (i.e., having the same velocity) by the expression:

$$R_b(M_b,z_b,p_b) = \left[\frac{M_b/M_a}{z_b^2/z_a^2}\right] R_a(M_a,z_a,p_a = p_b M_a/M_b) .$$

Photon Mass Attenuation Coefficients, Energy Deposition

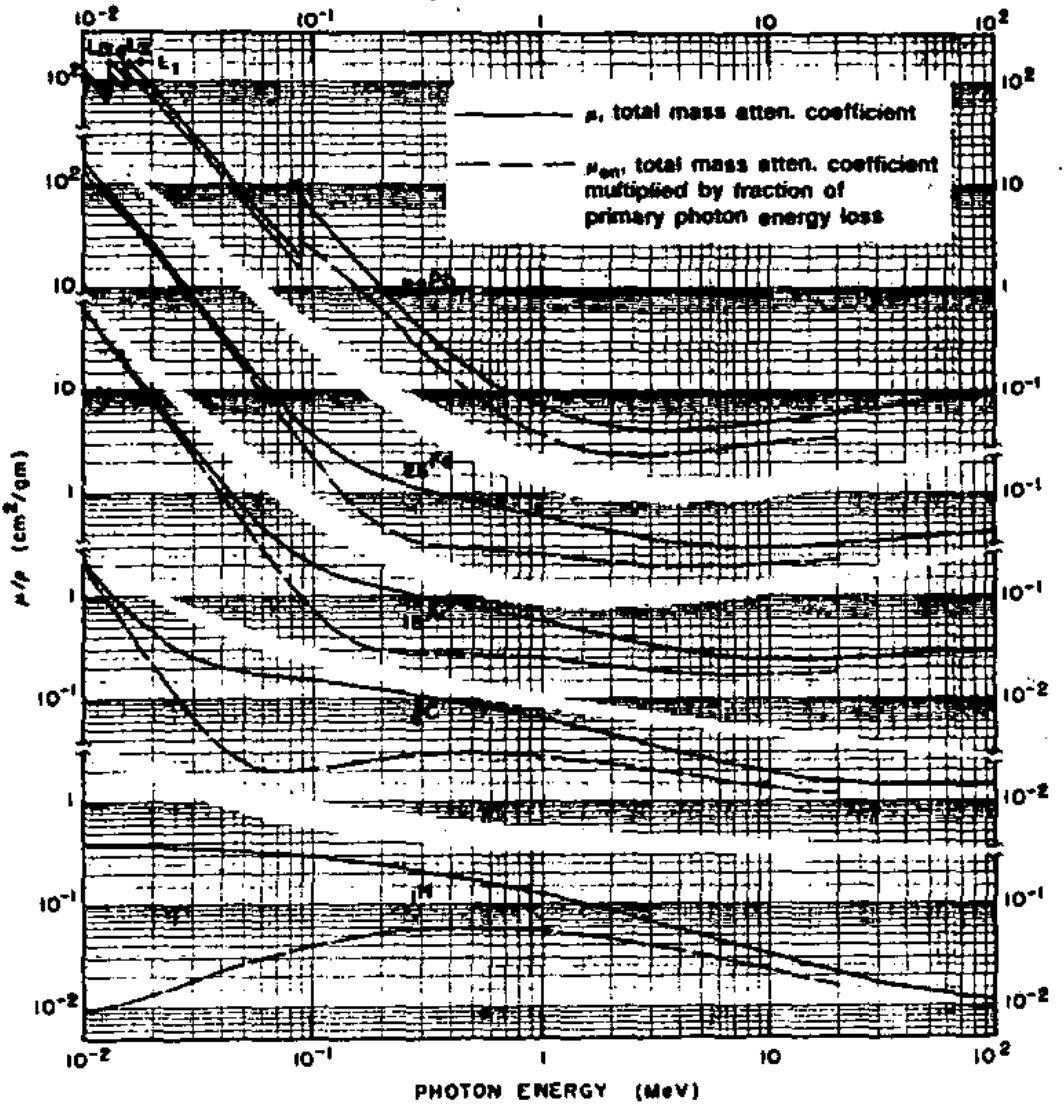

The photon mass attenuation coefficient μ for various absorbers as a function of photon energy (*solid curves*). For a homogeneous medium of density ρ, the intensity I remaining after traversal of thickness t is given by $I = I_0 \exp(-\mu t)$. The *accuracy* is a few percent. Interpolation to other Z should be done in the cross section $\sigma = (\mu/\rho)\, A/N_A$ cm^2/atom, where A is the atomic weight of the absorber material and N_A is Avogadro's number. For a chemical compound or mixture, use $(\mu/\rho)_{eff} \simeq \sum w_i(\mu/\rho)_i$, where w_i is the proportion by weight of the i^{th} constituent; this is accurate to a few percent. See next page for high energy range. The *dashed curves* give the mass energy-absorption coefficient μ_{en}, which is μ multiplied by the fraction of photon energy deposited in a small volume (assumed large enough to contain the ranges of most secondary electrons) about the interaction. This fraction is smaller than 1.0 because such processes as Compton scattering and electron bremsstrahlung imply radiation of some of the energy away from the immediate area. The absorption coefficient is an approximation to the energy available for chemical, biological, and other effects associated with exposure to ionizing radiation. At high energies, the range of secondary electrons tends to become comparable to the photon mean free path, and μ_{en} is not a useful approximation. From Hubbell, Gimm, and Øverbø, J. Phys. Chem. Ref. Data 9, 1023 (1980). See also J.H. Hubbell, Int. J. of Applied Rad. and Isotopes 33, 1269 (1982). Figures courtesy J.H. Hubbell.

Photon Mass Attenuation Coefficients (High Energy)

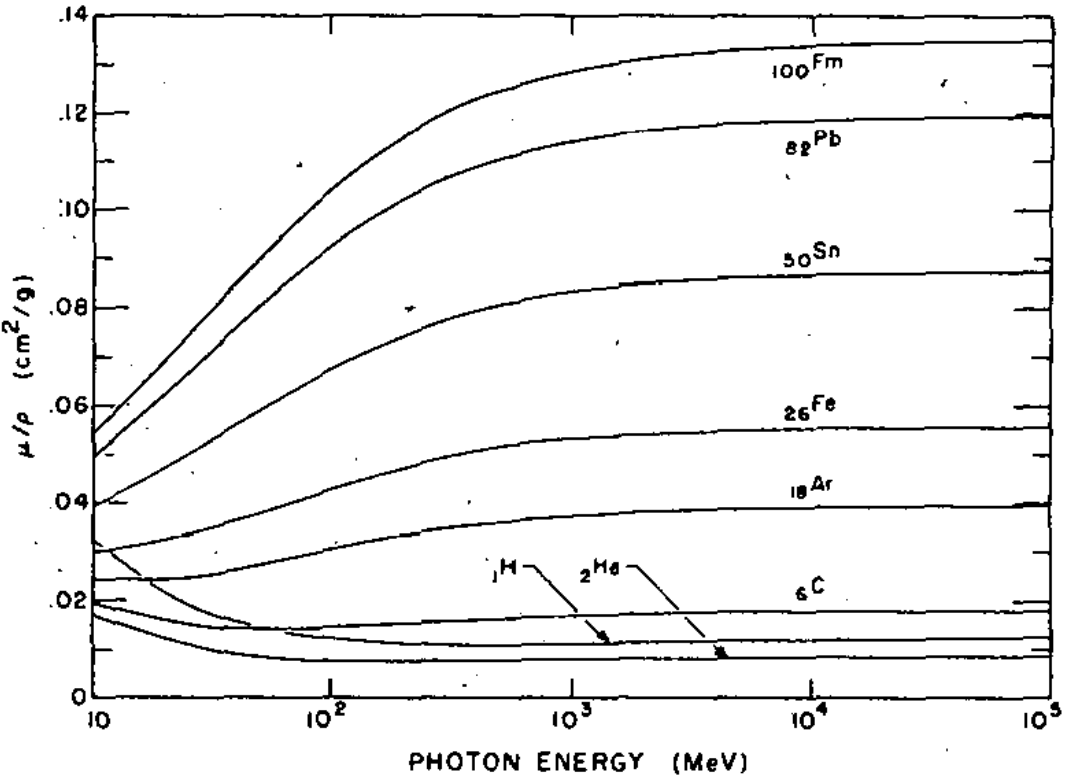

The photon mass attenuation coefficient, high energy range (note that ordinate is linear scale). See caption on previous page for details.

Fractional Energy Loss for Electrons and Positrons in Lead

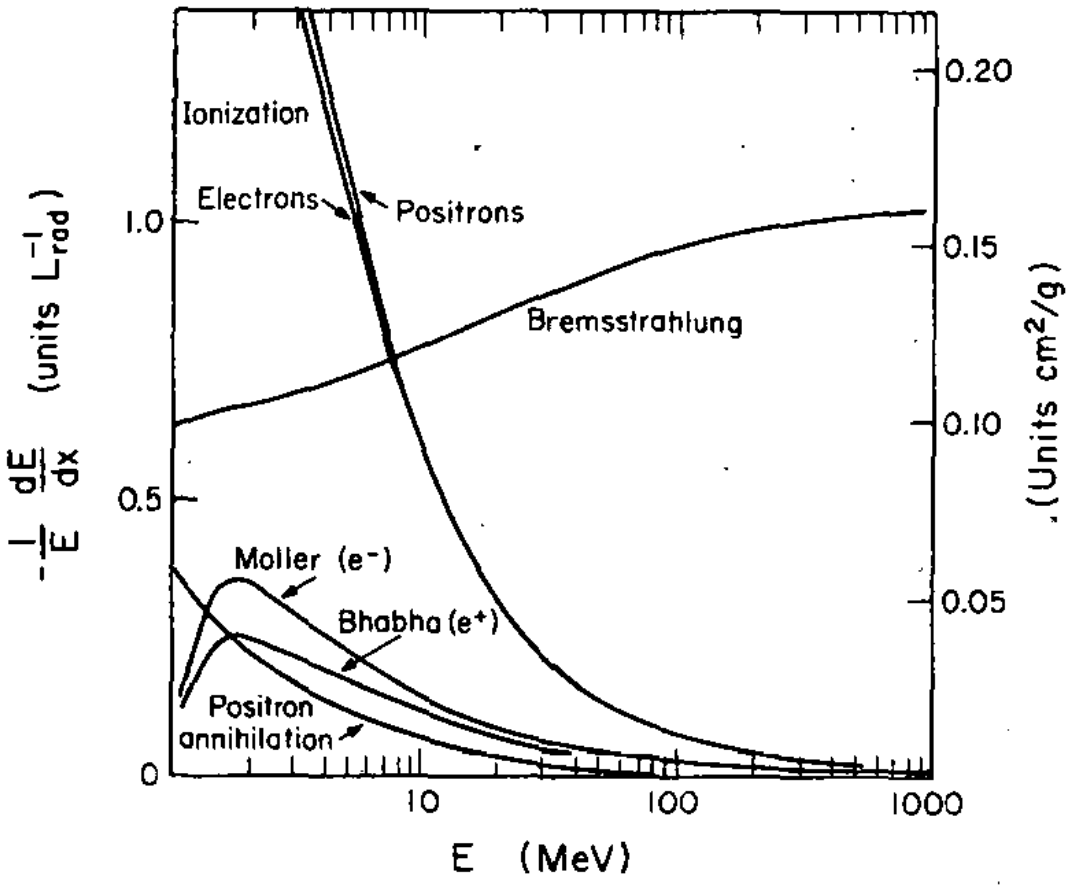

Fractional energy loss per radiation length in lead as a function of electron or positron energy. Electron (positron) scattering is considered as ionization when the energy loss per collision is below 0.255 MeV, and as Moller (Bhabha) scattering when it is above. Adapted from Fig. 3.2 from Messel and Crawford, *Electron-Photon Shower Distribution Function Tables for Lead, Copper, and Air Absorbers*, Pergamon Press, 1970. Messel and Crawford use $L_r(Pb) = 5.82$ g/cm^2, but we have modified the figures to reflect the value given in the Table of Atomic and Nuclear Properties of Materials (following), namely $L_r(Pb) = 6.4$ g/cm^2. The development of electron-photon cascades is approximately independent of absorber when the results are expressed in terms of inverse radiation lengths (i.e., scale on left of plot).

Contributions to Photon Cross Section in Carbon

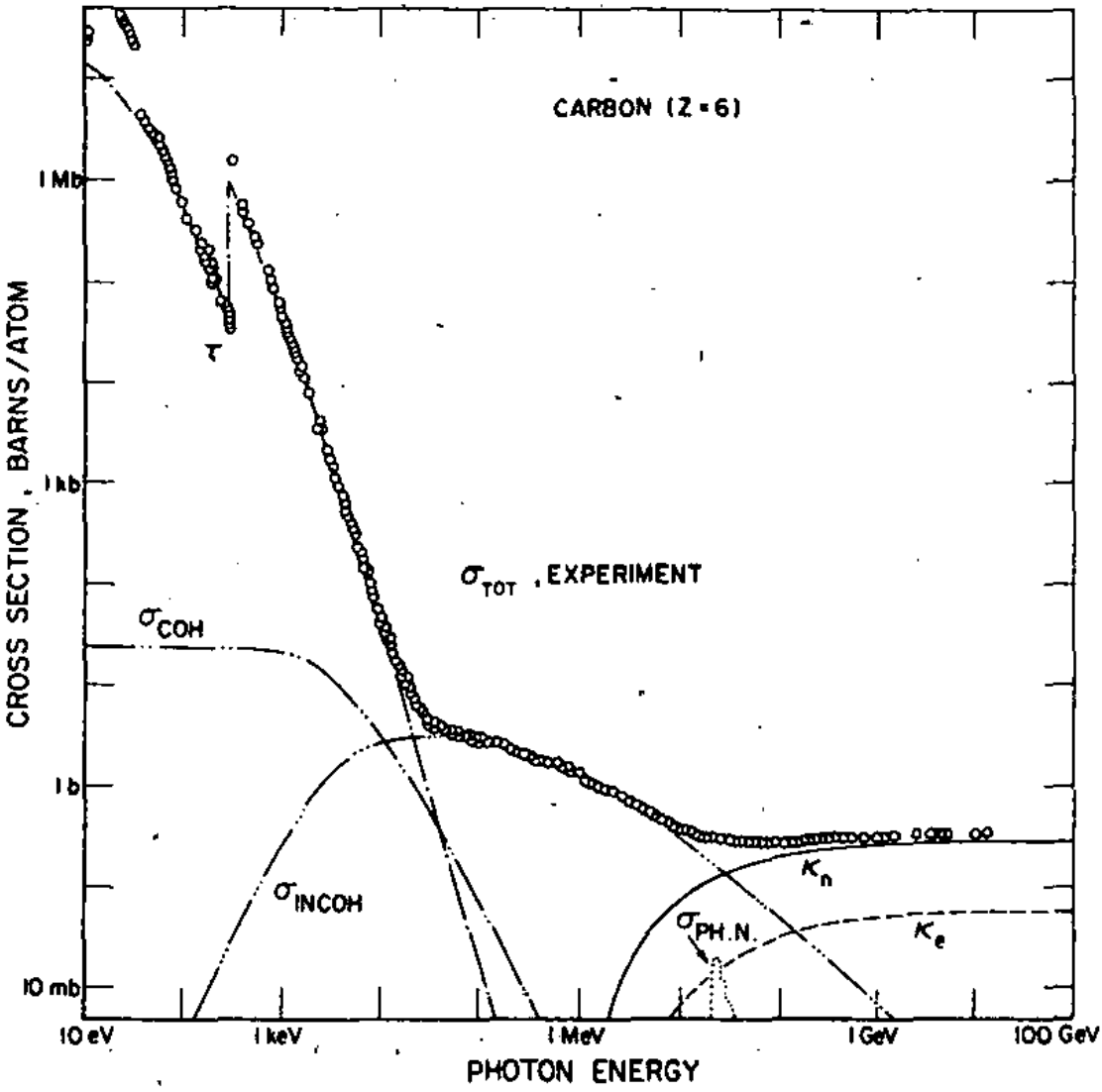

Photon total cross sections as a function of energy in carbon showing the contributions of different processes.

- τ = Atomic photo-effect (electron ejection; photon absorption)
- σ_{COH} = Coherent scattering (Rayleigh scattering — atom neither ionized nor excited)
- σ_{INCOH} = Incoherent scattering (Compton scattering off an electron)
- κ_n = Pair production, nuclear field
- κ_e = Pair production, electron field
- $\sigma_{PH.N.}$ = Photonuclear absorption (nuclear absorption, usually followed by emission of a neutron or other particle)

From Hubbell, Gimm, and Øverbø, J. Phys. Chem. Ref. Data 9, 1023 (1980). Figures courtesy J.H. Hubbell.

Contributions to Photon Cross Section in Lead

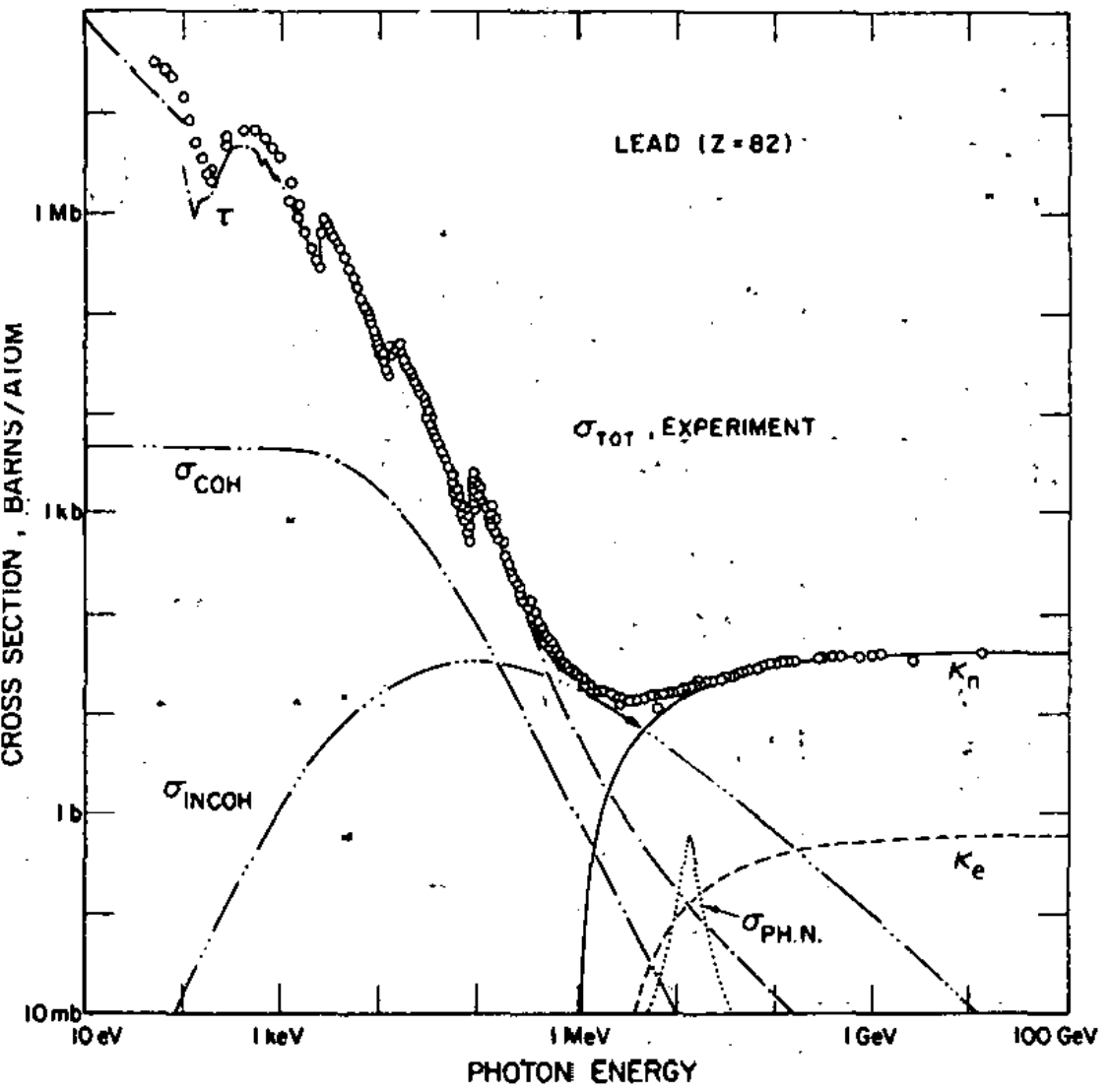

Photon total cross sections as a function of energy in lead showing the contributions of different processes.

τ	=	Atomic photo-effect (electron ejection, photon absorption)
σ_{COH}	=	Coherent scattering (Rayleigh scattering — atom neither ionized nor excited)
σ_{INCOH}	=	Incoherent scattering (Compton scattering off an electron)
κ_n	=	Pair production, nuclear field
κ_e	=	Pair production, electron field
$\sigma_{PH.N.}$	=	Photonuclear absorption (nuclear absorption, usually followed by emission of a neutron or other particle)

From Hubbell, Gimm, and Øverbø, J. Phys. Chem. Ref. Data 9, 1023 (1980). Figures courtesy J.H. Hubbell.

ELECTROMAGNETIC RELATIONS

Quantity	Gaussian CGS	MKSA
Units and conversions:		
Charge:	2.99792×10^{9} esu	= 1 coul = 1 amp-sec
Potential:	(1/299.792) statvolt = (1/299.792) erg/esu	= 1 volt = 1 joule/coul
Magnetic field:	10^{4} gauss = 10^{4} dyne/esu	= 1 tesla = 1 nt/amp-m
Electron charge:	$e = 4.803\,242\times10^{-10}$ esu	$= 1.602\,189\,2\times10^{-19}$ coul
Lorentz force:	$\mathbf{F} = q(\mathbf{E} + \frac{\mathbf{v}}{c}\times\mathbf{B})$	$\mathbf{F} = q(\mathbf{E} + \mathbf{v}\times\mathbf{B})$
Maxwell equations:	$\nabla\cdot\mathbf{D} = 4\pi\rho$ $\nabla\times\mathbf{E} = -\frac{1}{c}\frac{\partial\mathbf{B}}{\partial t}$ $\nabla\cdot\mathbf{B} = 0$ $\nabla\times\mathbf{H} = \frac{4\pi\mathbf{j}}{c} + \frac{1}{c}\frac{\partial\mathbf{D}}{\partial t}$	$\nabla\cdot\mathbf{D} = \rho$ $\nabla\times\mathbf{E} = -\frac{\partial\mathbf{B}}{\partial t}$ $\nabla\cdot\mathbf{B} = 0$ $\nabla\times\mathbf{H} = \mathbf{j} + \frac{\partial\mathbf{D}}{\partial t}$
Materials:	$\mathbf{D} = \epsilon\mathbf{E}$, $\mathbf{B} = \mu\mathbf{H}$	$\mathbf{D} = \epsilon\mathbf{E}$, $\mathbf{B} = \mu\mathbf{H}$
Dielectric constant:	$\epsilon_{vac} = 1$	$\epsilon_{vac} = \epsilon_0$
Magnetic susceptibility:	$\mu_{vac} = 1$	$\mu_{vac} = \mu_0$
Fields:	$\mathbf{E} = -\nabla V - \frac{1}{c}\frac{\partial\mathbf{A}}{\partial t}$ $\mathbf{B} = \nabla\times\mathbf{A}$	$\mathbf{E} = -\nabla V - \frac{\partial\mathbf{A}}{\partial t}$ $\mathbf{B} = \nabla\times\mathbf{A}$
Static potentials: (coulomb gauge)	$V = \sum_{\text{charges}} \frac{q}{r}$ $\mathbf{A} = \frac{1}{c}\sum_{\text{currents}} \frac{\mathbf{I}}{r}$	$V = \frac{1}{4\pi\epsilon_0}\sum_{\text{charges}} \frac{q}{r}$ $\mathbf{A} = \frac{\mu_0}{4\pi}\sum_{\text{currents}} \frac{\mathbf{I}}{r}$
Relativistic transformations: ($\mathbf{v}$ is the velocity of primed system as seen in unprimed system)	$\mathbf{E}'_{\parallel} = \mathbf{E}_{\parallel}$ $\mathbf{E}'_{\perp} = \gamma(\mathbf{E}_{\perp} + \frac{1}{c}\mathbf{v}\times\mathbf{B})$ $\mathbf{B}'_{\parallel} = \mathbf{B}_{\parallel}$ $\mathbf{B}'_{\perp} = \gamma(\mathbf{B}_{\perp} - \frac{1}{c}\mathbf{v}\times\mathbf{E})$	$\mathbf{E}'_{\parallel} = \mathbf{E}_{\parallel}$ $\mathbf{E}'_{\perp} = \gamma(\mathbf{E}_{\perp} + \mathbf{v}\times\mathbf{B})$ $\mathbf{B}'_{\parallel} = \mathbf{B}_{\parallel}$ $\mathbf{B}'_{\perp} = \gamma(\mathbf{B}_{\perp} - \frac{1}{c^2}\mathbf{v}\times\mathbf{E})$
	$4\pi\epsilon_0 = \frac{1}{c^2}10^{7}\frac{\text{coul}^2}{\text{nt sec}^2} = \frac{1}{8.987}55\times10^{-9}\frac{\text{coul}^2}{\text{nt m}^2}$ $\frac{\mu_0}{4\pi} = 10^{-7}\frac{\text{nt sec}^2}{\text{coul}^2}$; $c = 2.997\,924\,58\times10^{8}$ m sec^{-1}	

Impedances (MKSA)

ρ = resistivity in 10^{-8} Ωm:

~ 1.7 for Cu	~ 5.5 for W
~ 2.4 for Au	~ 73 for SS 304
~ 2.8 for Al	~ 100 for Nichrome
(Al alloys may have double this value.)	

For alternating currents, instantaneous current I, voltage V, angular frequency ω:

$$V = V_0 e^{i\omega t} = ZI .$$

Impedance of self-inductance L: $Z = i\omega L$.

Impedance of capacitance C: $Z = 1/i\omega C$.

Impedance of free space: $Z = \sqrt{\mu_0/\epsilon_0} = 376.7\ \Omega$.

Impedance per unit length of a flat conductor of width w (high frequency, ν):

$$Z = \frac{(1+i)\rho}{w\delta} \text{ , where } \delta = \text{effective skin depth ;}$$

$$\delta = \sqrt{\frac{\rho}{\pi\nu\mu}} \approx \frac{6.6 \text{ cm}}{\sqrt{\nu(\text{sec}^{-1})}} \text{ for Cu .}$$

Capacitance $\hat{C}$ and inductance $\hat{L}$ per unit length (MKSA)

Flat rectangular plates of width w, separated by $d \ll w$:

$$\hat{C} = \epsilon\frac{w}{d} ; \quad \hat{L} = \mu\frac{d}{w} ;$$

$\frac{\epsilon}{\epsilon_0}$ = 2 to 6 for plastics; 4 to 8 for porcelain, glasses.

Coaxial cable of inner radius r_1, outer radius r_2:

$$\hat{C} = \frac{2\pi\epsilon}{\ell n(r_2/r_1)} ; \quad \hat{L} = \frac{\mu}{2\pi}\ell n(r_2/r_1) .$$

Transmission lines (no loss):

Impedance: $Z = \sqrt{\hat{L}/\hat{C}}$.

Velocity: $v = 1/\sqrt{\hat{L}\hat{C}} = 1/\sqrt{\mu\epsilon}$.

Motion of charged particles in a uniform, static, magnetic field

The path of motion of a charged particle of momentum p is a helix of constant radius R and constant pitch angle λ, with the axis of the helix along **B**:

$$p(\text{GeV/c})\cos\lambda = 0.29979\ q\ B(\text{tesla})\ R(\text{m}),$$

where the charge q is in units of the electronic charge. The angular velocity about the axis of the helix is

$$\omega(\text{rad sec}^{-1}) = 8.98755\times10^{7}\ q\ B(\text{tesla})/E(\text{GeV}),$$

where E is the energy of the particle.

Synchrotron radiation (CGS)

For a relativistic particle of charge e, velocity β, γ, energy E, traveling in a circular orbit of radius R:

$$\text{Energy loss/revolution (MeV)} = \frac{4\pi}{3}\frac{e^2}{R}\beta^3\gamma^4$$

$$\simeq 0.0885\ [E(\text{GeV})]^4/R(\text{m}) \text{ for } e^{\pm} \text{ if } \beta \simeq 1.$$

Energy spectrum: The energy radiated into the photon energy interval $d(\hbar\omega)$ is

$$dI = \alpha\gamma F(\omega/\omega_c)d(\hbar\omega),$$

where $\alpha = e^2/(\hbar c)$ is the fine-structure constant,
$F(y) = 2\sqrt{3}y\int_{2y}^{\infty} dx\ K_{5/3}(x)$, with $K_{5/3}(x)$ a modified spherical Bessel function of the third kind, and $\omega_c = 3\gamma^3 c/R$ is a critical frequency;

$$\hbar\omega_c\ (\text{keV}) \simeq 4.44\ [E(\text{GeV})]^3/R(\text{m}) \text{ for } e^{\pm} \text{ if } \beta \simeq 1.$$

In the limit $\gamma \gg 1$,

for $\omega \ll \omega_c$:

$$\frac{dI}{d(\hbar\omega)} \simeq 3.3\alpha\left(\frac{\omega R}{c}\right)^{1/3};$$

for $\frac{\omega}{\omega_c} = (0.01, 0.1, 0.2, 1.0, 2.0)$:

$$\frac{dI}{d(\hbar\omega)} \simeq (1.0, 1.6, 1.6, 0.5, 0.08)\alpha\gamma \text{ , respectively;}$$

for $\omega \gtrsim 2\omega_c$:

$$\frac{dI}{d(\hbar\omega)} \simeq \sqrt{3\pi}\alpha\gamma \left(\frac{\omega}{\omega_c}\right)^{1/2} e^{-2\omega/\omega_c} .$$

The radiation is confined to angles $\lesssim 1/\gamma$ relative to the instantaneous direction of motion.

See J.D. Jackson, *Classical Electrodynamics*, 2nd edition (John Wiley & Sons, New York, 1975) for more formulae and details. (Prepared April 1974; revised April 1984.)

RADIOACTIVITY AND RADIATION PROTECTION

The International Commission on Radiation Units and Measurements (ICRU) recommends the use of SI units. Therefore we list SI units first, followed by cgs (or other common) units in parentheses, where they differ.

Unit of activity = becquerel (curie):
1 Bq = 1 disintegration/sec [$= 1/(3.7\times10^{10})$ Ci].

Unit of exposure, the quantity of X- or γ- radiation at a point in space integrated over time, in terms of charge of either sign produced by showering electrons in a small volume of air about the point:
= 1 coul/kg of air (roentgen; 1 R = 2.58×10^{-4} coul/kg
= 1 esu/cm^3 = 87.8 erg released energy per g of air); implicit in the definition is the assumption that the small test volume is embedded in a sufficiently large uniformly irradiated volume that the number of secondary electrons entering the volume equals the number leaving.

Unit of absorbed dose = gray (rad):
1 Gy = 1 joule/kg (= 10^4 erg/g = 10^2 rad)
= 6.24×10^{12} MeV/kg deposited energy.

Unit of dose equivalent (for biological damage) = sievert [= 10^2 rem (roentgen equivalent for man)]:
Dose equivalent in Sv = grays × Q, where Q (quality factor)

expresses long-term risk (primarily cancer and leukemia) from low-level chronic exposure; it depends upon the type of radiation and other factors. For γ rays and β particles, $Q \cong 1$; for protons, $Q \cong 1$ at $\sim$10 MeV, rising gradually to $\cong 2$ at $\sim$1 GeV; for thermal neutrons, $Q \cong 3$; for fast neutrons, Q ranges up to 10; and for α particles and heavy ions (assuming internal deposition — skin and clothing are usually sufficient protection against external sources), $Q \cong 20$.

Natural annual background, all sources: Most world areas, whole-body dose equivalent rate $\cong$ (0.4-4) mSv (40-400 millirems). Can range up to 50 mSv (5 rems) in certain areas. U.S. average $\cong$ 0.8 mSv. The lungs receive an additional $\cong$ 0.1 mSv ($\cong$ 10 mrem) from inhaled natural radioactivity, mostly radon and radon daughters (good to $\cong$ factor of 2 in open areas; can range an order of magnitude higher in buildings and up to 1000× in poorly ventilated mines).

Cosmic ray background in counters (Earth's surface): $\sim 10^4$/min/m^2/ster. For more accurate estimates and more details, see Sec. B of Particle Detectors, Absorbers, and Ranges.

Fluxes (per m^2) to deposit one Gy in one kg of matter, assuming uniform irradiation:

$\cong$ (**charged particles**) $6.24\times10^{12}/(dE/dx)$, where dE/dx (MeV m^2/kg), the energy loss per unit length, may be obtained (after conversion of units) from the Mean Range and Energy Loss figures.

$\cong 3.5\times10^{13}$ minimum-ionizing singly charged particles in carbon.

$\cong$ (**photons**) $6.24\times10^{12}/[E(MeV)(\mu_{en}/\rho)(m^2/kg)]$, for photons of energy E, mass energy absorption coefficient μ_{en}, and density ρ (see Photon Mass Attenuation Coefficients, Energy Deposition figure), for samples of thickness enough to contain the secondary electrons but $\ll 1/\mu_{en}$.

$\cong 2\times10^{15}$ photons of 1 MeV energy on carbon.

(Quoted fluxes good to about a factor of 2 for all materials.)

U.S. maximum permissible occupational dose for the whole body: 50 mSv/year (5 rem/year).

Lethal dose: Whole-body dose from penetrating ionizing radiation resulting in 50% mortality in 30 days (assuming no medical treatment), 2.5-3.0 Gy (250-300 rads) as measured internally on body longitudinal center line; surface dose varies due to variable body attenuation and may be a strong function of energy.

For a recent review, see E. Pochin, *Nuclear Radiation: Risks and Benefits* (Clarendon Press, Oxford, 1983).

PERIODIC TABLE OF THE ELEMENTS

IA	IIA											IIIA	IVA	VA	VIA	VIIA	
								1 H 1.0079									2 He 4.00260
3 Li 6.94	4 Be 9.01218											5 B 10.81	6 C 12.011	7 N 14.0067	8 O 15.9994	9 F 18.998403	10 Ne 20.17
11 Na 22.98977	12 Mg 24.305	IIIB	IVB	VB	VIB	VIIB	—	VIII	—		IB	IIB	13 Al 26.98154	14 Si 28.0855	15 P 30.97376	16 S 32.06	17 Cl 35.453	18 Ar 39.948
19 K 39.0983	20 Ca 40.08	21 Sc 44.9559	22 Ti 47.90	23 V 50.9415	24 Cr 51.996	25 Mn 54.9380	26 Fe 55.847	27 Co 58.9332	28 Ni 58.71	29 Cu 63.546	30 Zn 65.38	31 Ga 69.735	32 Ge 72.59	33 As 74.9216	34 Se 78.96	35 Br 79.904	36 Kr 83.80
37 Rb 85.467	38 Sr 87.62	39 Y 88.9059	40 Zr 91.22	41 Nb 92.9064	42 Mo 95.94	43 Tc 98.9062	44 Ru 101.07	45 Rh 102.9055	46 Pd 106.4	47 Ag 107.868	48 Cd 112.41	49 In 114.82	50 Sn 118.69	51 Sb 121.75	52 Te 127.60	53 I 126.9045	54 Xe 131.30
55 Cs 132.9054	56 Ba 137.33	57–71 Rare Earths	72 Hf 178.49	73 Ta 180.947	74 W 183.85	75 Re 186.207	76 Os 190.2	77 Ir 192.22	78 Pt 195.09	79 Au 196.9665	80 Hg 200.59	81 Tl 204.37	82 Pb 207.2	83 Bi 208.9804	84 Po (209)	85 At (210)	86 Rn (222)
87 Fr (223)	88 Ra 226.0254	89– Acti- nides	104 (260)	105 (260)	106 (263)												

57 La 138.9055	58 Ce 140.12	59 Pr 140.9077	60 Nd 144.24	61 Pm (145)	62 Sm 150.4	63 Eu 151.96	64 Gd 157.25	65 Tb 158.9254	66 Dy 162.50	67 Ho 164.9304	68 Er 167.26	69 Tm 168.9342	70 Yb 173.04	71 Lu 174.967	Rare earths (Lanthanide series)
89 Ac (227)	90 Th 232.0381	91 Pa 231.0359	92 U 238.029	93 Np 237.0482	94 Pu (244)	95 Am (243)	96 Cm (247)	97 Bk (247)	98 Cf (251)	99 Es (254)	100 Fm (257)	101 Md (258)	102 No (259)	103 Lr (260)	Actinide series

Upper number is atomic number, expressing the positive charge of the nucleus in multiples of the electronic charge e. Lower number is atomic mass weighted by isotopic abundance in earth's surface, relative to the mass of the carbon 12 isotope, which has been arbitrarily assigned a mass of 12.00000 atomic mass units (amu). Numbers in parentheses are mass numbers (the whole number nearest the value of the atomic mass, in amu) of most stable isotope of that element. Adapted from the *Handbook of Chemistry and Physics, 64th Ed., 1983-1984.* (Particle Data Group update, April 1984.)

CROSS SECTIONS AND RELATED QUANTITIES

NOTE: THE FIGURES IN THIS SECTION ARE INTENDED TO SHOW THE "BEST" OR "MOST REPRESENTATIVE" DATA IN THE OPINION OF THE COMPILER. THEY ARE NOT NECESSARILY COMPLETE COMPILATIONS OF ALL THE WORLD'S RELIABLE DATA.

Structure Functions

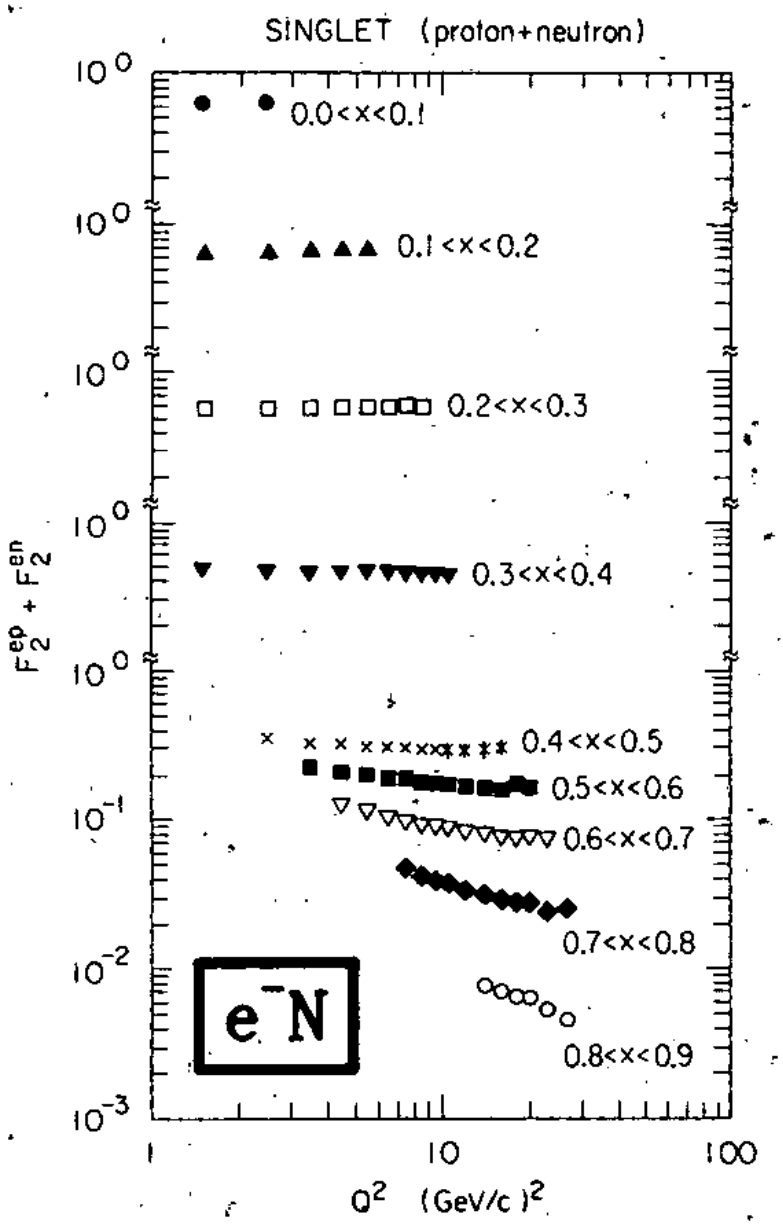

F_2 structure functions derived from inelastic electron-nucleon data taken at SLAC[1-4] with recoil mass > 2 GeV and four-momentum transfer squared $Q^2 > 1$ (GeV/c)^2 are shown. For definitions of F_2, x, and Q^2, see the Kinematics, Decays, and Scattering Section. $R \equiv \sigma_L/\sigma_T = 0.21$ [3] was assumed. Systematic errors are comparable in size to the data point symbols. Corrections for nucleon motion in

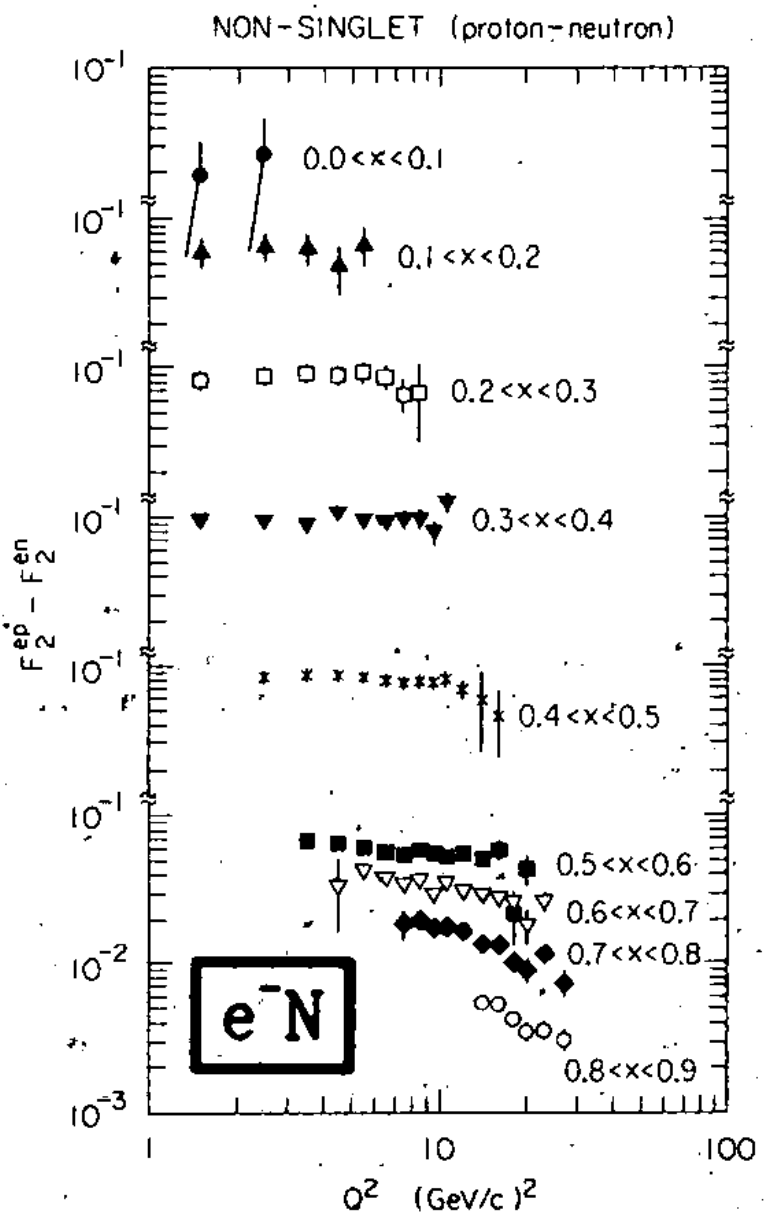

deuterium have been made. These corrections are small except for $x > 0.7$. No error was included to account for uncertainties in this correction. References: 1) A. Bodek et al., Phys. Rev. **D20**, 1471 (1979); 2) W.B. Atwood et al., SLAC Report No. 185 (1975); 3) M.D. Mestayer, SLAC Report No. 214 (1978); 4) S. Stein et al., Phys. Rev. **D12**, 1884 (1975). Courtesy W.B. Atwood, SLAC.

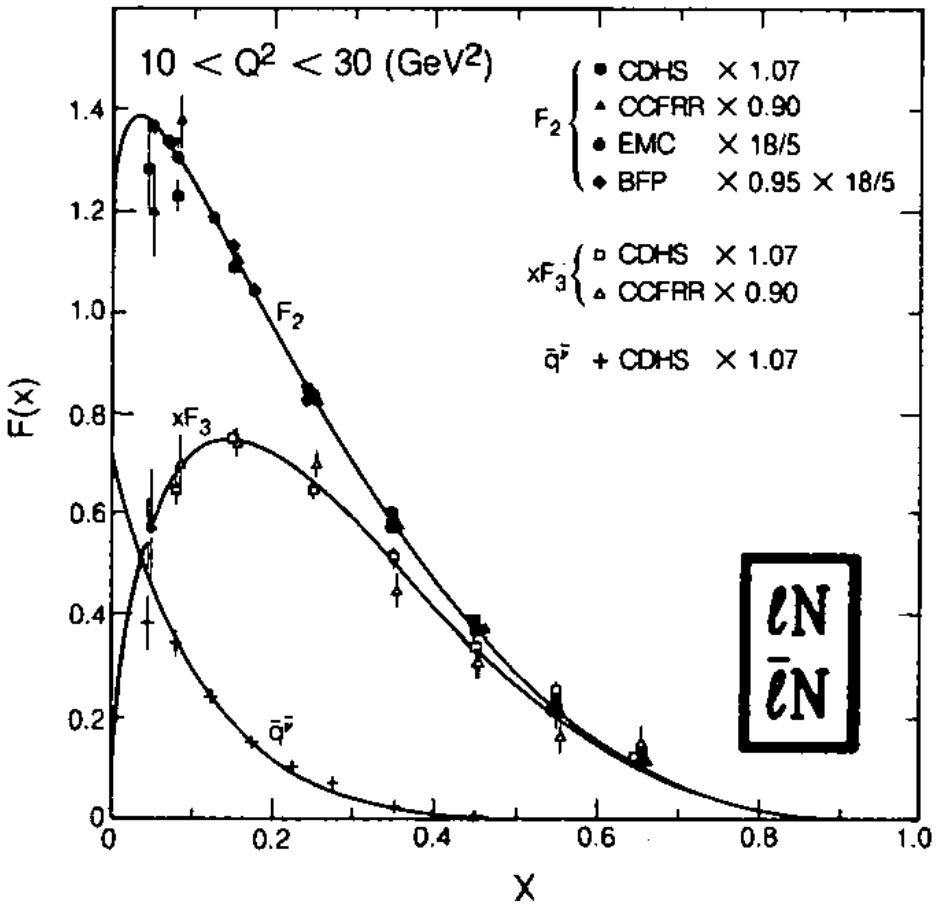

Structure functions F_2, xF_3, and $\overline{q}^{\nu}$, measured in different experiments, for fixed Q^2 versus x, plotted assuming $R = \sigma_L/\sigma_T = 0$. The electromagnetic structure function $F_2^{\mu N}$ measured by EMC and BFP is compared with the charged-current structure function $F_2^{\nu N}$ using the 18/5 factor from the average charge squared of the quarks. No correction has been applied for the difference between the strange and charm sea quarks so the interpretation is $F_2 = x\left[q + \overline{q} - \frac{3}{5}(s + \overline{s} - c - \overline{c})\right]$. (In this Q^2 range, $F_2^{\nu N}$ is depleted by a similar amount due to charm threshold effects in the transition $s \rightarrow c$.) The antiquark distribution measured from antineutrino scattering is $\overline{q}^{\nu} = x(\overline{u} + \overline{d} + 2\overline{s})$. The solid lines have the forms: $F_2 = 3.9x^{0.55}(1-x)^{3.2} + 1.1(1-x)^8$, $xF_3 = 3.6x^{0.55}(1-x)^{3.2}$, $\overline{q}^{\nu} = 0.7(1-x)^8$. Relative normalization factors have been fitted to optimize agreement between the different data sets, and absolute changes have been arbitrarily chosen as indicated. References: **CDHS** — H. Abramowicz et al., Zeit. Phys. **C17**, 283 (1983); **CCFRR** — F. Sciulli, private communication; **EMC** — J.J. Aubert et al., Phys. Lett. **105B**, 322 (1981); and A. Edwards, private communication; **BFP** — A.R. Clark et al., Phys. Rev. Lett. **51**, 1826 (1983); and P. Meyers, Ph.D. Thesis, LBL-17108 (1983), Univ. of Calif., Berkeley. Courtesy J. Carr, LBL.

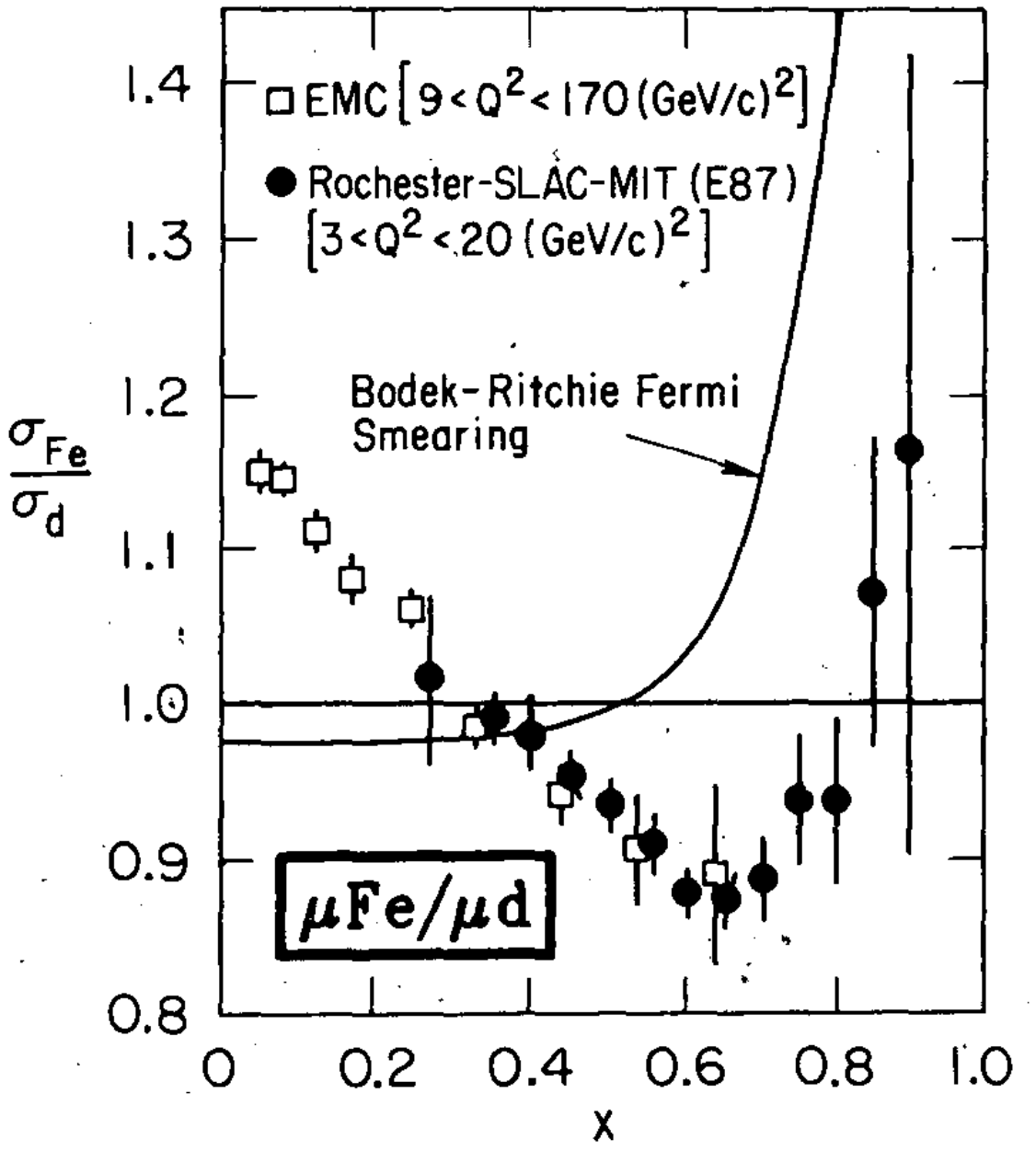

The "EMC" effect: the ratio of the differential cross section per nucleon, σ_{Fe}/σ_d, measured in electromagnetic deep inelastic scattering on iron and deuterium targets. (For equal values of $R = \sigma_L/\sigma_T$ on each target, $\sigma_{Fe}/\sigma_d = F_2^{Fe}/F_2^d$). The curve indicates the contribution to the ratio from Fermi motion in the nucleus [Phys. Rev. **D23**, 1070 (1981) and **D24**, 1400 (1981)]. The errors plotted are statistical only. The systematic errors are estimated as ± 0.011 for the Rochester-SLAC-MIT data, and ± 0.015 at $x = 0.35$ and ± 0.06 at $x = 0.05$ and $x = 0.65$ for the EMC data. References: **Rochester-SLAC-MIT** (electrons) — Phys. Rev. Lett. **50**, 1431 (1983); and **EMC** (muons) — Phys. Lett. **123B**, 275 (1983). Courtesy D. Coward, SLAC.

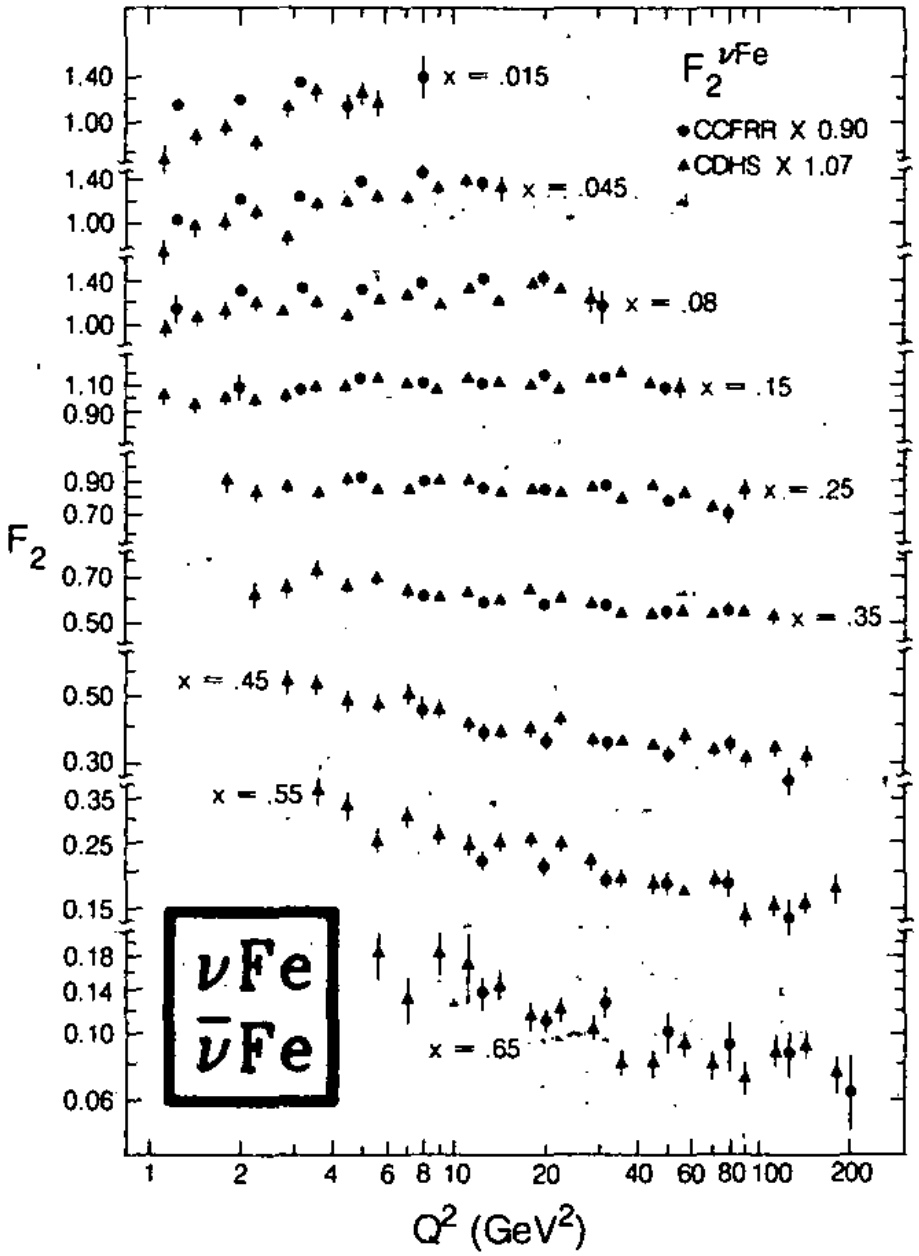

Structure functions F_2 and xF_3 for nucleons, measured in charged-current neutrino and antineutrino scattering from iron targets with $20 < E_\nu < 300$ GeV, versus Q^2 for fixed bins of x, plotted assuming $R = \sigma_L/\sigma_T = 0.1$. A relative normalization factor has been fitted to optimize the agreement between the different data sets, and absolute changes to the published data have been arbitrarily chosen as indicated. The point-to-point systematic errors for both experiments are generally smaller or of the same order as the statistical errors. In addition, CDHS quote an overall scale error of $\pm 6\%$ for F_2 and $\pm 8\%$ for xF_3, while for the CCFRR data the scale error is estimated to be

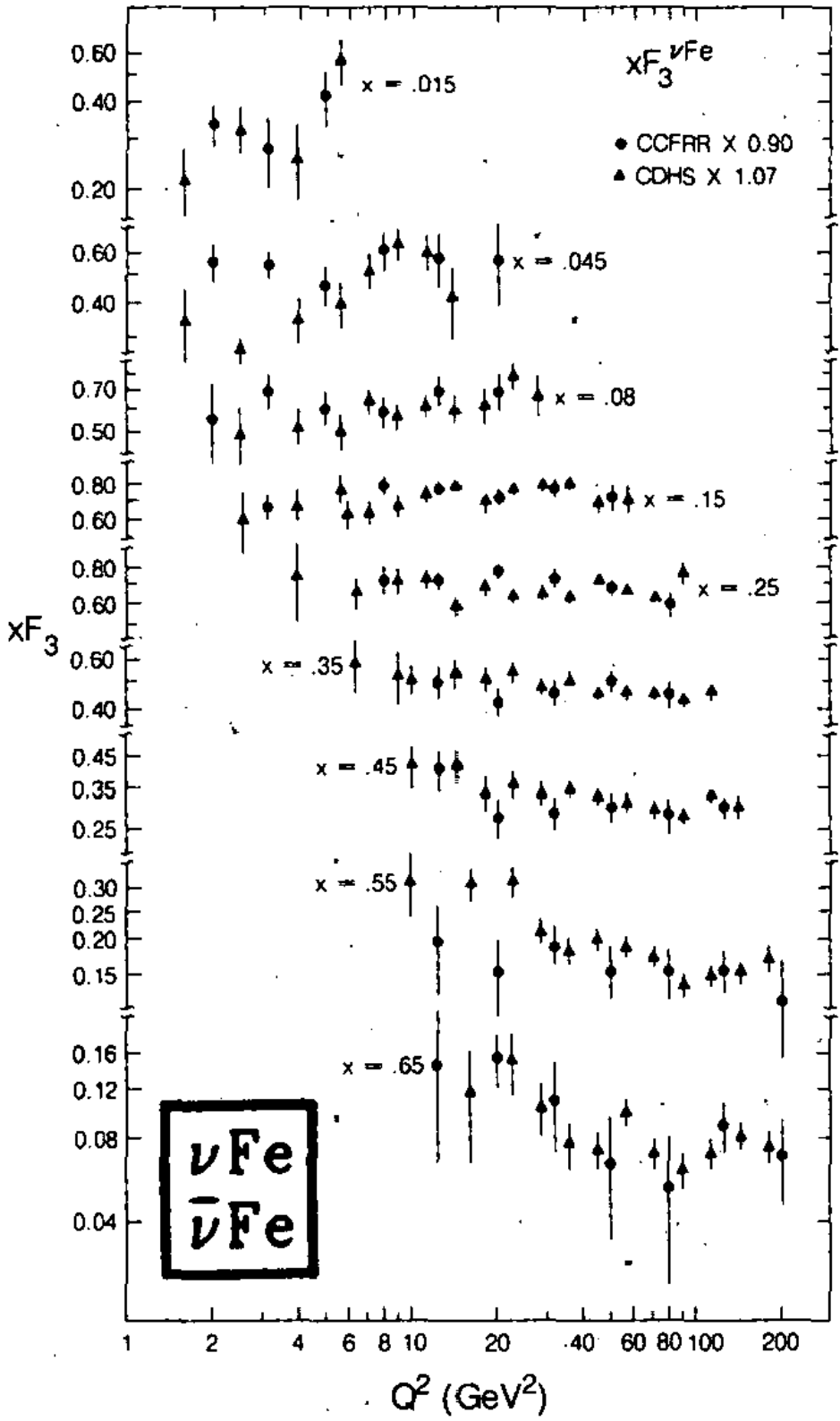

±4%. References: **CDHS** — H. Abramowicz et al., Zeit. Phys. C17, 283 (1983); **CCFRR** — F. Sciulli, private communication. Courtesy J. Carr, LBL.

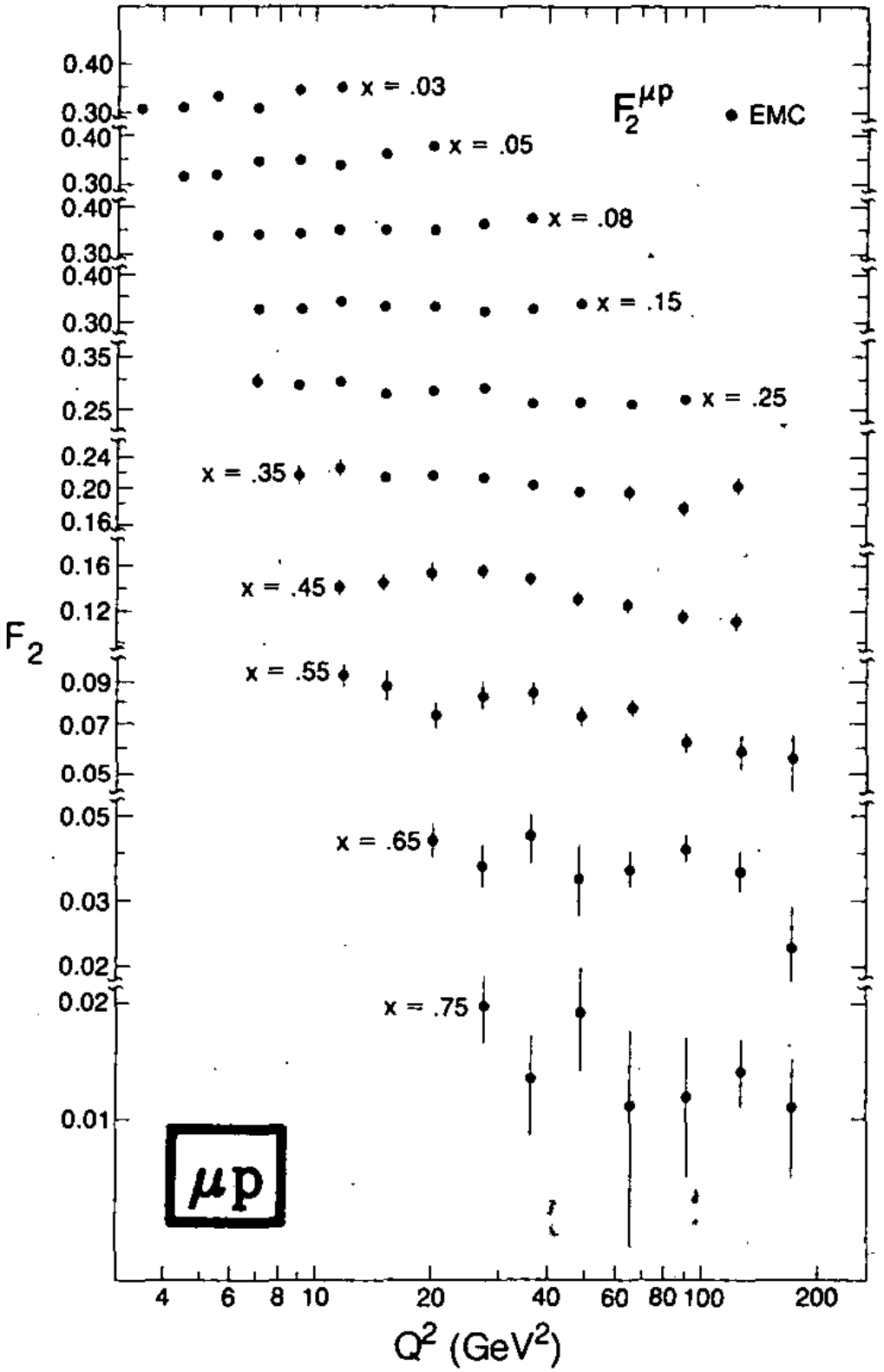

Structure function F_2^p, measured in electromagnetic muon scattering from a hydrogen target with beam energies 120, 200, 240, 280 GeV, versus Q^2 for fixed bins of x, plotted assuming $R = \sigma_L/\sigma_T = 0$. References: J.J. Aubert et al., Phys. Lett. **105B**, 315 (1981); and A. Edwards, private communication. Courtesy J. Carr, LBL.

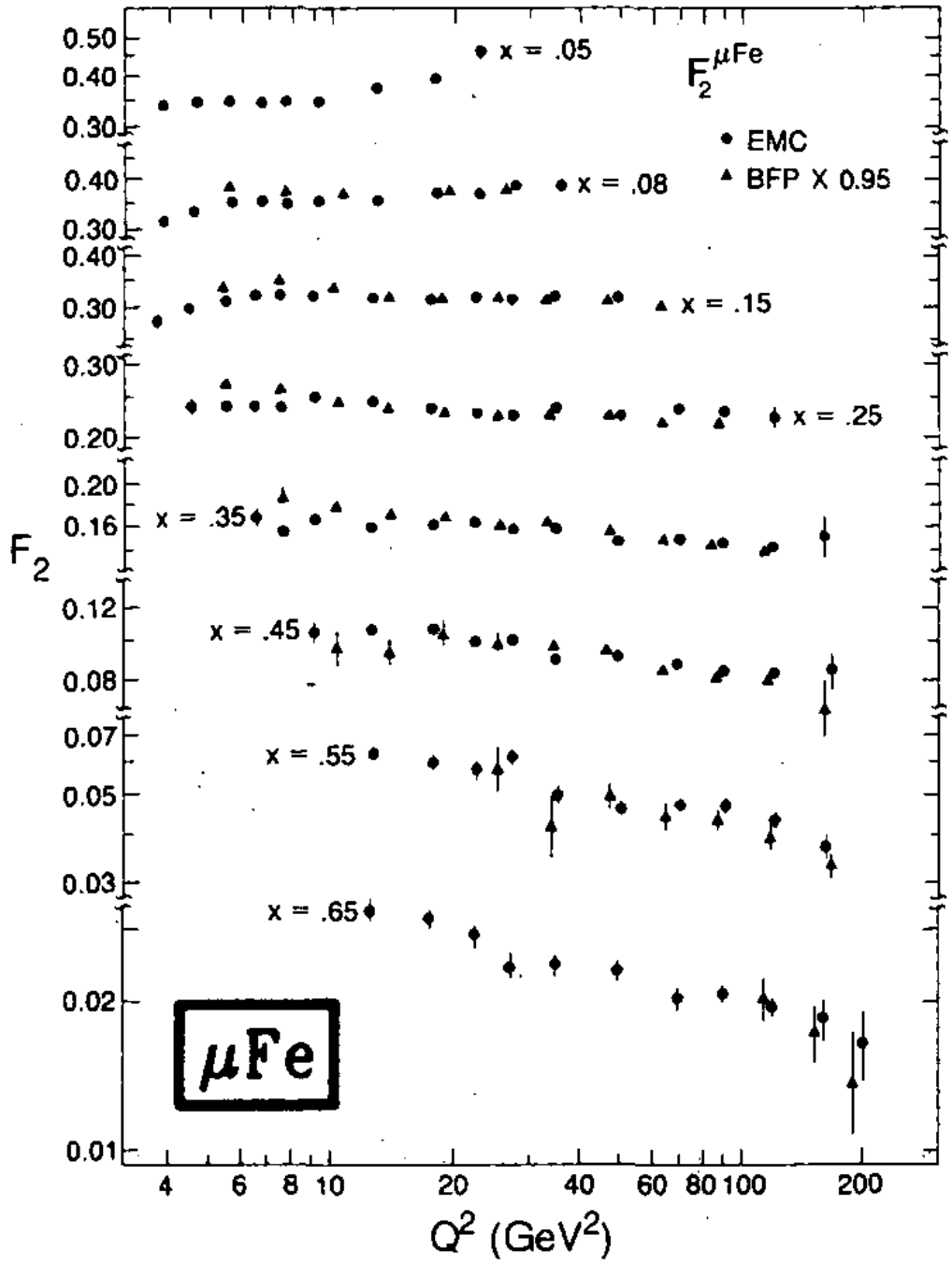

Structure function F_2 per nucleon, measured in electromagnetic muon scattering from iron targets with beam energies 120, 200, 250, 280 GeV (EMC) and 93, 215 GeV (BFP), versus Q^2 for fixed bins of x, plotted assuming $R = \sigma_L/\sigma_T = 0$. A relative normalization factor has been fitted to optimize agreement between the different data sets and has been arbitrarily applied to one data set as indicated. References: **EMC** — J.J. Aubert et al., Phys. Lett. **105B**, 322 (1981); and A. Edwards, private communication; **BFP** — A.R. Clark et al., Phys. Rev. Lett. **51**, 1826 (1983); and P. Meyers, Ph.D. Thesis, LBL-17108 (1983), Univ. of Calif., Berkeley. Courtesy J. Carr, LBL.

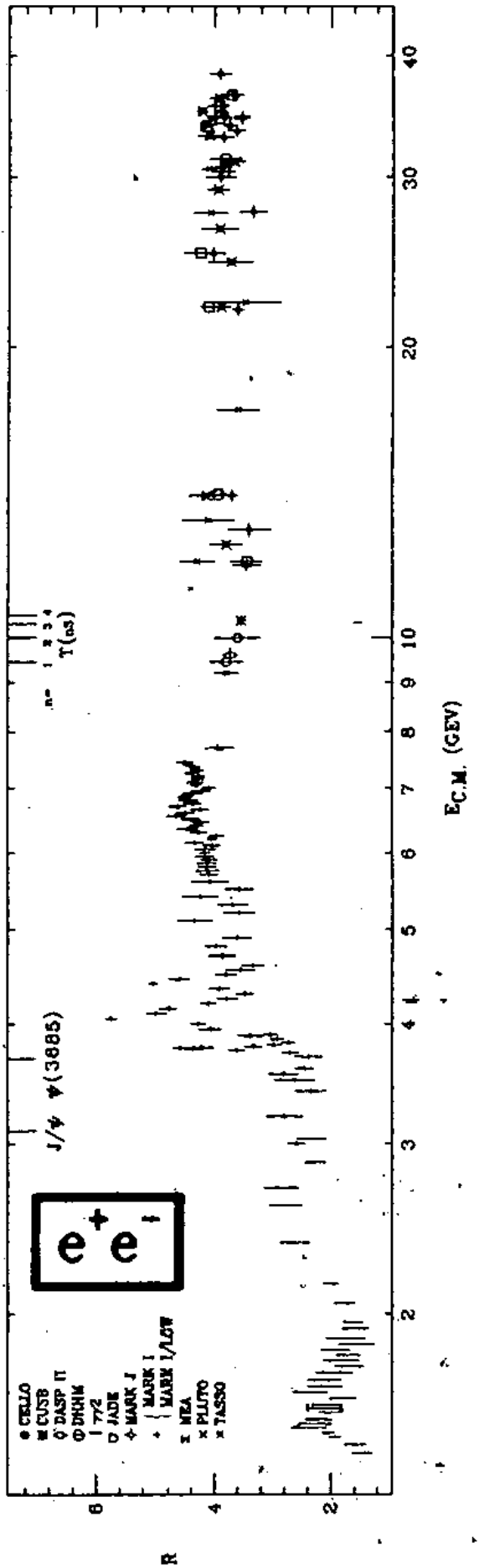
R
E_C.M. (GEV)
J/ψ ψ(3885)
n= 1 2 3 4
Υ(nS)
e+e-
CELLO
CUSB
DASP II
DHHM
7/2
JADE
MARK I
MARK I/LOW
MEA
PLUTO
TASSO

Measurements of $R \equiv \sigma(e^+e^- \to \text{hadrons})/\sigma(e^+e^- \to \mu^+\mu^-)$, where the annihilation proceeds via one photon. The denominator is a calculated quantity; see the section on Kinematics, Decays, and Scattering. Radiative corrections and, where important, corrections for two-photon processes and τ production have been made. Note that the ADONE data ($\gamma\gamma 2$ and MEA) is for ≥ 3 hadrons. The points in the $\psi(3770)$ region are from the MARK I - Lead Glass Wall experiment. The DASP [R. Brandelik et al., Phys. Lett. **76B**, 361 (1978)] and PLUTO (see references below) measurements have been omitted in the charm threshold region for clarity. Also for clarity, some points have been combined or shifted slightly (<4%) in $E_{c.m.}$, and some points with low statistical significance have been omitted. Systematic normalization errors are not included; they range from ~5 - 20%, depending on experiment. Note the suppressed zero. The horizontal extent of the plot symbols has no significance. The positions of the $J/\psi(3100)$, $\psi(3685)$, and the four known Υ vector-meson resonances are indicated at the top of the figure. References: **CELLO** — H.-J. Behrend et al., Phys. Lett. **B**, to be published (preprint DESY 81-029); **CUSB** — E. Rice et al., Phys. Rev. Lett. **48**, 906 (1982); **DASP II** — Phys. Lett. **116B**, 383 (1982); **DHHM** — P. Bock et al. (DESY-Hamburg-Heidelberg-MPI München Collab.), Zeit. fur Physik **C6**, 125 (1980); **$\gamma\gamma 2$** — C. Bacci et al., Phys. Lett. **86B**, 234 (1979); **JADE** — W. Bartel et al., Phys. Lett. **129B**, 145 (1983); **MARK J** — B. Adeva et al., Phys. Rev. Lett. **50**, 799 (1983); and H. Newman, private communication; **MARK I** — J.L. Siegrist et al., Phys. Rev. **D26**, 969 (1982); **MARK I + Lead Glass Wall** — P.A. Rapidis et al., Phys. Rev. Lett. **39**, 526 (1977); and P.A. Rapidis, thesis, SLAC-Report-220 (1979); **MEA** — B. Esposito et al., Lett. Nuovo Cimento **19**, 21 (1977); **PLUTO** — A. Bäcker, thesis Gesamthochschule Siegen, DESY F33-77/03 (1977); C. Gerke, thesis, Hamburg Univ. (1979); Ch. Berger et al., Phys. Lett. **81B**, 410 (1979); and W. Lackas, thesis, RWTH Aachen, DESY PLUTO-81/11 (1981); **TASSO** — R. Brandelik et al., Phys. Lett. **113B**, 499 (1982).

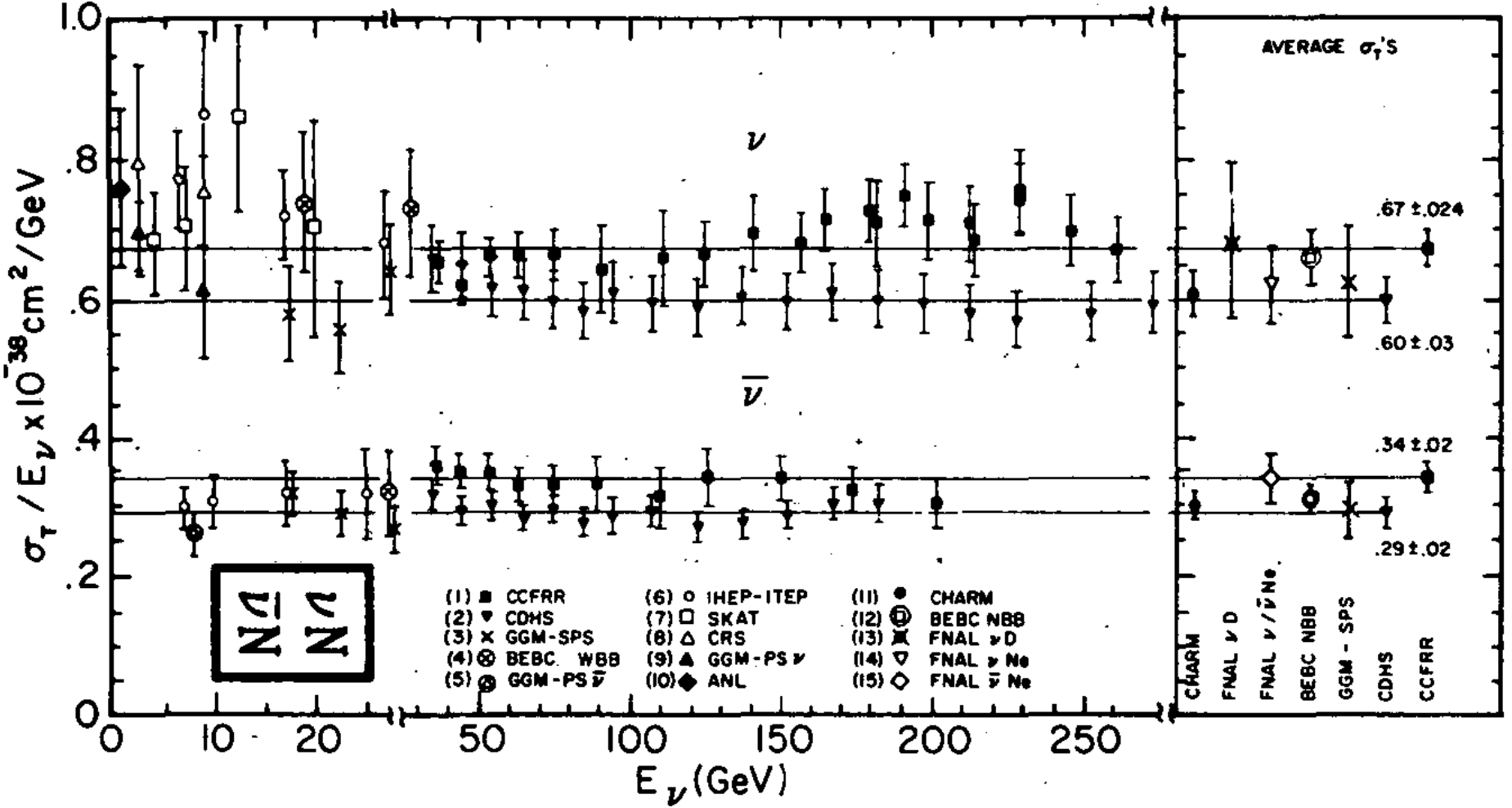
$\sigma_T / E_\nu \times 10^{-38} cm^2/GeV$
E_ν (GeV)
ν
$\bar{\nu}$
(1) CCFRR
(2) CDHS
(3) GGM-SPS
(4) BEBC WBB
(5) GGM-PS $\bar{\nu}$
(6) IHEP-ITEP
(7) SKAT
(8) CRS
(9) GGM-PS ν
(10) ANL
(11) CHARM
(12) BEBC NBB
(13) FNAL ν D
(14) FNAL ν Ne
(15) FNAL $\bar{\nu}$ Ne
AVERAGE σ_T'S
.67 ± .024
.60 ± .03
.34 ± .02
.29 ± .02
CHARM
FNAL ν D
FNAL $\nu/\bar{\nu}$ Ne
BEBC NBB
GGM - SPS
CDHS
CCFRR

σ_T/E_ν for the muon neutrino and antineutrino charged-current total cross section as a function of neutrino energy. The error bars include both statistical and systematic errors. The straight lines are averages for the CCFRR and CDHS measurements. Note the change in the energy scale between 20 and 50 GeV. The data points on the right give averages for other high energy measurements. References: (1) R. Blair et al., Phys. Rev. Lett. **51**, 343 (1983), and J.R. Lee, Ph.D. Thesis, Caltech (1981), "Measurements of νN Charged Current Cross Sections from E_ν = 25 GeV to E_ν = 260 GeV;" (2) H. Abramowicz et al., Zeit. fur Physik **C17**, 283 (1983); (3) J. Morfin et al., Phys. Lett. **104B**, 235 (1981); (4) D.C. Colley et al., Zeit. fur Physik **C2**, 187 (1979); (5) O. Erriquez et al., Phys. Lett. **80B**, 309 (1979); (6) A.S. Vovenko et al., Sov. J. Nucl. Phys. **30**, 527 (1979); (7) D.S. Baranov et al., Phys. Lett. **81B**, 255 (1979); (8) C. Baltay et al., Phys. Rev. Lett. **44**, 916 (1980); (9) S. Ciampolillo et al., Phys. Lett. **84B**, 281 (1979); (10) S.J. Barish et al., Phys. Rev. **D19**, 2521 (1979); (11) M. Jonker et al., Phys. Lett. **99B**, 265 (1981), E_ν = 20-200 GeV; (12) P. Bosetti et al., Phys. Lett. **110B**, 167 (1982), E_ν = 20-200 GeV; (13) T. Kitagaki et al., Phys. Rev. Lett. **49**, 98 (1982), E_ν = 10-200 GeV; (14) N.J. Baker et al., Phys. Rev. Lett. **51**, 735 (1983), E_ν = 10-240 GeV; (15) G.N. Taylor et al., Phys. Rev. Lett. **51**, 739 (1983), E_ν = 5-250 GeV. Courtesy M.H. Shaevitz, Columbia University (Nevis Laboratory).

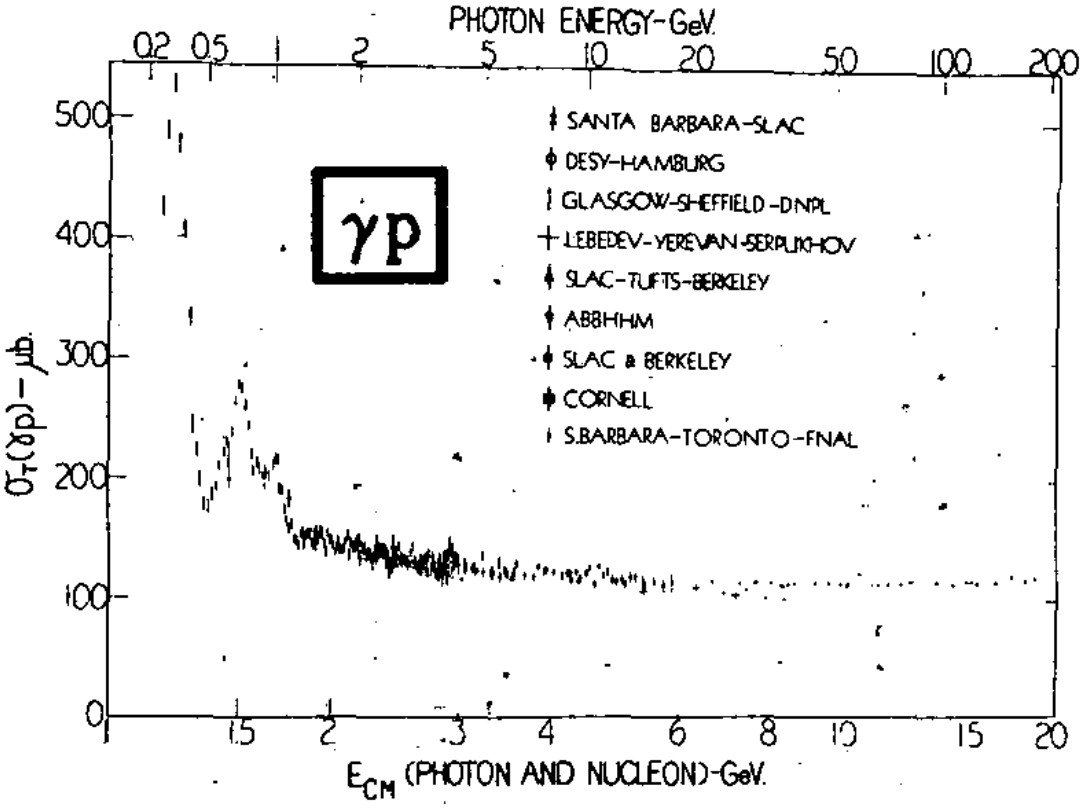

γp total cross section versus photon energy (top scale) and photon-plus-nucleon total center-of-mass energy (lower scale). References: **SANTA BARBARA-SLAC** — D.O. Caldwell et al., Phys. Rev. **D7**, 1362 (1973); **DESY-HAMBURG** — H. Meyer et al., Phys. Lett. **33B**, 189 (1970); **GLASGOW-SHEFFIELD-DNPL** — T.A. Armstrong et al., Phys. Rev. **D5**, 1640 (1972); **LEBEDEV-YEREVAN-SERPUKHOV** — A.S. Belousov et al., Preprint 19, Moscow, (1970); A. S. Belousov et al., Sov. Phys. Doklady **19**, 123 (1974); and A. S. Belousov et al., Sov. J. Nucl. Phys. **21**(3), 289 (1975); **SLAC-BERKELEY-TUFTS** — J. Ballam et al., Phys. Rev. **D5**, 545 (1972); **ABBHHM** — H.G. Hilpert et al., Phys. Lett. **27B**, 474 (1968); **SLAC** and **BERKELEY** — J. Ballam et al., Phys. Rev. Lett. **21**, 1544 (1968), and H.H. Bingham et al., Phys. Rev. **D8**, 1277 (1973); **CORNELL** — S. Michalowski et al., Phys. Rev. Lett. **39**, 737 (1977); **SANTA BARBARA-TORONTO-FNAL** — D.O. Caldwell et al., Phys. Rev. Lett. **40**, 1222 (1978). See, also, the ep data of E.D. Bloom et al., SLAC-PUB-653 (1969). Courtesy Gething M. Lewis, Glasgow.

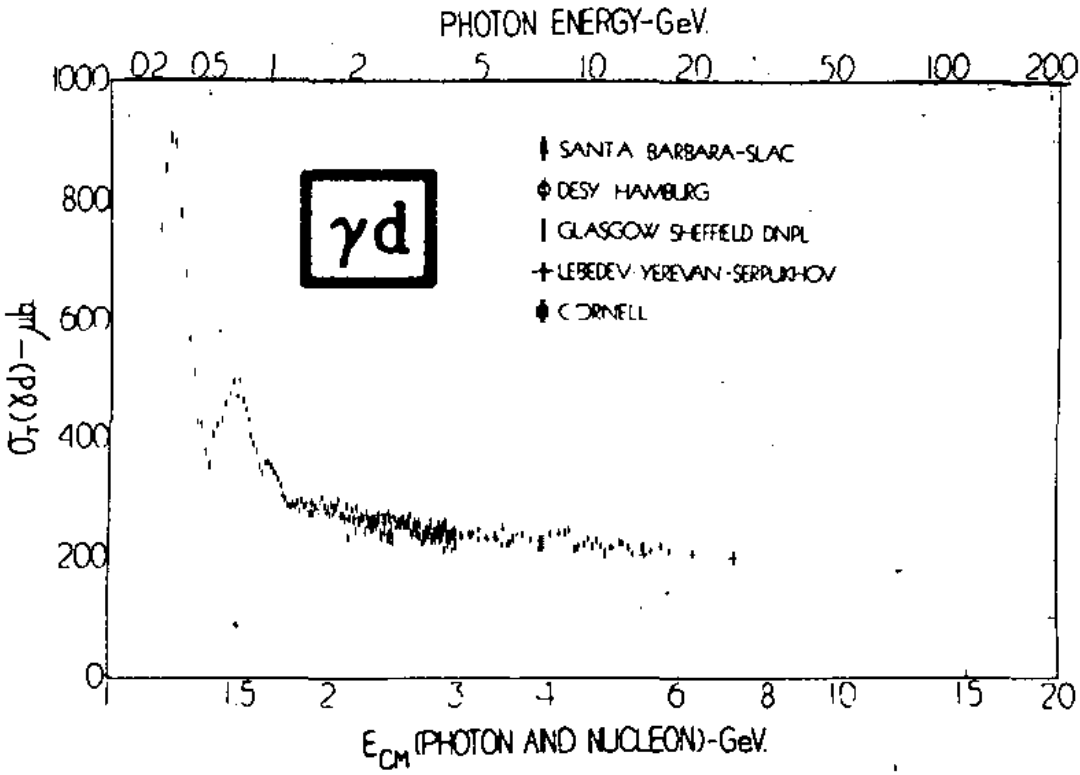

γd total cross section versus photon energy (top scale) and photon-plus-single-nucleon total center-of-mass energy (lower scale). References: SANTA BARBARA-SLAC — D.O. Caldwell et al., Phys. Rev. D7, 1362 (1973); DESY-HAMBURG — H. Meyer et al., Phys. Lett. 33B, 189 (1970); GLASGOW-SHEFFIELD-DNPL — T.A. Armstrong et al., Nucl. Phys. B41, 445 (1972); LEBEDEV-YEREVAN-SERPUKHOV — A.S. Belousov et al., Sov. J. Nucl. Phys. 21(3), 289 (1975); CORNELL — S. Michalowski et al., Phys. Rev. Lett. 39, 737 (1977). Courtesy Gething M. Lewis, Glasgow.

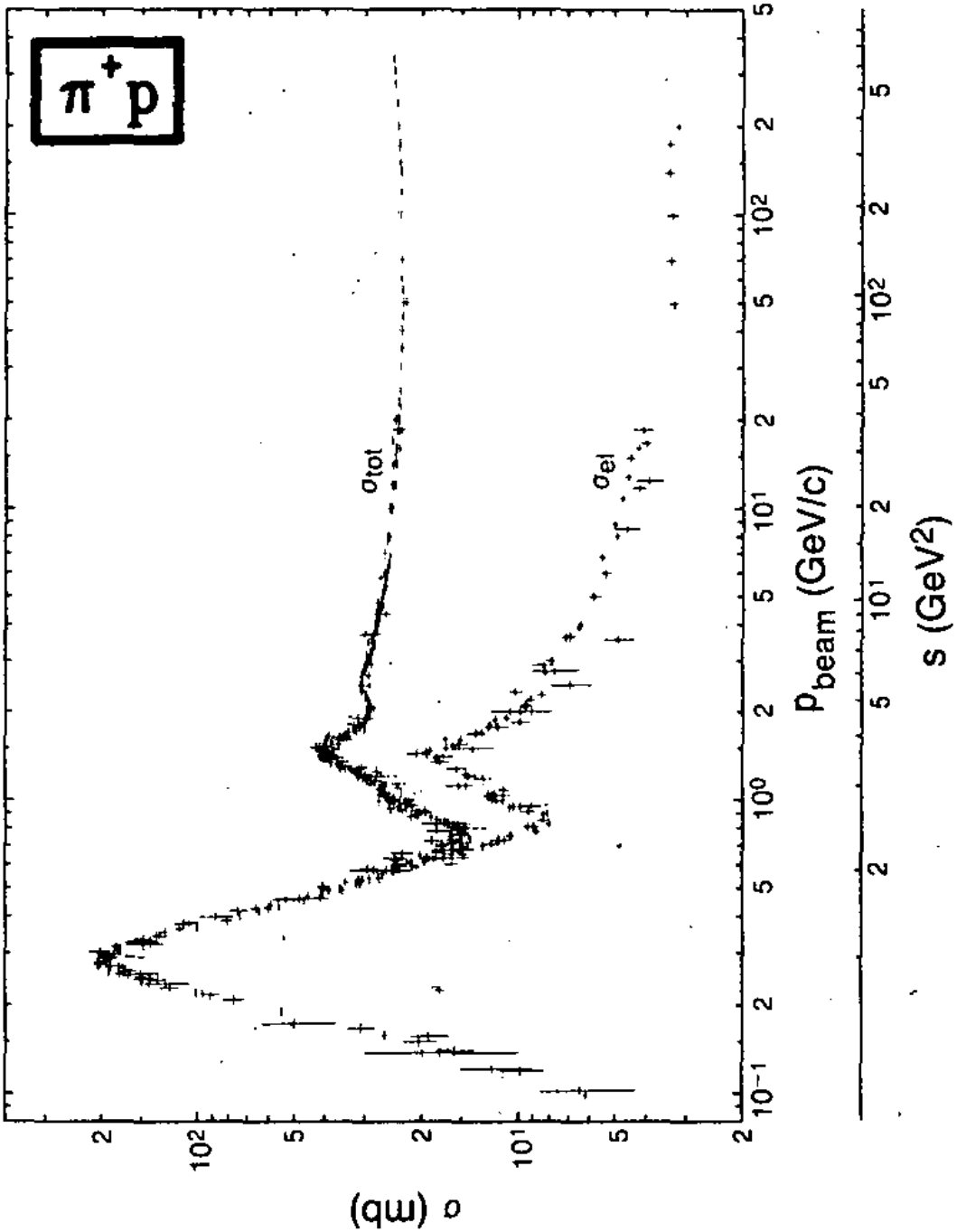

π^+p total and elastic cross sections vs. laboratory beam momentum p_{beam} and center-of-mass energy squared s. Figure courtesy V. Flaminio, W.G. Moorhead, D.R.O. Morrison, and N. Rivoire, CERN.

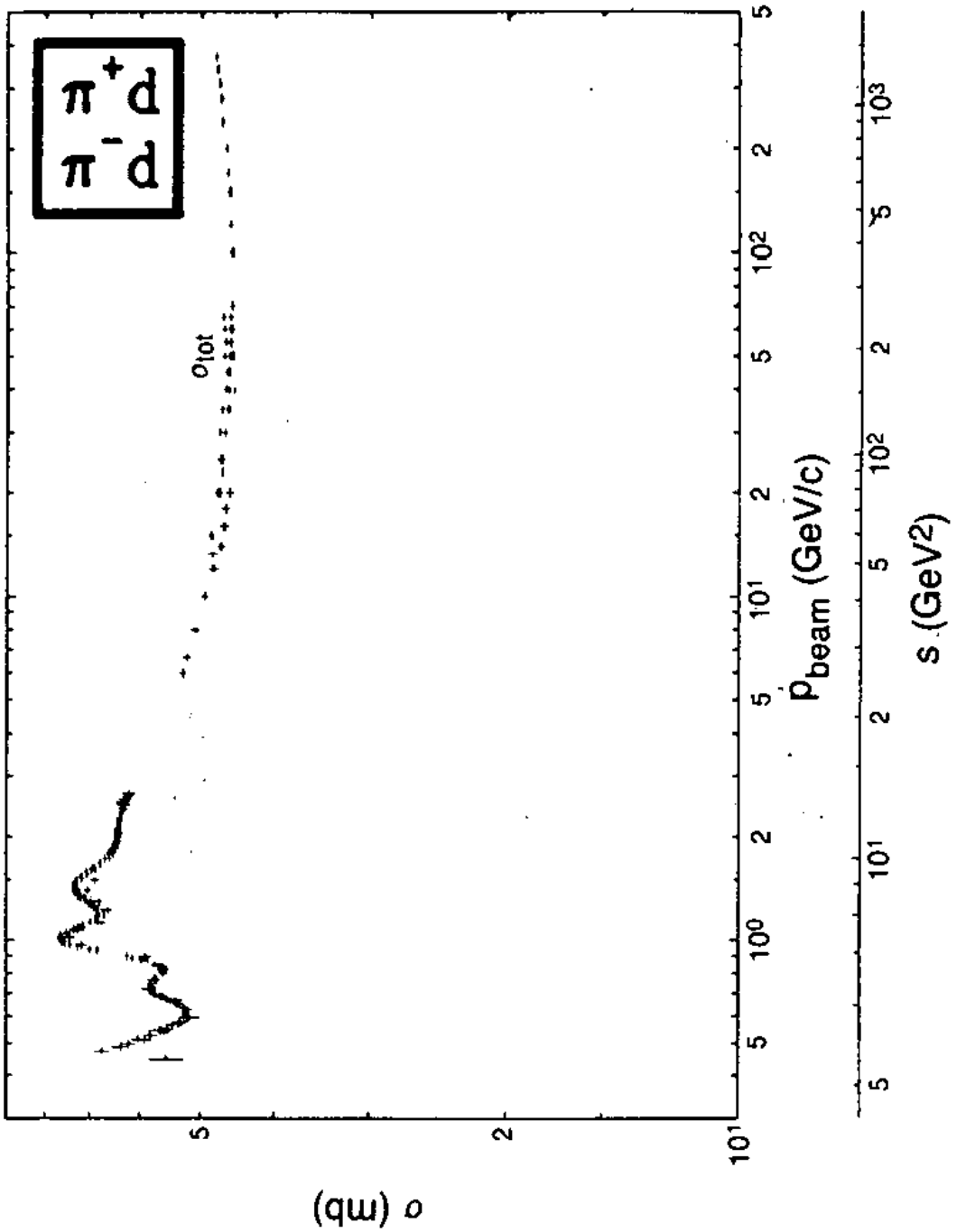

π^+d and π^-d total cross sections vs. laboratory beam momentum p_{beam} and center-of-mass energy squared s. Figure courtesy V. Flaminio, W.G. Moorhead, D.R.O. Morrison, and N. Rivoire, CERN.

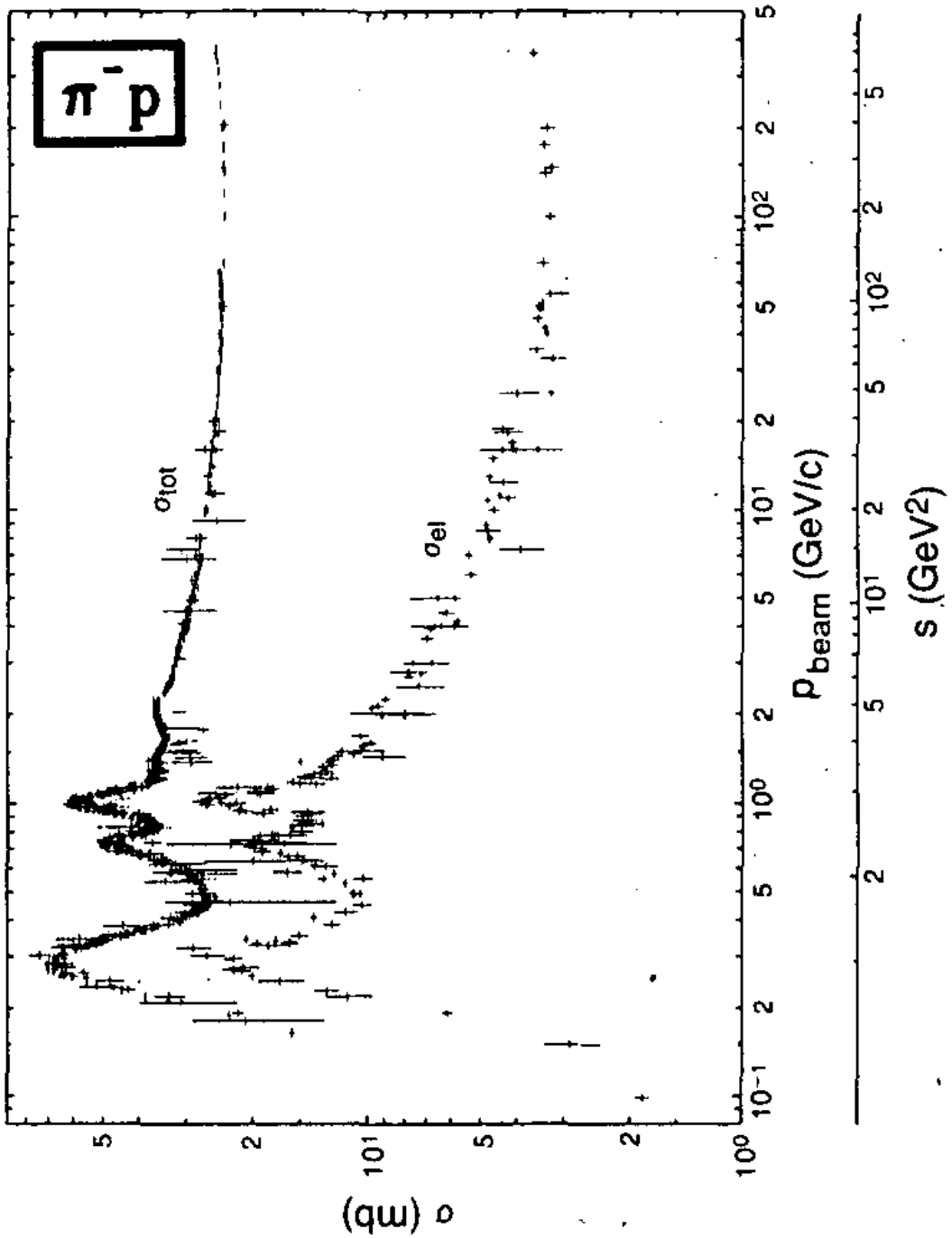

$\pi^- p$ total and elastic cross sections vs. laboratory beam momentum p_{beam} and center-of-mass energy squared s. Figure courtesy V. Flaminio, W.G. Moorhead, D.R.O. Morrison, and N. Rivoire, CERN.

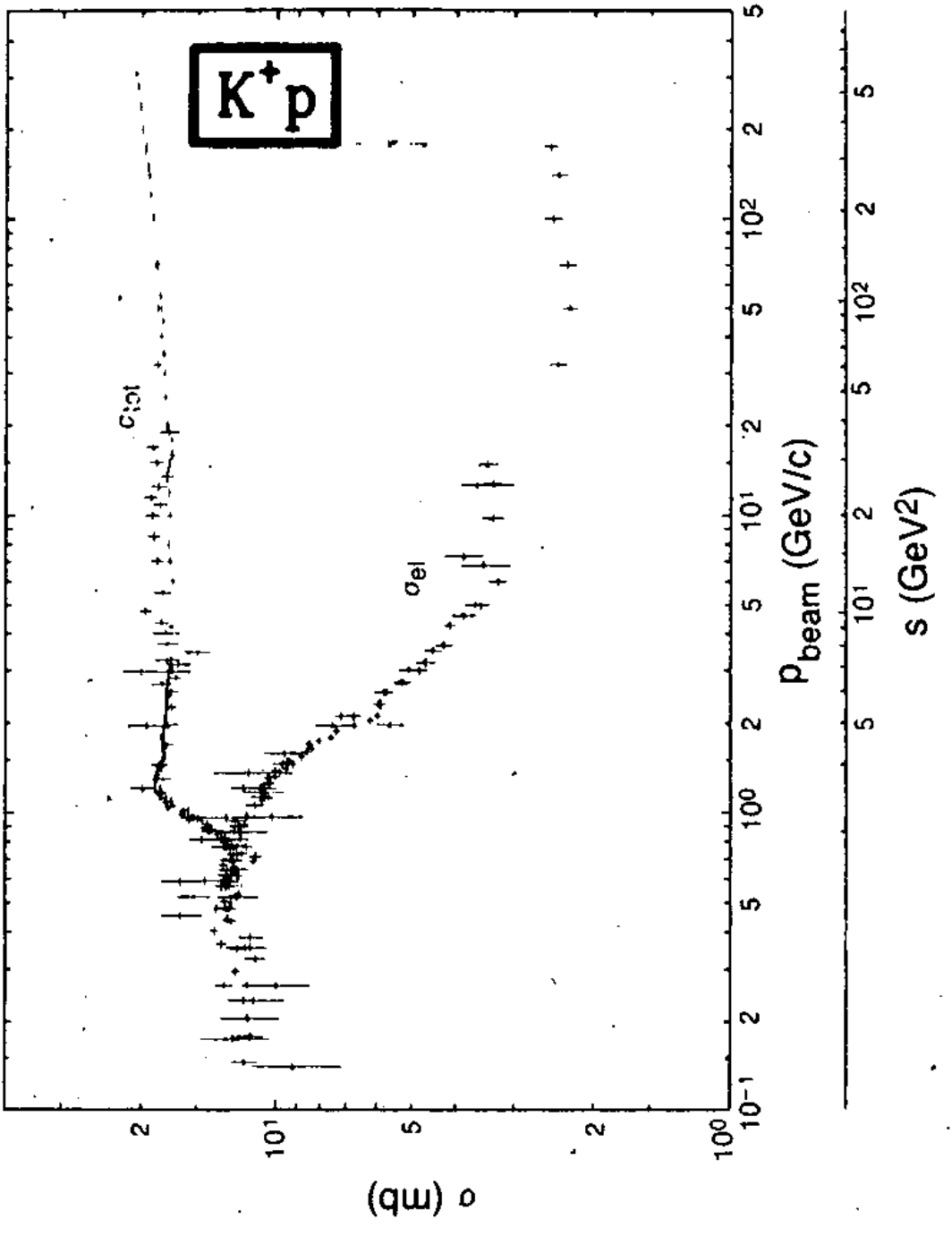

K^+p total and elastic cross sections vs. laboratory beam momentum p_{beam} and center-of-mass energy squared s. Figure courtesy V. Flaminio, W.G. Moorhead, D.R.O. Morrison, and N. Rivoire, CERN.

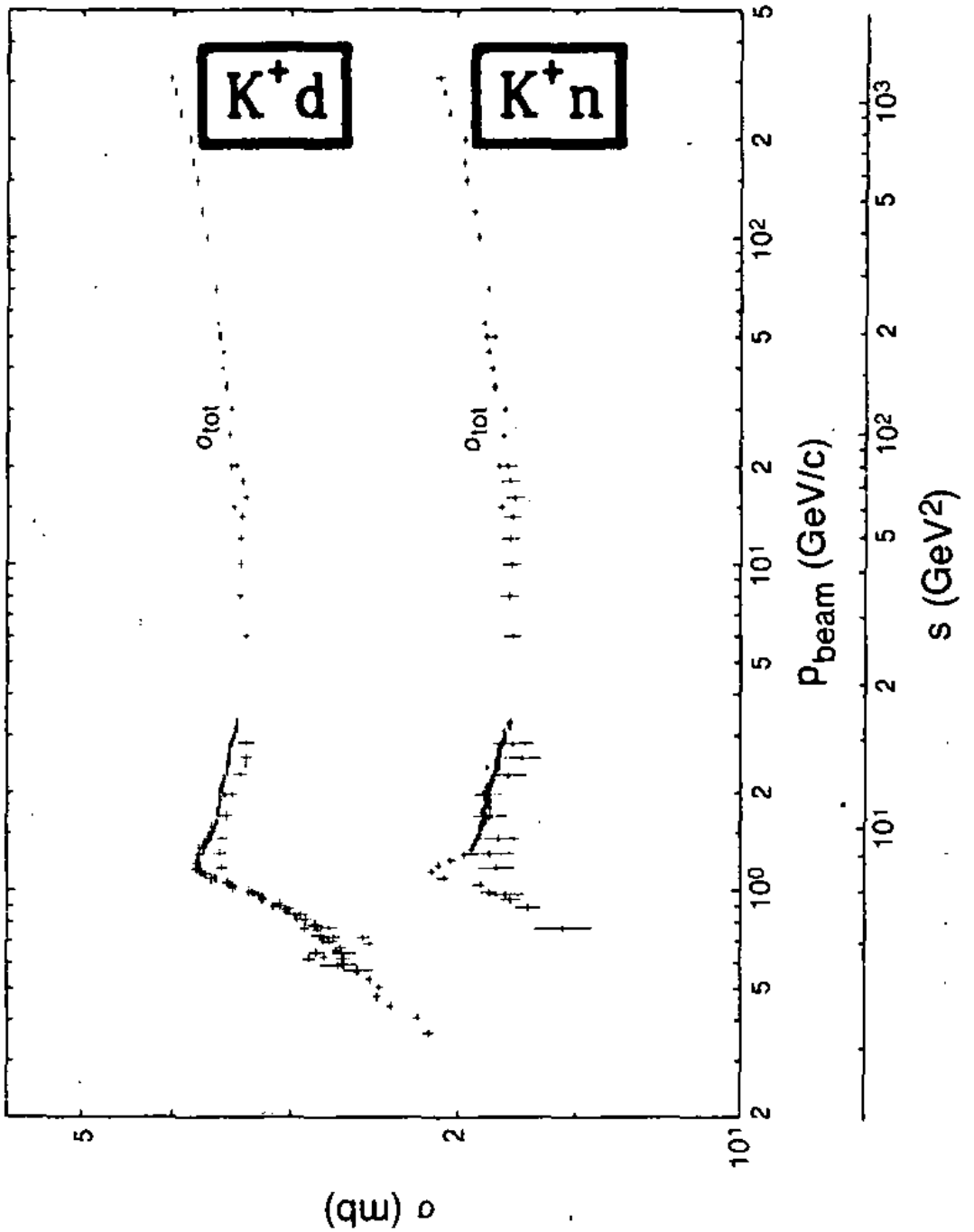

K^+d and K^+n total cross sections vs. laboratory beam momentum p_{beam} and center-of-mass energy squared s. Figure courtesy V. Flaminio, W.G. Moorhead, D.R.O. Morrison, and N. Rivoire, CERN.

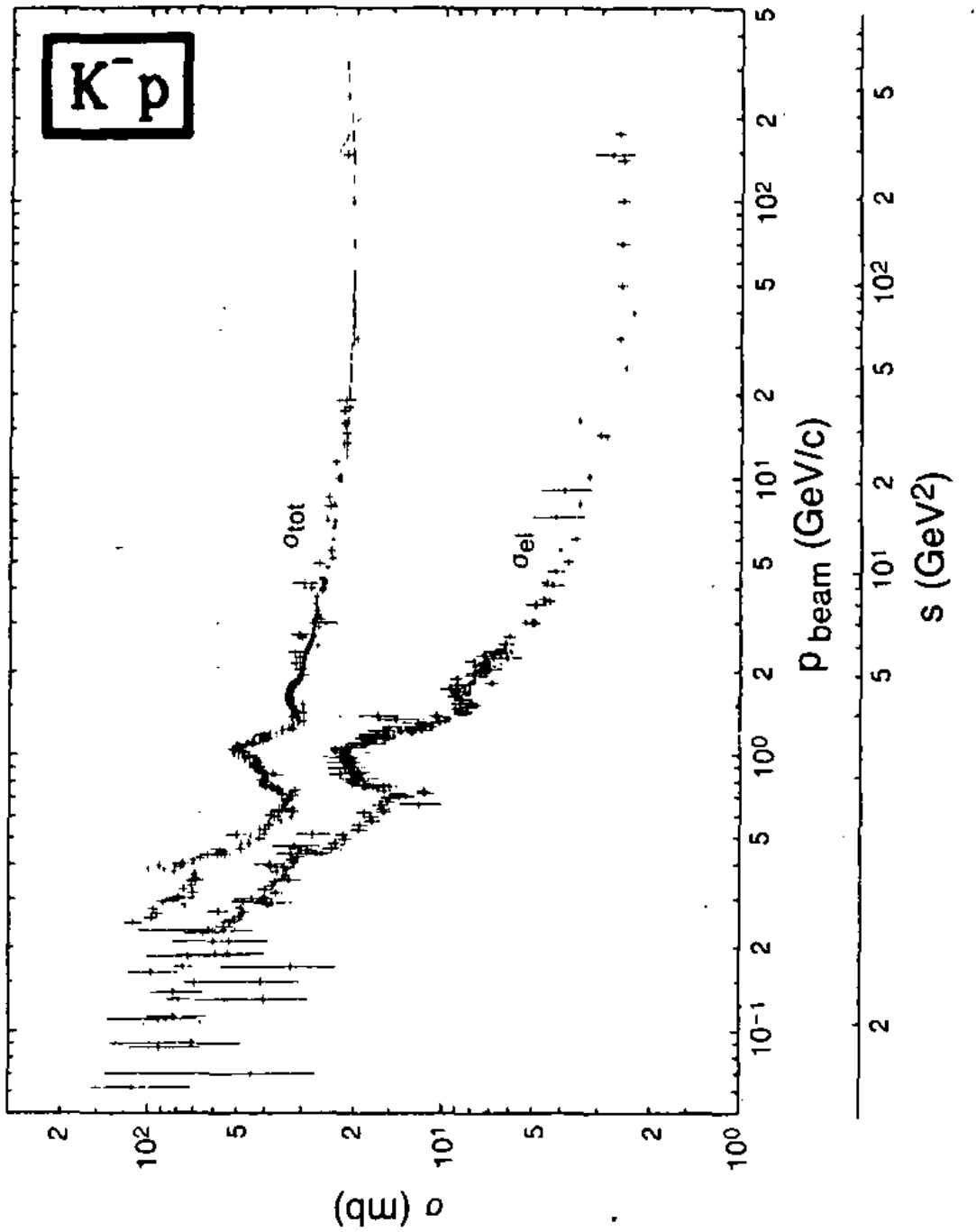

K^-p total and elastic cross sections vs. laboratory beam momentum p_{beam} and center-of-mass energy squared s. Figure courtesy V. Flaminio, W.G. Moorhead, D.R.O. Morrison, and N. Rivoire, CERN.

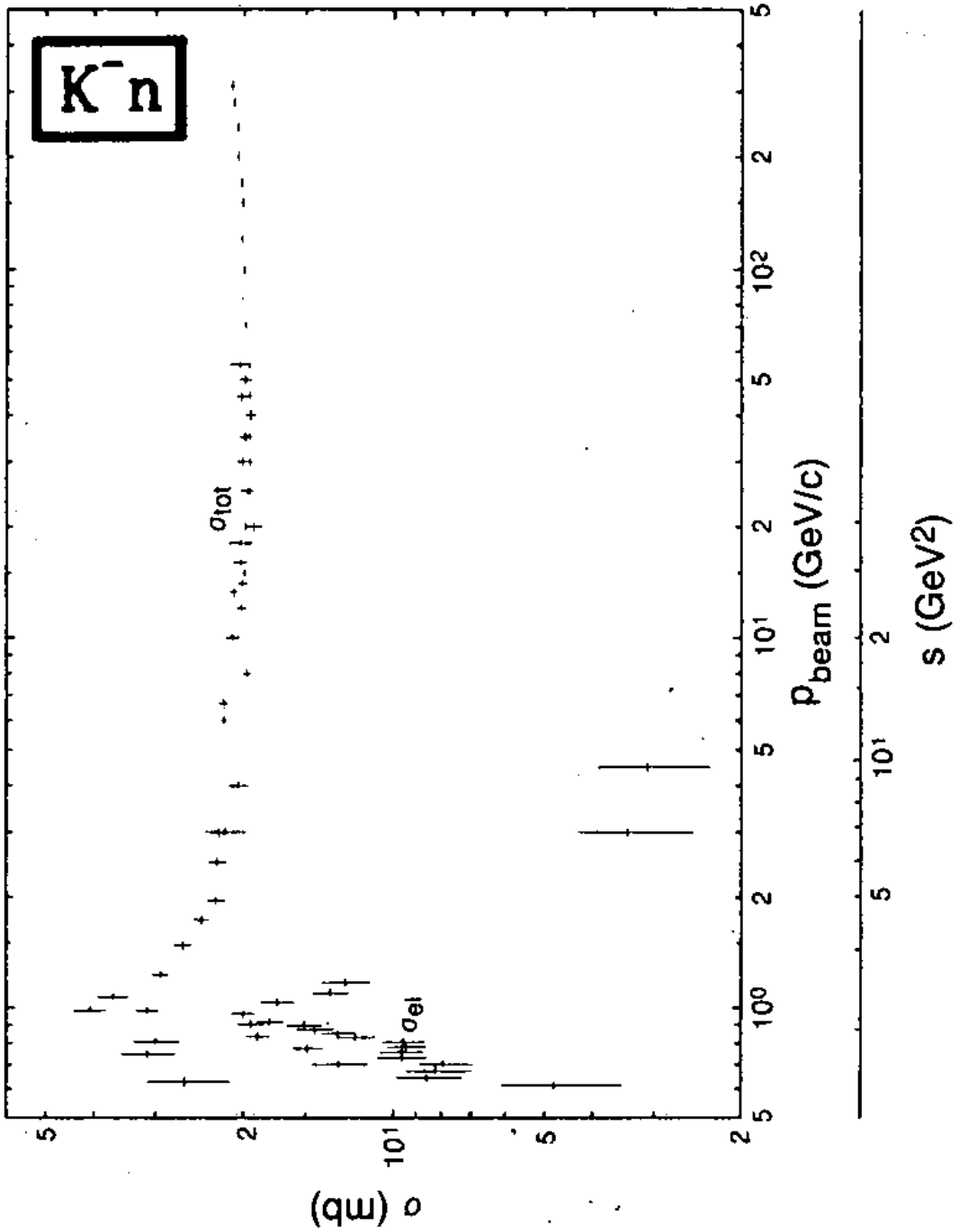

K^-n total and elastic cross sections vs. laboratory beam momentum p_{beam} and center-of-mass energy squared s. Figure courtesy V. Flaminio, W.G. Moorhead, D.R.O. Morrison, and N. Rivoire, CERN.

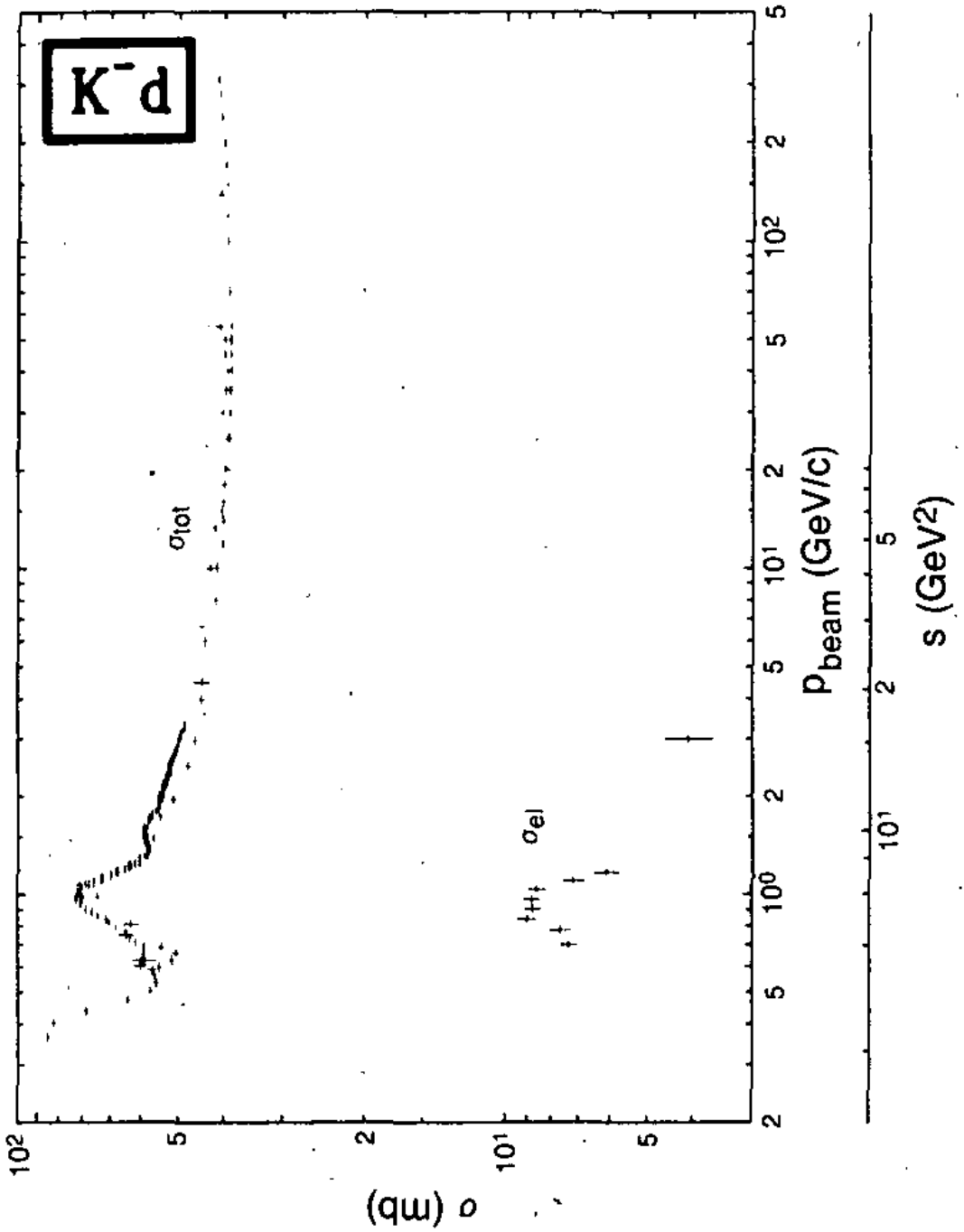

K^-d total and elastic cross sections vs. laboratory beam momentum p_{beam} and center-of-mass energy squared s. Figure courtesy V. Flaminio, W.G. Moorhead, D.R.O. Morrison, and N. Rivoire, CERN.

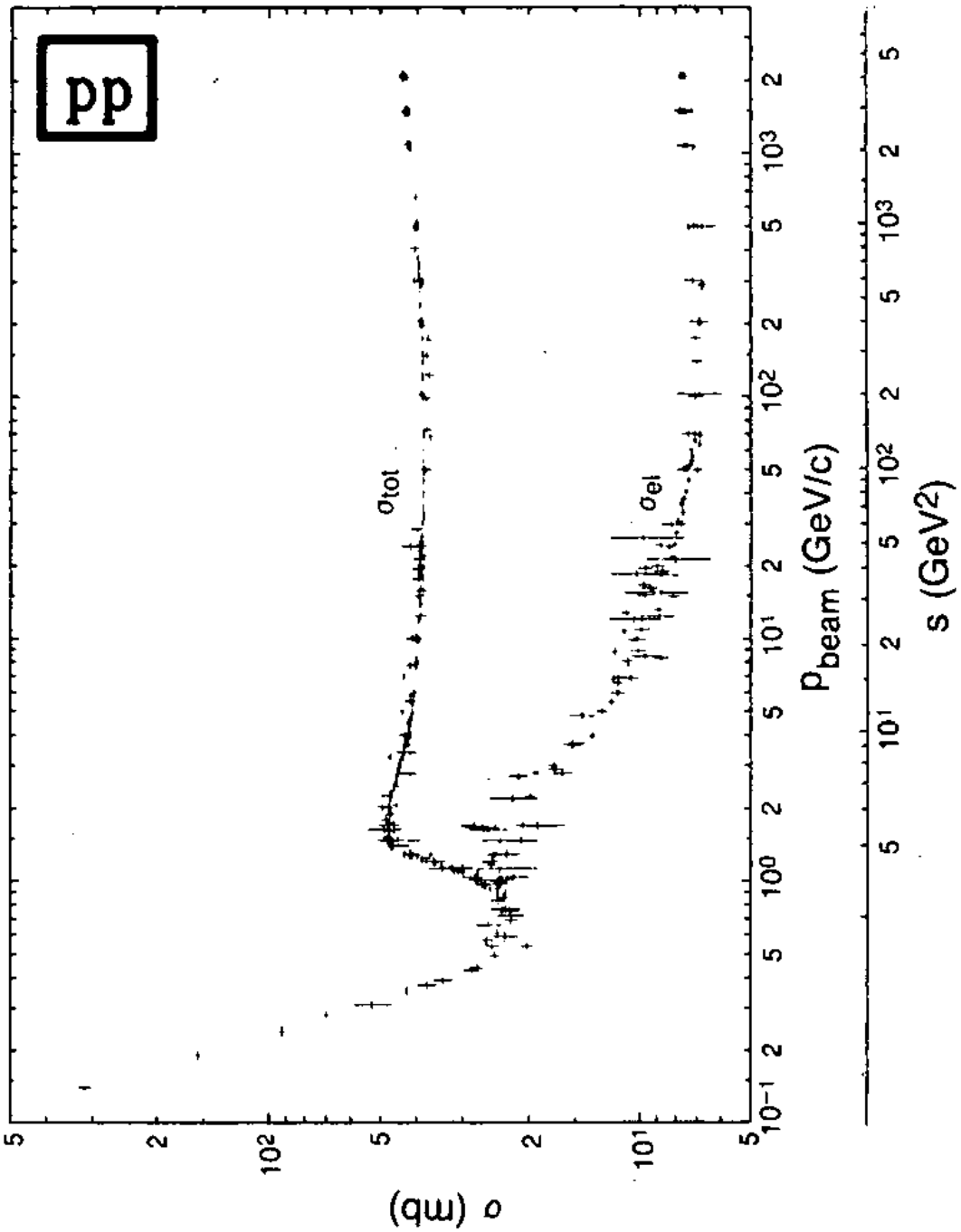

pp total and elastic cross sections vs. laboratory beam momentum p_{beam} and center-of-mass energy squared s. Figure courtesy V. Flaminio, W.G. Moorhead, D.R.O. Morrison, and N. Rivoire, CERN.

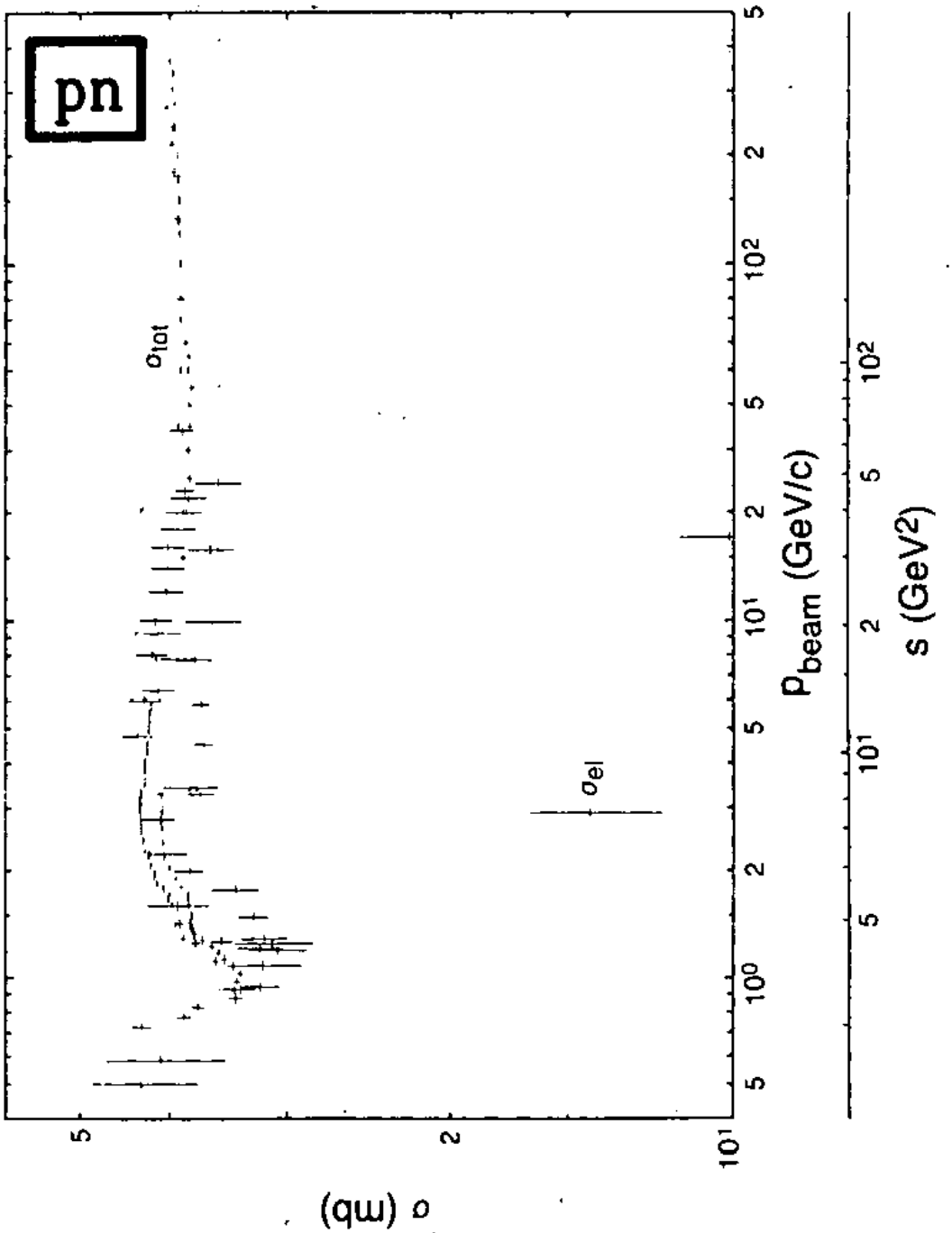

pn total and elastic cross sections vs. laboratory beam momentum p_{beam} and center-of-mass energy squared s. Figure courtesy V. Flaminio, W.G. Moorhead, D.R.O. Morrison, and N. Rivoire, CERN.

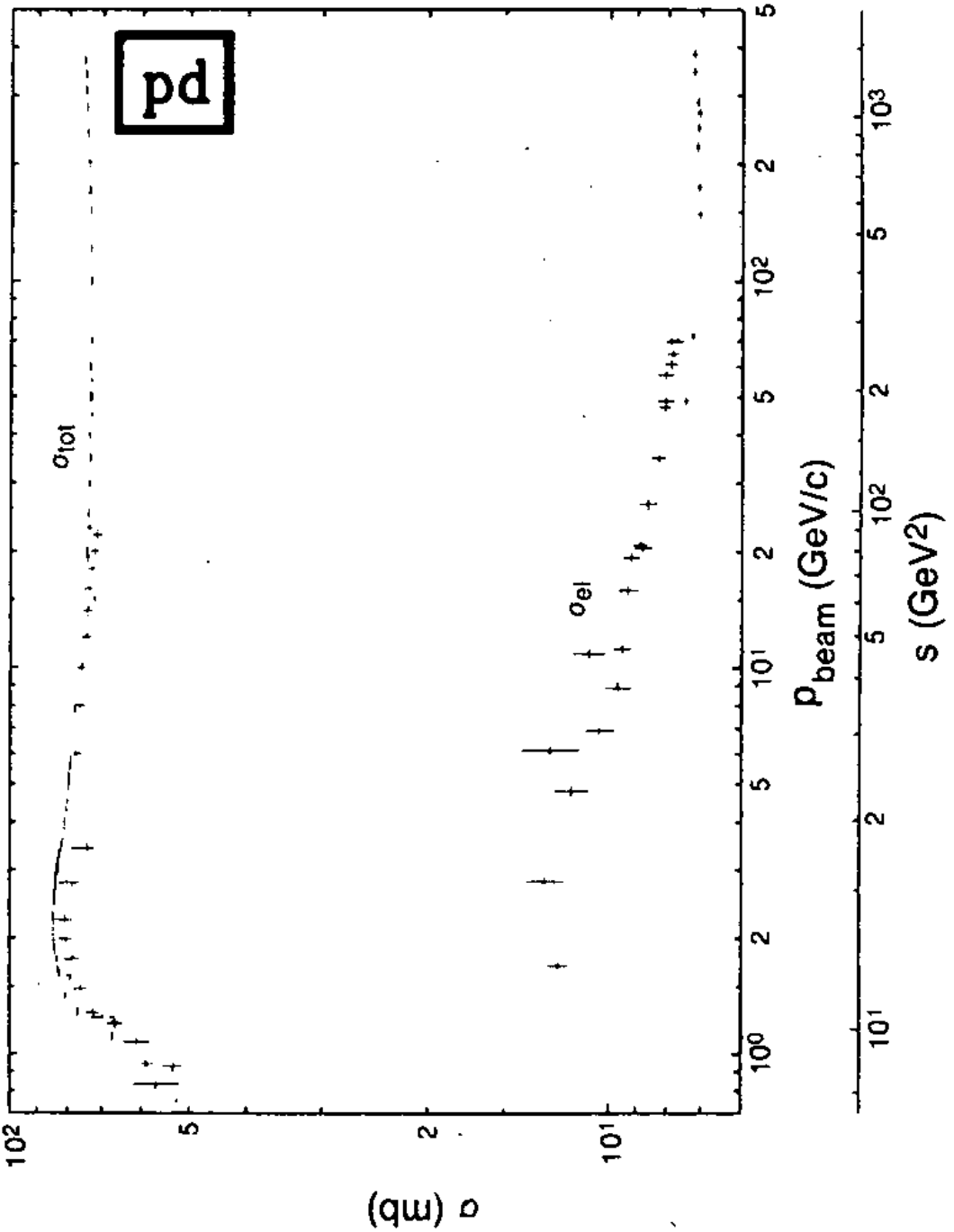

pd total and elastic cross sections vs. laboratory beam momentum p_{beam} and center-of-mass energy squared s. Figure courtesy V. Flaminio, W.G. Moorhead, D.R.O. Morrison, and N. Rivoire, CERN.

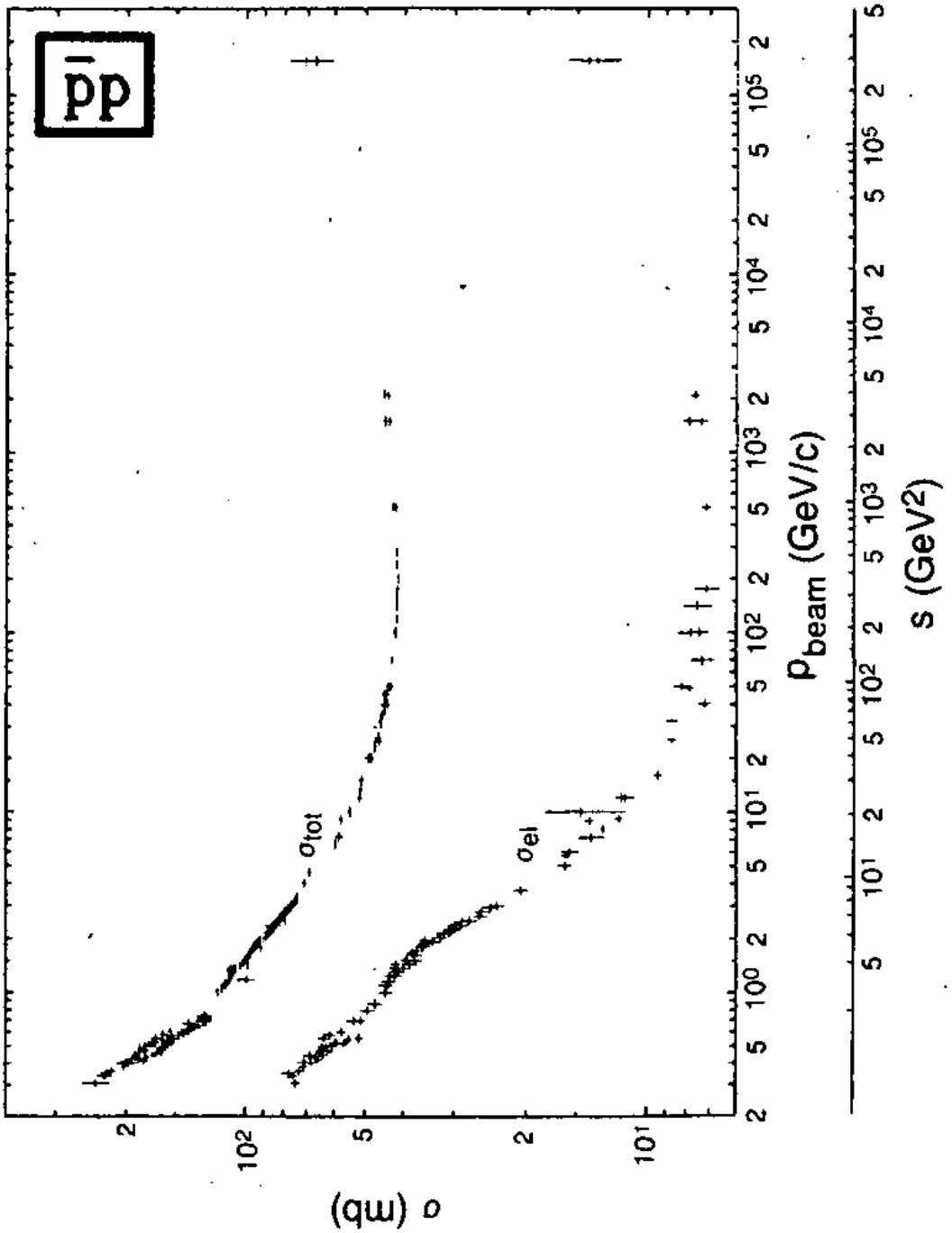

$\bar{p}p$ total and elastic cross sections vs. laboratory beam momentum p_{beam} and center-of-mass energy squared s. Figure courtesy V. Flaminio, W.G. Moorhead, D.R.O. Morrison, and N. Rivoire, CERN.

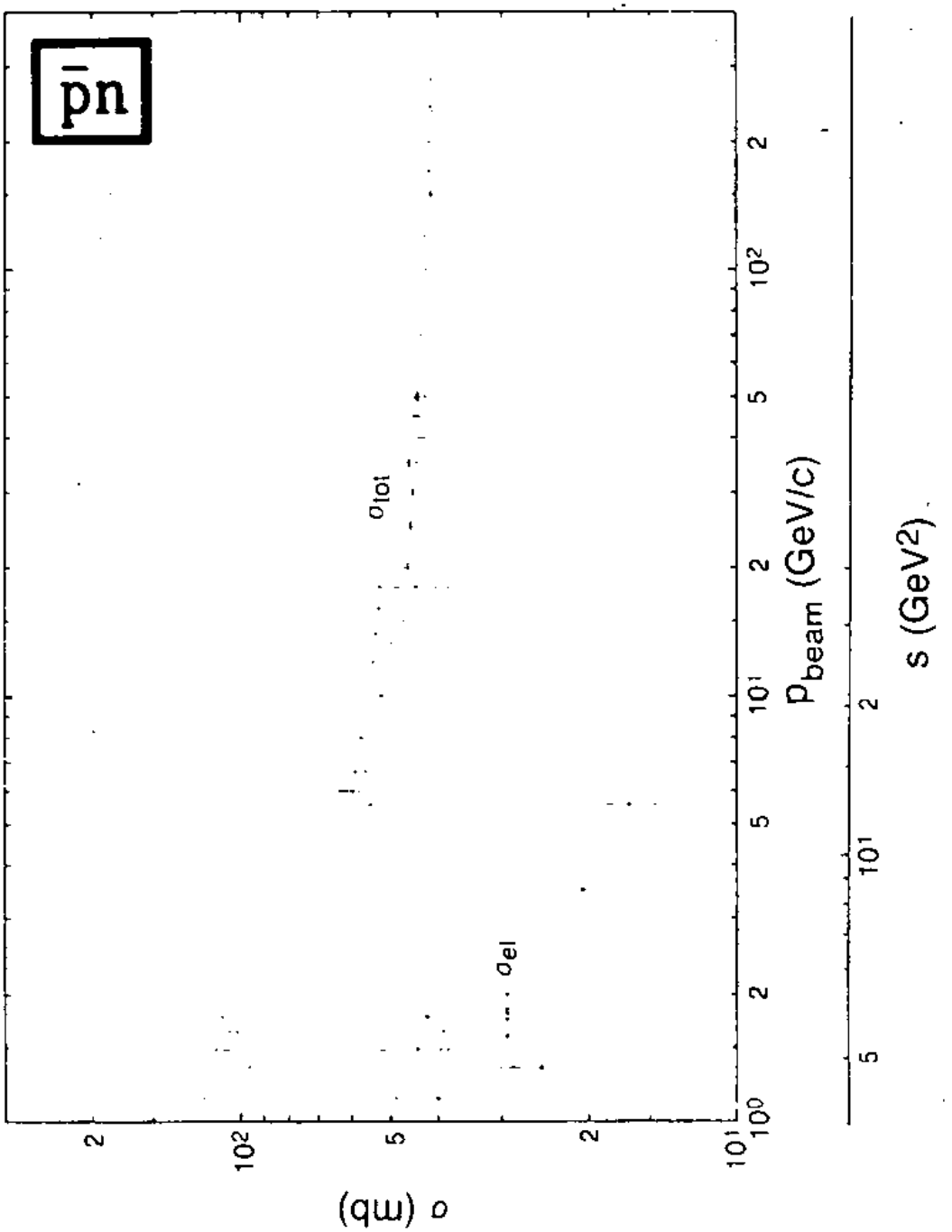

$\bar{p}n$ total and elastic cross sections vs. laboratory beam momentum p_{beam} and center-of-mass energy squared s. Figure courtesy V. Flaminio, W.G. Moorhead, D.R.O. Morrison, and N. Rivoire, CERN.

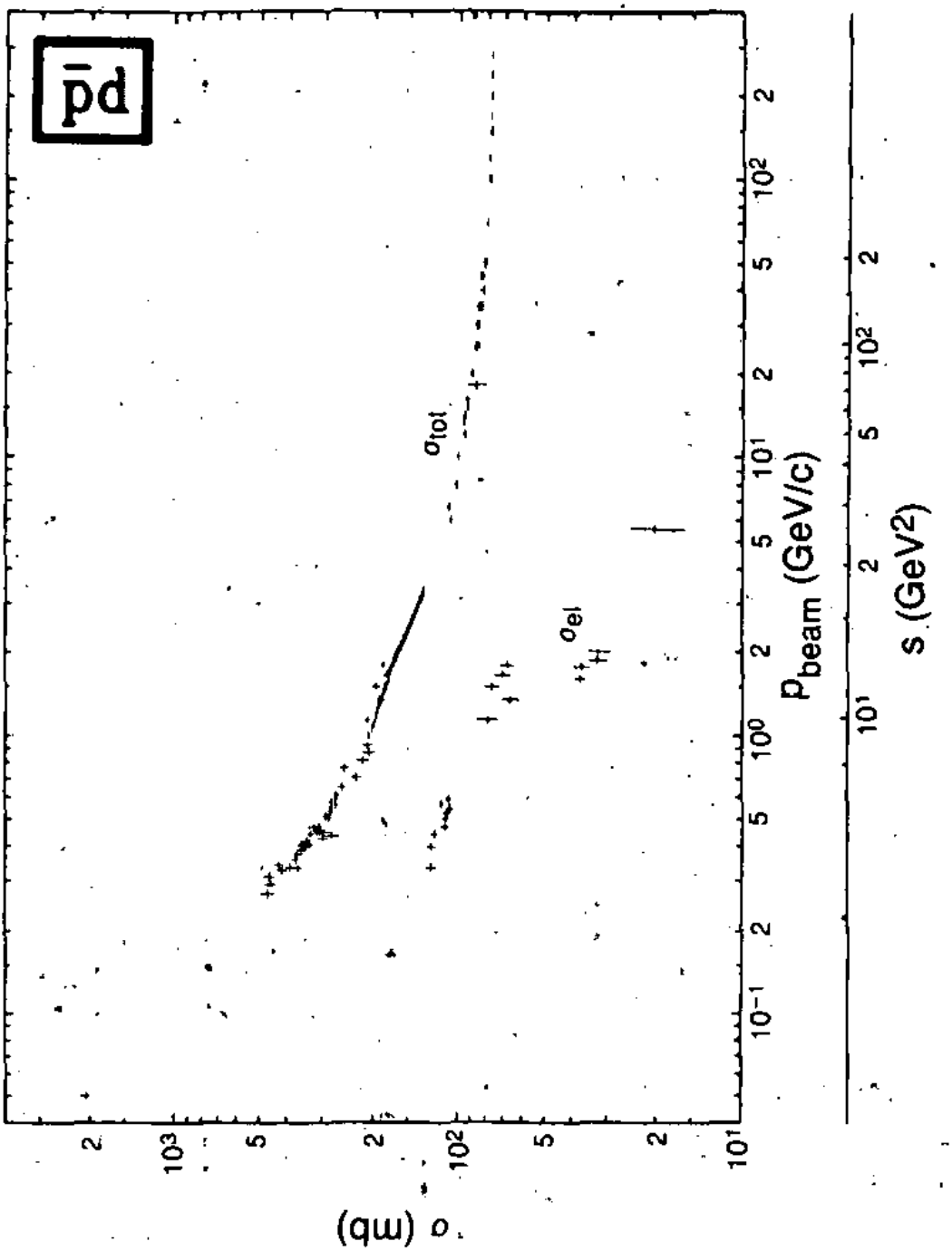

$\bar{p}d$ total and elastic cross sections vs. laboratory beam momentum p_{beam} and center-of-mass energy squared s. Figure courtesy V. Flaminio, W.G. Moorhead, D.R.O. Morrison, and N. Rivoire, CERN.

1984

JANUARY

S	M	T	W	T	F	S
1	2	3	4	5	6	7
8	9	10	11	12	13	14
15	16	17	18	19	20	21
22	23	24	25	26	27	28
29	30	31				

FEBRUARY

S	M	T	W	T	F	S
			1	2	3	4
5	6	7	8	9	10	11
12	13	14	15	16	17	18
19	20	21	22	23	24	25
26	27	28	29			

MARCH

S	M	T	W	T	F	S
				1	2	3
4	5	6	7	8	9	10
11	12	13	14	15	16	17
18	19	20	21	22	23	24
25	26	27	28	29	30	31

APRIL

1	2	3	4	5	6	7
8	9	10	11	12	13	14
15	16	17	18	19	20	21
22	23	24	25	26	27	28
29	30					

MAY

		1	2	3	4	5
6	7	8	9	10	11	12
13	14	15	16	17	18	19
20	21	22	23	24	25	26
27	28	29	30	31		

JUNE

					1	2
3	4	5	6	7	8	9
10	11	12	13	14	15	16
17	18	19	20	21	22	23
24	25	26	27	28	29	30

JULY

1	2	3	4	5	6	7
8	9	10	11	12	13	14
15	16	17	18	19	20	21
22	23	24	25	26	27	28
29	30	31				

AUGUST

			1	2	3	4
5	6	7	8	9	10	11
12	13	14	15	16	17	18
19	20	21	22	23	24	25
26	27	28	29	30	31	

SEPTEMBER

						1
2	3	4	5	6	7	8
9	10	11	12	13	14	15
16	17	18	19	20	21	22
23	24	25	26	27	28	29
30						

OCTOBER

	1	2	3	4	5	6
7	8	9	10	11	12	13
14	15	16	17	18	19	20
21	22	23	24	25	26	27
28	29	30	31			

NOVEMBER

				1	2	3
4	5	6	7	8	9	10
11	12	13	14	15	16	17
18	19	20	21	22	23	24
25	26	27	28	29	30	

DECEMBER

						1
2	3	4	5	6	7	8
9	10	11	12	13	14	15
16	17	18	19	20	21	22
23	24	25	26	27	28	29
30	31					

1985

JANUARY

S	M	T	W	T	F	S
		1	2	3	4	5
6	7	8	9	10	11	12
13	14	15	16	17	18	19
20	21	22	23	24	25	26
27	28	29	30	31		

FEBRUARY

S	M	T	W	T	F	S
					1	2
3	4	5	6	7	8	9
10	11	12	13	14	15	16
17	18	19	20	21	22	23
24	25	26	27	28		

MARCH

S	M	T	W	T	F	S
					1	2
3	4	5	6	7	8	9
10	11	12	13	14	15	16
17	18	19	20	21	22	23
24	25	26	27	28	29	30
31						

APRIL

	1	2	3	4	5	6
7	8	9	10	11	12	13
14	15	16	17	18	19	20
21	22	23	24	25	26	27
28	29	30				

MAY

			1	2	3	4
5	6	7	8	9	10	11
12	13	14	15	16	17	18
19	20	21	22	23	24	25
26	27	28	29	30	31	

JUNE

						1
2	3	4	5	6	7	8
9	10	11	12	13	14	15
16	17	18	19	20	21	22
23	24	25	26	27	28	29
30						

JULY

	1	2	3	4	5	6
7	8	9	10	11	12	13
14	15	16	17	18	19	20
21	22	23	24	25	26	27
28	29	30	31			

AUGUST

				1	2	3
4	5	6	7	8	9	10
11	12	13	14	15	16	17
18	19	20	21	22	23	24
25	26	27	28	29	30	31

SEPTEMBER

1	2	3	4	5	6	7
8	9	10	11	12	13	14
15	16	17	18	19	20	21
22	23	24	25	26	27	28
29	30					

OCTOBER

		1	2	3	4	5
6	7	8	9	10	11	12
13	14	15	16	17	18	19
20	21	22	23	24	25	26
27	28	29	30	31		

NOVEMBER

					1	2
3	4	5	6	7	8	9
10	11	12	13	14	15	16
17	18	19	20	21	22	23
24	25	26	27	28	29	30

DECEMBER

1	2	3	4	5	6	7
8	9	10	11	12	13	14
15	16	17	18	19	20	21
22	23	24	25	26	27	28
29	30	31				

1986

JANUARY

S	M	T	W	T	F	S
			1	2	3	4
5	6	7	8	9	10	11
12	13	14	15	16	17	18
19	20	21	22	23	24	25
26	27	28	29	30	31	

FEBRUARY

S	M	T	W	T	F	S
						1
2	3	4	5	6	7	8
9	10	11	12	13	14	15
16	17	18	19	20	21	22
23	24	25	26	27	28	

MARCH

S	M	T	W	T	F	S
						1
2	3	4	5	6	7	8
9	10	11	12	13	14	15
16	17	18	19	20	21	22
23	24	25	26	27	28	29
30	31					

APRIL

		1	2	3	4	5
6	7	8	9	10	11	12
13	14	15	16	17	18	19
20	21	22	23	24	25	26
27	28	29	30			

MAY

				1	2	3
4	5	6	7	8	9	10
11	12	13	14	15	16	17
18	19	20	21	22	23	24
25	26	27	28	29	30	31

JUNE

1	2	3	4	5	6	7
8	9	10	11	12	13	14
15	16	17	18	19	20	21
22	23	24	25	26	27	28
29	30					

JULY

		1	2	3	4	5
6	7	8	9	10	11	12
13	14	15	16	17	18	19
20	21	22	23	24	25	26
27	28	29	30	31		

AUGUST

					1	2
3	4	5	6	7	8	9
10	11	12	13	14	15	16
17	18	19	20	21	22	23
24	25	26	27	28	29	30
31						

SEPTEMBER

	1	2	3	4	5	6
7	8	9	10	11	12	13
14	15	16	17	18	19	20
21	22	23	24	25	26	27
28	29	30				

OCTOBER

			1	2	3	4
5	6	7	8	9	10	11
12	13	14	15	16	17	18
19	20	21	22	23	24	25
26	27	28	29	30	31	

NOVEMBER

						1
2	3	4	5	6	7	8
9	10	11	12	13	14	15
16	17	18	19	20	21	22
23	24	25	26	27	28	29
30						

DECEMBER

	1	2	3	4	5	6
7	8	9	10	11	12	13
14	15	16	17	18	19	20
21	22	23	24	25	26	27
28	29	30	31			

Notes

Notes

Notes

Additional copies of this Data Booklet, and of the complete Review of Particle Properties from which it is extracted, may be obtained from:

For North and South America, Australasia, and the Far East, write to:

Technical Information Department
Lawrence Berkeley Laboratory
Berkeley, California 94720
USA

All other areas write to:

CERN Scientific Information Service
CH-1211 Geneva 23
Switzerland

Prepared for the Department of Energy
under contract DE-AC03-76SF00098

Pub 72